ISSN 0973-8916

Current Trends in Biotechnology and Pharmacy

Volume 14 Issue 3 July 2020

www.abap.co.in

Current Trends in Biotechnology and Pharmacy
ISSN 0973-8916 (Print), 2230-7303 (Online)

Editors

Prof.K.R.S. Sambasiva Rao, India
krssrao@abap.co.in

Prof. Karnam S. Murthy, USA
skarnam@vcu.edu

www.abap.co.in

ISSN 0973-8916

Current Trends in Biotechnology and Pharmacy

(An International Scientific Journal)

Volume 14 Issue 3 July 2020

www.abap.co.in

Indexed in Chemical Abstracts, EMBASE, ProQuest, Academic SearchTM, DOAJ, CAB Abstracts, Index Copernicus, Ulrich's Periodicals Directory, Open J-Gate Pharmoinfonet.in Indianjournals.com and Indian Science Abstracts.

Current Trends in Biotechnology and Pharmacy
Vol. 14 (3) July 2020, ISSN 0973-8916 (Print), 2230-7303 (Online)

Association of Biotechnology and Pharmacy

(Regn. No. 28 OF 2007)

The *Association of Biotechnology and Pharmacy (ABAP)* was established for promoting the science of Biotechnology and Pharmacy. The objective of the Association is to advance and disseminate the knowledge and information in the areas of Biotechnology and Pharmacy by organising annual scientific meetings, seminars and symposia.

Members

The persons involved in research, teaching and work can become members of Association by paying membership fees to Association.

The members of the Association are allowed to write the title ***MABAP*** (Member of the Association of Biotechnology and Pharmacy) with their names.

Fellows

Every year, the Association will award Fellowships to the limited number of members of the Association with a distinguished academic and scientific career to be as Fellows of the Association during annual convention. The fellows can write the title ***FABAP*** (Fellow of the Association of Biotechnology and Pharmacy) with their names.

Membership details

(Membership and Journal)	India	SAARC	Others
Individuals – 1 year	Rs. 600	Rs. 1000	$100
LifeMember	Rs. 4000	Rs. 6000	$500
Institutions – 1 year	Rs. 1500	Rs. 2000	$200
(Journal only) Life member	Rs.10000	Rs.12000	$1200

Individuals can pay in two instalments, however the membership certificate will be issued on payment of full amount. All the members and Fellows will receive a copy of the journal free.

Association of Biotechnology and Pharmacy
(Regn. No. 28 OF 2007)
#5-69-64; 6/19, Brodipet
Guntur – 522 002, Andhra Pradesh, India

Current Trends in Biotechnology and Pharmacy
Vol. 14 (3) July 2020, ISSN 0973-8916 (Print), 2230-7303 (Online)

Current Trends in Biotechnology and Pharmacy

ISSN 0973-8916

Volume 14 (3) **July 2020**

CONTENTS

Current Trends in Biotechnology and Pharmacy
Vol. 14 (3) July 2020, ISSN 0973-8916 (Print), 2230-7303 (Online)

Information to Authors

The *Current Trends in Biotechnology and Pharmacy* is an official international journal of *Association of Biotechnology and Pharmacy*. It is a peer reviewed quarterly journal dedicated to publish high quality original research articles in biotechnology and pharmacy. The journal will accept contributions from all areas of biotechnology and pharmacy including plant, animal, industrial, microbial, medical, pharmaceutical and analytical biotechnologies, immunology, proteomics, genomics, metabolomics, bioinformatics and different areas in pharmacy such as, pharmaceutics, pharmacology, pharmaceutical chemistry, pharma analysis and pharmacognosy. In addition to the original research papers, review articles in the above mentioned fields will also be considered.

Call for papers

The Association is inviting original research or review papers and short comunications in any of the above mentioned research areas for publication in Current Trends in Biotechnology and Pharmacy. The manuscripts should be concise, typed in double space in a general format containing a title page with a short running title and the names and addresses of the authors for correspondence followed by Abstract (350 words), 3 – 5 key words, Introduction, Materials and Methods, Results and Discussion, Conclusion, References, followed by the tables, figures and graphs on separate sheets. For quoting references in the text one has to follow the numbering of references in parentheses and full references with appropriate numbers at the end of the text in the same order. References have to be cited in the format below.

Mahavadi, S., Rao, R.S.S.K. and Murthy, K.S. (2007). Cross-regulation of VAPC2 receptor internalization by m2 receptors via c-Src-mediated phosphorylation of GRK2. Regulatory Peptides, 139: 109-114.

Lehninger, A.L., Nelson, D.L. and Cox, M.M. (2004). Lehninger Principles of Biochemistry, (4th edition), W.H. Freeman & Co., New York, USA, pp. 73-111.

Authors have to submit the figures, graphs and tables of the related research paper/article in Adobe Photoshop of the latest version for good illumination and allignment.

Authors can submit their papers and articles either to the editor or any of the editorial board members for onward transmission to the editorial office. Members of the editorial board are authorized to accept papers and can recommend for publication after the peer reviewing process. The email address of editorial board members are available in website www.abap.in. For submission of the articles directly, the authors are advised to submit by email to krssrao@abap.co.in or krssrao@yahoo.com.

Authors are solely responsible for the data, presentation and conclusions made in their articles/research papers. It is the responsibility of the advertisers for the statements made in the advertisements.

Current Trends in Biotechnology and Pharmacy
Vol. 14 (3) 239-255, July 2020, ISSN 0973-8916 (Print), 2230-7303 (Online)
DOI: 10.5530/ctbp.2020.3.25

Variability in seed mineral composition of foxtail millet (*Setaria italica* L.) landraces and released cultivars

Gurulakshmi Kola[1#], Puli Chandra Obul Reddy[2#], Sameena Shaik[1], Mallikarjuna Gunti[1], Ramesh Palakurthi[1], H.S. Talwar[3] and Akila Chandra Sekhar*[1]

[1] Molecular Genetics and Functional Genomics Laboratory, Department of Biotechnology, School of Life Sciences, Yogi Vemana University, Kadapa - 516005, Andhra Pradesh, India
[2] Plant Molecular Biology Laboratory, Department of Botany, School of Life Sciences Yogi Vemana University, Kadapa - 516005, Andhra Pradesh, India
[3] Plant Physiology, ICAR-Indian Institute of Millet Research (IIMR) Rajendra Nagar-500030, Hyderabad, Telangana, India
Corresponding author : chandrasekhar_@yahoo.com

Abstract

Foxtail millet (*Setaria italica* L.) belongs to poaceae and an important research model plant to explore nutritional pathways. The present study represents a comprehensive micronutrient report of twenty landraces, four released cultivars, and their genetic variability in micronutrient content. FT-IR analysis recorded various absorption peaks at different wavelenths coressponding to certain chemical compounds and functional groups such as carbohydrates, alkenes, proteins, sulfur compounds, amines and lipids, etc, indicate that all the studied genotypes endowed with carbohydrates, proteins and lipids. The ICP-OES analysis revealed a wide range of variation in micronutrient concentrations across the studied genotypes *i.e* Iron (3.69 to 7.51mg/100g), Zinc (4.54 to 5.71 mg/100g), Calcium (13.13 to 39.58 mg/100g), Potassium (219.43 to 349.47 mg/100g), Copper (0.60 to1.09 mg/100g), Manganese (1.05 to 1.64 mg/100g). The PCA and cluster analaysis highlight a wide range of genetic variability among the genotypes. Further, these genotypes were clustered into six variables based on the micronutrient content. In overall performance of landraces better than released cultivars in terms of micronutrient content. Landraces like S1G4, S1G2; and relesed varity Narasimharaya recorded higher quatities of micronutrient compared to other genotypes studied. These genotypes would be useful to fish out the genes responsible for higher micronutrient occumulation and also as parental lines in breeding progrmmes to develop enhanced micronutrient genotypes.

Introduction

Plant-based foods contribute an array of nutrients that are essential for the day-to-day needs of human beings and they endorse good health. Humans require at least twenty-two micro and macro elements for their proper health, growth, and development (50). However, global estimates suggest that, over 60% of the people suffering from iron (Fe), 30% zinc (Zn), 30% iodine (I) and 15% selenium (Se) deficiencies. In addition to them, calcium (Ca), manganese (Mn), and copper (Cu) deficiencies are common in many of the developed and developing countries (40). Malnourishment is a global issue; especially developing countries from Asia and Africa facing severe micronutrient deficiencies in their dietary food (19, 42). The health and diet are co-dependent; the physiological functions of the human body are influenced by food components (29). Even though the requirements of micronutrients are minimal, they play a crucial role in proper growth and development. The deficiencies of micronutrients cause severe health complications such as physical and mental

Vol. 14 (3) 239-255, July 2020, ISSN 0973-8916 (Print), 2230-7303 (Online)
DOI: 10.5530/ctbp.2020.3.25

retardation, blindness, gastrointestinal health complications, reduced immunity, etc. (9). Newborn babies and pregnant women of India severely affected by micronutrient deficiency and most of the infants are born underweight. It is estimated that nearly 7.4 million children remain undernourished (19). Thus, functional foods are gaining importance in the prevention and/or treatment of diseases.

Among the plant-based foods, cereals alone play a key role as a staple food and provide ~50% of the dietary requirements of humans. Globally, among the cereals rice alone provides 50-60% of required calories to 2.7 billion people. However, the principle drawback of rice-based food products are being low in iron, zinc, proteins, vitamins, and other essential nutrients along with high water requirements for its cultivation (18, 50). On contrary small millets consists of diverse micronutrients, rich in essential amino acids and high water use efficient, grow in harsh environmental conditions, resistant to abiotic and biotic stress conditions. Hence, recently small millets gaining more importance and they might play a crucial role as functional foods.

The small millet, foxtail millet (*Setaria italica* L.) is an important nutritious crop belongs to the family Poaceae, known for its origin from China. Due to its drought tolerance capacity, it is very well grown in semi-arid regions such as South Asia and Sub-Saharan Africa as nutritional food. It is also cultivated in South Korea, North Korea, Japan, Russia, Australia, France and the United States as a forage crops, feed for birds and cattle (12). Foxtail millet endowed with high amounts of protein, vitamins, minerals, starch, and fat content (39). It has twice the content of protein and fat as compared to rice (35). Nutrient analysis of core collection of foxtail millet seeds revealed that it had a wide range of nutrients such as calcium (171.2–288.7 mg/kg), iron (58.2–68.0 mg/kg), zinc (54.5–74.2 mg/kg) and protein (15.6–18.5%) (43). However, due to the presence of anti-nutrients made them less bioavailable (1, 2, 15, 23, 30).

Bio-fortification of millets is an emerging approach to overcome the problem of anti-nutrients and to add more nutritional content to the crop plants. Conventional breeding, agronomical practices, and biotechnological strategies are the key approaches to improve the bio-fortification of crop plants. Agronomical practices such as supplementing the deficit soil with inorganic fertilizers were successfully practiced in Finland and Turkey for the high accumulation of Se and Zn in the seeds (50).

Genetic variation for the trait of interest is a prerequisite for plant breeding (13). Foxtail millet genotypes exhibited variation in seed protein, fat, starch, and amino acids (51); Fe content (31); vitamin E (25); cooking quality traits (38). Thippeswamy et al (2017) screened 25 genotypes and identified two genotypes namely GS78 and GS71 as superior for grain micronutrients (Zn, Fe, and Ca) and protein content (41). Four genotypes of foxtail millet genotype 00002, 0011 (red colour bran) and Slovenský, Friderica (yellow colour bran) displayed varied amounts of nutritive components, fatty acids, phenolic compounds and antioxidants (28). A greater amount of variability was observed in 78 elite genotypes for nutritional parameters such as moisture, protein, fat, crude fibre, carbohydrate, total minerals, total energy, and micronutrients (Cu, Mn, Zn, and Fe) (7, 21).

Landraces are a heterogeneous population, well adapted to local climatic conditions, and are extremely nutritious. They also serve as genetic material to breed high nutritional and stress adapted genotypes (11). Maxican maize landraces were successfully used to breed high-quality protein maize lines and cultivars (32). Similarly, Sorghum popular Indian landrace Maldandi (M35-1) was used in the breeding programme to develop several restorer lines (ICSR#) and cultivars (ICSV#) (34). In pearl millets West African drought tolerant landrace “Iniadi” was used to develop several cultivars e.g.: ICTP 8203 (33). As many as 245 foxtail millet traditional varieties from different regions of Shanxi, China was evaluated for seed folic acid variability and

Vol. 14 (3) 239-255, July 2020, ISSN 0973-8916 (Print), 2230-7303 (Online)
DOI: 10.5530/ctbp.2020.3.25

found a wide variability ranging (0.37–2.37 mg/g) of which 24 varieties with higher folic acid content were identified, among them, Jingu 21, a major leading cultivar, recorded folic acid content of 2 mg/g (36). Similarly, a panel of 92 foxtail millet landraces preserved by Taiwan indigenous peoples were assessed for seed amylase content (AC) using a rapid viscosity analyzer (RVA). A huge range of diversity (0.7% to 16.9%) in physiochemical properties was observed among the studied genotypes (52).

Thus, identification of elite genotypes for micronutrient content is very important towards the development of improved varieties through classical as well as modern tools. To identify the elite nutritious genotypes in the present study, twenty local landraces collected from various locations of Andhra Pradesh and four released cultivars were selected, nutrient content was analysed using modern analytical tools such as ICP-OES (Inductively coupled plasma atomic emission spectroscopy) and FT-IR (Fourier Transform Infrared Spectrophotometer) and data were subjected to multivariate statistical analysis.

Materials and Methods

Plant material : The seeds of foxtail millet landraces collected from the farmer fields of Rayalaseema region, Andhra Pradesh, and twenty pure lines were developed by single seed descent method (SSD). The details of their development and molecular characterization were described elsewhere (Ramesh et al., manuscript Unpublished). Twenty pure landraces along with four released cultivars (Table.1) were surfaced sterilized with 0.01% $HgCl_2$ followed by rinsing with distilled water. Seeds were sowed in the well-prepared seedbeds of natural field soil in a completely random blocked design with three replicates per sample. Each genotype was grown in three rows in net house at Yogi Vemana University, Kadapa, Andhra Pradesh under natural environmental conditions (30±1ºC/37±1ºC and relative humidity varied from 50-80%), by following standard agriculture practices. Seeds were harvested from panicles after maturation and stored in a cool dry place until further use. The seeds were de-husked and milled into flours by using a clean and sterilized mortar and pestle. The flours were kept at 55° C for 4-5 hours in a hot-air-oven to remove the moisture content if any. Dehydrated flours were subjected to nutrient analysis for macro, micronutrients, and essential biochemical groups.

Sample preparation and FTIR Analysis : Dehydrated flour of all twenty-four genotypes was used for the preparation of KBr (potassium bromide) pellets to analyze functional groups of flour. Ten mg of dehydrated seed flour was mixed with 100mg of KBr and vigorously ground into a fine powder with mortar and pestle. This mixture was compressed into diaphanous pellet discs using a hydraulic pressure pump. These diaphanous pellets were subjected to Fourier transformed infrared spectroscopy analysis using Perkin Elmer Spectrum Two (Perkin Elmer Inc., USA). Chemical and functional groups of the samples were obtained with 16 scans at a resolution of $2^{cm-1}$with the wavenumber range from 400^{cm-1} to 4000 $^{cm-1}$ at room temperature. The spectrometer has an auto-correction system to eliminate water vapor without purging with nitrogen.

Sample preparation and ICP-OES analysis : Five hundred mg of dehydrated flour of all twenty-four genotypes in three replications was taken into a clean acid prewashed polypropylene tube. The samples were digested with 2 ml of HNO_3 (65%V/V) and 0.5 ml of H_2O_2 (30% H_2O_2) in a closed vessel microwave digestion system and allowed the vessel to stand overnight at room temperature (cold digestion). The vessel is closed with a screw lid; sample-acid mixture was heated for 30 min at 125ºC for digestion. The samples were allowed to cool and make up to 10 ml with distilled water. The mixture was subjected to orbital shaker for 1 min for proper mixing. Finally, samples were filtered using Whatman No 1 filter paper. The supernatant was subjected to ICP-OES (ICPOES HD Prodigy –Lemans) for macro and micronutrient analysis. The ICP-OES operating conditions as

Vol. 14 (3) 239-255, July 2020, ISSN 0973-8916 (Print), 2230-7303 (Online)
DOI: 10.5530/ctbp.2020.3.25

followed: RF power 1.1kw; coolant flow 18 L/min; Auxiliary flow 0.0L/m; Nebulizer type Hildebrand Nebulizer; Nebulizer pressure 34 psi; Sample uptake rate 1.4 ml/min; Spray chamber cyclonic; Torch: Dual view; Pure gas Nitrogen; Pure gas flow- 0.7 L/min; Axial time-10 seconds; Radial time- 5 sec and Wash time – 40 seconds. All the samples analyzed in triplicates. The data was read by the inbuilt software of the instrument. The elemental parameters of studied macro and micronutrients of ICP-OES analysis are described in Table 2.

Statistical analysis: The ICP-OES data was subjected to XLSTAT 2019.3.1.60379 software for principal component analysis (PCA) followed by the "R" program for multivariate hierarchical cluster analysis. The data of mineral content of 24 Foxtail millet genotypes are expressed as mean± Standard deviation of at least three replicates. The PCA analysis was used to determinate correlation among seed residues from wild and released cultivars of Foxtail millet. The analyzed data were statistically subjected to analysis of variance technique using STATISTIX 8.1 Software and the significance was evaluated by least significance test (LSD) at 5% probability level (Table 3).

Table 1 : 20 Landraces and 4 released cultivars of Foxtail millet

S No	Name of Foxtail millet genotype	Variety type	Origin
1	S1G1	Landrace	Eipperu, Anantapur
2	S1G2	Landrace	Eipperu, Anantapur
3	S1G4	Landrace	Eipperu, Anantapur
4	S1G5	Landrace	Eipperu, Anantapur
5	S1C1	Landrace	Eipperu, Anantapur
6	S1C2	Landrace	Rakatla, Anantapur
7	S2G1	Landrace	Korrapadu, Kadapa
8	S2G2	Landrace	Korrapadu, Kadapa
9	S2C1	Landrace	Korrapadu, Kadapa
10	S2C2	Landrace	Korrapadu, Kadapa
11	S3G1	Landrace	Dudyala, Kadapa
12	S3G2	Landrace	Dudyala, Kadapa
13	S3G3	Landrace	Dudyala, Kadapa
14	S3G4	Landrace	Dudyala, Kadapa
15	S3G5	Landrace	Dudyala, Kadapa
16	RED	Landrace	Punganur, Chittoor
17	BLACK	Landrace	Basavanapalli, Anantapur
18	Srilakshmi	Released Cultivar	RARS, Nandyal, AP, India
19	Prasad	Released Cultivar	RARS, Nandyal, AP, India
20	Krishnadevaraya	Released Cultivar	RARS, Nandyal, AP, India
21	Narasimharaya	Released Cultivar	RARS, Nandyal, AP, India
22	S4G4	Landrace	Maddikera, Kurnool
23	S4C4-G	Landrace	Maddikera, Kurnool
24	S4C4	Landrace	Maddikera, Kurnool

Vol. 14 (3) 239-255, July 2020, ISSN 0973-8916 (Print), 2230-7303 (Online)
DOI: 10.5530/ctbp.2020.3.25

Table 2: Elemental parameters of ICPOES analysis

Element	View	Wave length
Potassium	Radial	766.490
Calcium	Radial	317.993
Iron	Axial	259.940
Zinc	Axial	213.856
Manganese	Axial	257.610
Copper	Axial	327.393

Results

In the present study, twenty-four foxtail millet genotypes were analyzed for their micro and macronutrient analysis using FTIR and ICP-OES analysis. FTIR analysis was recorded at 400^{cm-1} to 4000^{cm-1}region to identify different functional groups such as amino acids, carbohydrates, alkenes, proteins, Sulphur compounds, amines, and lipids present the flour. IR spectrum data was presented in Fig. 1.

The absorbance regions below 800 $^{cm-1}$, between 800 $^{cm-1}$-1500 $^{cm-1}$ (fingerprint region); 2800-3000 $^{cm-1}$ (C-H stretch region) and 3000-3600 $^{cm-1}$ (O-H stretch region) indicates the presence of starch. All of the genotypes exhibited similar kinds of peaks below 800$^{cm-1,}$ C-H stretch region, and O-H stretch region. However, the genotypes S4C4-G and S4C4 displayed very weak infrared peaks at 1015.11 $^{cm-1}$ and 1017.45^{cm-1} respectively, in contrast to other genotypes. The IR peaks at 1022 $^{cm-1}$ indicates the amorphous structure of flour and the peak at 1041^{cm-1} sensitive to the crystalline structure of flour. The genotype S1G4, S3G2, S3G5 shows absorption peaks at 1020.73^{cm-1}, 1021.88^{cm-1}, 1023.09^{cm-1} respectively, and could be highly amorphous. The genotype S2G1 displays a peak at 1041$^{cm-1,}$ indicates the crystalline structure of flour.

The absorption peaks at 1660^{cm-1}and 1550^{cm-1}detects the two forms of proteins amide I and amide II. The peak at 1660^{cm-1}detects C=O of the Amide I, the peak at 1550 $^{cm-1}$ detects NH bending of amide II in the crude protein. The strong absorption peak of the NH bond in the FTIR spectrum indicates that genotype protein richness. In the present study, the strong absorbance peak of the NH group was observed at 1543.69 $^{cm-1}$, 1543.09^{cm-1} in the genotypes S1G2, S4G4 respectively, which are considered to be as protein rich genotypes compared to other genotypes. The released cultivars Prasad and Narasimharaya have absorption peaks at 1542.45 $^{cm-1}$ and 1542 $^{cm-1}$ respectively. The genotype S4C4-G has a maximum absorbance at 1664.45 $^{cm-1}$which is a strong amide I bond and might contain very low protein content. The IR spectral peaks in the region 1600^{cm-1}- 1700^{cm-1} and 1550^{cm-1}-1570^{cm-1}indicates the presence of crude fat. In the present study, all the analyzed genotypes recorded peaks at 1645^{cm-1} and 1664.45^{cm-1}. However, the genotype S4C4-G and S4C4 did not record peaks in the region 1550 $^{cm-1}$ -1570 $^{cm-1}$. The moisture content of the flour can be determined by measuring OH stretching and H bending vibrations at IR spectral peaks from 1640 $^{cm-1}$ to 3300 $^{cm-1}$. All the genotypes in the present study recorded strong peaks in the prescribed spectral region. The IR spectral peaks at 1648.28^{cm-1}, 1658.84^{cm-1} indicates the occurrence of carbonyl group and amines 1 bond, IR peak at 2923.12 $^{cm-1}$ specifies presence of C-H compound (lipids). All the genotypes of present study displayed peak at 2923.12^{cm-1} and 1648.28^{cm-1} indicating the presence of lipids and aromatic compounds in their flour. The presence of thin bands at 2923.12^{cm-1} is associated with symmetric stretching vibrational modes of the C-H bonds in alkylic CH2 and CH3 groups, which are mainly due to the presence of lipids in flour.

The ICP-OES data of twenty-four genotypes seed flour indicates that there was a high genotypic variation for Fe, Zn, Mn, Cu, Ca, and K as showed in Table 3. Analysis of variance indicates that foxtail millet genotypes displayed non-significance variation ($P< 0.05$) for Fe content. Most of the studied genotypes recorded high Fe content, which is ranging from 3.69±0.38 to

Vol. 14 (3) 239-255, July 2020, ISSN 0973-8916 (Print), 2230-7303 (Online)
DOI: 10.5530/ctbp.2020.3.25

7.51±0.68 mg/100gm. Especially, the genotype S1G4 recorded high Fe content in its seed flour and followed by the released cultivars Krishnadevaraya, Prasad, and Narasimharaya. The low concentration of Fe noticed in landrace S2C2 (3.69±0.38 mg/100g). Almost all the studied genotypes recorded a greater amount of Zn ranging from 4.54± 0.34 to 5.71± 0.33 mg/100gm. The maximum content of Zn (5.71± 0.33) found in the landrace Black and followed by the genotypes S2C1, RED, S2C2, and S2G2. The genotype S1G1 contains a minute amount of Zn. However, genotypes recorded non- significant variation in Zn content (P< 0.05). The calcium content in foxtail millet germplasm under study varied from 13.13±0.57 mg/100g to 39.58±0.83 mg/100g. The genotypes displayed huge variation for Ca content (P< 0.05). Highest concentration of Ca was observed in the landrace S4C4 (39.58±0.83), followed by S1G2 (32.91±0.64), S3G1 (31.03±0.45) and S1C1 (28.12±0.83mg/100g). The low Ca content was observed in the landrace S4C4-

Table 3: Analysis of Variance (one way-Least significance test) showing the results of different macro and micro nutrient concentrations (mean value and SD) of 24 genotypes of Foxtail millet (At 5% probability level)

	Fe	Zn	Ca	K	Mn	CU
S1G1	4.92±0.34^{bcde}	4.54±0.34^{a}	23.72±0.29^{d}	258.03±0.69^{ji}	1.49±0.16^{abc}	0.63±0.16^{de}
S1G2	6.3±0.42^{abcd}	5.33±0.42^{a}	32.9173±0.64^{b}	251.057±0.49^{j}	1.38±0.16^{abc}	0.64±0.30^{de}
S1G4	7.51±0.68^{a}	4.65±0.38^{a}	21.09±0.72^{defgh}	267.63±0.41^{h}	1.49±0.20^{abc}	1.02±0.13^{abc}
S1G5	5.07±0.44^{bcde}	5.16±0.50^{a}	18.27±0.59^{hijk}	219.433±0.32^{n}	1.16±0.14^{bc}	1.09±0.17^{a}
S1C1	5.39±0.65^{abcde}	5.2±0.56^{a}	28.12±0.83^{c}	250.48±0.61^{l}	1.13±0.13^{c}	0.92±0.27^{abcd}
S1C2	5.63±0.60^{abcde}	4.69±0.48^{a}	20.83±0.43^{defgh}	349.54±0.81^{a}	1.59±0.20^{ab}	1.05±0.21ab
S2G1	5.28±0.76^{abcde}	5.4±0.37^{a}	21.53±0.38^{defgh}	238.75±0.54^{m}	1.28±0.12^{abc}	0.85±0.18^{abcde}
S2G2	4.81±0.73^{cde}	5.45±0.29^{a}	18.52±0.51^{ghij}	238.70±0.73^{m}	1.38±0.24^{abc}	0.73±0.07^{cde}
S2C1	5.83±0.86^{abcde}	5.67±0.35^{a}	15.11±0.75^{jkl}	257.41±0.42^{ijk}	1.31±0.10^{abc}	0.71±0.08^{de}
S2C2	3.69±0.38^{e}	5.59±0.40^{a}	19.29±0.50^{ghi}	255.16±0.83^{jkl}	1.19±0.10^{bc}	0.8±0.09^{abcde}
S3G1	5.06±0.54^{bcde}	4.64±0.24^{a}	31.03±0.45^{bc}	300.65±0.69^{f}	1.47±0.19^{abc}	0.67±0.07^{de}
S3G2	5.08±0.45^{bcde}	4.65±0.31^{a}	18.05±0.46^{hijk}	253.08±0.63^{kl}	1.49±0.15^{abc}	0.81±0.11^{abcde}
S3G3	4.48±0.56^{cde}	4.87±0.36^{a}	18.27±0.48^{hijk}	290.05±0.64^{g}	1.31±0.17^{abc}	0.6±0.10^{e}
S3G4	5.54±0.06^{abcde}	4.96±0.28^{a}	22.87±0.69^{def}	317.54±0.53^{cd}	1.64±0.21^{a}	0.77±0.09^{bcde}
S3G5	4.16±0.21^{de}	5.11±0.39^{a}	15.79±0.56^{ijkl}	313.51±0.32^{de}	1.2±0.14^{abc}	0.69±0.07^{de}
Red	4.76±0.52^{cde}	5.65±0.33^{a}	14.79±0.49^{kl}	271.4±0.57^{h}	1.12±0.10^{c}	0.83±0.11^{abcde}
Black	4.45±0.66^{cde}	5.71±0.33^{a}	23.70±0.28^{d}	261.08±0.60^{i}	1.33±0.15^{abc}	0.63±0.06^{de}
S4G4	5.58±0.93^{abcde}	5.56±0.25^{a}	15.06±0.55^{jkl}	316.98±0.53^{cd}	1.38±0.21^{abc}	0.79±0.10^{bcde}
S4C4-G	3.87±0.27^{e}	4.65±0.19^{a}	13.13±0.57^{l}	309±0.41^{e}	1.05±0.16^{c}	0.71±0.04^{de}
S4C4	3.8±0.42^{e}	4.66±0.26^{a}	39.58±0.83^{a}	317.58±0.35^{cd}	1.08±0.13^{c}	0.79±0.08^{bcde}
Srilakshmi	3.99±0.31^{e}	5.26±0.23^{a}	19.95±0.49^{fgh}	320.92±0.64^{c}	1.33±0.12^{abc}	0.74±0.05^{cde}
Prasad	6.63±0.76^{abc}	5.45±0.37^{a}	20.011±0.39^{efgh}	321.29±0.42^{c}	1.12±0.10^{c}	0.83±0.11^{abcde}
Krishnadevaraya	7.15±0.72^{ab}	5.04±0.35^{a}	22.06±0.70^{defg}	303.67±0.55^{f}	1.15±0.14^{bc}	0.69±0.07^{de}
Narasimharaya	6.48±0.69^{abc}	5.31±0.40^{a}	23.25±0.79^{de}	333.58±0.54^{b}	1.09±0.19^{c}	0.66±0.03^{de}
Mean	5.23	5.13	21.55	284.07	1.30	0.78
LSD<0.05	1.929	1.103	11.263	48.331	0.422	0.282
CV	26.78	16.34	10.04	1.05	20.91	22.91

Vol. 14 (3) 239-255, July 2020, ISSN 0973-8916 (Print), 2230-7303 (Online)
DOI: 10.5530/ctbp.2020.3.25

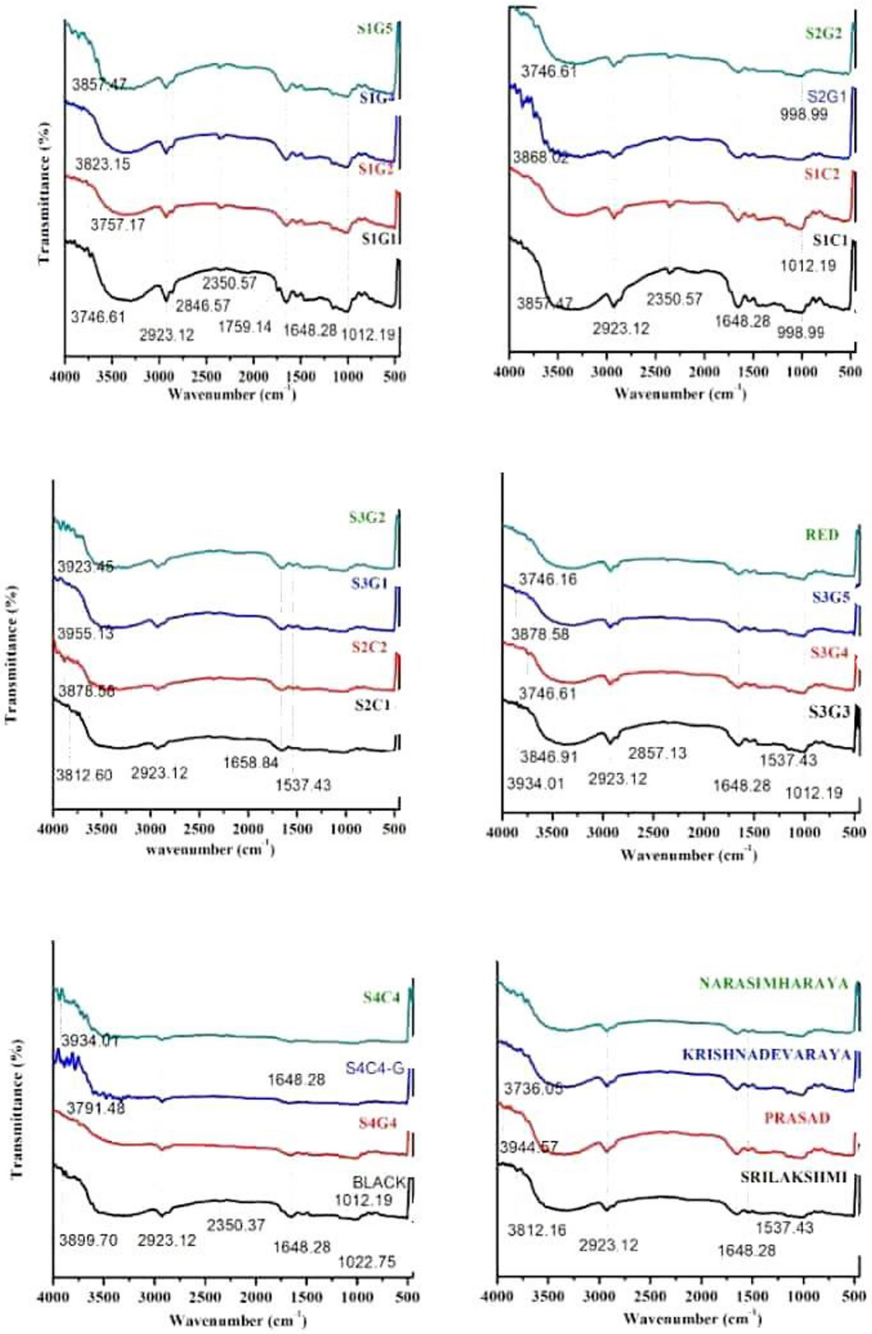

Fig 1: FTIR Spectra showing the functional groups of the organic and inorganic compounds of 20 Landraces and 4 released cultivars

Vol. 14 (3) 239-255, July 2020, ISSN 0973-8916 (Print), 2230-7303 (Online)
DOI: 10.5530/ctbp.2020.3.25

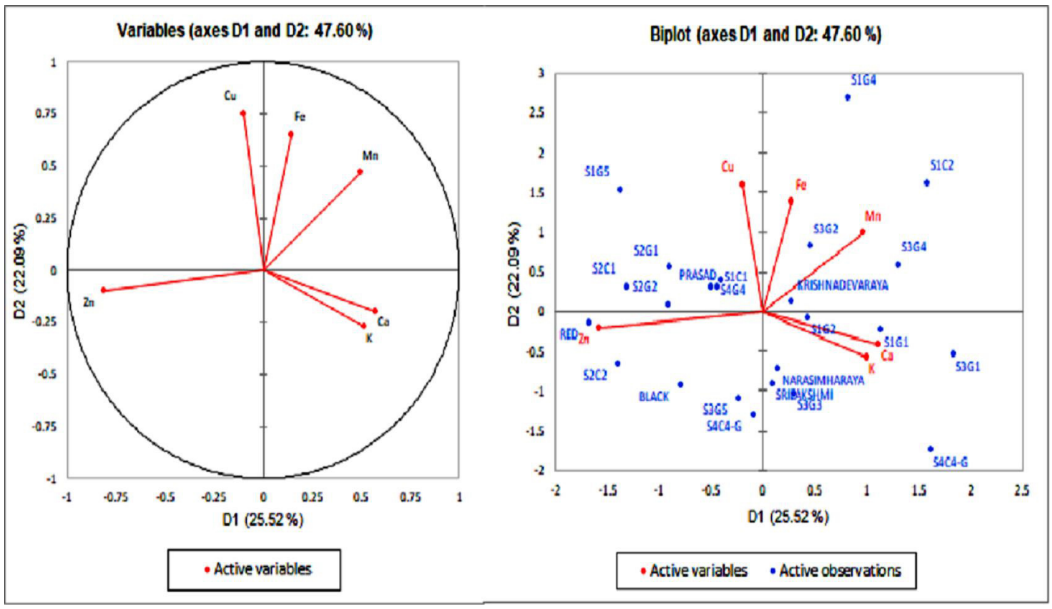

Fig 2: Scatter plot of variables and Biplot of 24 foxtail millet genotypes for first two Principal components contributing 47.60 per cent to total variability

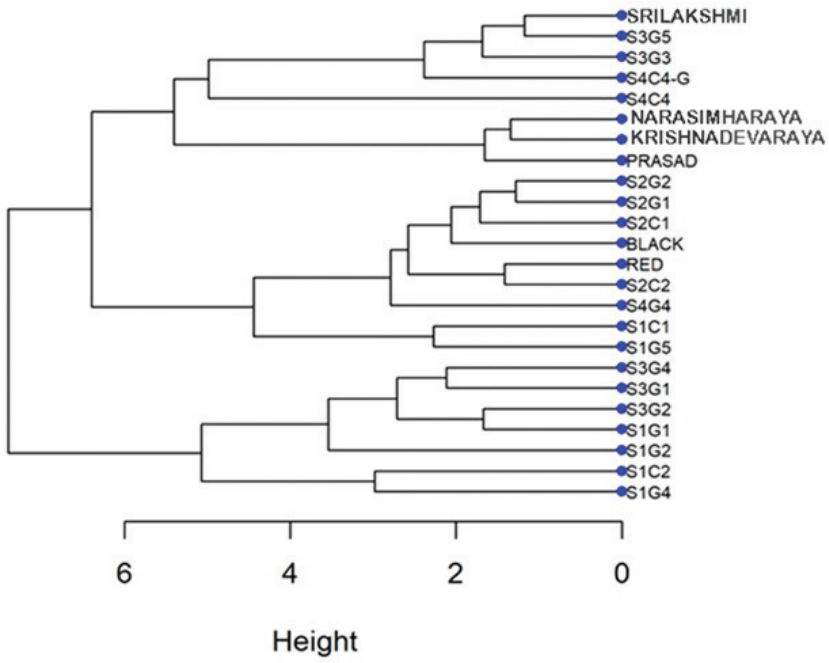

Fig 3: Hierarchical cluster dendrogram showing clusters in 24 Foxtail millet genotypes under various micro and macronutrient concentration

Vol. 14 (3) 239-255, July 2020, ISSN 0973-8916 (Print), 2230-7303 (Online)
DOI: 10.5530/ctbp.2020.3.25

G (13.13±0.57mg/100g). The grain Cu content of genotypes ranged from 0.60±0.10 mg/100g to 1.09±0.17 mg/100g. However, genotypes displayed non significance variation (P< 0.05) in Cu content. The greater amount of Cu observed in S1G5 (1.09±0.17 mg/100g), while the genotypes S1C2 and S1G4 had the medium range 1.05±0.21, 1.02±0.13 mg/100g respectively. The lowest concentration of Cu was recorded in the landrace S3G3 (0.60±0.10 mg/100g). Genotypes exhibited non-significance variation (P< 0.05) for manganese. The Mn concentration in genotypes ranged from 1.05±0.16 to 1.64±0.14 mg/100g. The genotype S3G4 has the highest Mn concentration, followed by S1C2, S3G2, S1G1, and S1G4. The genotype S4C4-G recorded the lowest concentration of Mn (1.05±0.16 mg/100g). Foxtail millet genotypes displayed a high significance of variation for potassium content (P< 0.05). The K content in foxtail millet germplasm was ranging from 219.43±0.32 mg/100g to 349.47±0.81 mg/100g. The landrace S1C2 accumulated the highest concentration (349.47±0.81), followed by Narasimharaya, Prasad, Srilakshmi, and S4C4. The genotype S1G5 accumulated a low concentration of K among all studied genotypes. Overall, the landraces S1C2, S3G4, S1G5 have the highest concentration of K, Mn, and Cu respectively.

Principal component analysis: The PCA analysis was applied to the determinate correlation of mean values of six micronutrients of the genotypes. The principal component analysis grouped the genotypes based on the variables of Iron, Zinc, Calcium, Potassium, Copper, and Manganese. PCA demonstrated that out of six; the first two principle components elucidated superiority of total variation. These two principal components have eigenvalue >1 and contributed 47.601% percent of total variability and were plotted to examine the relationships between different clusters with PC1 on X-axis and PC II on Y-axis (Fig. 2). Out of six PC's, PC I and PC II have eigenvalues of 1.557, and 1.299 respectively. PC III had the eigenvalue 0.964 and PC IV had the eigen value of 0.907 (Table 4). The PC I contributed maximum regards variability (25.953%) followed by PC II (21.648%), PC III (16.074%) and PC IV (15.112%). The first four components contributed for 78.78% the variability of all the data and the remaining two components contributed 21.22% of variability among the 24 genotypes for micronutrient and macronutrient concentration. In the present study, the PC I had the highest positive loading for Zinc (0.803) and higher negative loading for Manganese (-0.617), Calcium (-0.480). In PC II, Copper (0.745), Iron (0.569) has positive loadings and Potassium having a negative loading (-0.419). PC III attributed to Potassium (0.764), Iron (0.228), and Calcium (-0.559) with positive and negative loadings respectively. The PC IV consists of variables regards to Iron (0.622), Calcium (0.502) and Zinc (0.285) with positive loadings and Manganese (-0.414) negative loadings (Table 4).

The score values of each principal component for 24 foxtail millet genotypes were represented in Table 5. Based on the factor scores, the PC1 component explains that Zn concentrations are higher in RED followed by S2C2, S2C1, BLACK, and S2G2 and lower in S1C2, S1G4, S3G1, S3G4, S1G1, and S4C4. The PC II reveals that Cu, Fe, Mn and Zinc concentrations are higher in S1G4, S1G5, S1C2, S2G1, and S2C1 and lower in S4C4, S4C4-G, S3G1, and S3G3. The PC III loadings elucidated that concentrations of K, Fe, Zn and Cu are higher in Prasad, S4G4, S1C2, Narasimharaya, and S4C4-G, lower in S1G2, S4C4, S2G1 and S1C1. The PC IV loadings represent Fe, Ca, Zn and K concentrations are higher in Narasimharaya, Krishnadevaraya, S1G2, Prasad, S1C1 and S4C4-G, lower in S3G2, S4C4-G and S1G1.

In the present investigation, the principal component score plot of PC I and PC II differentiated the genotypes into four quadrants depending on the concentrations of six trace metals. Out of four quadrants based on the compositions of macro and micronutrients,

Vol. 14 (3) 239-255, July 2020, ISSN 0973-8916 (Print), 2230-7303 (Online)
DOI: 10.5530/ctbp.2020.3.25

genotypes were scattered into three quadrants in PC analysis. The genotypes on the top right quadrant represent Zinc concentration. The genotypes that were scattered in the top left quadrant were associated to Mn, Fe, Cu concentrations. The genotypes on the left bottom quadrant were corresponding to their Ca and K concentrations. However, the genotypes in the right bottom quadrant did not exhibit any associations in the measured traits.

Hierarchical cluster analysis: Further, to identify the genetic variability more accurately in the genotypes, the hierarchical cluster analysis was performed based on the concentrations of their macro and micronutrients by using R Program software package. The analysis in the form of dendrogram revealed that the investigated genotypes were separated with a euclidean distance ranging from 0 to 6; which indicates a high genetic variation between the genotypes. The dendrogram classified the genotypes into four main clusters as shown in Fig. 3. The first main cluster (I) consists of only two genotypes *i.e.*, S1G4, and S1C2. This cluster was characterized by genotypes with high Fe and K contents, moderate levels of Mn, Cu and Zn and lowest concentration of Calcium. Cluster II consists of genotypes S3G4, S3G1, S3G2, S1G1, and S1G2 with the moderate levels of all macro and micronutrients. However, the genotype S3G2 recorded lowest concentration of Ca, K and S3G4 has the highest Manganese content compared to other genotypes of Cluster II. Cluster III consists of eight genotypes namely, S1C1, S1G5, S4G4, S2C2, RED, BLACK, S2C1, S2G1, and S2G2. This cluster consists of genotypes with high levels of Fe, Zn, Cu, K, and Mn. The lowest calcium content genotypes were also identified in this group. The genotype S2C2 consists of a low level of Fe concentrations. The fourth cluster consists of eight genotypes namely PRASAD, KRISHNADEVARAYA, NARASIMHARAYA, S4C4, S4C4-G, S3G3, S3G5, and SRILAKSHMI. The three genotypes PRASAD, KRISHNA DEVARAYA, and NARASIMHARAYA were mainly separated from this cluster due to high levels of Fe, Zn, K, Mn and lowest contents of Ca and Cu. The genotype S4C4 was separated from this cluster due to highest concentration of Ca.

Discussion

Recently, millets are gaining importance due to their survivability under extreme environments, low glycemic index, gluten-free rich protein, and affluence in minerals, vitamins, and antioxidants (24). The seed mineral composition depends on the nature of the genotype, uptake, and acquisition, allocation capacity of minerals into seeds. Due to their cost effectiveness, the research community more focused on the enrichment of mineral nutrients in the millets through genetic improvement programs. Understanding the natural genetic variants for mineral nutrition and identification of genotypes with greater mineral content is an important step in this direction and landraces might serve as great primary resources. Until recently, the scientific community reluctant to use exotic germplasm due to the fear of loss of co-adapted gene complexes, linkage drag, and lengthened pre-breeding time (11). However, recent research community started focusing ion exotic germplasm for improvement of abiotic stress resistance, and improved nutritional capacity due to the advantage of improved plant phenotyping facilities, genomics resources and discovery, exploration of allelic diversity (11).

FTIR technique in combination with multivariate statistical analysis; has been successfully applied for chemical mapping of minerals in several agriculture products (17, 49). In a previous study, Fourier transform near infrared spectroscopy (FT-NIRS) was used to evaluating 259 foxtail millet genotypes of China, based on the analysis of Protein, Fat, Starch and Amino acids (51). Similarly, in the present study, FTIR analysis revealed the presence of organic and inorganic components in foxtail millet genotypes. The IR spectra as depicted in Fig.1, displayed the presence of biochemical constituents such as amino acids, carbohydrates, alkenes, proteins,

Vol. 14 (3) 239-255, July 2020, ISSN 0973-8916 (Print), 2230-7303 (Online)
DOI: 10.5530/ctbp.2020.3.25

Sulphur compounds, amines, and lipids in all of the genotypes. The absorption spectra 800-1500^{cm-1} is a highly overlapping region, which displays various peaks with complex spectra, and identification of specific peaks is very difficult (46). The location and glycosidic linkage bands also affect the presence of peaks in the fingerprint region. The infrared spectra of polysaccharides (amylose, amylopectin, cellulose, and starch) which are present in the fingerprint region are majorly evaluated, from the vibrational bands of monomeric unit glucose (8, 47, 47). The infrared bands 1022 $^{cm-1}$ and 1041 $^{cm-1}$ are attributed to amorphous structure and crystalline structure respectively, as reported previously in flours of raw foxtail millet and rice (48) (20). The genotypes S1G4, S3G2 and S3G5 displayed amorphous starch structure, which might contain more amylopectin, whereas genotype S2G1 displayed the characteristic features of crystalline starch. The IR peaks at 1022^{cm-1}and 1048^{cm-1}are associated to the C-O bond stretching of the C-O-C group in the anhydrous glucose ring (45). The IR region between1640-3300^{cm-1} indicates the moisture content; the presence of strong peaks in that region indicates the presence of moisture in flour (27). Moisture content can be detected by its OH stretching and H bending vibrations (10). However, it is very difficult to quantify moisture content based on IR spectral peaks as the other OH group- containing compounds such as alcohols, phenols, hydro -peroxides also interfere spectral bonding of H and OH groups (10). We did not observe any genotypic variation for moisture content in the present investigation. A strong absorption peak of the NH bond in the FTIR spectrum indicates the protein richness of the sample (3). We have observed a high genetic variation for the NH group among the studied genotypes. The presence of a strong absorbance peak of the NH group in S1G2, S4G4, Prasad and Narasimharaya signifies their protein richness in the flour. The presence of amide II spectral bond at 1550 $^{cm-1}$ in the landraces S1G2 and S4G4 mostly from the NH bending secondarily from the CN stretch effect indicates these landraces are rich in protein (3). The released cultivars Prasad and Narasimharaya have been considered as second-ranking genotypes with regards to protein content having an absorption peak at 1542.45 $^{cm-1}$ and 1542 $^{cm-1}$ respectively. The landrace S4C4-G, considered as low protein rich genotype having a very weak NH bond in its spectrum of flour. These results are in agreement with the wheat genotypes (3). FTIR spectroscopy has been widely used as a quality control method to detect fat and moisture in high-fat products (44). The absorption spectra in the range of 1600 $^{cm-1}$ to 1700 $^{cm-1}$ and 1550 $^{cm-1}$ to 1570 $^{cm-1}$ indicate the presence of fat. In the present investigation, we have not observed genotypic variation for fat content among the studied genotypes. The IR peak 1648.28^{cm-1}, 1658.84^{cm-1}and 2923.12 $^{cm-1}$indicates the presence of carbonyl group, amines 1 bond, and C-H compound (regards lipids) respectively. All the investigated genotypes exhibited similar kinds of peaks for carbonyl groups, amines 1 and lipids. These results are in agreement with the data obtained for finger millet flour and pearl millet flour (14).

Principle component analysis is one of the important statistical techniques, which can summarize the data from complex data sets (6). The PCA of six characteristics such as Fe, Zn, Ca, K, Mn, and Cu considered for the total variability. The eigenvalue of PCA, which is greater than 1, recognized as significant, and the PCA were greater than ±0.3 identified as meaningful (16). In the present investigation, PCA delivered a high variability among the studied foxtail millet genotypes in the range of 78.78%, which indicates a considerable level of genotypic variation among the genotypes for mineral content. PCA can analyze the genotypes through verification of studied variables such as Fe, Zn, Ca, K, Mn and Cu as explained by the first two principal components. The first principal component occupies most of the variation in the analysis as possible. The second principal component displays much longer variation and mostly incorporeal to the PC I. By analyzing PC I and PC II, one can explain the correlation between

Vol. 14 (3) 239-255, July 2020, ISSN 0973-8916 (Print), 2230-7303 (Online)
DOI: 10.5530/ctbp.2020.3.25

Table 4: Principal component analysis of six mineral elements in foxtail millet genotypes showing factor loadings, Eigen values and their percentage contribution to the total variation.

Factor loadings	F1	F2	F3	F4
Fe	-0.344	0.569	0.228	0.622
Zn	0.803	0.168	0.066	0.285
Ca	-0.480	-0.369	-0.559	0.502
K	-0.403	-0.419	0.764	0.101
Mn	-0.617	0.284	-0.105	-0.414
Cu	-0.146	0.745	0.004	-0.076
Eigen value	1.557	1.299	0.964	0.907
Variability (%)	25.95	21.64	16.07	15.11
Cumulative (%)	25.95	47.60	63.67	78.78

variables (macro and micronutrients), factor loadings, factor scores, interpretation of genotypes in the scattered plot, similarities and differences (CAMO SOFTWARE AS, 1998). In the present investigation, high loadings and high factor scores are obtained for some variables and low loadings and low factor scores are obtained for other variables (Table 4). The high loading present in particular variables involved a greater contribution to the variation among studied genotypes. The distance between the positions of any two genotypes on the score plot is directly proportional to the degree of similarity or difference between them. Therefore, the genotypes are scattered to very close proximity having similar variation, genotypes near the origin having distinctive variation and far from the central axis of score plot having an extreme variation. The extreme genotypes are useful for breeding programs due to differentiation in their biochemical concentrations compared to other genotypes. The genetic diversity of studied foxtail millet genotypes were categorized based on the mineral concentration as followed; the landraces RED and S2C2 for Zn, landraces S1G4 and S1G5 for Cu, Fe, and Mn, released cultivar Prasad and landrace S4G4 for K, released cultivars Narasimharaya, Krishnadevaraya, and S1G2 for high calcium.

Cluster analysis is a diagrammatic representation and reliable visual method to analyze the complex union of multiple traits and differentiation in the genotypes at various mineral nutrition concentrations. ICP-OES coupled with multivariate statistical analysis was used in several crop species for seed mineral content. Shergo et al., (2013) conducted a genetic diversity study for characterization of mineral, total starch, total sugar and protein contents using multivariate statistical analysis for the selection of parents for hybridization (37). Multivariate analysis was employed to study the genetic divergence among pearl millet germplasm based on their agro morphological traits and grain nutritional values (5). The genetic diversity studies were also carried out in indigenous germplasm lines of finger millet for their mineral nutrients using multivariate analysis (4). Cluster analysis measures the data based on the genetic distance among the landraces and released cultivars (26). Previously, a similar study was conducted for micro and

Table 5: The scores of the four rotated principal components.

Factor scores	F1	F2	F3	F4
S1G1	-1.249	-0.668	-1.081	-0.954
S1G2	-0.486	-0.244	-1.574	1.601
S1G4	-2.039	2.613	-0.004	0.345
S1G5	1.012	2.164	-1.057	-0.395
S1C1	0.323	0.563	-1.200	0.970
S1C2	-2.521	1.175	1.350	-0.880
S2G1	0.846	0.922	-0.929	0.109
S2G2	1.045	0.422	-0.817	-0.611
S2C1	1.419	0.818	0.235	0.178
S2C2	1.908	-0.203	-0.624	-0.626
S3G1	-1.951	-1.252	-0.761	-0.001
S3G2	-0.869	0.717	-0.599	-1.388
S3G3	0.047	-1.217	0.211	-0.861
S3G4	-1.778	0.152	0.437	-0.606
S3G5	0.708	-1.100	1.004	-0.801
RED	2.028	0.461	0.453	-0.085
BLACK	1.297	-0.710	-0.811	0.078
S4G4	0.471	0.530	1.438	-0.128
S4C4-G	0.620	-1.364	1.122	-1.227
S4C4	-1.215	-2.471	-1.212	0.952
Srilakshmi	0.244	-1.008	0.683	-0.781
Prasad	0.391	0.502	1.458	1.558
Krikrishnadevaraya	-0.374	0.030	0.897	1.697
Narasimharaya	0.123	-0.831	1.383	1.858

Vol. 14 (3) 239-255, July 2020, ISSN 0973-8916 (Print), 2230-7303 (Online)
DOI: 10.5530/ctbp.2020.3.25

macronutrient analysis using a multivariate statistical analysis of 60 pearl millet genotypes (22). In the present investigation through PCA and dendrogram of clusters, it was identified that genotypes included in this study displayed high genetic variability for seed mineral content and might serve as valuable sources for the foxtail millet improvement programs. As the studied genotypes dispersed into different clusters, they might belong to highly heterotrophic groups for breeding programs. Therefore, the present study genetic diversity analysis of foxtail millet genotypes would be crucial for foxtail millet breeders to identify genotypes to enhance their nutritional importance.

Conclusion

The present study represents a comprehensive comparison of the foxtail millet landraces and released cultivars for their micronutrient content through ICP-OES and FTIR coupled with multivariate statistical analysis. The data generated in this study would be not only helpful for the identification of elite genotypes regarding seed mineral content, but also to tap the alleles responsible for high mineral content in foxtail millet. Our findings highlighted the importance of landraces that are being underutilized earlier in the breeding programs.

Anknowledgement

Authors in YVU, acknowledge the financial support (No. CRG/2018/003280 dated 30th May, 2019) from Department of Science and Technology, Science and Engineering Research Board (DST-SERB), New Delhi, India. The authors thankful to Prof.Arjula R. Reddy, Emeritus Professor, Department of Plant Sciences, School of Life Sciences, University of Hyderabad, Hyderabad for his inputs in the form of critical comments for the improvement of manuscript. GK acknowledge the financial support (IF-140991 dated 31st December, 2014) from DST-INSPIRE for providing INSPIRE Fellowship for her to complete the work. Authors in YVU, acknowledge the Central Lab and AGRI-Science park Lab for research facilities in the Yogi Vemana University, Kadapa.

References

1. Abdalla, A.A., El Tinay, A.H., Mohamed, B.E. and Abdalla A.H. (1998). Proximate composition, starch, phytate and mineral contents of 10 pearl millet genotypes. *Food Chem.*63 243–246.
2. AbdelRahman, S.M., Babiker, E.E. and El Tinay, A.H. (2005). Effect of fermentation on antinutritional factors and HCl extractability of minerals of pearl millet cultivars. *J. Food Tech.*3 (4): 516–522.
3. Amir, R.M., Faqir, M.A., Anjum, F.M., Khan, M.I., Khan, M.R., Pasha, I. and Nadeem, M. (2011). Application of Fourier transform infrared (FTIR) Spectroscopy for the identification of Wheat Varieties. Food Sci Technol 50(5): 1018-1023
4. Badigannavar, A. and Ganapathi, T.R. (2018) Genetic variability for mineral nutrients in indigenous germplasm lines of finger millet (*Eleusine coracana* Gaertn.), J. Cereal Sci. (2018), 8:1-6.
5. Bashir, E.M.A., Ali, A.M., Ali, A.M., Melchinger A.E., Parzies, H.K and Haussmann, B.I.G. (2014). Characterization of Sudanese pearl millet germplasm for agro-morphological traits and grain nutritional values. Plant Genet. Resour. 12(1); 35–47.
6. Basilevsky, A. (1994). Statistical Factor Analysis and Related Methods, Theory and Applications. Jhon Willey & Sons, New York, NY. DOI: 10.1002/9780470316894.
7. Brunda, S.M., Kamatar, M.Y., Naveen Kumar, K.L., Ramaling Hundekar and Umesh Kumar (2017). Genetic Variability in the Foxtail Millet (*Setaria italica*) Germplasm as Determined by Nutritional Traits. Int. J. Pure App. Biosci. 5(1):453-458.
8. Cael, J. J., Koenig, J. L. and Blackwell, J (1973). Infrared and Raman spectroscopy of carbohydrates. Part III: Raman spectra of the polymorphic forms of amylose. *Carbohydr. Res.*, *29*, 123- 134.

Vol. 14 (3) 239-255, July 2020, ISSN 0973-8916 (Print), 2230-7303 (Online)
DOI: 10.5530/ctbp.2020.3.25

9. Deshpande, J.D., Joshi, M.M. and Giri, P.A. (2013). Zinc: the trace element of major importance in human nutrition and health. Int. J. Med. Sci. Publ. Health 2, 1–6.

10. Dong, J., van de Voort, F.R., Ismail A.A., Akochi-Koble, E. and Pinchuk, D. (2000). Rapid determination of the carboxylic acid contribution to the total acid number of lubricants by Fourier transform infrared spectroscopy. Lubr Eng 56(6):12–17.

11. Dwivedi, S.L., Ceccarelli, S., Blair, M.W., Upadhyaya, H.D., Are. A.K. and Ortiz, R. (2016). Landrace Germplasm for Improving Yield and Abiotic Stress Adaptation. Trends Plant Sci. 2016: 21(1):31-42.

12. Gai, J. (2003). Millet breeding. In: Gai J, ed. Crop breeding science Beijing: China Agriculture press, 200-201(in Chinese).

13. Govindaraj, M., Vetriventhan, M., and Srinivasan, M. (2015). Importance of genetic diversity assessment in crop plants and its recent advances: an overview of its analytical perspectives. *Genet. Res. Int.* 2015, 431487–431487.

14. Gull, A., Prasad, K. and Kumar, P. (2015). Evaluation of functional, antinutritional, pasting and microstructural properties of millet flours. J. Food Meas. Charact. 10(1):1-8.

15. Gupta V. P. (1980). "Genetics of quality improvement," in *Trends in Genetical research on Pennisetums* eds Gupta V. P., Minnocha J. L., editors. (Ludhiana: Punjab Agricultural University) 291–294.

16. Hair, J.F., Andrson, J.R., Tatham R.E. and Black, W.C. (1998). Multivariate data analysis, 5th Edn, Prentice-Hall international, Inc, London.

17. Himmelsbach, D.S., Khahili, S. and Akin, D.E. (1998). Micro spectroscopic imaging of flax (Linum usitatissimum L.). Cell Mol Biol 44:99–108.

18. Hirshi, K.D. (2009). Nutrient Bio fortification of food crops. Annu. Rev. Nutr. 29: 401-421.

19. Jaiswal, V., Bandyopadhyay. T., Gahlaut, V., Gupta, S., Dhaka, A., Ramachiary, N. and Prasad. M. (2019). Genome – wide association study (GWAS) delineates genomic loci for ten nutritional elements in foxtail millet (*Setaria italica* L.). J. Cereal Sci. 85:48-55.

20. Ji, Y., Zhu, K., Zhou, H. and Qian, H. (2010). Study of the retro gradation behaviour of rice cake using rapid visco analyser, Fourier transform infrared spectroscopy and X ray analysis. Int. J. Food Sci. Technol. 45(5): 871-876.

21. Kamatar, M.Y., Brunda, S.M., Sanjeevsingh, R., Sowmya, H.H., Giridhar, G. and Hundekar Ramaling (2015). Nutritional composition of seventy-five elite germplasm of foxtail millet (*Setaria italica*). Int. J. Eng. Res. Technol. 4(4): 1-6.

22. Kiprotich, F., Kimurto, P., Ombui, P., Towett, B., Jeptanui, L., Henry, O. and Lagat, N. (2015). Multivariate analysis of nutritional diversity of selected macro and micronutrients in Pearl millet (*Pennisetum glaucum*) varieties. African J. Food Sci. (9)3: 103-112.

23. Kumar, A. and Chauhan, B.M. (1993). Effect of phytic acid on protein digestibility (in vitro) and HCl-extractability of minerals in pearl millet sprouts. *Cereal Chem.*70 504–506.

24. Kumar, A., Tomer, V., Kaur, A., Kumar, V. and Gupta, K. (2018). Millets: a solution to agrarian and nutritional challenges. Agric. Food Secur. 7:31.

25. Li, G.Y., Fan, Z.Y., Lu, P., Liu, F., Zhang, P., Li, W.X. and Zhu, Z.X. (2009) Identification and evaluation of tocopherol content in primary core-collection of foxtail millet. J. Plant Genet. Resour, 10: 378-384 (in Chinese).

Vol. 14 (3) 239-255, July 2020, ISSN 0973-8916 (Print), 2230-7303 (Online)
DOI: 10.5530/ctbp.2020.3.25

26. Liu, Y., Zhang, X., Tran, H., Shan, L., Kim, J., Childs, K., Ervin, E.H., Frazier, T. and Zhao, B. (2015). Assessment of drought tolerance of 49 Switch grass (*Panicum virgatum*) genotypes using physiological and morphological parameters. Biotechnol Biofuels 8:152.

27. Manley M., Zyl L.V. and Osborne B.G. (2002). Using Fourier transform near infrared spectroscopy in determining kernel hardness, protein, and moisture content of whole-wheat flour. J Near Infrared Spectrosc 10:71–76.

28. Mikulajova, A., et al. (2017) "Genotypic variation in nutritive and bioactive composition of Foxtail millet." Cereal Research Communications, vol. 45, no. 3, 2017, p. 442+.

29. Milner, JA (1999) Functional foods and health promotion. Journal of Nutrition129, Suppl. 7, 1395S–1397S.

30. Oberleas, D. P. (1973). "Phytates," in *Toxicants Occurring Naturally in Foods* ed. Strong F. M., editor. (Washington DC: National Academy of Sciences ;) 363–371.

31. Phillip, J. and Maloo, S. R. (1996). An evaluation of *Setaria italica* for seed iron content. 82: ISMN 37.

32. Prasanna, B.M. (2012). Diversity in global maize germplasm: characterization and utilization. *J. Biosci.* 37: 843-855.

33. Rai, K N., Kumar, K A., Andrews, D J., Rao, A S., Raj, A G B. and Witcombe, J R (1990) *Registration of 'ICTP 8203' pearl millet.* Crop Science, 30 (4). p. 959.

34. Rakshit, S., Gomashe, S., Ganapathy, K. N., Elangovan, M., Ratnavathi, C., Seetharama, N. and Patil, J. Morphological and molecular diversity reveal wide variability among sorghum Maldandi landraces from India. *J. Plant Biochem. Biotechnol.* 21: 145-156.

35. Saleh, S. M., Zhang, Q., Chen, J., & Shen, Q. (2013). Millet grains, nutritional quality, processing and potential health benefits. Compr. Rev. Food Sci. Technol, 12(3), 281-295.

36. Shao, L.H., Wang, L., Bai, W.W., and Liu, Y.J. (2014). Evaluation and analysis of folic acid content in millet from different ecological regions in Shanxi province. J Integr Agric 47:1265-1272.

37. Shegro, A., Labuschagne, M.T., Shargie, N.G.and Biljon, A.V. (2013). Multivariate analysis of Nutritional Diversity in Sorghum Landrace Accessions from Western Ethiopia. J. Biol. Sci. 13(2): 67-74.

38. Shilpa Huchchannanavar, L.N. Yogesh and S.M. Prashant. 2019. Nutritional and Physicochemical Characteristics of Foxtail Millet Genotypes. Int. J. Curr. Microbiol. App. Sci. 8(01): 1773-1778.

39. Suma, P.F. and Urooj, A. (2012). Antioxidant activity of extracts from Foxtail millet (*Setaria italica*) J Food Sci Technol 49(4): 500-504

40. Thacher, T.D., Fischer, P.R., Strand, M.A. and Pettifor, J.M. (2006). Nutritional rickets around the world: causes and future directions. Ann. Trop. Paediat. 26: 1–16.

41. Thippeswamy, V., Sajjanar, G.M., Nandini, C., Bhat, S and Doddaraju, P. (2017). Characterization of Genotypes for Nutritional traits in Foxtail Millet [*Setaria italica* (L.) Beauv.]. Int. J Microbiol. Appl. Sci. 6 (12): 97-101.

42. Tiwari, C., Wallwork, H., Arun, B., Mishra, V.K., Velu, G. and Stangoulis, J. (2016). Molecular mapping of quantitative trait loci for zinc, iron and protein content in the grains of hexaploid wheat. Euphytica 207: 563–570.

Vol. 14 (3) 239-255, July 2020, ISSN 0973-8916 (Print), 2230-7303 (Online)
DOI: 10.5530/ctbp.2020.3.25

43. Upadhyaya, H.D., Pundir, R.P.S., Gowda, C.L.L., Reddy, V.G., Singh, S., (2008). Establish-ing a core collection of foxtail millet to enhance the utilization of germplasm of an underutilized crop. Plant Genet. Resour. 7(2); 177–184.

44. Van de Voort, F.R., Sedman, J., Emo, G. and Ismail, A.A. (1992). Assessment of Fourier transform infrared analysis of milk. J Assoc off Anal Chem 75(5):780–785.

45. Van Soest, J.J.G. (1996). Starch plastics: Structure-Property Relationships, PhD thesis, University of Utrecht, Koninklijke Bibliotheca Den Haag. ISBN 90-393-1072-6.

46. Vasko, P. D., Blackwell, J. and Koenig, J. L. (1971). Infrared and Raman spectroscopy of carbohydrates. Part I: Identification of O-Hand C-H related vibrational modes for D-glucose, maltose, cellobiose, and dextran by deuterium-substitution methods. Carbohydr. Res. *19*, 297-310.

47. Vasko, P. D., Blackwell, J. and Koenig, J. L. (1972). Infrared and Raman spectroscopy of carbohydrates. Part II: Normal and coordinate analysis of R-D-glucose. Carbohydr. Res. *23*, 407-416.

48. Wang, R., Chen, C. and Guo, S. (2017). Effects of drying methods on starch crystallinity of gelatinized foxtail millet (á-millet) and its eating quality. J. Food Eng. 207: 81-89

49. Wetzel, D.L. and Reffner J.A. (1993). Using spatially resolved Fourier transform infrared micro beam spectroscopy to examine microstructure of wheat kernels. Cereal Foods World 38:9–20.

50. White, P.J. and Broadley, M.R. (2008). Biofortification of crops with seven mineral elements often lacking in human diets – iron, zinc, copper, calcium, magnesium, selenium and iodine. New Phytologist (2009) 182:49-84

51. Yang, X.S., Wang, L.L., Zhou, X.R., Shuang, S.M., Zhu, Z.H., Li, N., Li, Y., Liu, F., Liu, S.C., Lu, S.C., Lu, P., Ren G.X. and Dong, C. (2013). Determination of Protein, Fat, Starch and Amino acids in Foxtail millet (*Setaria italica* (L.) Beauv.) by Fourier Transform Near Infrared Reflectance Spectroscopy. Food Sci. Biotechnol. 22(6):1495-1500.

52. Yin, S. Y., Kuo, S. M., Chen, Y. R., Tsai, Y. C., Wu, Y. P., & Lin, Y. R. (2019). Genetic Variation of Physicochemical Properties and Digestibility of Foxtail Millet (*Setaria italica*) Landraces of Taiwan. Molecules, *24*(23): 4323.

Current Trends in Biotechnology and Pharmacy
Vol. 14 (3) 256-262, July 2020, ISSN 0973-8916 (Print), 2230-7303 (Online)
DOI: 10.5530/ctbp.2020.3.26

Development of in-house indirect enzyme linked immunosorbent assay (iELISA) for detection of *Salmonella enteritidis* dpecific antibodies in poultry

P. Navaneetha[1,2], M. Anil[1,2], A. Vijay Kumar [3], M. Manasa[1,2], P. Janardhan Reddy[1,2], P. Sudhakar [4], P. Rathnagiri[1,2,5*]

[1]Department of Medical Microbiology, Genomix Molecular Diagnostics Pvt. Ltd., Hyderabad – 500072. Telangana, India.
[2]Department of Veterinary Microbiology, Genomix CARL Pvt. Ltd., Pulivendula – 516390, A.P., India.
[3]Department of veterinary public health and epidemiology, P.V.N.R Telangana, Veterinary university, Hyderabad.
[4]Department of Biotechnology, Acharya Nagarjuna University, Guntur-522510, A.P.,India.
[5]Genomix Biotech Inc, Atlanta, GA 30345, USA.
*Corresponding author : giri@genomixbiotech.com

Abstract

Salmonella enteritidis is a most important pathogenic bacterium of avian and mammals. *Salmonella* Enteritidis is the main cause of Salmonellosis in poultry flocks. *S. enteritidis* majorly infects the chicks, eggs and vertically transmitted to their off springs. The majority of the food infections to the humans are caused by *salmonella* by eating chicken meat and eggs. Monitoring of poultry farms with the bacteriological methods were time consuming and labour intensive process. The present study was development an in-house indirect enzyme linked immunesorbent assay (iELISA) for the detection of antibodies against *Salmonella enteritidis* in chicken serum samples. For detection of antibodies, *Salmonella enteritidis* LPS was used as antigen and rabbit anti chicken IgG HRP was used as the secondary antibody to detect antibodies against *Salmonella enteritidis*. The developed in-house ELISA was compared with the Rapid plate agglutination test. The purified LPS antigen 200ng/well, test sample serum at a dilution of 1:100 and rabbit anti chicken IgG HRP 1:10000 were used as optimal concentration of the assay and OD was measured at 450nm. A total of 1020 chicken serum samples were collected and performed the assay along with known Positive and negative controls. Out of these samples 592 and 566 samples were seropositive with iELISA and RPA respectively. Out of 1020 samples 58% samples shown positive immune response with iELISA and 55.6% samples were shown positive immune response to Rapid plate agglutination assay. The major prevalence of SE antibodies against SE antigen were shown in 20-25 weeks birds was 65.5%.The findings suggested that an in-house indirect ELISA based on *S.enteritidis* LPS can be a useful as a rapid and sensitive assay for the detection of antibodies to *S.enteritidis* and can be best assay for regular monitoring of *Salmonella Enteritidis* infection in flocks.

Key words: Antibody, antigen, LPS, RPA, HRP conjugate, ELISA

Abbreviations: SE-*Salmonella enteritidis*, LPS-Lipopolysaccharide, RPA-Rapid Plate agglutination ELISA – Enzyme linked immunosorbent assay; SDS-PAGE – Sodium dodecylesulphate – Polyacrylamide Gel Electrophoresis; HRP – Horse radish peroxidase; IgG – Immunoglobulin G; PBS – Phosphate buffered saline; TMB – 3,32 ,5,52 -Tetramethyl benzidine; nm – nanometer;

Introduction

Salmonella enteritidis is one of the important pathogen of many mammals and birds, it cause Salmonellosis.It is one of the dominant *salmonella*

Vol. 14 (3) 256-262, July 2020, ISSN 0973-8916 (Print), 2230-7303 (Online)
DOI: 10.5530/ctbp.2020.3.26

sero type and it is consided for its economical impact all over the world including India, it is also the major food borne pathogen associated with poultry meat and eggs. In recent years the majority of food borne pathogen outbreaks caused by the contamination of chicken meat and with contaminated eggs has increased.*Salmonella enteritidis* is a gram negative, flagellated, rod shaped, facultative aerobic bacterium.The contaminated environment with *Salmonella* serovars are main source of infection, by the reason of this *Salmonella* can remain in the environment for a long period of time, hereafterthe *Salmonella* have being transmitted to suitable hosts, where it can shed in their faeces for long time.(1) Poultry farms may carry few *Salmonella* serovars without showing any clinical symptoms of disease and without causing any harmful effects to chickens (2). To combat *salmonella* infections in flocks poultry sectorfacing most difficult problems and not only worried for poultry industry as well as concerned for public health hazard(3) because it causes problems in food safety.To overcome these problems in poultry there is a need for suitable assays to use as a screening test to detect *S.enteritidis* infection in poultry flocks based on clinical symptoms. Routine bacteriological procedures for the isolation and identification of *S.enteritidis* were laborious and time consuming method.Molecular methods such as PCR, ribotyping or restriction endonuclease analysis which have the epidemiological importance but these methods were more expensive to test each bird The diagnosis of infection traditionally has been done by serologically. Several serological assays have been used to detect SE antibodies they are the most reliable for flock screening rather than for testing individual birds.The most widely used serological assays are the serum agglutination test, ELISA, tube and micro agglutination tests.In the Serum plate agglutination test serum or whole blood samples from individual birds were tested. But the assay method is crude, inaccurate and insensitive (4).coming to the immunological assays Enzyme-linked immunosorbent assay (ELISA) methods were emerged as best tools for diagnosis the disease and monitoring the immune status of the poultry flocks and ELISA assays were developed for the detection of *salmonella* antibodies (5). Most ELISAs currently in use for the detection of *S.enteritidis* infected flocks identify antibodies to either crude surface-extracted antigens or flagellar antigens. Lipopolysaccharide (LPS) is the major antigenic and immunogenic structure on the surface of *S.enteritidis*, it consist three components: lipid A, inner core and O-side chain oligosaccharides. Lipid A is the endotoxic principle of LPS and activates macrophages. Several factors released from the macrophages exert biological effects associated with fever and shock (6).

The main objective of this study was to develop an indirect enzyme-linked immunosorbent assay (iELISA) for the detection *of S.enteritidis*-specific antibodies in chicken sera samples. *S.enteritidis* LPS has been used as an antigen for the detection of *S.enteritidis* in chicken flocks.

Materials and Methods

Bacterial strain and growth conditions : *Salmonella* enterica subsp enteric serovar Enteritidis (ATCC 13076TM) was obtained from American Type Culture Collection (ATCC). It was maintained as pure culture as recommended by ATCC and was revived periodically by successive transfers on same medium. The culture was grown on nutrient agar for 24 hrs at 37^{o}C.The culture was harvested in 5% phenol and it was centrifuged at 5000 rpm for 10 min. The weight of the harvested bacterial cell pellet was measured and further used for the extraction LPS. The entire procedure was carried out in a Class II bio-safety cabinet.

Extraction of LPS : Extraction of LPS was done by hot phenol water method without any modifications (7). 12 g (wet weight) of cells was suspended in 105 ml distilled water pre-warmed to 65-70°C. Equal volume of 90% aqueous phenol prewarmed to 65-70°C was added to the cell suspension. The mixture was stirred vigorously

Vol. 14 (3) 256-262, July 2020, ISSN 0973-8916 (Print), 2230-7303 (Online)
DOI: 10.5530/ctbp.2020.3.26

at 65-70°C for 15 min. The mixture was chilled on ice for 15 min. Mixture was centrifuged at 8000 rpm (Remi cooling centrifuge C-24 BL) at 4°C for 15 min for separation of aqueous and phenol phase. The LPS was collected from the aqueous phage in a fresh tube. Then carefully collected aqueous phase was dialyzed against distilled water in dialysis membrane of MWCO (Molecular weight cut off) 3.5 kd till absorbance at 260 nm of water outside dialysis membrane became zero. The aqueous phase was centrifuged at 8000 rpm for 15 min to remove insoluble impurities. The LPS precipitation was done by Ethanol precipitation in which sodium acetate was added to LPS at final concentration of 0.15 M. Tube was placed on ice and four volumes of chilled 96% (v/v) ethanol was added and kept at -20°C for 24 hours (8). Precipitates of LPS were collected by centrifugation at 5500 g. 10 mg LPS pellet was reconstituted in 2 ml phosphate buffered saline and stored at 4°C.

SDS-PAGE and silver staining : 10 microliter of LPS preparations were mixed with 10 ìlLaemmli sample buffer (62.5 mMTris-HCl with pH-6.8, 25% glycerol, 2% SDS, 0.01% bromophenol blue and 5% â mercaptoethanol) and heated at 90°C for 5 min. Samples were loaded in gel consisting of 12% resolving gel and 5% stacking gel. The SS-PAGE gel Electrophoresis was done by using (BIORAD's Mini Protean Tetra Cell apparatus). LPS was visualized by standard silver staining procedure (9).

Development of an immunoassay to measure immune response against *S.enteritidis*

Sample collection: This study was conducted with approval from the Institutional animal ethics committee of the Genomix Private Ltd. A total 1020 serum samples were randomly collected from 9 (MSB Farms, Gold chick hatcheries, Srinivasa hatcheries, GSV poultry Bindhu poultry farm VR poultry, Sneha farms, Gagana farms and Abhudaya hatcheries)different chicken flocks in and around Hyderabad, Telangana State of India in between June and July 2019 with no prior history of vaccination. . Three milliliter of blood was drawn from each bird randomly and all collected samples were subjected to centrifugation at 3000 rpm for 5 minutes. The clear sera were harvested using the pasteur pipette decantation method. The serum samples were then stored at 4°C and further used for the serological investigation in the present study. The reference sera used in this study for optimization of assay and field sample analysis were provided by Department of Veterinary Public Health and Epidemiology, P.V.N.R Telangana Veterinary University, Hyderabad.

Assay development and test procedure : The reagents used for ELISA were commercially procured to develop iELISA. The rabbit anti chicken HRP conjugate (Sigma Aldrich, USA), tetramethy lbenzidine/H_2O_2 (Abcam, USA) and 96 well ELISA plates (Nunc polysorpthermo fishers) were used. Positive serum sample from PCR confirmed cases of *S.enteritidis* were obtained by Department of Veterinary Public Health and Epidemiology, P.V.N.R Telangana Veterinary University, Hyderabad. The optimal working condition for dilutions of the coating Antigen LPS-SE, blocking solution, Serum samples, HRP conjugate were found out by checker board titration for their usage in developing ELISA. Briefly, the antigen concentrations optimized by assaying 0.5ìg/ml to 16 ìg/ml concentrations and antibody dilutions tested at 1:25, 1:100, 1:200, 1:400, 1:800, 1:1600 and secondary antibody that is rabbit anti chicken IgG HRP antibody tested at 1:5000, 1:10,000, 1:20,000.The known positive (PCR confirmed) and negative (SPF Sera) controls used for standardizing the assay and in order to get the high differential ratio between positive and negative sera. The validation of the In-house iELISA was carried out by 156 reference serum samples provided by P.V.N.R Telangana Veterinary University. After validation, in-house iELISA were tested with field sera samples along with other laboratory serological assay(SE RPA test).Preparation of ELISA micro titer plates are done as follows the nunc poly sorp micro titter

Vol. 14 (3) 256-262, July 2020, ISSN 0973-8916 (Print), 2230-7303 (Online)
DOI: 10.5530/ctbp.2020.3.26

plates are coated with the LPS-SE antigen at concentration of 2ug/ml with coating buffer (0.2M sodium carbonate and bicarbonate) pH 9.2 and they were incubated at 4°C overnight. The plates were then washed thrice with PBS-Tween 20. The remaining protein sites were blocked by adding 300ìl of 3% (Amul) skimmed milk powder prepared with 1X phosphate buffered saline, respectively to all wells of the plate and incubated at 37°C for 1 hr. The plates were then washed thrice with wash buffer. The test sera and control sera was diluted to 1:100 and they were added to the wells. The plates were then incubated at 37°C for 1 hr. The plates were washed thrice and then, the100 microliter of rabbit anti chicken immunoglobulin IgG in HRP (1:10000 diluted in 1XPBS) was added to each well and incubated for 1hr at 37°C. The plates were washed thrice and they were treated with 100 ìl of TMB/H_2O_2 for 15 min. Finally, the reaction was stopped by adding 100 ìl of stop solution (0.5M H_2SO_4). The OD readings were taken with an Elisa micro titter plate reader instrument (Robonik, India) at 450 nm. The values obtained by the assay were used to calculate by the percent positivity (PP) value.

Percent positivity value (PPV=True Positive / (True Positive+ False Negative) X 100).

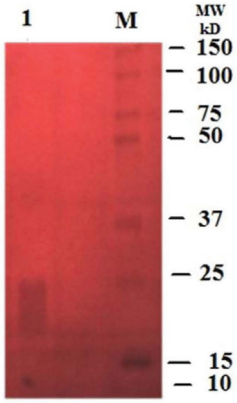

Fig. 1. SDS-Page/silver staining of LPS from *Slamonella enteritidis,* Lane M : Bio-Rad precision plus protein standard, 1-LPS from *Slamonella enteritidis.*

The SE RPA (*Salmonella enteritidis* Rapid Plate Agglutination) Test : The SE RPA test is carried out by using Biovac SE-RPA (Biovac SERPA TESTS AS2 Biovac animal health care) assay is a colored inactivated suspension of *Salmonella Enteritidis* antigen that are used for the detection of antibodies against *S.Enteritidis* in chickens by making a visible agglutination reaction.

Procedure : In the biovac rapid plate agglutination test, a drop of test sample was placed on a clean glass plate and a drop of biovac*S.enteritidis* antigen from was taken with dropper and deposited on plate, then the glass plate was gently rocked and rotated 30 to 40 seconds to ease the agglutination process. Read the results within 50 sec. Positive reaction was noted by the formation of clumps and negative reaction by without any clumps or clear solution.

Results

The LPS extracted from the *S.enteritidis* was run by SDS-PAGE, the gels were stained by Silver nitrate LPS was visualized and characterized upon staining the gel by silver staining method. SDS-PAGE followed by silver staining of LPS showed that molecular weight the LPS of *S.enteritidis* was ranging from ~14 kD to 25 kD. The Concentration of the Extracted S.E LPS was 2.07 mg/ml (Fig. 1).In house iELISA and RPA were compared with 156 reference serum samples. Cut off valuewas selected according to differentiate ratio between positive and negative values based on PP values.The sensitivity, specificity and accuracy of indirect ELISA using SE Antigen are sensitivity is 94.4%, specificity is 96.6% and accuracy is 93.5%.The Indirect ELISA assay for field samples were performed with a total number of 1020 serum samples from 9 individual commercial flocks and with a set of known reference samples, along with iELISA and another laboratory rapid plate agglutination assay also performed for all the collected serum samples. Among these, 592 (58.03%) serum samples are positive by iELISA and 566 (55.4%) serum samples were positive by Rapid plate

Vol. 14 (3) 256-262, July 2020, ISSN 0973-8916 (Print), 2230-7303 (Online)
DOI: 10.5530/ctbp.2020.3.26

agglutination test respectively. The Percentage positivity of the SE antibodies in commercial flocks are MSB Farms (57.1%) and 55.3%, Gold chick hatcheries was 55% and 53.3%, Srinivasa Hatcheries was 57% and 53.5, GSV poultry was 47% and 45%, Bindhu poultry farm was 64% and 60.4%, VR poultry was 78% and 74%, Sneha farms pvt, ltd was 44% and 42%, Gagana farms was 68% and 67%, Abhyudaya hatcheries was 39% and 36.2 % and the positive % of reference sera was 100% and 98% (Fig.2). In this study the age of the chickens used was in between 20 to 35 weeks and according to the age of the birds the serological response of the SE antibodies against SE pathogen 20-25 weeks was given 65.5%, 26-30 weeks were given 47% and 31-35 weeks were given 47.2% immune response (Table 1). Among the birds of all age groups, young birds are given higher serological response to the *Salmonella enteritidis* antigen.

Discussion

The objective of the present study was to gauge the development of an indirect ELISA for the detection of IgG antibody against *Salmonella enteritidis* in poultry flocks. To develop this assay *Salmonella enteritidis* LPS (Lipopoly sacharide) used as antigen in ELISA were assessed together with serum plate agglutination test. For this study a total 1020 number of chicken serum samples were collected from birds of different age groups of 9 commercial poultry farms and performed iELISA and RPA test. In this study, we isolated LPS (Lipopolysacharide) from *Salmonella* Enteritidis purified cells by hot phenol-water extraction method. The LPS was obtained in upper aqueous phase and it was subjected precipitate the LPS by ethanol. Thereafter LPS was dialyzed and the isolated LPS concentration was determine it was 2.07 mg/ml. The LPS had given a band in between 14 to 25 kD on SDS PAGE. The SDS-

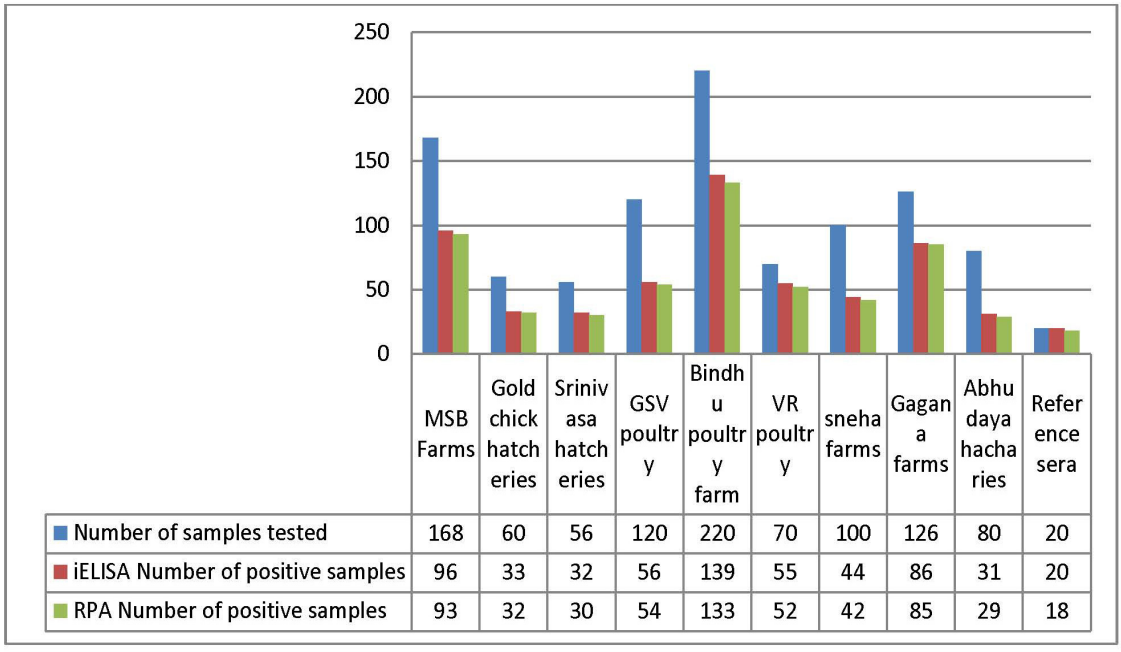

	MSB Farms	Gold chick hatcheries	Srinivasa hatcheries	GSV poultry	Bindhu poultry farm	VR poultry	sneha farms	Gagana farms	Abhudaya hacharies	Reference sera
Number of samples tested	168	60	56	120	220	70	100	126	80	20
iELISA Number of positive samples	96	33	32	56	139	55	44	86	31	20
RPA Number of positive samples	93	32	30	54	133	52	42	85	29	18

Fig. 2: Graph showing the sero positivity of chicken samples

Vol. 14 (3) 256-262, July 2020, ISSN 0973-8916 (Print), 2230-7303 (Online)
DOI: 10.5530/ctbp.2020.3.26

Age of birds(weeks)	Number of sera tested	Number of positive	Prevalence % samples
20-25	604	396	65.5
26-30	120	56	47
31-35	296	140	47.2

Table 1: Table showing the Age wise analysis of *Salmonella* Enteritidis infection

PAGE showed low molecular weight LPS was the characteristic for the repeated some sugar units as reported earlier by others (10,11).The iELISA With SE purified LPS was developed, to know the seroprevalance of *Salmonella enteritidis* in chickens and this showed that iELISA was robust tool for its mass screening and has many advantages than the other diagnostic methods. Similar reports have been showed by cooper (12) who detects the immune status of the SE antibodies in three flocks which gave high titer value than the other tests (12). In this study more than 1,000 sera were sampled among these chicken serum samples 592 (58.03%) and 566 (55.4%) were found to be seropositive for iELISA and RPA test respectively. Serological investigation of age-wise analysis shown that highest infection rate was 65.5% in 20-25 weeks age group followed by 47% in 26-30 weeks and 47.2% in 31 to 35 weeks. Among the birds of all age groups, younger birds are given higher serological response to the *Salmonella enteritidis* antigen.

Conclusion

This study stated that the iELISA immunoassay of SE was superior, rapid, easy to perform and most reliable test to screen the large number of birds for *S.enteritidis* infection and best use full tool for serosurvivalance to control the vertical and horizontal transmission of *S.enteritidis* in flocks.

References

1. Newell, D. G., Koopmans, M., Verhoef, L., Duizer, E., Aidara-Kane, A., Sprong, H., Giessen, J. v. d. and Kruse, H. (2010). Food-borne diseases-the challenges of 20 years ago still persist while new ones continue to emerge. International Journal of Food Microbiology 139: S3-S15. doi:10.1016/j.ijfoodmicro.2010.01.021.
2. Jarquin, R., Hanning, I., Ahn, S. and Ricke, S.C. (2009) Development of rapid detection and genetic characteriza-tion of *Salmonella* in poultry breeder feeds. *Sens. (Basel)*, 9(7): 5308-5323.
3. Galis, A.M., Marcq, C., Marlier, D., Portetelle, D., Van, I., Beckers, Y. and Thewis, A. (2013) Control of *Salmonella* contamination of shell eggs-preharvest and postharvest methods: A review. *Compr. Rev. Food Sci. Food Saf*., 12: 155-182.
4. Barrow, P.A., 1992. Further observations on the serological response to experimental *Salmonella* typhimurium in chickens measured by ELISA. Epidem. Infect, 108: 231-241.
5. Barrow, P. A. 1994. Serological diagnosis of *Salmonella* serotype *enteritidis* infections in poultry by ELISA and other tests. Int. J. Food Microbiol. 21:55–68.
6. Shoko Suzuki Pathogenicity of *Salmonella enteritidis*in poultry *International Journal of Food .~licrobiolo~',* 21 (1994) 89-105
7. H. Iihara, T. Niwa, M.M. Shah, P.H. Nhung, S.X. Song, M. Hayashi, K. Ohkusa, Y. Itoh, S. Makino, T. Ezaki, Rapid multiplex

immunofluorescent assay to detect antibodies against Burkholderiapseudomallei and taxonomically closely related nonfermenters, Japanese Journal of Infectious Diseases, 60-4 (2007) 230-234

8. R. Perdomo, V. Montero, Purification of E. coli 055:B5 lipopolysaccharides by size exclusion chromatography, Biotecnología Aplicada. 23 (2006) 124-129.

9. Chevallet M, Luche S, Rabilloud T. Silver staining of proteins in polyacrylamide gels. *Nat Protoc*. 2006;1(4):1852#1858. doi:10.1038/nprot.2006.288

10. Brooks BW, Perry MB, Lutze-Wallace CL, MacLean LL (2008) Structural characterization and serological specificities of lipopolysaccharides from *Salmonella* entericaserovar Gallinarumbiovar Pullorum standard, intermediate and variant antigenic type strains. Vet Microbiol 126(4):334–344

11. Peter GJ, Parker TC, Asokan K, Carlson WR (1999) Clinical and veterinary isolates of *Salmonella* entericaserovar *enteritidis* defective lipopolysaccharides O- chain polymerization. Appl Environ Microbiol 65(5):2195–2201

12. Cooper GL, Nicholas RA, Bracewell CD. Serological and bacteriological investigations of chickens from flocks naturally infected with *Salmonella enteritidis*. Vet Rec 1989; 125: 567-72.

Current Trends in Biotechnology and Pharmacy
Vol. 14 (3) 263-270, July 2020, ISSN 0973-8916 (Print), 2230-7303 (Online)
DOI: 10.5530/ctbp.2020.3.27

Formulation of pullulan/plasticizer blended films for their physical and biodegradability studies

V S Rama Krishna Ganduri[1,*], Usha Kiranmayi M[2], K.R.S.Sambasiva Rao[3], Sudhakar Poda[3]
[1]Department of Biotechnology, Koneru Lakshmaiah Education Foundation, Vaddeswaram- 522502, A.P., India.
[2]Department of Microbiology and Botany, Acharya Nagarjuna University, Nagarjuna Nagar, Guntur- 522510, A.P., India.
[3]Department of Biotechnology, Acharya Nagarjuna University, Nagarjuna Nagar, Guntur- 522510, A.P., India.
Corresponding author : krishna.ganduri@kluniversity.in

Abstract

The present investigation utilizes the eco-efficient pullulan polysaccharide as film forming biopolymer. Pullulan-based edible films offer good physical, thermal and mechanical properties which enable them to use in shelf-life preservation of fresh produce. Blends of other film forming polysaccharides, plasticizers and an antioxidant with pullulan (Pu) solution were prepared in order to determine physical and optical parameters of those films. The morphological and biodegradable studies were attempted to identify the changes on the films' surfaces. The films made from (only) pullulan (10Pu), pullulan composited with sodium alginate(10Pu_0.5SA), gelatin (10Pu_0.5G), polyethylene glycol (10Pu_0.5PG), calcium chloride and lemon juice (10Pu_1CC_2L) resulted heavier film densities, higher whiteness indexes and lower total color difference values.All the films were tested for their biodegradability in soil, where visual changes were appreciated after 15 days, partial and complete degradation took place at the end of 34 days and 53 days, respectively. Thus, these pullulan blended films could be a better replacement for synthetic films towards environmental problems.

Keywords: Pullulan, Plasticizers, antioxidant, edible film, biodegradable

Introduction

Use of bio-active packaging materials for extending shelf-life of fresh produce replaces the traditional petroleum-based (synthetic) packaging polymers (1,2). Edible films using thin wrapping materials, generally have packaging properties that shield the inner part from outer environment by limiting gas and water vapor transportation and improve the shelf-life of fresh produce by protecting them from physical, chemical and microbiological deteriorations (3). Traditionally, waxes, soymilk proteins, gelatin, sucrose and sugar derivatives were used as edible coatings to extend the storage life of many food items (4). Later, due to increased demand of coatings on food was served by petroleum-based coatings on food package. Further, dramatic increase of petroleum costs led to high packaging costs of fresh food materials. The past three decades, researchers have shown tremendous concern over cheaper edible materials for healthy packaging alternatives that lead to the commercial edible films prepared (5, 6, 7).

Typically, edible film composed of film forming compound, plasticizer, additive, and solvent to formulate a film forming dispersion (8). Characteristics of edible films, generally, affected by composition of film forming material, type and concentration of additives (9). In the present study, film forming materials viz., Pullulan (EPS from

Aureobasidium pullulans), Gelatin, Sodium Alginate, Agar and Starch; plasticizers like Poly-Ethylene Glycol 4000, Sorbitol, Glycerol and Calcium chloride; and Citric acid (in lemon juice) as an antioxidant additive were used in combinations to prepare variety of edible films. The prepared edible films were analyzed for organoleptic (color, whitening index), physical (opacity, light transparency), topographical properties and biodegradability.

Materials and methods

Materials used : All the chemicals (of analytical grade) were purchased from M/s. Qualigens Biochemicalswere purchased from M/s. HIMEDIA chemicals Ltd. Standard Pullulan of medium molecular weight (viscosity:180 centipoise)was purchased from M/s. Kumar Organics Pvt. Ltd., Bengaluru. Deionized water was used from a Millipore Simplicity system.

Film formation : Pullulan (10% w/v) was dissolved in distilled water and heated by a hot plate stirrer at 80°C, 500 rpm for 60 min; and then solution was cooled down to room temperature. Different mixed concentrations (% w/v) of other film forming materials (Gelatin, Starch, sodium Alginate, Agar), plasticizers (Glycerol, Sorbitol, Calcium chloride, Polyethylene glycol-4000, 6000), and additive (Citric acid) were mixed with 10 (% w/v) Pullulan suspension to form variety of film formulations (Table 1). Pullulan based edible films were formed by the casting method and dried at 60°C and 40% relative humidity (RH) in an environment chamber (S.K. Scientific & Surgical, India), for 24 h prior to characterization.

Color parameters measurement : Color Flex EZ 45/0°color spectrophotometer (Hunterlab, Reston, VA, USA) was used to test the color parameters of the edible films, according to ASTM E308. The CIE lab scale measurements were made, and the instrument was calibrated with a standard white plate (*L'* = 91.83, *a'* = - 0.73, *b'* = 1.52) as film background before the measurements. Results were expressed as *L** (luminosity), *a** (red/green) and *b** (yellow/blue) parameter values of the film samples sample and *L'*, *a'* and *b'* are the color parameter values of the standard white plate. A mean value of five repetitions of film's top and bottom side was recorded.

The total color difference (*ÄE*) was calculated using the following equation (10):

$$\Delta E = \langle [L^* - L']^2 + [a^* - a']^2 + [b^* - b']^2 \rangle^{\frac{1}{2}}$$

The Whitening Index (*WI*) of edible films was calculated as described by Bolin and Huxsoll (1991):

$$WI = 100 - \sqrt{[100 - L^{*2}] + a^{*2} + b^{*2}}$$

Film thickness and density measurement : Film thickness was measured by using Mini Electronic Dial Thickness Indicator (Gauge Tester, Joro). The thickness reading was made of mean value of three experimental tests in ten different positions, each twice per second measuring a minimum, a maximum and an average value, with a resolution of 0.001 mm, at room temperature. The density of each film (in g/cm^3) was determined and expressed as an average of three measurements and standard deviation.

Film transparency measurement : Transparency of pullulan-based films was measured according to the procedure of Han and Floros, 1997 (11) using a spectrophotometer (Biospectrometer® kinetic, Eppendorf, New York, USA), as per ASTM method D1746-92 (12). Edible film's transparency was calculated using following equation (13):

$$\text{Transparency} = \frac{A_{600}}{b} \text{ or } \frac{\log T_{600}}{b}$$

where T_{600} is transmittance at 600 nm, A_{600} is absorbance, and *b* is the length of the light path through the medium (i.e., film thickness).

Morphology evaluation : The films' morphology was determined by using a microscope (Olympus CX31 HD Digital Microscope, Feasterville, PA)

Vol. 14 (3) 263-270, July 2020, ISSN 0973-8916 (Print), 2230-7303 (Online)
DOI: 10.5530/ctbp.2020.3.27

with a standard light. Film strips were observed in black and white and the images were recorded at a 20X magnification (13).

Biodegradability in soil : Biodegradation of prepared films was tested in soil under controlled laboratory conditions (25ºC, 25% humidity and pH=7). Samples were placed onto the soil located in plastic containers which were covered by aluminium foil in order to keep the films free of dirt. Biodegradation was studied taking photographs at regular time intervals (14).

Results and Discussion

Color related characteristics : The consumer acceptance of any edible film depends, primarily, on film's color that in turn influenced by the ingredient composition by means which it was formulated (15). The different composition of film forming compounds, plasticizers, additive used for pullulan based edible films and film thickness, total color difference (*ÄÅ*), whiteness index (*WI*), and Transparency values were tabulated in the Table 2. The presence of various materials significantly affected the films formation and their characterization. All the pullulan-based films have shown the thickness range of 0.04 to 0.1 mm. Thickness can affect barrier properties, particularly water vapor permeability due to differences between the water vapor pressure below the film and that of the moisture build-up above the film (16). To obtain films with similar thickness, same suspension volumes were used. However, films prepared with plasticizers exhibited higher thickness that those prepared with other polysaccharides. The films' thickness values are in good agreement with previous studies (17, 18).

The Hauntercolor parameters results (L^*, a^*, b^*) were used to calculate the total color difference (*ÄÅ*) and whiteness index (*WI*), the values shows significant variation of color characteristics ($p<0.05$). The films made from (only) pullulan, pullulan composited with sodium alginate, gelatin, polyethylene glycol, calcium chloride and lemon juice resulted heavier film densities, higher whiteness indexes and lower total color difference values. The similar results were also reported in previous study (15, 18). The transparency (based on absorbance at 600 nm wavelength) values of these films were very high, also attracts the packaging visual characteristics in both product consumer acceptability and food quality, when these are applied on fresh produce. So, these five films were used in the mechanical and thermal characterization. The same trend was also reported by Bertan et al., 2005 (19) andTaqi et al., 2011 (20).

Microstructure of films : Edible films are usually hydrophilic in nature, whereas conventional plastic films are non-polar, as reported by Antarés and Chiralt, 2016 (21). The incorporation of various plasticizers and additives in the film forming

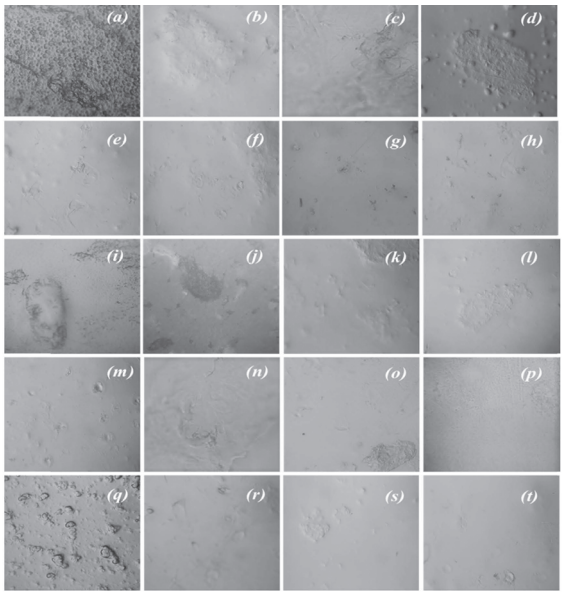

Fig. 1: Surface micrographs of Pullulan based edible films (a)10 Pu, (b) 10 Pu_0.5 SA, (c) 10 Pu_0.5 G, (d) 10 Pu_0.5 St, (e) 10 Pu_0.5 A, (f) 10 Pu_0.5 G*, (g) 10 Pu_0.5 S*, (h) 10 Pu_1 CC, (i) 10 Pu_0.5 PG, (j) 10 Pu_0.5 PG*, (k) 10 Pu_0.5 G*_0.5 S*, (l) 10 Pu_0.5 G_0.5 G*, (m) 10 Pu_0.5 SA_0.5 G, (n) 10 Pu_0.5 SA_ 0.5 G*, (o) 10 Pu_0.5 SA_1 PG, (p) 10 Pu_1 CC_1 PG, (q) 10 Pu_1 PG_2.5St, (r) 10 Pu_1 CC_2 L, (s) 10 Pu_1 CC_2 S*, (t) 10 Pu_2 L

Vol. 14 (3) 263-270, July 2020, ISSN 0973-8916 (Print), 2230-7303 (Online)
DOI: 10.5530/ctbp.2020.3.27

dispersion is done by homogenization of polymer aqueous solution. When the film is dried, plasticizers and additives embedded into the polymer matrix, as observed by microscopy. The drying time plays an important role in determining the arrangement of the components during the film-forming step, thus the final microstructure of the edible films. Morphological analysis of the films under study was carried out by optical microscopy (20X magnification), to evaluate the homogeneity and the structure of the prepared films. Fig. 1 shows the surface micrographs of all the prepared films. Pullulan composited films presented a more homogeneous and uniform structure than pullulan (alone) ones. Starch containing films (Fig. 1. (*d*), (*q*)) shows a mild change (agglomerations) in the structure of films due to non-uniform distribution of starch. The most irregular structure was observed in Pullulan film (Fig. 1. (*a*)). The morphology of the films supported the tensile results, evidencing that a different structural arrangement of the components in the film forming dispersion significantly influences both mechanical and gas barrier properties. The similar surface micrographs were also observed by many researchers for edible films (13, 14, 18).

Biodegradability tests : Edible films made from biopolymers takes advantage of reducing environmental pollution clean-up (14). The pullulan-based films were visualized using a digital camera. Fig. 2 (a) and (b) shows the surface of pullulan blended films at 0, 4, 8, 15, 27, 34, 41, 46 and 53 days in contact when buried under fertile soil. The visual images outline the films' surface change indicating cracks, holes, color changes and microorganism's appearance, in a progressive manner. Over the time, microorganism's(present

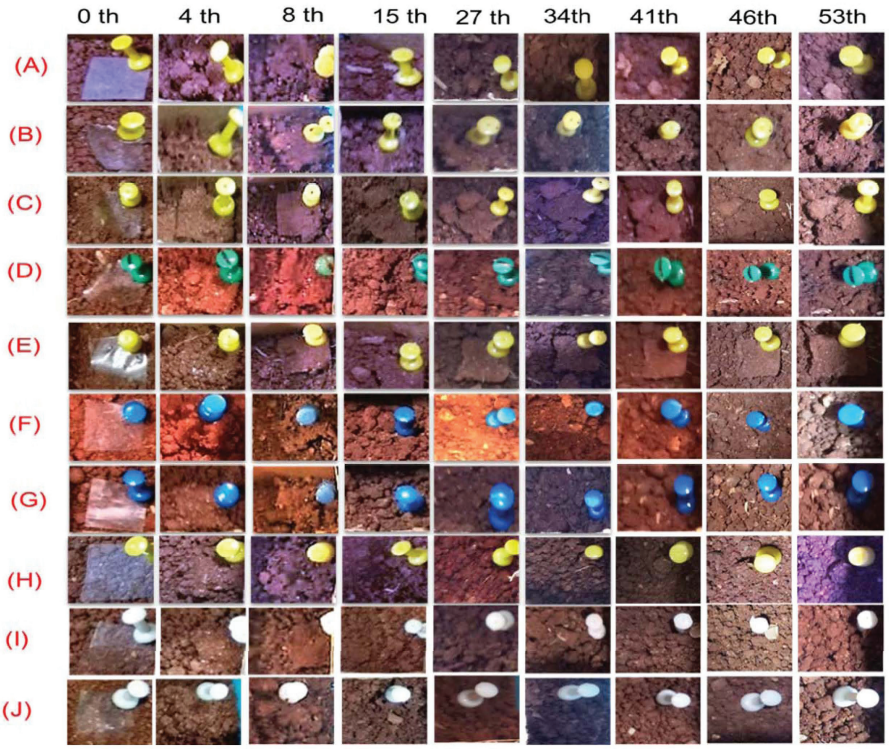

Fig. 2 (a). Pullulan based edible films degraded in soil after different (0, 4, 8, 15, 27, 34, 41, 46 and 53) days: (A)10 Pu, (B) 10 Pu_0.5 SA, (C) 10 Pu_0.5 G, (D) 10 Pu_0.5 St, (E) 10 Pu_0.5 A, (F) 10 Pu_0.5 G*, (G) 10 Pu_0.5 S*, (H) 10 Pu_1 CC, (I) 10 Pu_0.5 PG, (J) 10 Pu_0.5 PG*

Vol. 14 (3) 263-270, July 2020, ISSN 0973-8916 (Print), 2230-7303 (Online)
DOI: 10.5530/ctbp.2020.3.27

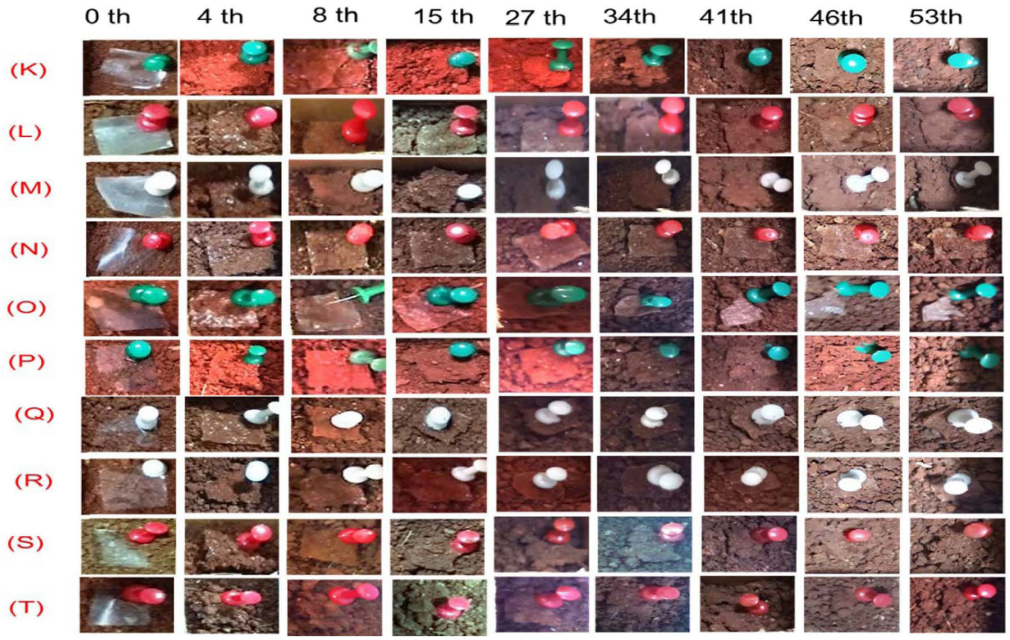

Fig. 2 (b). Pullulan based edible films degraded in soil after different (0, 4, 8, 15, 27, 34, 41, 46 and 53 days: (K) 10 Pu_0.5 G*_0.5 S*, (L) 10 Pu_0.5 G_0.5 G*, (M) 10 Pu_0.5 SA_0.5 G, (N) 10 Pu_0.5 SA_ 0.5 G*, (O) 10 Pu_0.5 SA_1 PG, (P) 10 Pu_1 CC_1 PG, (Q) 10 Pu_1 PG_2.5St, (R) 10 Pu_1 CC_2 L, (S) 10 Pu_1 CC_2 S*, (T) 10 Pu_2 L

in soil) attack on the film's surface was gradually spreaded.The gravimetric biodegradation studies were not performed, due to the microbial degradation of film surface. Almost all the films were slowly degraded after 5 weeks (34 days) in soil but visual changes were only appreciated after the 15 days. By the end of 53 days, all the films were completely degraded by soil microorganisms and disappeared (Fig. 2 (a), (b)). Microorganism proliferation was enhanced by the humidity of films which was favoured by the pullulan content. The similar observations were also reported by Debandi et al., 2016 (13) for films made with Chitosan/ Glycerol.

Conclusion

Use of different polysaccharides, plasticizers and additives were blended to pullulan, edible biopolymer, to formulate the edible thin films was attempted. Film physical, optical, surface and biodegradability properties were evaluated.Out of twenty different pullulan-based edible films, only the films formulated with plasticizers have shown high film thicknesses. High value of density, whiteness index and low value of color difference was observed in 10Pu, 10Pu_0.5SA, 10Pu_0.5G, 10Pu_0.5PG and 10Pu_1CC_2L films. Different morphological changes were also seen in all these pullulan blended films. Biodegradability, of all these films, in soil elucidates the use of these pullulan-based films would be an alternate for plastic films that completely eradicates the environment pollution.

Acknowledgements

First and corresponding author is thankful to SYST-SEED, Department of Science & Technology, Government of India for providing financial support under the Research Grant No.: SP/YO/026/2016(G))and the management of KLEF, Vaddeswaram for providing facilities to carry out this work.

Vol. 14 (3) 263-270, July 2020, ISSN 0973-8916 (Print), 2230-7303 (Online)
DOI: 10.5530/ctbp.2020.3.27

Table 1. Pullulan blended films classification based on composition

Film symbol	Film Forming Material (% w/v)				Plasticizer (% w/v)						Additive (% w/v)
	Pu	SA	G	St	A	G*	S*	CC	PG	PG*	L
10 Pu	10.0	–	–	–	–	–	–	–	–	–	–
10 Pu/0.5 SA	10.0	0.5	–	–	–	–	–	–	–	–	–
10 Pu/0.5 G	10.0	–	0.5	–	–	–	–	–	–	–	–
10 Pu/0.5 St	10.0	–	–	0.5	–	–	–	–	–	–	–
10 Pu/0.5 A	10.0	–	–	–	0.5	–	–	–	–	–	–
10 Pu/0.5 G*	10.0	–	–	–	–	0.5	–	–	–	–	–
10 Pu/0.5 S*	10.0	–	–	–	–	–	0.5	–	–	–	–
10 Pu/1 CC	10.0	–	–	–	–	–	–	1.0	–	–	–
10 Pu/0.5 PG	10.0	–	–	–	–	–	–	–	0.5	–	–
10 Pu/0.5 PG*	10.0	–	–	–	–	–	–	–	–	0.5	–
10 Pu/0.5 G*/0.5 S*	10.0	–	–	–	–	0.5	0.5	–	–	–	–
10 Pu/0.5 G/0.5 G*	10.0	–	0.5	–	–	0.5	–	–	–	–	–
10 Pu/0.5 SA/0.5 G	10.0	0.5	0.5	–	–	–	–	–	–	–	–
10 Pu/0.5 SA/ 0.5 G*	10.0	0.5	–	–	–	0.5	–	–	–	–	–
10 Pu/0.5 SA/1 PG	10.0	0.5	–	–	–	–	–	–	1.0	–	–
10 Pu/1 CC/1 PG	10.0	–	–	–	–	–	–	1.0	1.0	–	–
10 Pu/1 PG/2.5St	10.0	–	–	2.5	–	–	–	–	1.0	–	–
10 Pu/1 CC/2 L	10.0	–	–	–	–	–	–	1.0	–	–	2.0
10 Pu/1 CC/2 S*	10.0	–	–	–	–	–	2.0	1.0	–	–	–
10 Pu/2 L	10.0	–	–	–	–	–	–	–	–	–	2.0

Pu- Pullulan, SA-Sodium Alginate, G- Gelatin, St- Starch, A- Agar, G*-Glycerol, S*- Sorbitol, CC-Calcium chloride, PG- Polyethylene Glycol4000, PG*- Polyethylene Glycol6000, L- Lime juice

Vol. 14 (3) 263-270, July 2020, ISSN 0973-8916 (Print), 2230-7303 (Online)
DOI: 10.5530/ctbp.2020.3.27

Table 2. Pullulan based edible films thickness, density, color properties and transparency.

Film symbol	Thickness (mm)	Density (g/cc)	Color Difference, E	Whiteness Index, (Abs)	Transparency WI
10 Pu	0.06±0.001§	10.46±0.2¶	13.48±0.55¡	78.39±0.21¢	36.13±0.21¤
10 Pu/0.5 SA	0.05±0.001	7.95±0.1	16.77±0.47	75.09±0.43	19.08±0.34
10 Pu/0.5 G	0.05±0.002	7.24±0.21	16.47±0.24	75.39±0.34	1.66±0.07
10 Pu/0.5 St	0.05±0.002	0.954±0.09	37.29±0.59	54.56±0.54	2.22±0.12
10 Pu/0.5 A	0.04±0.001	1.450±0.23	29.05±0.24	62.72±0.13	2.35±0.54
10 Pu/0.5 G*	0.07±0.003	0.716±0.08	22.51±0.76	69.45±0.52	2.25±0.27
10 Pu/0.5 S*	0.04±0.001	1.600±0.17	21.38±0.35	70.45±0.31	2.07±0.35
10 Pu/1 CC	0.05±0.002	1.03±0.05	33.46±0.53	58.36±0.28	2.66±0.31
10 Pu/0.5 PG	0.05±0.001	9.10±0.13	16.86±0.37	75.17±0.17	4.30±0.42
10 Pu/0.5 PG*	0.10±0.004	1.463±0.06	35.64±0.45	56.13±0.56	8.42±0.25
10 Pu/0.5 G*/0.5 S*	0.04±0.002	1.075±0.02	39.80±0.55	52.09±0.23	4.95±0.32
10 Pu/0.5 G/0.5 G*	0.04±0.001	1.575±0.01	34.34±0.52	57.45±0.47	4.27±0.38
10 Pu/0.5 SA/0.5 G	0.07±0.001	1.31±0.03	19.73±0.13	72.05±0.87	1.63±0.54
10 Pu/0.5 SA/ 0.5 G*	0.06±0.003	1.233±0.02	27.68±0.65	64.12±0.76	2.21±0.23
10 Pu/0.5 SA/1 PG	0.04±0.001	1.30±0.04	37.75±0.16	54.05±0.58	3.70±0.54
10 Pu/1 CC/1 PG	0.10±0.005	1.854±0.05	36.17±0.56	55.63±0.52	12.02±0.33
10 Pu/1 PG/2.5St	0.06±0.002	1.850±0.21	36.17±0.32	55.63±0.43	2.31±0.26
10 Pu/1 CC/2 L	0.05±0.002	10.35±0.34	19.14±0.44	72.61±0.87	32.62±0.45
10 Pu/1 CC/2 S*	0.04±0.003	1.04±0.02	24.79±0.54	67.56±0.45	4.23±0.28
10 Pu/2 L	0.04±0.001	1.650±0.04	36.47±0.24	55.33±0.37	2.72±0.36

Data shows mean ± standard deviation and different superscript letters (§, ¶, ¡, ¢, ¤) in each column indicated significant differences ($p<0.05$)

References

1. S. Guilbert, (2011). Technology and application of edible protective films, in: Mathlouthi M (Ed.), Food packaging and preservation, Elsevier Applied Sci., London, UK, pp.371–394.
2. Vanessa, D.A., Suzana, M., Adelaide, B. and Maria, V.E. (2007). Effect of glycerol and amylose enrichment on cassava starch films properties, J. Food Eng. 78(3): 941–946.
3. Vargas, M., Albors, A., Chiralt, A. and González-Martínez, C. (2009). Characterization of chitosan–oleic acid composite films. Food Hydrocolloids, 23(2):536-547.
4. Bourtoom, T. (2008). Edible films and coatings: characteristics and properties. International food research journal, 15(3):237-248.
5. Antoniou, J., Liu, F., Majeed, H., Qazi, H. J. and Zhong, F. (2014). Physicochemical

Vol. 14 (3) 263-270, July 2020, ISSN 0973-8916 (Print), 2230-7303 (Online)
DOI: 10.5530/ctbp.2020.3.27

and thermomechanical characterization of tara gum edible films: Effect of polyols as plasticizers. Carbohydrate polymers, 111:359-365.

6. Giteru, S. G., Coorey, R., Bertolatti, D., Watkin, E., Johnson, S. and Fang, Z. (2015). Physicochemical and antimicrobial properties of citral and quercetin incorporated kafirin-based bioactive films. Food chemistry, 168:341-347.
7. Ma, Q., Hu, D., Wang, H., & Wang, L. (2016). Tara gum edible film incorporated with oleic acid. Food Hydrocolloids, 56:127-133.
8. Zhang, P., Zhao, Y. and Shi, Q. (2016). Characterization of a novel edible film based on gum ghatti: Effect of plasticizer type and concentration. Carbohydrate polymers, 153:345-355.
9. Lazaridou, A. and Biliaderis, C. G. (2002). Thermophysical properties of chitosan, chitosan–starch and chitosan–pullulan films near the glass transition. Carbohydrate polymers, 48(2):179-190.
10. Sothornvit, R. and Pitak, N. (2007). Oxygen permeability and mechanical properties of banana films. Food Research International, 40(3):365-370.
11. Han, J. H. and Floros, J. D. (1997). Casting antimicrobial packaging films and measuring their physical properties and antimicrobial activity. Journal of Plastic Film & Sheeting, 13(4):287-298.
12. Irissin-Mangata, J., Bauduin, G., Boutevin, B. and Gontard, N. (2001). New plasticizers for wheat gluten films. European polymer journal, 37(8):1533-1541.
13. Siracusa, V., Romani, S., Gigli, M., Mannozzi, C., Cecchini, J. P., Tylewicz, U. and Lotti, N. (2018). Characterization of active edible films based on citral essential oil, alginate and pectin. Materials, 11(10):1980.
14. Debandi, M. V., Bernal, C. and Francois, N. J. (2016). Development of biodegradable films based on chitosan/glycerol blends suitable for biomedical applications. J. Tissue Sci. Eng, 3(4172):2157-7552.
15. Zhang, B., Wang, D. F., Li, H. Y., Xu, Y. and Zhang, L. (2009). Preparation and properties of chitosan–soybean trypsin inhibitor blend film with anti-Aspergillus flavus activity. Industrial crops and products, 29(2-3):541-548.
16. Wu, J., Chen, S., Ge, S., Miao, J., Li, J. and Zhang, Q. (2013). Preparation, properties and antioxidant activity of an active film from silver carp (Hypophthalmichthys molitrix) skin gelatin incorporated with green tea extract. Food Hydrocolloids, 32(1):42-51.
17. Gounga, M. E., Xu, S. Y. and Wang, Z. (2007). Whey protein isolate-based edible films as affected by protein concentration, glycerol ratio and pullulan addition in film formation. Journal of Food Engineering, 83(4):521-530.
18. Hedayati Rad, F., Khodaiyan, F., Hossaini, S. E. and Sharifan, A. (2018). Preparation and Characterization of Pullulan-Soy Protein Concentrate Biocomposite Film. Journal of Food Biosciences and Technology, 8(2):19-28.
19. Bertan, L. C., Tanada-Palmu, P. S., Siani, A. C. and Grosso, C. R. F. (2005). Effect of fatty acids and 'Brazilian elemi'on composite films based on gelatin. Food hydrocolloids, 19(1):73-82.
20. Taqi, A., Askar, K. A., Nagy, K., Mutihac, L. and Stamatin, L. (2011). Effect of different concentrations of olive oil and oleic acid on the mechanical properties of albumen (egg white) edible films. African Journal of Biotechnology, 10(60):12963-12972.
21. Atarés, L. and Chiralt, A. (2016). Essential oils as additives in biodegradable films and coatings for active food packaging. Trends in Food Science & Technology, 48: 51-62.

Current Trends in Biotechnology and Pharmacy
Vol. 14 (3) 271-278, July 2020, ISSN 0973-8916 (Print), 2230-7303 (Online)
DOI: 10.5530/ctbp.2020.3.28

Generation of gamma irradiated mutagenized population in *Solanum lycopersicum* CV. Arka Vikas

Pottipadu John Elia Prashanth, Nambi Rajesh, Jogi Gurucharan Padma, E.C. Surendranatha Reddy and Pinjari Osman Basha*
Department of Genetics and Genomics, Yogi Vemana University, Kadapa
*Corresponding author : osmanbasha@yahoo.co.in

Abstract

Natural and induced mutants are the primary resource for understanding the functions of the genes. The study of lethal dose (LD) and development of 300Gy, 400Gy, and 500Gy gamma irradiation population in *Solanum lycopersicum* L. cv. ArkaVikas was carriedout in the present investigation. The highest germination percentage was recorded in control (98.53%). The germination percentage reduction, seedling height decline, and decreased pollen fertility in M_1 generation was noted with the increasing gamma radiation dose. The 300Gy irradiation caused 41.73% seed germination reduction and was considered an appropriate irradiation dose to develop a mutagenized population. A total of 3000 seeds have been irradiated with 300Gy of gamma rays and 1,748 (58.26%) M_1 mutagenized plants have survived and out of these 1,185 viable fertile plants were noted. In M_1 generation two chlorophyll mutants have been identified. Six plants from each M_2 line were screened based on morphological alterations and six putative mutants (0.51%) were identified. The identified mutant lines displayed a varied range of morphological variations that include altered chlorophyll content, elongated fruits, and orange color fruit.

Keywords: *Solanum lycopersicum L.*, gamma irradiation, mutagenesis, morphological variations.

Introduction

Globally, Solanum lycopersicum L. occupies the second place in the fresh vegetable market and the food processing industry. Tomato belongs to the Solanaceae family, with a small genome size, various mapped traits and EST clones (1). Tomato bears a fleshy berry fruit and emerged as a model plant for fruit ripening studies. The genome size of tomato was predicted to be approximately 900 Mb with 12 chromosomes and 34,727 protein-coding genes (2). Out of these predicted protein-coding genes, 30,855 genes are supported by RNA sequencing (RNA-Seq) data (2). Mutagenized population development and mutant collection is a fundamental and key resource for gene function investigation and several researchers have developed a mutagenized tomato population (3 and 4). Induced mutagenesis is one of the effective approaches to the genetic enhancement of crop plants (5). Significant efforts have been made to generate large scale induced mutagenized population by chemical (EMS, and DEB), physical (X-rays, gamma rays, and fast and thermal neutrons) and biological (T-DNA and Transposans) mutagens (3, 6, 7, 8, 9 and 10). Mutagenesis frequency, spectrum, screening, and usability were varied from one to another approach.

The tomato genetic resource center (University of California, Davis) collected and cataloged 1,050 monogenic stocks, including morphological mutants, alloenzyme markers, and 1,153 wild tomato accessions (http://tgrc.uctavis.edu). Physical and chemical mutagenesis causes high-frequency mutations in plants (11). Gamma rays and fast neutrons are widely used as physical mutagens for the development of a mutagenized popu-

Vol. 14 (3) 271-278, July 2020, ISSN 0973-8916 (Print), 2230-7303 (Online)
DOI: 10.5530/ctbp.2020.3.28

lation and these populations are used for mutants screening (12, 13 and 14). Forward genetics is one of the approaches, in which the gene responsible for the natural mutant or induced mutant phenotype is determined. Gamma-rays have the capacity to induce large-scale deletions, sometimes the reconstitution of chromosomes and useful mutants have been isolated with low and medium doses (15).

The availability of complete genome sequence and dense genetic maps has enabled researchers to develop systematic approaches to discover the function of identified alleles. Several approaches such as TILLING (Targeting Induced Local Lesions IN Genomes), De-TILLING and insertional mutagenesis (T-DNA or transposon tagging) enable high-throughput gene functions characterization (16, 17, 18, 19 and 20). TILLING is one of the strategies in which point mutations introduced in genome by alkylating agent ethyl methanesulfonate followed by mutation detection (21 and 22). Li et al. (9) developed a fast neutron based delete-a-gene reverse genetics approach in Arabidopsis, which is dependent on PCR strategy to detect deletions using shorter extension times to allow preferential amplification of short deletion in gene at high pooling depths.

Mutant resources have contributed to both plant breeding and functional genomics. Moreover, the rate of mutant recovery in EMS mutagenized population was actually higher than gamma rays irradiation mutagenesis (15). This may be due to gamma irradiation, which often causes larger DNA deletion (15, 23 and 24) and most mutants with extreme deletions of DNA may not have survived. Thus, there is still a need to develop large scale deletion mutagenized genetic resources and development of more efficient detection methods. Here, we describe the development of mutagenized gamma-irradiated M2 population of Solanum lycopersicum L. cv. Arka Vikas, and this population exploits for the screening of mutants. The generated M2 deletion mutagenized population may contribute to the genetic resources for breeding and functional genomics in tomato.

Materials and Methods

Plant material and determination of optimal dose for mutagenesis : Solanum lycopersicum cv. Arka Vikas seeds were procured from the Indian Institute of Horticulture Research (IIHR), Bangalore, India. Cultivar Arka Vikas seed batches were treated with 300Gy, 400Gy, and 500Gy gamma irradiation doses. The gamma radiation treatment was carried out at Baba Atomic Research Institute (BARC), Trombay, Bombay, India in 2016. In order to record the results of seed germination and seedling survival, the treated seeds were placed on moisture filter paper in petri plates in a growth chamber at 25±2°C.

Development of mutagenized population: The gamma irradiated seeds were manually sown in the nursery bed. The seedlings were transplanted in an open field after three weeks of germination. Fertilization and herbicide treatments were applied once and the field was regularly irrigated by flood irrigation. The M1 plants were allowed to self-pollinate to produce M2 seeds. Red ripe fruits were harvested from individual plants at the end of the plant life cycle and M2 seeds were collected for construction of the M2 families.

Phenotypic screening of M2 population: Around ten seeds of each M2 family were sown in nursery beds. As mentioned above, six plants from each of the M2 lines were grown in open field. Each M2 plant was tagged and a systematic phenotypic assessment of the mutant population was carried out based on the visual characterization. Phenotypic variations were captured using the digital camera (Sony NEX-3N). All the M3 seeds were collected from individual M2 plants.

Results and Discussion

Mutants with favorable genetic variations have attracted the breeders to develop the new cultivars. It is therefore very essential to develop a wide range of induced mutagenized populations by various mutagenesis approaches. An Indian cultivar 'Arka Vikas' was used in the present investigation for the development of the mutant resource. Geneticists have used natural and induced

Vol. 14 (3) 271-278, July 2020, ISSN 0973-8916 (Print), 2230-7303 (Online)
DOI: 10.5530/ctbp.2020.3.28

mutations for the genetic enhancement of economically important crops (25) these mutations have also been used as tools for the study of gene function. Natural or chemically induced genetic diversity is considered to be an important genetic resource and has been used for cultivation without any stringent regulatory restrictions imposed by national and international agencies.

Three specific doses of gamma radiation, i.e. 300 Gy, 400 Gy, and 500 Gy, were chosen to determine the optimal dose of mutagen for the development of the gamma-irradiated mutagenized population of the cv. Arka Vikas. The lethal dose in the cv. Arka Vikas at 300 Gy, 400 Gy, and 500 Gy, was 41.73, 67.63, and 86.33% respectively, whereas 98.53% seed germination was observed in control (Table 1). The frequency of seed germination and survival of M1 seedlings decreased with an increased dose of gamma radiation. The LD50 values of various mutagens vary greatly in plant species and induced mutagenized populations are developed based on LD50 values. Mutation induction in the genome is a random phenomenon, and a mutation's recovery depends on the chance of survival of the individual plants, consecutively which affects the likelihood of a desirable mutant being identified.

Okabe et al. (26) reported one mutation per 1,237 Kb and these mutations affected an average of three alleles per kilobase from EMS mutagenized population. Till et al. (27) reported one putative mutation per 300 Kb from 1.5% EMS mutagenized Nipponbare population. In Arabidopsis thaliana, averages of 720 mutations were detected in each M2 plant (28). Nevertheless, the EMS mutagenesis typically causes random G/C to A/T transitions and the incidence of truncated mutations is lower than 5% (29) and expected to result in a large percentage of leaky mutation. In addition, these leaky mutations were probably undetected morphologically and remained in the mutagenized population, and the efficient detection of mutations required further screening of the lines. An occurrence of lower mutation frequency in the gamma-irradiated population was noted in literature, and this may be due to the lethality of larger deletions. Naito et al. (13) irradiated the buds with gamma-rays and used the pollen to fertilize the open flowers and further studies revealed that in the most mutant's large deletions of up to 6 Mbp were found, the majority of which were not transmitted to progeny. They also reported mutations containing 1- or 4-bp deletions that were normally transmitted to the next generation (13).

Parameters for assessing the mutagen mutagenicity are seed germination, lethality, sterility, chimeric plants in M1 generation and viable mutant frequency (3, 14 and 30). In addition, the adverse effects of physical and chemical mutagens on various biological parameters have been reported earlier (31 and 32). In this study, we developed a total of 1,449 M2 gamma-irradiated lines. A total of 1,185 M1 plants survived and produced fertile offsprings from germinated 1,748 M1 seedlings belonging to 300 Gy gamma-irradiated seeds (Table 2). A total of 235 and 29 M1 seedlings were survived from 400 Gy and 500 Gy gamma-irradiated seeds, respectively (Table 2). The 300 Gy dose is chosen as the best possible irradiation dosage after careful evaluation of the seed germination and M1 seedling survival percentages. Physical and chemical mutagens have induced a wide range of morphological mutations in various crops (3, 4, 23, 33, 34, 35, 36 and 37). Chimeric plants have also been identified in the M1 generation of the developed gamma-irradiated mutagenized population.

Six individual plants were transplanted to the field from each M2 line and screened for morphological and developmental variation. A total of six lines were identified as putative mutant candidates with morphological changes. The observed phenotypic variations were reduced chlorophyll content (Fig. 1D), increased chlorophyll content in leaves (Fig. 1E), elongated fruits (Fig. 1 F & G), orange color ripened fruit mutant (Fig. 1 H) and pale yellow flower (Fig. 1I). All six mutant candidates were identified from 300 Gy gamma-irradiated mutagenized populations. The mutant frequency was measured as the number of mutants

Vol. 14 (3) 271-278, July 2020, ISSN 0973-8916 (Print), 2230-7303 (Online)
DOI: 10.5530/ctbp.2020.3.28

detected from total families screened. The mutation frequency was measured as 0.51% (6/1,185) and is an approximate rough index of the frequency of gamma irradiation mutagenesis. In the present investigation, 0.168% of the germinated M2 seedlings showed chlorophyll mutants. Gamma-ray irradiation in rice resulted in the identification of one mutation per 6.19Mb and the point mutation rate was relatively lesser than the EMS mutagenesis, however, the rate of knockout mutations was higher in gamma-ray irradiation than the EMS mutagenesis (38). A total of 10.88% M2 plants with morphological phenotypes were identified on the basis of primary screening from the EMS mutagenized population (3).

One of the drawbacks of gamma-radiation mutagenesis is that there no efficient method of

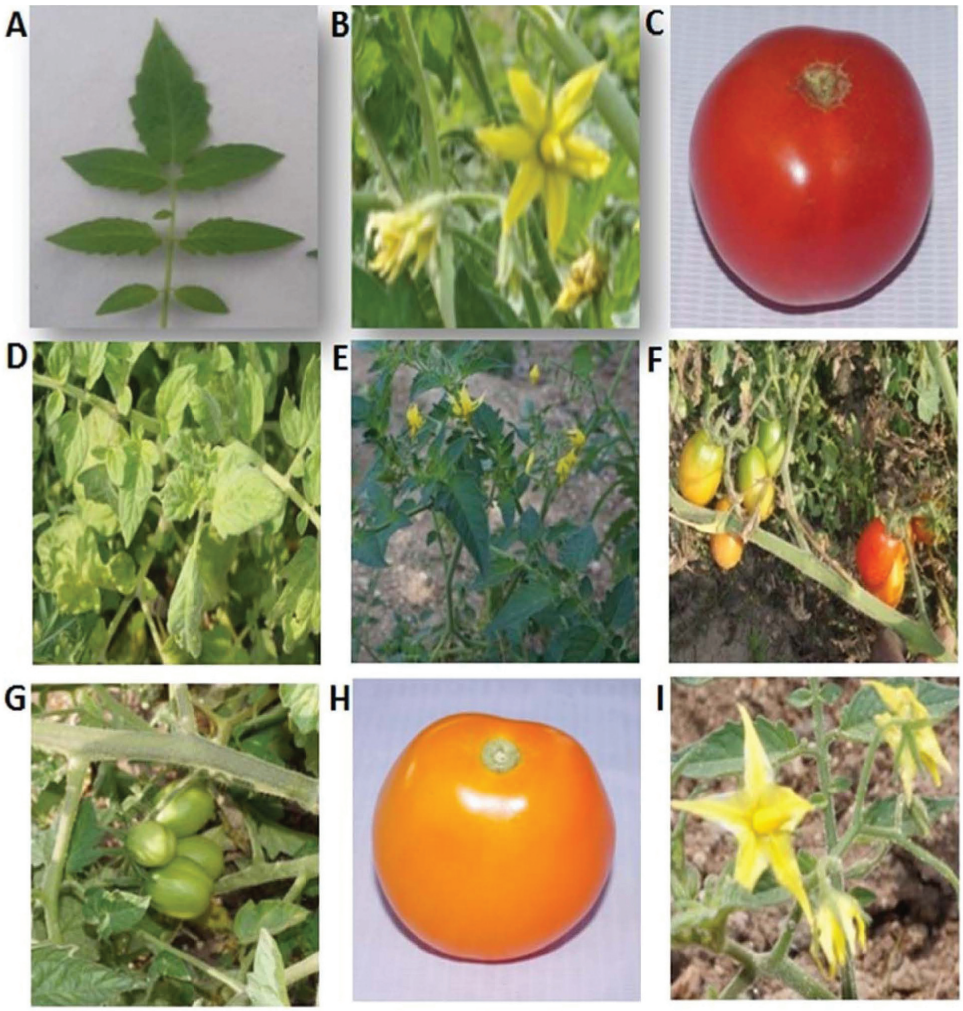

Fig. 1: Morphological mutants identified fromã-irradiated mutagenized population. (A) (B) & (C): Wild type (cv. ArkaVikas); (D) Leaf color: Reduced chlorophyll mutant; (E) Leaf color: Increased chlorophyll mutant; (F) & (G) Fruit shape: Elongated fruit; (H): Fruit color: Orange color fruit mutant; (I): Flower color: Pale yellow color.

Vol. 14 (3) 271-278, July 2020, ISSN 0973-8916 (Print), 2230-7303 (Online)
DOI: 10.5530/ctbp.2020.3.28

Table 1: Effects of Gamma-irradiation on seed germination in Solanum lycopersicum L. cv. Arka Vikas.

S.No	γ-radiation dose	Total Number of seeds	Number of seeds germinated	% of seeds germinated seeds	Number of seeds not germinated	% of seeds not germinated (LD)
1	Control (0 Gy)	3000	2956	98.53%	44	1.46%
2	300 Gy	3000	1748	58.26%	1252	41.73%
3	400 Gy	3000	971	32.36%	2029	67.63%
4	500 Gy	3000	410	13.66%	2590	86.33%

Table 2: Effect of Gamma radiation on M1 plant's survival and fertility.

S.No	γ-radiation dose	Number of gamma radiated seeds germinated	Number of fertile M1 plants survived	% M1 plants survived
1	300 Gy	1748	1185	67.79%
2	400 Gy	971	235	24.2%
3	500 Gy	410	29	7.07%

reverse genetics approach for detecting the smaller to larger deletions in the genome. However, there are few reports in literature for the identification of deletions in the genome. The technique of TILLING (Targeting Induced Local Lesions IN Genome) was introduced to recognize the point mutations (39) and the technique was applied to various crops, such as rice, tomato, wheat, barley (26, 27, 40 and 41). The TILLING technique is also effective in detecting 2–4bp deletions induced by gamma-rays (38). Li et al. (9) developed a reverse genetics approach to discovering deletions in targeted genes in Arabidopsis and has identified deletions in 84% of targeted regions by using a total of 51, 840 lines. Furthermore, they reported deletions in rice genome using a similar approach.

Acknowledgments

The authors are thankful to the University Grant Commission (UGC), New Delhi, India, for financial support.

References

1. Adamu, A. K. (2004). Gamma rays (60Co) and thermal neutron induced mutants in popcorn (Zea mays var. Praccox Sturt). *Nigerian J. Sci. Res*, *4*(2), 52-63.
2. Ahloowalia, B. S., & Muluszynksi, M. (2001).Induced mutations- A new paradigm in plant breeding. Euphytica,118(2), 167-173.
3. Alonso, J. M., Stepanova, A. N., Leisse, T. J., Kim, C. J., Chen, H., Shinn, P., & Gadrinab, C. (2003). Genome-wide insertional mutagenesis of Arabidopsis thaliana. *Science*, *301*(5633), 653-657.
4. Caldwell, D. G., McCallum, N., Shaw, P., Muehlbauer, G. J., Marshall, D. F., & Waugh, R. (2004). A structured mutant population for forward and reverse genetics in Barley (Hordeum vulgare L.). *The Plant Journal*, *40*(1), 143-150.

Vol. 14 (3) 271-278, July 2020, ISSN 0973-8916 (Print), 2230-7303 (Online)
DOI: 10.5530/ctbp.2020.3.28

5. Colbert, T., Till, B. J., Tompa, R., Reynolds, S., Steine, M. N., Yeung, A. T., &Henikoff, S. (2001). High-throughput screening for induced point mutations. *Plant physiology*, *126*(2), 480-484.

6. Dakshinamurthy, A., Nyswaner, K. M., Farabaugh, P. J., &Garfinkel, D. J. (2010). BUD22 affects Ty1 retrotransposition and ribosome biogenesis in Saccharomyces cerevisiae. *Genetics*, *185*(4), 1193-1205.

7. Dumanovic´ J, Denic´ M, Jovanovic´ C, Ehrenberg L (1968) Radiation-induced heritable variation of quantitative characters in wheat. Hereditas 62: 221–238

8. Emmanuel, E., & Levy, A. A. (2002). Tomato mutants as tools for functional genomics. *Current opinion in plant biology*, *5*(2), 112-117.

9. Greene EA, Codomo CA, Taylor NE, Henikoff JG, Till BJ, Reynolds SH, Enns LC, Burtner C, Johnson JE, Odden AR, et al (2003) Spectrum of chemically induced mutations from a large-scale reverse-genetic screen in Arabidopsis. Genetics 164: 731–740.

10. Knapp S, Larondelle Y, Robberg M. Furtek D, Theres K (1994) Transgenic tomato lines containing Ds elements at defined genomic positions as tools for targeted transposon tagging. Mol Gen Genet 243: 666–673

11. Kon, E., Ahmed, O. H., Saamin, S., & Majid, N. M. (2007). Gamma radiosensitivity study on long bean (Vignasesquipedalis). *Am. J. Applied Sci*, *4*(12), 1090-1093.

12. Krysan, P. J., Young, J. C., &Sussman, M. R. (1999). T-DNA as an insertional mutagen in Arabidopsis. *The plant cell*, *11*(12), 2283-2290.

13. Li X, Song Y, Century K, Straight S, Ronald P, Dong X, Lassner M, Zhang Y (2001) A fast neutron deletion mutagenesis-based reverse genetics system for plants. Plant J 27: 235–242

14. Matsukura, C., Yamaguchi, I., Inamura, M., Ban, Y., Kobayashi, Y., Yin, Y. G., & Nishimura, S. (2007). Generation of gamma irradiation-induced mutant lines of the miniature tomato (Solanum lycopersicum L.) cultivar 'Micro-Tom '. *Plant Biotechnology*, *24*(1), 39-44.

15. McCallum CM, Comai L, Greene EA, Henikoff S (2000a) Targeted screening for induced mutations. Nature Biotechnol 18: 455–457

16. McCallum CM, Comai L, Greene EA, Henikoff S (2000b) Targeting induced local lesions in genomes (TILLING) for plant functional genomics. Plant Physiol 123: 439–442.

17. Mehandjiev A, Kosturkova G, Mihov M. 2001. Enrichment of Pisumsativum gene resources through combined use of physical and chemical mutagens. Israel J. Plant Sci., 49: 279-284.

18. Meissner, R., Jacobson, Y., Melamed, S., Levyatuv, S., Shalev, G., Ashri, A., & Levy, A. (1997). A new model system for tomato genetics. *The Plant Journal*, *12*(6), 1465-1472.

19. Menda, N., Semel, Y., Peled, D., Eshed, Y., &Zamir, D. (2004). In silico screening of a saturated mutation library of tomato. *The Plant Journal*, *38*(5), 861-872.

20. Morita, R., Kusuba, M., Iida, S., Yamaguchi, H., Nishio, T., &Nishima, M. (2009). Molecular characterization of mutations induced by gamma irradiation in rice. *Genes & genetic systems*, 84(5), 361-370.

21. Naito, K., Kusaba, M., Shikazono, N., Takano, T., Tanaka, A., Tanisaka, T., & Nishimura, M. (2005). Transmissible and nontransmissible mutations induced by

Vol. 14 (3) 271-278, July 2020, ISSN 0973-8916 (Print), 2230-7303 (Online)
DOI: 10.5530/ctbp.2020.3.28

irradiating Arabidopsis thaliana pollen with ã-rays and carbon ions. *Genetics*, *169*(2), 881-889.

22. Okabe, Y., Asamizu, E., Saito, T., Matsukura, C., Ariizumi, T., Brès, C., &Ezura, H. (2011). Tomato TILLING technology: development of a reverse genetics tool for the efficient isolation of mutants from Micro-Tom mutant libraries. *Plant and cell physiology*, *52*(11), 1994-2005.

23. Parinov, S., &Sundaresan, V. (2000). Functional genomics in Arabidopsis: large-scale insertional mutagenesis complements the genome sequencing project. *Current opinion in biotechnology*, *11*(2), 157-161.

24. Rajesh, N., Prashanth, P. J. E., &Basha, P. O. (2014). Development of a Mutant Genetic Resource of Tomato Solanum lycopersicum L. cv. ArkaVikas. *Annals of Biological Research*, *5*(11), 1-6.

25. Rawat, N., Sehgal, S. K., Joshi, A., Rothe, N., Wilson, D. L., McGraw, N., Gill, B. S. (2012). A diploid wheat TILLING resource for wheat functional genomics. *BMC plant biology*, *12*(1), 205.Sikder,S P. Biswas, P. Hazra, S. Akhtar A. Chattopadhyay, A. M. Badigannavar and S. F. D'Souza (2013) Induction of mutation in tomato (Solanum lycopersicum L.) by gamma irradiation and EMS Indian Journal of Genetics 73(4): 392-399

26. Sabetta, W., Alba, V., Blanco, A., &Montemurro, C. (2011). sunTILL: a TILLING resource for gene function analysis in sunflower. *Plant methods*, *7*(1), 20.

27. Saito, T., Ariizumi, T., Okabe, Y., Asamizu, E., Hiwasa-Tanase, K., Fukuda, N., &Ezura, H. (2011). TOMATOMA: a novel tomato mutant database distributing Micro-Tom mutant collections. *Plant and cell physiology*, *52*(2), 283-296.

28. Sato Y, Shirasawa K, Takahashi Y, Nishimura M, Nishio T (2006) Mutant selection from progeny of gamma-ray-irradiated rice by DNA heteroduplex cleavage using Brassica petiole extract. Breeding Sci 56: 179–183

29. Sato, S., Shirasawa, K., &Tabata, S. (2013). Structural analyses of the tomato genome. *Plant Biotechnology*, 13-0707.

30. Schreiber, M., Barakate, A., Uzrek, N., Macaulay, M., Sourdille, A., Morris, J.,& Waugh, R. (2019). A highly mutagenised barley (cv. Golden Promise) TILLING population coupled with strategies for screening-by-sequencing. *Plant methods*, *15*(1), 99.

31. Sessions A, Burke E, Presting G, Aux G, McElver J, Patton D, Dietrich B, Ho P, Bacwaden J, Ko C, Clarke JD, Cotton D, Bullis D, Snell J, Miguel T, Hutchison D, Kimmerly B, Mitzel T, Katagiri F, Glazebrook J, Law M, Goff SA.(2002) A High throughput Arabidopsis revers genetics system. Plant Cell 14(12):2985-94.

32. Sikder, S., Ravat, V. K., Basfore, S., &Hazra, P. (2015). Research Article Isolation of induced mutants using gamma ray and ethyl methane sulphonate in Tomato (Solanum lycopersicum L.). *Electronic Journal of Plant Breeding*, *6*(2), 464-471.

33. Stöber, G., Nöthen, M. M., Pörzgen, P., Brüss, M., Bönisch, H., Knapp, M.,& Propping, P. (1996). Systematic search for variation in the human norepinephrine transporter gene: identification of five naturally occurring missense mutations and study of association with major psychiatric disorders. *American journal of medical genetics*, *67*(6), 523-532.

34. Sussman, M. R., Amasino, R. M., Young, J. C., Krysan, P. J., & Austin-Phillips, S. (2000). The Arabidopsis knockout facility at

Vol. 14 (3) 271-278, July 2020, ISSN 0973-8916 (Print), 2230-7303 (Online)
DOI: 10.5530/ctbp.2020.3.28

the University of Wisconsin–Madison. *Plant Physiology*, *124* (4), 1465-1467.

35. Tadege, M., Wen, J., He, J., Tu, H., Kwak, Y., Eschstruth, A.,&Ratet, P. (2008). Large scale insertional mutagenesis using the Tnt1 retrotransposon in the model legume Medicagotruncatula. *The Plant Journal*, *54*(2), 335-347.

36. Tanksley S.D., (1993) Mapping Polygenes. Annual Review of Genetics Vol. 27:205-233.

37. Thomas CM, Jones DA, English JJ, Carroll BJ, Bennetzen JL, Harrison K, Burbidge A, Bishop GJ, Jones JD (1994) Analysis of the chromosomal distribution of transposon-carrying T-DNAs in tomato using the inverse polymerase chain reaction. Mol Gen Genet 242: 573–585.

38. Till, B. J., Cooper, J., Tai, T. H., Colowit, P., Greene, E. A., Henikoff, S., &Comai, L. (2007). Discovery of chemically induced mutations in rice by TILLING. *BMC plant biology*, *7*(1), 19.

39. Till, B. J., Reynolds, S. H., Greene, E. A., Codomo, C. A., Enns, L. C., Johnson, J. E.,&Henikoff, J. G. (2003). Large-scale discovery of induced point mutations with high-throughput TILLING. *Genome research*, *13*(3), 524-530.

40. Till, B. J., Reynolds, S. H., Weil, C., Springer, N., Burtner, C., Young, K.,& Greene, E. A. (2004). Discovery of induced point mutations in maize genes by TILLING. *BMC plant biology*, *4*(1), 12.

41. Wani, A. A. (2009). Mutagenic effectiveness and efficiency of gamma rays, ethyl methane sulphonate and their combination treatments in chickpea (Cicer arietinum L.). *Asian Journal of Plant Sciences*, *8*(4), 318.

42. Wu, J. L., Wu, C., Lei, C., Baraoidan, M., Bordeos, A., Madamba, M. R. S.,& Bruskiewich, R. (2005). Chemical-and irradiation-induced mutants of indica rice IR64 for forward and reverse genetics. *Plant molecular biology*, *59*(1), 85-97.

43. Xin, Z., Wang, M. L., Barkley, N. A., Burow, G., Franks, C., Pederson, G., & Burke, J. (2008). Applying genotyping (TILLING) and phenotyping analyses to elucidate gene function in a chemically induced sorghum mutant population. *BMC Plant Biology*, *8*(1), 103.

Current Trends in Biotechnology and Pharmacy
Vol. 14 (3) 279-288, July 2020, ISSN 0973-8916 (Print), 2230-7303 (Online)
DOI: 10.5530/ctbp.2020.3.29

Enhanced L-lysine production through chemical mutagenesis in *Corynebacterium glutamicum* MTCC 25069

Ramesh Malothu*[1]
[1]School of Biotechnology, Institute of Science and Technology, Jawaharlal Nehru Technological University, Kakinada - 533003, A.P, India
*Corresponding author : ramesh_biotech@jntuk.edu.in

Abstract

Lysine is one of the most commercially available amino acid, which is chiefly used as a feed additive, human medicine and as a dietary supplement. In the present day, *Corynebacterium glutamicum* is the most popularly known microorganism for the industrial biosynthesis of lysine. The purpose of this study was to improve the yield of lysine production by chemical mutagenesis. In this study the culture conditions were optimized and the maximum growth was observed at 37p C, pH-7.4 for 72 hours.

The chemical mutagen, N Ethyl N Nitroso Urea (ENU) was used to develop the auxotrophic mutants by treating the wild type strain with different concentrations of ENU (i.e.,35mM, 50mM, 70mM, and 100mM) at different time periods (i.e.,0, 5, 10, 15, 20, and 25mins). The obtained mutants were then inoculated in seed culture medium enriched with methionine and threonine and all the mutants obtained were screened for lysine concentrations.

The most potent auxotrophic mutant developed in this study produced 30.2 g/l lysine when the culture was exposed to ENU of 70mM concentration for 10 minutes.

Keywords: L-lysine, *Corynebacterium glutamicum,* N Ethyl N NitrosoUrea (ENU), mutagenesis, auxotrophs, seed culture medium.

Introduction

L Lysine is one of the most important essential amino acids which could be used in many biophysical mechanisms in the living organisms. Corynebacterium glutamicum is used to produce L Lysine commercially[1]. L-Lysine is an essential amino acid which is utilized in many biochemical reactions like phosphorylation and also used as an additive for fodder crops[2]. Annually around 80, 00, 00 tones were produced which made L Lysine second among global amino acid synthesis at industrial scale[3,4]. Chemical synthesis, enzymatic method, fermentation, extraction from protein Hydrolysate, genetic engineering and protoplast fusions were several kinds of technologies employed in L Lysine synthesis from Corynebacterium glutamicum[3,26]. L-lysine is one of the most deficient components found in the food of both human and animals. Animal feed generally contains a less quantity of L-lysine and is not synthesized by cattle, poultry or other livestock, so L-lysine will be added as a food supplement for animals to meet feed requirements[6]. L-Lysine, one of the eight essential amino acids for animals and humans which is used as feed additives, dietary supplements and also as an ingredient of pharmaceuticals and cosmetics[7].

Corynebacterium glutamicum is a non-lethal and non-emulsifying gram-positive bacterium. It exhibits a low protease activity in the culture and

Vol. 14 (3) 279-288, July 2020, ISSN 0973-8916 (Print), 2230-7303 (Online)
DOI: 10.5530/ctbp.2020.3.29

can secrete protease-sensitive proteins into the culture supernatant[14]. C. glutamicum is a gram-negative bacteria with the absence of lipopolysaccharide removed in the production of therapeutic proteins[15] increases the yield by reducing the purification steps. C. glutamicum is generally recognized as safe (GRAS) for the industrial biochemical production of L Lysine and L glutamate[16].

Corynebacterium glutamicum is one of the major microorganisms used in amino acid synthesis. The Corynebacterium glutamicum is a rod-shaped bacteria, aerobic and gram-positive bacteria grows in the soil, on the surfaces of vegetables and fruits[17]. C.glutamicum has the capability to metabolize glucose, fructose, and sucrose[18, 29]. C. glutamicum utilizes many different kinds of carbohydrates, organic acids, and alcohol as a carbon and energy source for rapid microbial growth and for many amino acids synthesis[24, 25]. The glucose, or sucrose or any carbon source is utilized by the Corynebacterium glutamicum for l lysine synthesis by fermentation[28]. The time of incubation is reported for maximum L Lysine is between 48 hrs to 72 hrs[30, 31]. The ddh recombinant Corynebacterium glutamicum MTCC 25069 produces more amounts of L Lysine compared to Wild type. This is because of the expression of more amount of ddh which acts as an enzyme for the substrate 2,6 dicarboxylic acid with the participation of less number of enzymes. Chemical mutagenesis with ENU increased the yield of L Lysine in the mutant than the Wild type strain[27]. The ENU causes insertion or deletion mutation and shows its effect on protein synthesis. The ENU causes mutation in Homoserine dehydrogenase gene to cause the Homoserine Auxotrophs of C. glutamicum[21].

Generally, the Aspartyl â semialdehyde is produced in two ways. In the Krebs cycle of Corynebacterium glutamicum, the Oxaloacetic acid (OAA)[19,20] undergoes transamination reaction with the presence of *glutamate: oxaloacetate: transaminase* enzymes produce aspartyl â semi aldehyde which further produces homoserine and L L diaminopimelate (2,3 meso- DAP) by two different pathway[1]. The Aspartyl â semialdehyde is also formed from *Aspartate dehydrogenase* from Aspartyl phosphate which was formed from Aspartate by *Aspartate kinase*[2,19]. The aspartyl â-semi aldehyde acts as a common substrate to produce L Lysine through L L diaminopimelate (2,3-DAP) and Methionine or threonine through homoserine[1,28]. The aspartylâ-semi aldehyde converts to Homoserine by reacting with *homoserine dehydrogenase*[4] which participates in the Homoserine pathway in the production of Threonine and Methionine[22,23]. Homoserine reacts with *MetA*[6] and produces O-Acetylhomoserine which reacts with *Met B* synthesize Cystathionine further reacts with *C*[7] to produce Homocysteine finally reacts with *Met E* or *Met H* to produce methionine or Homoserine reacts with homoserine kinase produces L homoserine phosphate and converts to threonine[11] by Threonine synthase in Homoserine pathway. Aspartyl â semi aldehyde reacts with *2,3 Dihydrodipicolinate synthase* produces 2,3 Dihydropicolinate which further reduces to 2,6 Dicarboxylic acids by 2,3 *Dihydrodipicolinate reductase*. Corynebacterium glutamicum chose three kinds of enzymes namely *Acetyltransferase* or *Succinyl Transferase* or *diaminopimelate dehydrogenase (ddh)* to produce L L diaminopimelate (2,3 meso DAP). The LL diaminopimelate (2,3 meso DAP) converts to L Lysine by *Lysine synthase*. By Recombination with ddh gene with a constitutive promoter enhances the productivity of L Lysine by diverting the acetyltransferase and succinic transferase pathway to ddh pathway. The Chemical Mutagen N-nitroso-N-ethyl urea **(**ENU)[3,9] has the capability to cause deletion or insertion mutation in the *Homoserine dehydrogenase*[18] enzyme and blocks the Homoserine Pathway which generally leads to the production of threonine and Methionine. This block in the homoserine pathway diverts the aspartic â-semialdehyde to react with 2,3 Dihydrodipicolinate synthase the enzyme to produce more amounts of "-diaminopimelate (" DAP) through ddh pathway.2,3 Dihydrodipicolinate synthase [35] converts aspartic β-semialdehyde to

Vol. 14 (3) 279-288, July 2020, ISSN 0973-8916 (Print), 2230-7303 (Online)
DOI: 10.5530/ctbp.2020.3.29

2,3 Dihydropicolinate. In the presence of reductase 2,3 Dihydropicolinate reduces to Piperidine 2,6, dicarboxylic acid. The formation of DAP will be done by binding of Piperidine 2,6, dicarboxylic acid with three different enzymes acetyltransferase or Succinyl transferase or diaminopimelate dehydrogenase enzymes leads to three different pathways for the L Lysine production through DAP. 2,6 dicarboxylic acid reacts with *acetyl transferase* produces the N – acetyl 2 –amino 6-keto L-pimelate which reacts with the enzyme *aminotransferase* produces N- Acetyl- L- L - diaminopimelate produces L- L- DAP by *deacetylase* in the acetyltransferase pathway which is a three-step pathway. 2,6 dicarboxylate reacts with Succinyl transferase to produce N Succinyl 2- amino 6 keto L pimelate which reacts with *dap C* Produces N Succinyl L-L diaminopimelate which again reacts with *dap E* gives L L diaminopimelate is also a three step pathway. The ddh recombinant strain produces more L L diaminopimelate (2,3 meso DAP) by overexpression of ddh enzyme which follows ddh pathway for the production of L L diaminopimelate (2,3 meso-DAP) by reacting with 2,6 Dicarboxylic acid as substrate by eliminating the more number of reactions that were in the remaining *acetyltransferase* and *Succinyltransferase* pathways by overexpression of *ddh* by the ddh recombinant strain of C. glutamicum MTCC 25069 strain with constitutive promoter.

Materials and Methods

Chemicals used in this study: Seed culture medium: (Peptone 5 g/l, Yeast extract 3.75 g/l, NaCl 5 g/l, KH_2PO_4 25 g/l, K_2HPO_4 25 g/l,) [D-Glucose 10 g/l, $(NH_4)_2SO_4$ 17.46 g/l, $ZnSO_4$ 0.05 g/l, $FeSO_4.7H_2O$ 0.02 g/l, $MnSO_4.5H_2O$ 0.02 g/l, $MgSO_4.7H_20$ 0.04 g/l, Methionine 2 g/l, Threonine 2 g/l].

Optimization of Corynebacterium glutamicum MTCC 25069 : The culture conditions of *Corynebacterium glutamicum* were optimized to improve the the yield of L-lysine.

Optimal pH: In order to find optimal pH, the temperature and time of incubation were kept constant. The 24hr broth culture which was incubated at different pH levels was centrifuged and the quantification of protein was done by Lowry's method.

Optimal temperature: To find the optimal temperature, the pH and time of incubation were kept constant. The 24hr broth culture which was incubated at different pH levels was centrifuged and the quantification of protein was done by Lowry's method.

Optimal time: In order to find the optimal time, pH and temperature of the bacterial cultures were kept constant. The cultures were incubated at different time intervals. The samples were then collected and the total protein was estimated by lowry's method.

Mutation of Corynebacterium glutamicum MTCC 25069 : The bacterial strain *Corynebacterium glutamicum* MTCC 25069 was mutated by using the chemical mutagen N Ethyl N NitrosoUrea. The mutation of this bacteria was carried out at different concentrations of ENU (i.e., 35mM, 50mM, 70mM, and 100mM) and the auxotrophs were isolated as per given below. Seed culture medium was used for the growth of mutant bacterial cells.

Procedure: The wild type bacterial cells were grown on Luria Bertani (LB) broth and 10ml of LB broth was taken in eight falcon tubes and was inoculated with the growth. These tubes were incubated at 37p C for 24 hours and were used for mutagenesis purpose. After 24 hours the tubes were centrifuged at 10000 RPM for 5 minutes and the pellets were collected. The pellets were suspended in 3ml Sodium Citrate buffer (pH 4.1) and again centrifuged at 10000 RPM for 5 minutes. The pellets were again resuspended in Sodium Citrate buffer containing 1.2ml ENU solution. The cultures were incubated for 0, 5, 10, 15, 20 and 25 minutes. The growth culture without adding mutagen was also run along with the test samples

Vol. 14 (3) 279-288, July 2020, ISSN 0973-8916 (Print), 2230-7303 (Online)
DOI: 10.5530/ctbp.2020.3.29

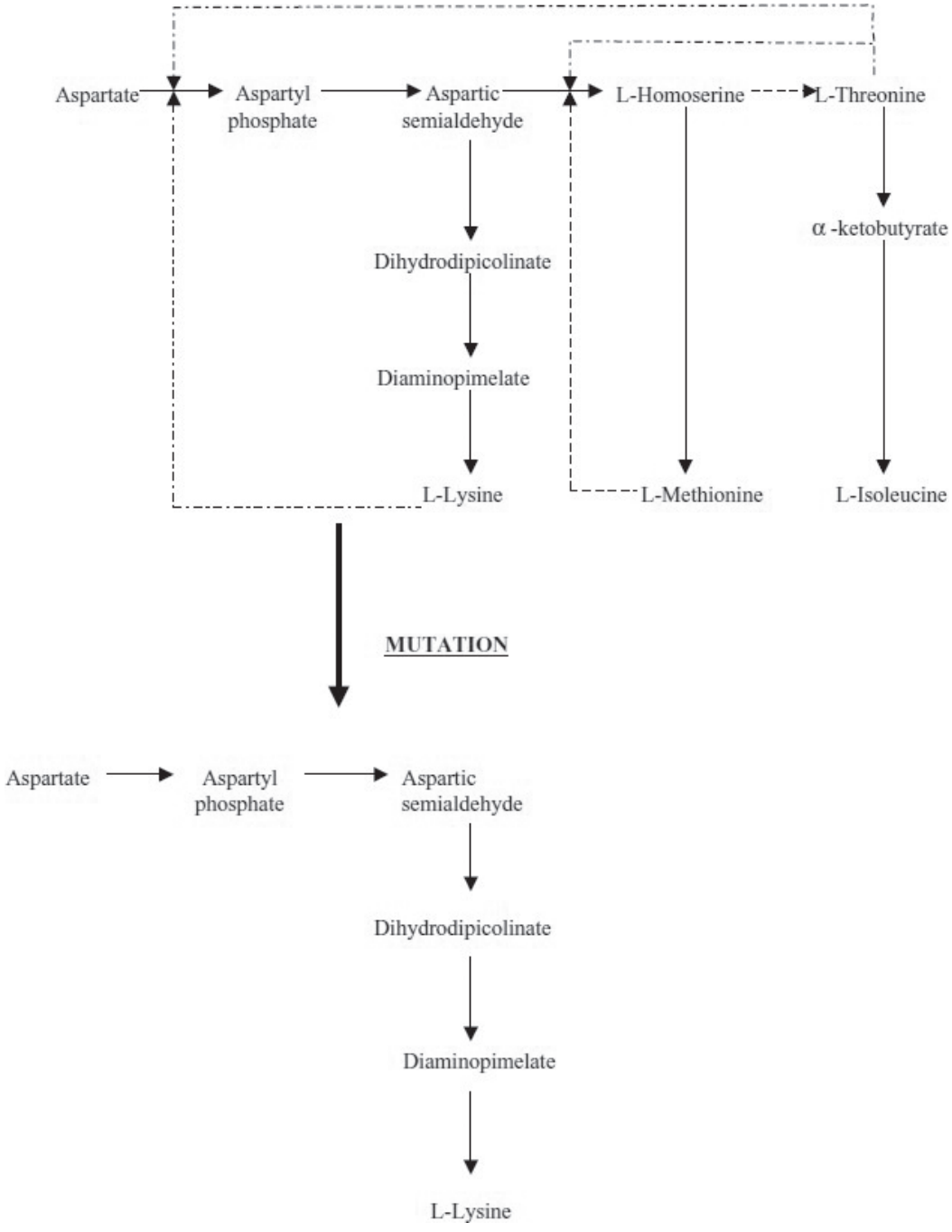

Fig. 1: Deregulation of lysine synthesis in auxotrophs (Nakayama, 1985).

Vol. 14 (3) 279-288, July 2020, ISSN 0973-8916 (Print), 2230-7303 (Online)
DOI: 10.5530/ctbp.2020.3.29

under similar conditions. After incubation, the samples were centrifuged at 10000 RPM for 5 minutes and the pellets were collected. The pellets were now washed with 3ml Sodium Citrate buffer and again centrifuged at 10000 RPM for 5 minutes to remove ENU and the resultant pellets were resuspended in 3ml of Sodium Citrate buffer. These pellets were inoculated in seed culture medium enriched with methionine and threonine and were incubated at 37p C for 3 days.

Isolation of auxotrophs: The growth obtained was inoculated in 1ml seed culture medium containing no methionine and threonine. To this, 100 units of penicillin G was added and incubated on shaking incubator for 20 hours at 37p C. After 20 hours, 50 units of penicillinase was added to each tube and left for 10 minutes.100ul of this growth was inoculated on seed culture medium plates without methionine and threonine and with seed culture medium with methionine and threonine. These plates were incubated at 37p C for 3 days. Colonies that grow on seed culture medium with methionine and threonine but not on seed culture medium without methionine and threonine were isolated. These isolated colonies were screened for lysine production. The samples were centrifuged at 15000 rpm for 10 minutes. The supernatant was collected and analyzed for lysine concentration.

Qualitative and quantitative analysis: For the qualitative analysis of lysine, paper chromatography was used whereas quantitative estimation was done by using the Ninhydrin method.

Results and Discussion :

Optimal pH: The pH of the media's were adjusted to 2, 5, 7.4, 9 and 11. From the values obtained from growth turbidity, (For total protein estimation) an efficient growth for *Corynebacterium glutamicum* MTCC 25069 was observed at an optimal pH of **7.4** (as shown in Fig. 3).

Optimal temperature: The cultures were incubated at different temperatures (i.e. 10p C, 25p C, 37p C, and 45p C). The optimal temperature required for the growth of *Corynebacterium glutamicum* MTCC 25069 is 37p C (as shown in Fig. 4).

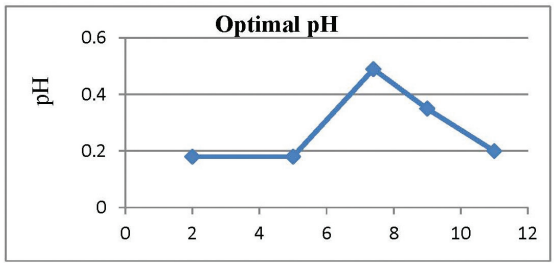

Fig. 2: Optimal pH

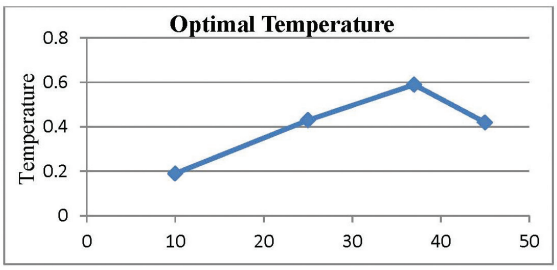

Fig. 3: Optimal temperature

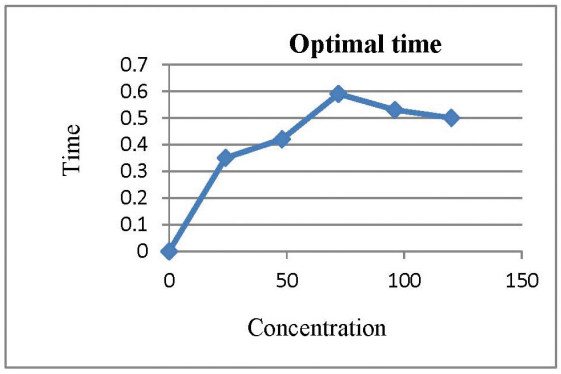

Fig. 4: Optimal time

Optimal time: Fermentation was carried out for 120 hours and for every 24 hours the samples were collected to measure growth turbidity.The growth turbidity has increased after 48 hours and was maximum at 72 hours. Later the concentration of protein gradually decreased (as shown in Fig. 5).

Vol. 14 (3) 279-288, July 2020, ISSN 0973-8916 (Print), 2230-7303 (Online)
DOI: 10.5530/ctbp.2020.3.29

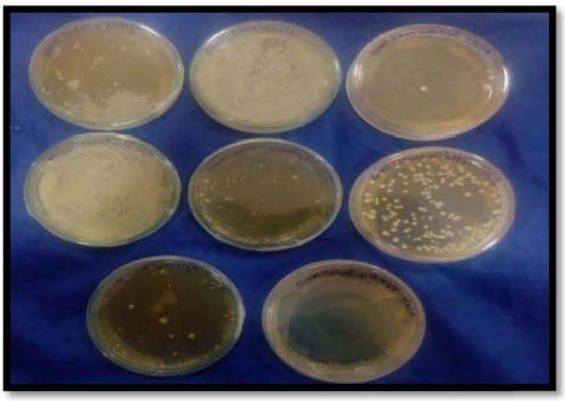

Fig. 5: Culture plates treated with 35mM concentration of ENU.

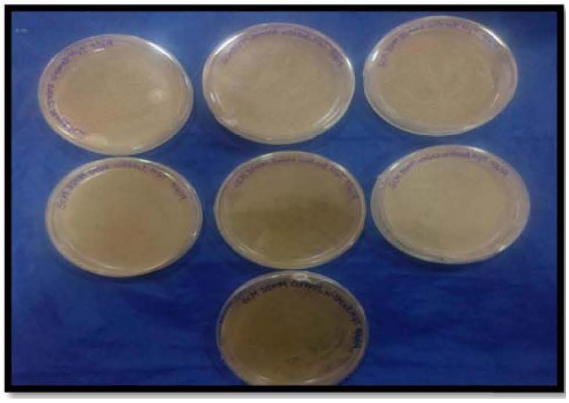

Fig. 6: Culture plates treated with 50mM concentration of ENU.

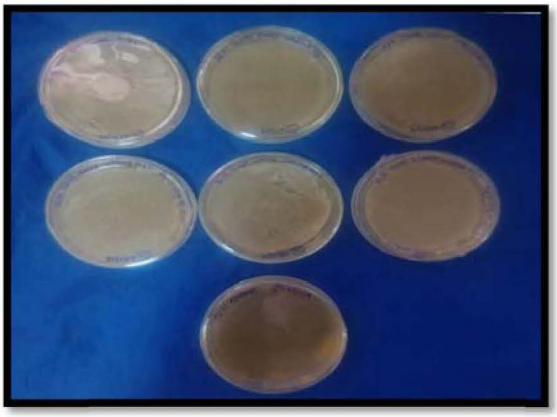

Fig. 7: Culture plates treated with 70mM concentration of ENU.

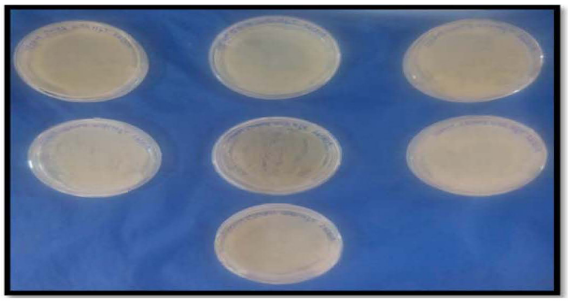

Fig. 8: Culture plates treated with 100mM concentration of ENU.

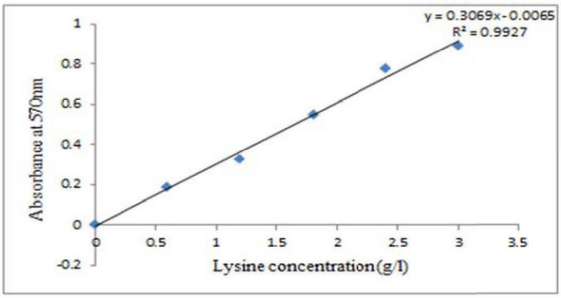

Fig. 9: Standard graph for Ninhydrin method.

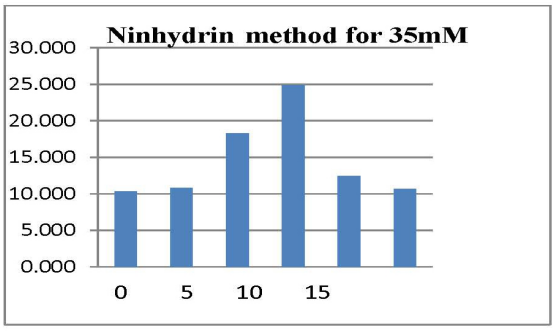

Fig. 10: Ninhydrin method for 35mM.

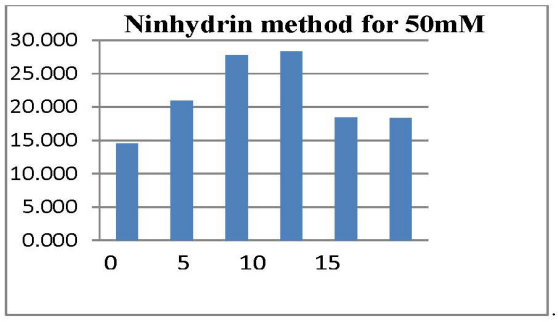

Fig. 11: Ninhydrin method for 50mM.

Vol. 14 (3) 279-288, July 2020, ISSN 0973-8916 (Print), 2230-7303 (Online)
DOI: 10.5530/ctbp.2020.3.29

Table 1: Concentration of Lysine in mutants developed from Corynebacterium glutamicum MTCC 25069

Mutants	Lysine
Wild type	concentration (g/l)
MTCC 25069	14.959
A0	10.318
A5	10.835
A10	18.275
A15	24.873
A20	12.453
A25	10.706
B0	14.507
B5	20.927
B10	27.784
B15	28.302
B20	18.437
B25	18.356
C0	26.701
C5	30.275
C10	24.356
C15	19.051
C20	18.614
C25	17.838
D0	11.790
D5	10.027
D10	10.431
D15	6.970
D20	13.180
D25	5.790

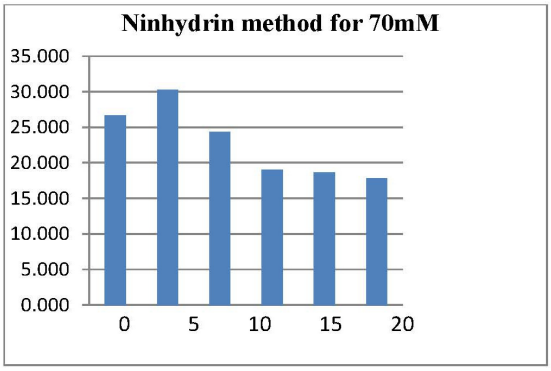

Fig. 12: Ninhydrin method for 70mM.

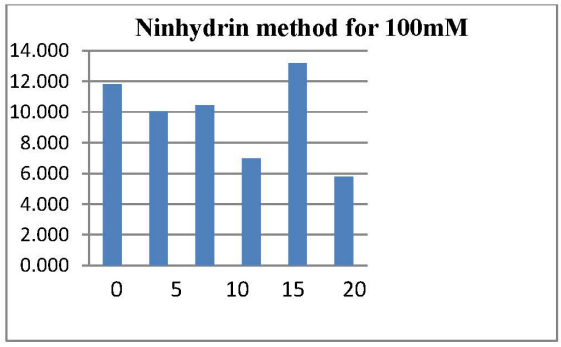

Fig. 13: Lysine estimation by Ninhydrin method for 100mM.

Well no.1 and 2: reference
Well no 3 to 6: A15, B15, C5, D20.

Fig. 14: SDS-PAGE gel showing lysine bands

Vol. 14 (3) 279-288, July 2020, ISSN 0973-8916 (Print), 2230-7303 (Online)
DOI: 10.5530/ctbp.2020.3.29

Isolation of auxotrophs: The Auxotrophs were isolated after spreading chemically (ENU) mutated samples onto the seed culture medium containing methionine and threonine and on to the seed culture medium without methionine and threonine. Colonies that grow only on methionine and threonine containing plates but not on plates without methionine and threonine were considered as auxotrophs. These auxotrophs were isolated after several repeats and a reduced growth was observed on the plates which were analyzed for lysine production. (From Fig 6 to Fig 9)

Quantitative analysis:

Ninhydrin method: This method was used to quantify lysine concentration in both mutated samples and in the wild type strain of *Corynebacterium glutamicum* MTCC 25069.

Here y = absorbance at 440nm and x = Concentration of lysine (g/l) (Fig. 11).

The concentration of lysine was calculated and presented in Table 15:

Out of 24 mutants, only 13 (represented in bold in the table) showed an increase in the lysine

yield, compared to the wild type strain which is grown in the seed culture medium.

In both the sets A and B, the mutants obtained by treating the cultures with ENU for 15 minutes showed higher lysine concentration compared to the remaining samples.

In set A, the concentration of lysine has increased only in A10 and A15 mutants. Whereas in set B all the mutants showed an increase in lysine yield except B0.

All the mutants of set C showed an increase in the lysine concentration with the highest maximum yield of 30.275g/l by C5 mutant. All the mutants of set D showed a negative effect on the mutants as there was no increase in the lysine yield.

Graphs were plotted for each set of ENU concentrations from the values obtained from the Ninhydrin test (i.e., for 35mM,50mM,70mM, and 100mM).

From the (Fig. 16), it can be interpreted that, at 35mM concentration of ENU, the mutant sample treated for 15 minutes showed the highest lysine concentration compared to the remaining mutant samples.

From (Fig. 13), it can be inferred that the mutant sample obtained by treating the wild type strain with 50mM ENU for 15 minutes produced the highest lysine concentration.

From the (Fig. 14), it can be interpreted that, at 70mM concentration of ENU, the mutant sample at 5 minutes showed the highest maximum lysine concentration.

The mutant samples obtained by treating the wild type strain with 100mM concentration of ENU at different time periods showed different concentrations of lysine, with the highest yield at 20minutes (Fig. 15).

SDS-PAGE: This method was performed to confirm whether lysine is present in the mutated sample and wild type strain.

At different concentrations of ENU, the mutant samples producing the highest lysine concentrations from each set were selected (i.e., A15, B15, C5, and D20).

In the above gel picture, the first two wells are loaded with L-lysine (reference) and the remaining wells are loaded with samples. After staining and destaining of the gel, bands were visible and they stand along the same line with lysine and by comparing with the reference (L-lysine) it can be inferred that lysine was present in the mutant samples (Fig. 16).

Conclusion

According to lysine production statistics in 2015, approximately 2.4 metric million tons of L-lysine is required every year, but there is an enormous shortage in the production of this amino acid as only 2 million tons of L-lysine is produced annually. Due to the increasing demand in the world market for this amino acid, there is a growing interest in the development and optimization in the fermentative process of L-lysine production.

Vol. 14 (3) 279-288, July 2020, ISSN 0973-8916 (Print), 2230-7303 (Online)
DOI: 10.5530/ctbp.2020.3.29

Of all the bacteria present, *Corynebacterium glutamicum* is an industrially important microorganism for the production of various amino acids, hence it has been selected for this study. Mutagenesis is carried out by using N Ethyl N NitrosoUrea (ENU) which is one of the potent alkylating chemical mutagens. (ENU) adds alkyl groups (an Ethyl group in ENU) to many positions on all four bases, mutagenesis is best correlated with an addition to the oxygen at the 6th position of guanine to create an O-6 alkylguanine. This addition results in GC '! AT transitions and would lead to direct mispairing with thymine.

In this study, the bacterial culture conditions were optimized and the maximum growth was observed at 37p C, pH 7.4 for 72 hours. The auxotrophic mutants were obtained by treating the wild type bacterial strain with different concentrations of ENU (i.e. 35mM,50mM,70mM, and 100mM) for different time periods (i.e 0, 5, 10, 15, 20 and 25 minutes). 13 out of 24 mutants showed a significant difference in the yield and productivity compared to the wild type strain.

The auxotrophic mutant treated with 70mM ENU for 5 minutes showed the highest lysine concentration of 30.2g/l.

From this, we can conclude that the mutagenic effect of ENU was significant when cells of *Corynebacterium glutamicum* MTCC 25069 were treated with 70mM concentration of ENU for 5 minutes.

Reference

1) Leuchtenberger, W. (1996). Amino acids–technical production and use. *Biotechnology: products of primary metabolism*, 465-502.

2) Schmid R D (2002) Pocket Atlas of biotechnology and genetic engineering. Wiley-VCH publishing company, First Edition.

3) Tosaka O, Takinami K, Aida K, Chibata I, Nakayama I, Takinami K, Yamada H (1986) *Biotechnology of amino acid production* 152–172.

4) Kinoshita S, Udaka S, Akita S (1961) Method of producing l-glutamic acid by fermentation. United States Patent Office, number 3.003.925 (Patented Oct. 10. 1961).

5) Wartenberg A (1989) Introduction to Biotechnology. Gustav Fischer Verlag, Stuttgart.

6) Eggeling, L., &Sahm, H. (1999). L-Glutamate and L-lysine: traditional products with impetuous developments. *Applied microbiology and biotechnology*, Anastassiadis, S. (2007). L-Lysine fermentation. *Recent patents on Biotechnology*, *1* (1), 11-24.

7) Blombach B, Schreiner M E, Holatko J, Bartek T, Oldiges M, Eikmanns B J (2007) L- Valine Production with Pyruvate Dehydrogenase Complex-Deficient *Corynebacterium glutamicum. Applied and Environmental Microbiology* 73: 2079-20.

8) Kumar, D., Garg, S., Bisaria, V. S., Sreekrishnan, T. R., & Gomes, J. (2003). Production of methionine by a multi-analogue resistant mutant of *Corynebacterium lilium*. *Process Biochemistry*, *38* (8), 1165-1171.

9) Lee, H. S., & Hwang, B. J. (2003). Methionine biosynthesis and it's regulation in *Corynebacterium glutamicum*: parallel pathways of transsulfuration and direct sulfhydrylation. *Applied microbiology and biotechnology*, *62*(5-6), 459-467.

10) Kumar, D., & Gomes, J. (2005). Methionine production by fermentation. *Biotechnology advances*, *23*(1), 41-61.

11) Kodym, A., &Afza, R. (2003). Physical and chemical mutagenesis. In *Plant functional genomics* (pp. 189-203). Humana Press.

12) Heslot, H., Ferrary, R., Levy, R., and Monard, C. (1959) Recherchessur les substances mutagenes (halogeno 2–ethyle)amines, derives oxygenes du sulfure de bis (chloro-

Vol. 14 (3) 279-288, July 2020, ISSN 0973-8916 (Print), 2230-7303 (Online)
DOI: 10.5530/ctbp.2020.3.29

2–ethyle), ester sulfoniques et sulfuriques, C.R. Seanc. Hebd. Acad. Sci., Paris 248, 729.

13) Heslot, H., Ferrary, R., Levy, R., and Monard, C. (1961) Induction de mutations chez l'orge. Efficacite relatives des rayons gamma, du sulfated'ethyle, du methane sulfonated'ethyleet de quelquesautres substances. Effects of ionizing radiation on seeds (Proc. Conf. Karlsruhe, 1960), IAEA, Vienna, 243–250.

14) Van Harten, A. M. (1998) Mutation Breeding Theory and Practical Applications. Cambridge University Press, Cambridge.

15) Malumbres, M., & Martin, J. F. (1996). Molecular control mechanisms of lysine and threonine biosynthesis in amino acid-producing corynebacteria: redirecting carbon flow. *FENU microbiology letters*, *143*(2-3), 103-114.

16) Anonymous,. Mechanisms of Gene Mutation (2004).

17) Ralph Kirby,. Fundamentals of biochemistry, cell biology and biophysics. Vol. 2,. Prokaryote Genetics (2003).

18) Textbook of *Industrial Microbiology*, *2nd edition* (*Biotechnology*) by *W*. *Cruger*and A.*Cruger*, Sinauer Associates, Sunderland, US (2004).

19) Jeremy W. Dale and Simon F. Park. Molecular Genetics of Bacteria, 5th edition. A John Wiley & Sons, Ltd., Publication (2010).

20) Nakayama K, Araki K, Kase H (1978) Microbial production of essential amino acid wit *Corynebacterium glutamicum* mutants. *Advances in Experimental Medicine and Biology* 105: 649-661.

21) Nakayama H V, Araki K (1973) Process for producing l-lysine. US patent 3,708,395.

22) Kelle R, Hermann T, Bathe B (2005) l-lysine production. In: Eggeling L, Bott M (eds) Handbook of *Corynebacterium glutamicum*. CRC Press, Boca Raton, 465–488.

23) Samanta T K, Y, Das S, Mondal S P, Chatterjee (1988) L-lysine production by auxotrophic mutants of Arthro-bacterglobiformis. *Acta Bio-technologica* 8: 527-533.

24) Sambanthamurthi R, P D Laverack and P H Clarke (1984) Lysine excretion by mutant strain of Pseudomonas aeruginosa. *FENU Microbiology Letters* 23: 11-15.

25) Fitzgerald G, Williams S (1975) Modified penicillin enrichment procedure for the selection of bacterial mutants. *Journal of bacteriology* 122:345-346.

26) Eggeling L, Sahm H (2005) New ubiquitous translocators: amino acid export by *Corynebacterium glutamicum* and *Escherichia coli. Archives of Microbiology* 180: 155 – 160.

Current Trends in Biotechnology and Pharmacy
Vol. 14 (3) 289-301, July 2020, ISSN 0973-8916 (Print), 2230-7303 (Online)
DOI: 10.5530/ctbp.2020.3.30

Green synthesis of silver nanoparticles from fractionated *Annona reticulata* leaf extract in different solvents and analysis of its antioxidant and antibacterial activity

Sugunakar.Y.J[1], Chandramati Shankar P[2]*.
[1, 2.] Department of Biotechnology, Yogi Vemana University, Kadapa, 516005
Andhra Pradesh, INDIA.
*Corresponding author : pchandra20@gmail.com

Abstract

Silver nanoparticles were synthesized from fractionated leaf extract in Hexane, Chloroform and Water. Synthesis of AgNPs was confirmed by change in color of leaf extract solution, followed by confirming of reduction of silver ions in the leaf extract by UV-Visible spectroscopy. The Surface Plasmon resonance (SPR) peak was observed from 400 to 450nm. The biosynthesized AgNPs were characterized by dynamic light scattering measurement (DLS), Zeta potential and Transmission electron microscopy (TEM). The XRD, Fourier transform infrared spectroscopy (FTIR), X-ray diffraction (XRD) analysis confirmed the crystalline nature of AgNPs and the presence of elemental silver. The size of the silver nano particles ranged from 10-50nm and were spherical in shape as found by DLS and TEM studies. The synthesized AgNPs showed higher antioxidant activity by DPPH assay as compared to the crude leaf extract. Antibacterial activity was higher in the synthesized AgNPs on observing the inhibition zone of Gram positive and Gram Negative bacteria.

Key words: AgNPs, Biosynthesis, Crystalline, Phytochemicals,Zeta potential.

Introduction

During the past decade production of Silver nanoparticles (AgNPs) has gained wide exposure due to its applications in different industries based on the unique physical, chemical, optical and biological properties of AgNPs. Biosynthesis of AgNPs can be carried out by Microorganisms and plant extracts or by physical and chemical methods. In case of Microorganisms, the synthesis is slow and time consuming, while in Physical method high energy radiation, microwave irradiation and inert gas condensation are used which is expensive . Whereas in chemical methods hazardous chemicals such as reductants, stabilizers and organic solvents, are used. The plant mediated biosynthesis of Silver Nanoparticles using plant extracts as a source of natural reductants has gained importance because of its higher stability, easier preparation procedure and no hazards to the environment as compared to chemical methods. The small size of AgNPs has paved the path to improve and gain more importance in pharmacological applications, electronics, optics, catalysis, food industry, agriculture, and textile industry and water treatment. Several studies have been carried out on synthesis of silver nanoparticles from plant extracts and it has been reported that the plant species is one main factor responsible for reduction of the silver ions. Apart from acting as reductants, Plant extracts also help in capping and stabilizing of nanoparticles (1).

Annona reticulata belongs to Annonaceae, a very large family of plants which comprise about 120 genera and more than 2000 species (2). *Annona reticulata*., is commonly known as

Vol. 14 (3) 289-301, July 2020, ISSN 0973-8916 (Print), 2230-7303 (Online)
DOI: 10.5530/ctbp.2020.3.30

Ramphal (Hindi), Ramasitapalam (Telugu), Ramachita (Tamil), Manilanilam (Malayalam), and Ramaphala (Kanada). It grows in tropical and subtropical region. It is a small tree with a height of seven to eight meters. Leaves of the plant are membranous, lanceolate, oblong lanceolate, acute, cuneate rounded at the base (3). It is a large evergreen shrub or small tree, grown commercially for its fruit.The leaves of *A. reticulata* have great medicinal properties due to the presence of phytochemicals like Annoreticuin, Solamin, Dopamine, Coclaurine, Acetogenin, Squamone (4). The leaves possess good antioxidant and antimicrobial activity. It is a medicinal plant used widely in ayurvedic system of medicine for the treatment of several diseases like dysentery, worm infections, hemorrhage, constipation, dysuria, and ulcer (5). *A. reticulata* possess various phytochemical constituents in Stem, Leaf and Root. The plant is reported to contain acetogenins which posses potential anticancer and anti-inflammatory property (6). Various plant parts like leaves, bark, seed and root are medicinally useful and they show many therapeutic activities as anticancer, CNS depressant, analgesic, antihyperglycemic, anti-inflammatory, antiproliferative, wound healing and antiulcer activity (7). The root contains aporphine alkaloids like liriodenine, norushinsunine, reticuline and one acetogenin neoannonin(8).

This is the first report of the biosynthesis of AgNPs using different leaf extract fractions in polar solvents like Hexane, Chloroform and Water. The Phytochemicals fractionated with different polar solvents of *A.reticulata* leaf were used to synthesize AgNPs. The synthesized AgNPs were characterized by UV-Vis spectroscopy, Dynamic Light Scattering (DLS), Zeta sensitizer, Fourier Transform Infrared spectroscopy (FTIR), X-ray diffraction (XRD) and Transmission Electron Microscopy (TEM). Various biological assays like Antioxidant and Antibacterial activities were carried out to evaluate their biomedical and pharmacological applications of *A.reticulata* leaf extract.

Materials and Methods

Silver nitrate was purchased from Avra synthesis Pvt.Ltd.,Nacharam, Hyderabad, Telangana State, India. Fresh leaves of *Annona reticulata* were collected from Mittapalem, Srinivasamangapuram village, Tirupathi region, Chittoor Disrict, Andhra Pradesh, India. The harvested leaf sample was authenticated by Dr. A. Mudhusudan Reddy, Assistant Professor, Department of Botany, Yogi Vemana University, Kadapa, Andhra Pradesh, India, and deposited in the herbarium with a voucher specimen number (AMR4855YVUH).

Preparation of Annona reticulata leaf powder: *A. reticulata* leaves were thoroughly washed with tap water, shade dried and then grounded into smooth powder and then transferred to air tight container and preserved at -20^{o}C in darkness till further use.

Extraction and fractionation of Annona reticulata leaf extract with hexane, chloroform and water *:* 500gm of *A.reticulata* leaf powder was soaked in 1000ml of 90% methanol for 48 hrs on rotary shaker for agitation at 35^{o}C. This leaf extract was later filtered and extracted by using Whatman filter paper No1. The filtrate was then concentrated on a rotary evaporator (Hidolph Germany make) at 35^{o}C temperature and under reduced pressure. This concentrated methanol extract of *A.reticulata* leaf was referred to as Crude (ArL Crude). The *A. reticulata* crude extract (ArL Crude) was dissolved in 500ml of distilled water and filtered to which 500ml of Hexane solvent was added this was followed by vigorous shaking. The layers were then allowed to separate by shaking for 6hr in a separating funnel (9). The separated hexane layer was collected and labelled as Fraction 1 *A. reticulata* Leaf Hexane Extract (F1-ArL HE). Similar procedure was followed and repeated with Chloroform solvent and this extract was labeled as Fraction 2 *A.reticulata* Leaf Chloroform Extract (F2-ArL CE), and the remaining aqueous extract was labeled as Fraction 3 *A.reticulata* Leaf Water Extract (F3- ArL WE). Each of the fractions obtained were dried and

Vol. 14 (3) 289-301, July 2020, ISSN 0973-8916 (Print), 2230-7303 (Online)
DOI: 10.5530/ctbp.2020.3.30

concentrated by using Rota vapor. The concentrated samples were collected into vials and stored at -20ÚC until further use.

Biosynthesis of silver nanoparticles (AgNPs) in fractionated A. reticulata leaf extracts : 100mg of all three fractions (hexane, chloroform and water) of leaf extracts were taken separately and added in individual flasks containing 100ml of 1mM $AgNO_3$ aqueous solution and then incubated in an oven at 80° C in darkness. This incubation leads to reduction of silver ions to AgNPs after 24hrs in darkness. The change in the color of the leaf extract fractions from green to dark brown in color indicated the formation of Silver Nano particles (10). The synthesized AgNPs in Hexane fraction of leaf extract was labelled as *A.reticulata* Leaf Hexane Extract AgNPs(ArL HE AgNPs), the synthesized AgNPs by chloroform extract was labelled as *A.reticulata* Leaf Chloroform Extract AgNPs(ArL CE AgNPs) and the synthesized AgNPs by water extract was labelled as *A.reticulata* Leaf Water Extract AgNPs (ArL WE AgNPs) respectively.

Characterization of synthesized AgNPs of A. reticulata leaf extract fractions : The reduction of silver ions in silver nitrate solution by *A. reticulata* leaf fractions was monitored by UV-visible spectroscopy (UV-1800 Shimadzu Co., Japan) ranging from 200 to 800nm at resolution of 1nm (11)

The particle size of the synthesized AgNPs were determined by Dynamic Light Scattering (DLS) technique and zeta potential was determined by using Zetasizer (HORIBA scientific sz-100) with a range of 0.1 to 10000nm at scattering of angle of 90° and 25°. For diameter measurement 1ml of sample was transferred to a plastic cuvette, and automatically equilibrated for 2min. For zeta potential analysis, 1ml of the sample was injected in to the zeta cell, and the measurement was repeated thrice.

The FTIR spectra analysis was carried out by JASCO FTIR-4700 with a range of 399.193$cm^{-1}$to 4000cm^{-1}.The synthesized AgNPs after the reaction were subjected to centrifugation at 10,000 rpm for 10min and then the precipitate was washed with deionized water to eliminate the uncoordinated biomolecules on the surface of AgNPs. The final product was collected and dried in a vacuum oven.

The X-ray diffraction (XRD) analysis of biosynthesized AgNPs was performed on the X-ray diffractometer (Brucker, D8 advance, Germany) operated at a voltage of 40kV and a current of 30mA at a wave length of 1.5406A, at scattering angle of 30°-80° range (12).

Transmission Electron Microscopy (TEM) studies was performed at 100kV, to determine the size and morphology of the biosynthesized AgNPs. Thus was done by taking one drop of the reaction mixture on silicon wafer and then the sample was evaporated and dried completely for further analysis.

Antioxidant assay (DPPH free radical scavenging activity) : 1, 1-Diphenyl 1-2-picrylhydrazyl (DPPH) free radical scavenging potential of phytochemical fractions and AgNPs of *A. reticulata* were evaluated by preparing 1mM of DPPH in Methanol solution (13). Phytochemicals of all fractions and AgNPs at different concentrations (0.1, 0.2, 0.3, 0.4, 0.5, 0.6, 0.7, 0.8, 0.9, and 1mg) were added to 1ml of 1mM of DPPH solution. The reactions was carried out under dim light and incubated for 30min. The change in the color of the reaction mixture from purple to yellow was monitored and measured at 517nm. Ascorbic acid (Vitamin C) was used as reference and methanol was taken as blank.

% of DPPH scavenged = (A ctrl – A test) / A ctrl x 100

A ctrl = Absorbance of the control reaction

A test = Absorbance of the test sample with DPPH

Antibacterial activity : The bacterial strains were obtained from Institute of microbial Technology (IMTEC), Chandigarh, India. The antibacterial

Vol. 14 (3) 289-301, July 2020, ISSN 0973-8916 (Print), 2230-7303 (Online)
DOI: 10.5530/ctbp.2020.3.30

assay was performed by disc diffusion method (14) against pathogenic bacteria like *Staphylococcus aureus* (MTCC-87)and *Bacillus subtilis* (MTCC 10619) which are (Gram-positive) and *Salmonella ebony* (MTCC 3384) and *Salmonella enteric* (MTCC 3858) which are Gram-negative bacteria. The bacteria were cultured in nutrient broth and kept for incubation at 35°C in an rotary shaker for 24hr. After incubation, 100µl of bacterial culture was uniformly spread on the surface of the freshly prepared nutrient agar petridishes with the help of sterile 'L' shaped glass rod. Simultaneously presterilized circular filter paper discs with a diameter of 25mm are dipped in 10µl of each sample leaf extracts with a concentration of 1mg and were placed on the surface of the bacterial plated petridish. Standard antibiotic Ampicillin (1mg/ml) was used as a positive control. Eventually the zone of inhibition was measured after incubation time of 24hr at 37°C.

Results and Discussion

UV-Visible spectroscopy analysis: The initial formation of AgNPs was monitored by change in color of all leaf extracts samples in all three solvents. The color was initially green and later turned to dark brown (Fig.1).

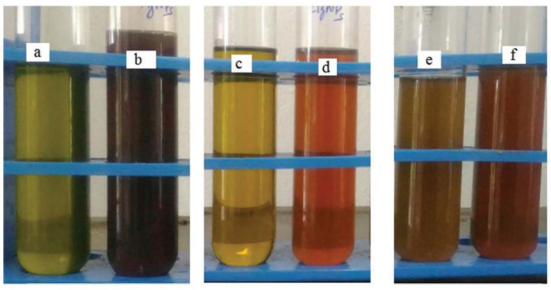

Fig. 1: Synthesis of AgNPs in *A.reticulata* leaf extracts in different solvents.

a. Leaf extract in Hexane
b. Synthesis of AgNPs in Hexane extract
c. Leaf extract in Chloroform
d. Synthesis of AgNPs in Chloroform extract
e. Leaf extract in Water
f. Synthesis of AgNPs in Water extract

The biosynthesized AgNPs exhibited a strong absorption Surface Plasmon resonance (SPR) band by UV visible spectral analysis as shown in (Fig.2). The well-defined SPR absorption at 446 nm, confirmed the synthesis of ArLHEAgNPs (Fig 2.a). SPR absorption peak at 439 nm, confirmed the synthesis of ArLCEAgNPs (Fig2.b) and SPR absorption peak at 441 nm, confirmed the synthesis of ArLWEAgNPs (Fig2 c).

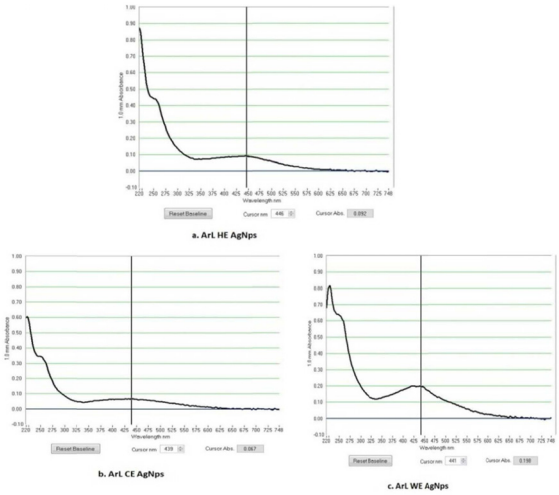

Fig. 2: UV–Vis absorption spectra of the synthesized AgNPs by *A.reticulata* leaf extract

(2.a) *A.reticulata* Hexane Extract AgNPs Shows the SPR absorption peak at 446 nm.
(2.b) *A.reticulata* Chloroform Extract AgNPs Shows the SPR absorption peak at 439 nm.
(2.c) *A.reticulata* Water Extract AgNPs Shows the SPR absorption peak at 441nm.

Determination of particle size by Dynamic Light Scattering (DLS) analysis: The synthesized AgNPs of *A. reticulata* Leaf extract was analyzed by DLS to determine the partical size and diameter.The average particle size is as shown in Table.1 and Fig .3. The results have shown that the average particle size of ArL HE AgNPs is

Vol. 14 (3) 289-301, July 2020, ISSN 0973-8916 (Print), 2230-7303 (Online)
DOI: 10.5530/ctbp.2020.3.30

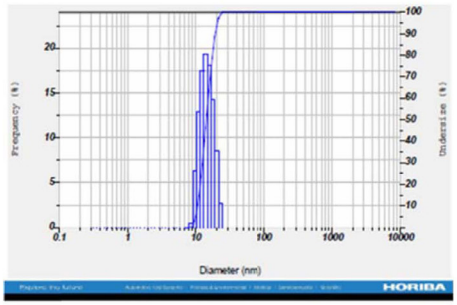

a. ArL HE AgNps

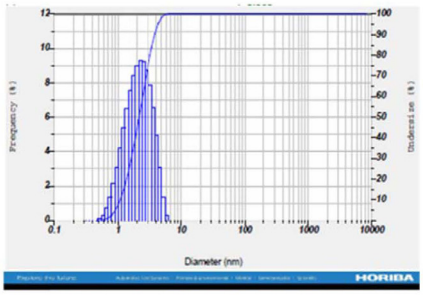

b. ArL CE AgNps

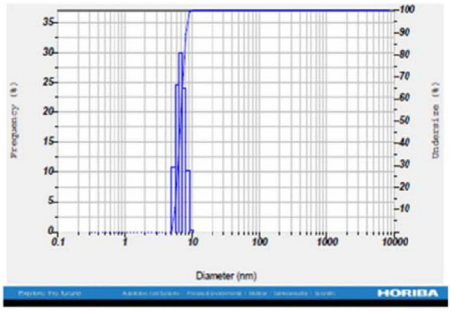

c. ArL WE AgNps

Fig. 3. Particle size of AgNPs synthesized by fractionated *A. reticulata* leaf extract. (a) Hexane Extract AgNPs (b) Chloroform Extract AgNPs (c) Water Extract AgNPs.

Table. 1. The average particle size of biosynthesized AgNPs from *A.reticulata* leaf extract

S.No	AgNPs of different solvent extracts	Particle size
1.	Hexane Extract AgNPs (ArL HE AgNPs)	14.1nm
2.	Chloroform Extract AgNPs (ArL CE AgNPs)	2.3 nm
3.	Water Extract AgNPs (ArL WE AgNPs)	6.8 nm

Table.2. The Zeta potential of AgNPs synthesized from fractionated *A. reticulata* leaf extract in different solvents.

S.No	AgNPs of different solvent extracts	Zeta potentialin mv
1.	Hexane Extract AgNPs (ArL HE AgNPs)	-28.0 mv
2.	Chloroform Extract AgNPs (ArL CE AgNPs)	-31.3 mv
3.	Water Extract AgNPs (ArL WE AgNPs)	-30 mv

Vol. 14 (3) 289-301, July 2020, ISSN 0973-8916 (Print), 2230-7303 (Online)
DOI: 10.5530/ctbp.2020.3.30

14.1nm, ArL CE AgNPs is 2.3nm and particle size of ArL WE is 6.8nm.

Zeta potential : The Zeta potential of the AgNPs of *A. reticulata* leaf extract fractions in Hexane, Chloroform and water was analyzed and is as shown in Table.2 and Fig.4.(a,b,c) shows the graphical representation of the Zeta potential. The negatively charged Nanoparticles prevented the agglomeration formation and lead to long term stability of the nanoparticles. In this study the synthesized AgNPs showed very high value of zeta potential and confirms the existence of repulsive force among the particles thus increasing the long term stability of the AgNPs.

FT-IR analysis : FT-IR analysis with synthesized AgNPs in different solvents to investigate the surface chemistry composition of AgNPs capped by the biomolecules in *Annona reticulata* leaf extract showed different peaks which is because of different functional groups involved in the synthesis and stabilization of AgNPs (Fig.5.a,b,c) various functional groups involved in the formation of AgNPs leaf extract in different solvents.

Table. 3. The various functional groups involved in the formation of AgNPs in different solvents (a) Hexane extract (b) Chloroform Extract and (c) Water Extract.

AgNps Sample Different solvents	FTIR peak (cm^{-1})	Functional group	Reference no
a. ArL HE AgNPs	3272.92	N–H stretching of amide II	15
(Hexane)	2941.98	–C–H stretching of –CH2 of Protein	16
	2128.37	CC or CN triple bond	17
	1618.19	C–C stretching	18
	1328.06	C–O stretching/ O–H	19
	1080.52	C–OH of the phenols	20
b. ArL CE AgNPs (chloroform)	3334.34	N–H stretching of the secondary amide of the protein	21
	2320.60	N–H/C–O stretching	22
	2093.32	CC or CN triple bond	23
	1608.74	C–O/aromaticC–C stretching	24
	1337.04	C–O stretching/ O–H	25
	1064.38	C–OH of the phenols	26
c. ArLWEAgNps(Water)	3300.43	N–H stretching of the secondary amide ofthe protein	27
	2914.47	–C–H stretching of –CH2 ofProtein	28
	2320.90	N–H/C–O stretching	29
	2128.37	CC or CN triple bond	30
	1618.19	C–O/aromaticC–C stretching	31
	1314.15	C–O stretching/ O–H	32

Vol. 14 (3) 289-301, July 2020, ISSN 0973-8916 (Print), 2230-7303 (Online)
DOI: 10.5530/ctbp.2020.3.30

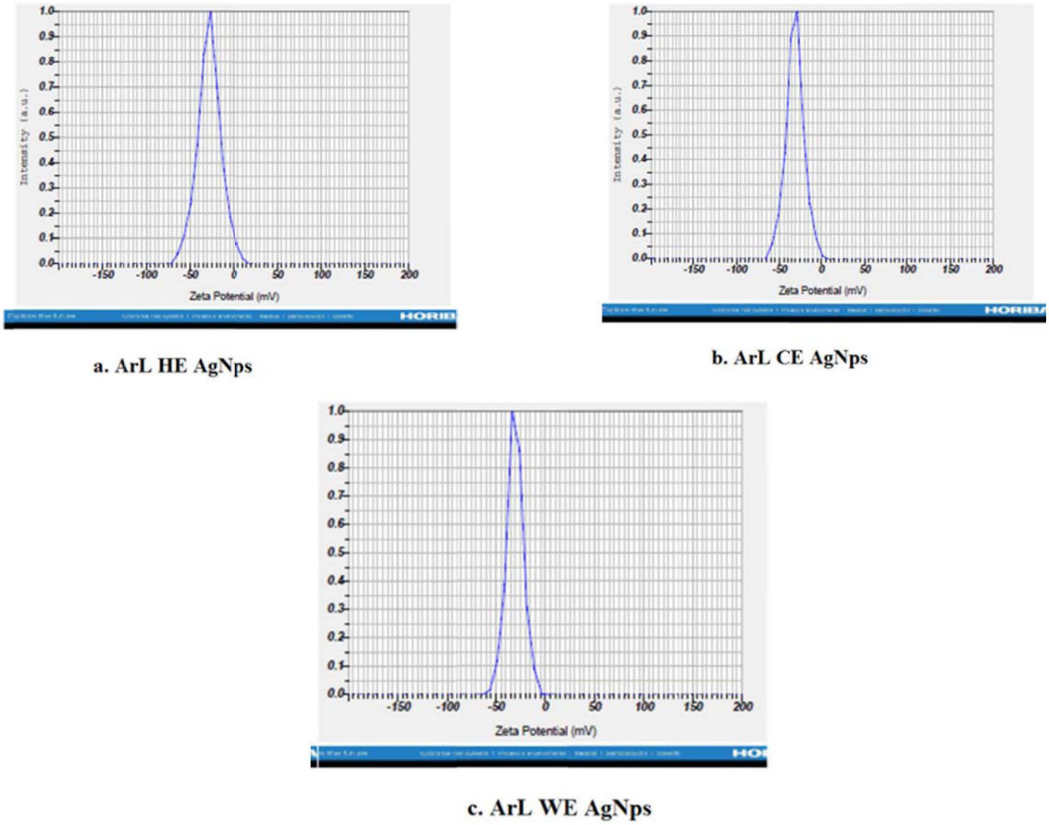

Fig. 4. Zeta potential of AgNPs synthesized by fractionated *A.reticulata* leaf extract in different solvent. (a) Hexane extract AgNPs (b) Chloroform Extract AgNPs (c) Water extract AgNPs.

(a) A.reticulata Hexane Extract AgNPs

(b) *A.reticulata* Chloroform Extract AgNPs

(c) *A.reticulata* Water Extract AgNPs.

XRD Studies : The crystalline nature of the biosynthesized AgNPs was confirmed by XRD pattern as displayed in Fig. 6. These patterns revealed four diffraction peaks at the 2è values of the three samples at 38.31æ%, 44.58æ%, 64.71æ%, 77.71æ%, and 81.92æ% .This could be indexed to (111), (200), (220), (311), and (222) crystallographic planes respectively. This suggested that all the peaks of the prepared AgNPs corresponded to face-centered cubic (FCC) lattice phase of silver and showed consistency with the standard JCPDS (File No 04-0783) data.

TEM Analysis : The TEM Micrographs revealed the spherical morphology of all the AgNPs. The AgNPs segregated based on their diameters which ranged diameters ranging from 10nm-100nm as seen in the (Fig.7).

Antioxidant activity (1, 1-Diphenyl-2-picrylhydrazyl radical scavenging activity) : Anti oxidant activity if different solvent fractions (F1 ArL HE, F2 ArL CE and F3 ArL WE), of *A.reticulata* leaf extract and its synthesized AgNPs varied as in Table.4 and Fig.8. The best antioxidant activity was observed at 1.0 mg conc., (97.84%) in AgNPs synthesized in water extract and crude leaf water extract sample (97.516%). Among all the synthesized AgNPs in different solvents, the lowest antioxidant activity was

Vol. 14 (3) 289-301, July 2020, ISSN 0973-8916 (Print), 2230-7303 (Online)
DOI: 10.5530/ctbp.2020.3.30

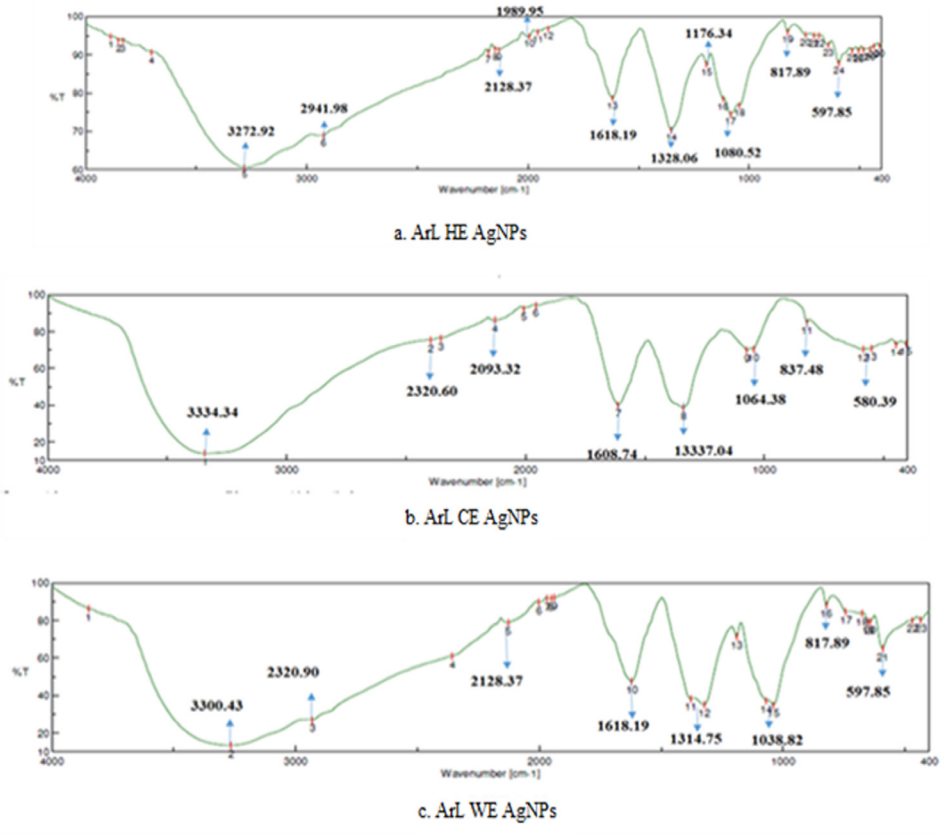

Fig. 5. Shows the various functional groups observed by the different peaks of AgNps Synthesized by *A. reticulata* leaf extracts in different solvents.

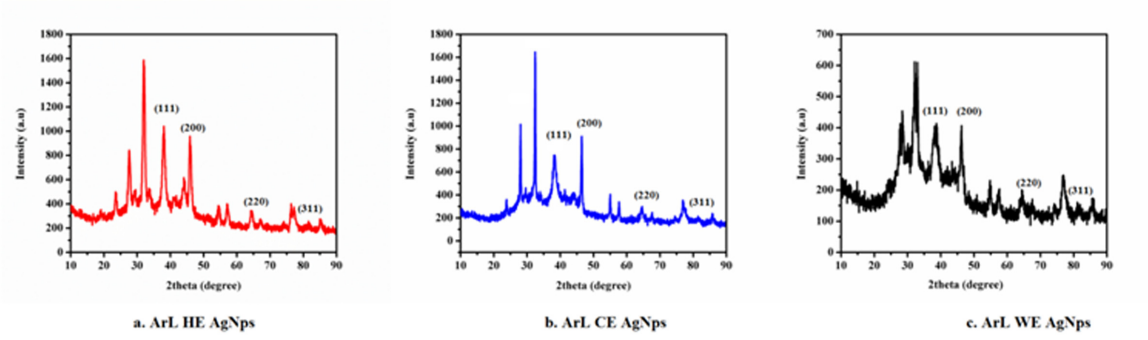

Fig. 6. XRD pattern studies confirming the crystal nature of the AgNPs by showing the Braggs peaks corresponding to(111), (200), (220) and (311) planes of (a) *A.reticulata* Hexane Extract AgNPs (b) *A.reticulata* Chloroform Extract AgNPs (c) *A.reticulata* Water Extract AgNPs.

Vol. 14 (3) 289-301, July 2020, ISSN 0973-8916 (Print), 2230-7303 (Online)
DOI: 10.5530/ctbp.2020.3.30

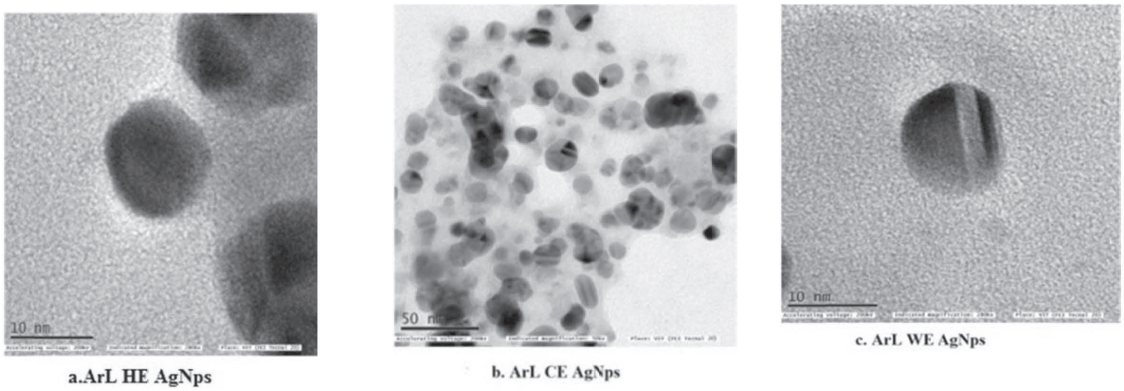

Fig. 7. Shows TEM micrograph of synthesized AgNPs in different solvent fractionated *A.reticulata* Leaf extracts.(a) *A.reticulata* Hexane Extract AgNPs (b) *A.reticulata* Chloroform Extract AgNPs (c) *A.reticulata* Water Extract AgNPs.

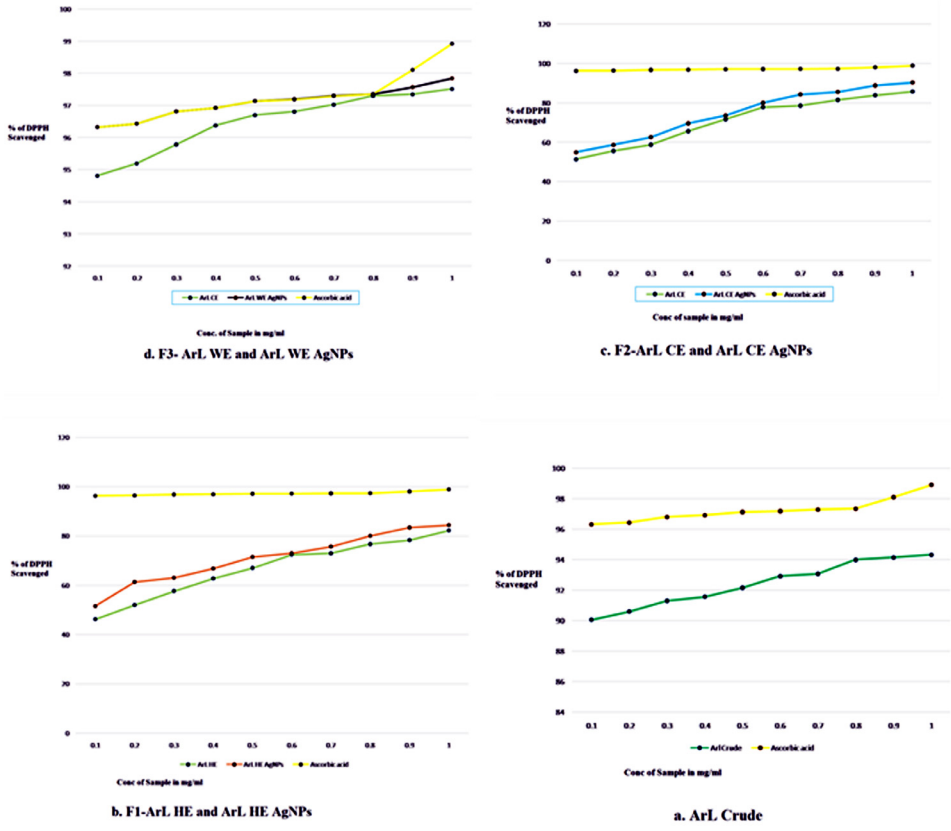

Fig. 8. shows the graphical representation of antioxidant activity of fractionated *A.reticulata* leaf extracts and its synthesized AgNPs.

Vol. 14 (3) 289-301, July 2020, ISSN 0973-8916 (Print), 2230-7303 (Online)
DOI: 10.5530/ctbp.2020.3.30

Table.4: Showing the percentage DPPH radical scavenging activity of A. reticulatafractionated leaf extracts and its synthesized AgNPs.

Conc.,of Samplein mg/ml	%of DPPH Scavenged byArLCrude	%of DPPH Scavenged by F1ArLHE	%of DPPH Scavenged by ArL HE AgNps	%of DPPH Scavenged by F2ArLCE AgNPS	%of DPPH Scavenged by ArLCE WE	%of DPPH Scavenged by F3ArL	%of DPPH by ArLWE AgNps	%of DPPH Scavenged by Ascorbic Acid
0.1	90.064	46.220	51.619	51.349	55.021	94.816	96.328	96.328
0.2	90.604	51.943	61.339	55.561	58.747	95.194	96.436	96.436
0.3	91.306	57.667	63.067	58.747	62.635	95.788	96.814	96.814
0.4	91.576	62.742	66.792	65.604	69.600	96.382	96.922	96.922
0.5	92.170	67.008	71.436	71.652	73.596	96.706	97.138	97.138
0.6	92.926	72.408	73.002	77.807	80.075	96.814	97.192	97.192
0.7	93.088	73.002	75.647	78.617	84.287	97.030	97.300	97.300
0.8	94.006	76.727	80.021	81.479	85.529	97.300	97.354	97.354
0.9	94.168	78.347	83.369	83.909	88.768	97.354	97.570	98.110
1	94.330	82.235	84.341	85.745	90.280	97.516	97.840	98.920

ArL = Annonareticulata leaf, HE = Hexane extract, CE = Chloroform, WE = Water extract

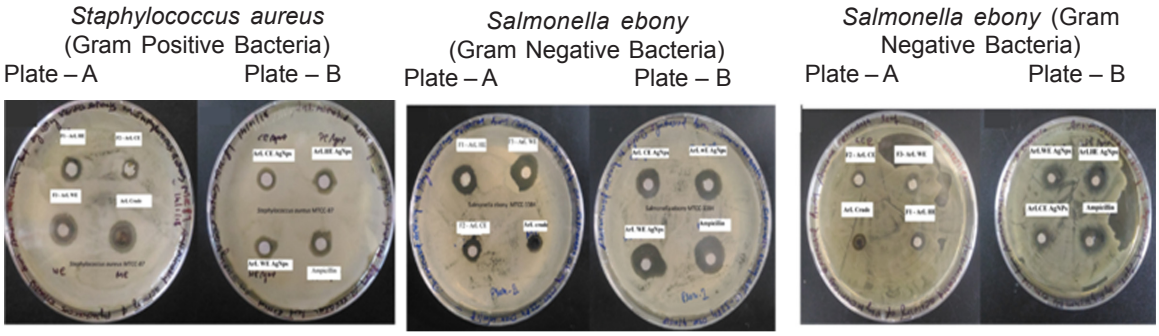

Fig. 9. Showing the Zone of inhibition of *A. reticulata* fractionated leaf extracts and its synthesized AgNPs towards the Gram positive and Gram negative bacteria

observed in AgNPs synthesized in Hexane leaf extract(84.34%). The antioxidant activity increased with an increase in concentration of leafextract . The lowest concentration used of leaf extract in different solvents is (0.1mg). The hexane extract (F1 fraction) showed the least Antioxidant activity (46.220%) and the highest antioxidant activity in concentration (0.1mg) of water extract. Synthesized AgNPs all the synthesized AgNPs showed a better response (84.341, 90.280 & 97.840) as compared to the crude leaf extract showed a steady increasing antioxidant activity with increase in leaf sample concentration(0.1 to 1.0mg conc.,). The F3 fraction of *A.reticulata* leaf extract in water and its synthesized AgNPs antioxidant activity (97.516% and 97.840%) was very near to the Ascorbic acid(98.920%).

Vol. 14 (3) 289-301, July 2020, ISSN 0973-8916 (Print), 2230-7303 (Online)
DOI: 10.5530/ctbp.2020.3.30

Anti-bacterial activity : After incubation period for 24hr, growth (ZOI) was observed around discs impregnated with AgNPs and leaf fractions. Fig.9 shows the plating of bacteria with the test samples. Plate a. with normal leaf fractions Whereas plate b. with synthesized AgNPs and Ampicillin against Gram positive and Gram-negative bacteria. ArL WE AgNPs showed Maximum ZOI against *Stephylococcus aureus* (5.43±0.08) , *Salmonella abony*(6.26±0.08), *Salmonella enteric* (6.3±0.05). The results of Antibacterial activity has shown that ArL WE AgNPs showed the highest activity against the bacteria . he Zone of inhibition of samples were measured and is shown in Table.5. It is clear from the obtained results that the AgNPs showed a higher antibacterial activity compared to the normal plant extract samples.

Plate. a: *A. reticulata* leaf extract fractions,

Plate.b: Synthesized AgNPs by *A. reticulata* leaf extract fractions

Conclusion:

Plant mediated biosynthesis of silver Nanoparticles was performed by using various fractions of *Annona reticulata*.L leaf extract fractionated by Hexane, Chloroform, and Water solvents . It was found that various phytochemical constituents of leaf extract were responsible for the formation of AgNPs. The size, morphology, crystalline nature and stability of AgNPs were characterized by using advanced techiniques like UV Visible spectroscopy, Dynamic light scattering, zeta potential, FTIR, X-Ray diffraction and Transmission electron microscope. The synthesized AgNPs were spherical in shape with size ranging 10 to 100nm, as observed in TEM and XRD. Among three different fractions, aqueous leaf extract fraction of *A. reticulata* has shown good antioxidant and antibacterial activity. The synthesized AgNPs have also shown enhanced activity of phytoconstituents compared to the normal leaf extract fractions due to the decrease in the size of the particle and increase in the

Table .5. Antibacterial activity of different extracts and their synthesized AgNPs against gram positive and gram negative bacteria.

ZOI = Zone of Inhibition

Samples	***Stephylococcusaureus*** (MTCC-87) **ZOI in (mm)**	***Salmonella abony*** (MTCC 3384) **ZOI in (mm)**	***Salmonella enteric*** (MTCC 3858) **ZOI in (mm)**
ArL Crude	2.4±0.15	2.43±0.08	2.23±0.08
F1-ArL HE	3.3±0.05	4.2±0.05	3.3±0.05
F2-ArL CE	2.56± 0.14	3.26±0.03	4.3±0.05
F3-ArL WE	3.73±0.08	5.13±0.16	4.36±0.03
ArL HE AgNps	5.33±0.12	5.5±0.05	6.26±0.08
ArLCEAgNps	3.33±0.08	5.2±0.05	5.46±0.06
ArL WE AgNps	5.43±0.08	6.26±0.08	6.3±0.05
Ampicillin	6.73±0.12	8.16±0.08	7.63±0.08

Vol. 14 (3) 289-301, July 2020, ISSN 0973-8916 (Print), 2230-7303 (Online)
DOI: 10.5530/ctbp.2020.3.30

surface volume ratio. Thus, the study concluded that plant mediated biosynthesis of AgNPs is a cost effective and ecofriendly which would establish its importance in biomedicine.

References

1. Bo Rao and Ren-Cheng Tang,(2017), Green synthesis of silver nanoparticles with antibacterial activities using aqueous *Eriobotryanaponica* leaf extract, Adv., in Nat., sci., Nanotechnol 015014
2. Biba V. S., Amily A., Sangeetha S., and Remani P. (2014), Antioxidant And Antimicrobial Activity Of Annonaceae Family,World Journal of Pharmacy and Pharmaceutical Sciences,Vol 3, Issue 3,1595-1604.
3. Prasad G. Jamkhande , Amruta S. Wattamwar , Ashish D. Kankudte , Priti S. Tidke, Mohan G. Kalaskar (2015). Assessment of *Annonareticulata* Linn. leaves fractions for invitroantioxidative effect and antimicrobial potential against standard human pathogenic strains, Alex J Med.
4. Nirmal SA, Gaikwad SB, Dhasade VV, Dhikale RS, Kotkar PV, DigheSS. (2010), Anthelmintic activity of *Annonareticulata* leaves. Res J Pharm BiolChem Sci.; 1:115e118.
5. Kamaruz Zaman1, Kalyani Pathak (2013), Pharmacognostical and Phytochemical Studies on the Leaf andStem Bark of *Annonareticulata*Linn.Journal of Pharmacognosy and Phytochemistry,Vol. 1 No. 5.
6. Tran DinhThang, Ping-Chung Kuo , Guan-Jhong Huang , Nguyen Huy Hung , Bow-Shin Huang, Mei-Lin Yang, Ngo Xuan Luong and Tian-Shung Wu 4, (2013), Chemical Constituents from the Leaves of *Annonareticulata* and Their Inhibitory Effects on NO Production, Molecules, 4477-4486.
7. Bhalke RD, Chavan MJ.(2011) Analgesic and CNS depressant activities of extracts of Annona reticulate Linn. bark. Phytopharmacology;1(5):160e5.
8. Suresh HM, Shivakumar B, Shivakumar SI. Inhibitory potential of the ethanol extract of Annona reticulata Linn. Against melanoma tumor. Journal of Natural Pharmaceuticals 2011;2(4):168e72.
9. Mohan Penumala, Raveendra Babu Zinka, Jeelan Basha Shaik, and Damu Amooru Gangaiah, (2017), Vitro Screening of Three Indian Medicinal Plants for Their Phytochemicals, Anticholinesterase, Antiglucosidase, Antioxidant, and Neuroprotective Effects, BioMed Research International Volume.Article ID 5140506.
10. Gaddam SA, Kotakadi VS, Gopal DVRS, Rao YS, Reddy AV. (2014), Efficent and robust biofabrication of silver nanoparticles by*Cassiaalata* leaf extract and their antimicrobial activity.JNanostructChem 4(82):1–9.
11. Kotakadi VS, Gaddam SA, Rao YS, Prasad TNVKV, Reddy AV,Gopal DVRS .(2014). Biofabrication of silver nanoparticles byAndrographispaniculata. Eur J Chem 73:135–140.
12. Rafie MH, Shaheen T, Mohamed AA, Hebeish A (2012) Biosynthesis and applications of silver nanoparticles onto cotton fabrics. Carbohydrate Pol 90:915–920
13. C. Sarikurkcu, K. Arisoy, B. Tepe, A. Cakir, G. Abali, and E. Mete, (2009), “Studies on the antioxidant activity of essential oil and different solvent extracts of *Vitexagnuscastus* L. fruits from Turkey,” Food andChemical Toxicology, vol. 47, no. 10, pp. 2479– 2483.
14. Litvin VA, Minaev BF (2013) Spectroscopy study of silver nanoparticles fabrication using synthetic humic substances and their antimicrobial activity. SpectrochimActa Part AMolBiomolSpectrosc 108:115–122.

Vol. 14 (3) 289-301, July 2020, ISSN 0973-8916 (Print), 2230-7303 (Online)
DOI: 10.5530/ctbp.2020.3.30

15. Gaddam SA, Kotakadi VS, Gopal DVRS, Rao YS, Reddy AV (2014) Efficent and robust biofabrication of silver nanoparticles by Cassia alata leaf extract and their antimicrobial activity. J Nanostruct Chem 4(82):1–9.
16. Valli JS, Vaseeharan B (2012) Biosynthesis of silver nanoparticles by Cissus quadrangularis extracts. Mater Lett 82:171–173
17. M. Jannathul Firdhouse (2013) Biosynthesis of silver nanoparticles using the extract of Alternanthera sessilis—antiproliferative effect against prostate cancer cells. Cancer Nanotechnol 4(6): 137–143.
18. Salprima YS, Notriawan D, Angasa E, Suharto TE, Hendri J, Nishina Y (2013) Green synthesis of silver nanoparticles using aqueous rinds extract of Brucea javanica (L.) Merr at ambient temperature. Mater Lett 97:181–183
19. Kumar MHV, Gupta YK (2002) Effect of different extracts of Centella asiatica on cognition and markers of oxidative stress in rats. J Ethnopharmacol 79:253–260
20. Litvin VA, Minaev BF (2013) Spectroscopy study of silver nanoparticles fabrication using synthetic humic substances and their antimicrobial activity. Spectrochim Acta Part A Mol Biomol Spectrosc 108:115–122
21. Bozanic DK, Trandafilovic LV, Luyt AS, Djokovic V (2010) Green' synthesis and optical properties of silver–chitosan complexes and nanocomposites. React Funct Polym 70:869–873
22. Tran TTT, Havu TT, Nguyen TH (2013) Biosynthesis of silver nanoparticles using Tithonia diversifolia leaf extract and their antimicrobial activity. Mater Lett 105:220–223
23. M. Jannathul Firdhouse (2013) Biosynthesis of silver nanoparticles using the extract of Alternanthera sessilis—antiproliferative effect against prostate cancer cells. Cancer Nanotechnol 4(6): 137–143.
24. Kumar MHV, Gupta YK (2002) Effect of different extracts of Centella asiatica on cognition and markers of oxidative stress in rats. J Ethnopharmacol 79:253–260
25. Babu TD, Kuttan G, Padikkala J (1995) Cytotoxic and anti-tumour properties of certain taxa of Umbelliferae with special reference to Centella asiatica (L.) Urban. J Ethnopharmacol 48:53–57
26. Litvin VA, Galagan RL, Minaev BF (2012) Kinetic and mechanism formation of silver nanoparticles coated by synthetic humic substances. Colloids and surf A: Physicochem Engg Asp 414:234–243
27. Bozanic DK, Trandafilovic LV, Luyt AS, Djokovic V (2010) 'Green' synthesis and optical properties of silver–chitosan complexes and nanocomposites. React Funct Polym 70:869–873
28. Vanaja M, Annadurai G (2012) Coleus aromaticus leaf extract mediated synthesis of silver nanoparticles and its bactericidal activity. Appl Nanosci 3:217–223
29. Tran TTT, Havu TT, Nguyen TH (2013) Biosynthesis of silver nanoparticles using Tithonia diversifolia leaf extract and their antimicrobial activity. Mater Lett 105:220–223
30. M. Jannathul Firdhouse (2013) Biosynthesis of silver nanoparticles using the extract of Alternanthera sessilis—antiproliferative effect against prostate cancer cells. Cancer Nanotechnol 4(6): 137–143.
31. Babu TD, Kuttan G, Padikkala J (1995) Cytotoxic and anti-tumour properties of certain taxa of Umbelliferae with special reference to Centella asiatica (L.) Urban. J Ethnopharmacol 48:53–57
32. Kumar MHV, Gupta YK (2002) Effect of different extracts of Centella asiatica on cognition and markers of oxidative stress in rats. J Ethnopharmacol 79:253–260

Current Trends in Biotechnology and Pharmacy
Vol. 14 (3) 302-310, July 2020, ISSN 0973-8916 (Print), 2230-7303 (Online)
DOI: 10.5530/ctbp.2020.3.31

Anticancer potential of D-limonene and hispolon against colon cancer cell lines

K. Chandra Sekhar[1, 2], A. Rajanikanth[1], Md. Nazneen Bobby[2] and Jagadeeswara Reddy Kanala[1*]

[1]Sugen Life Sciences Pvt. Ltd, Tirupati – 517505, AP, India
[2]Department of Biotechnology, Vignan University, Vadlamudi, Guntur-522213, AP, India
*Corresponding author : kjreddy32@gmail.com.

Abstract

Natural products and associated combination therapy have gained prominent role in decreasing the adverse effects of synthetic drugs engaged in the severity of colon cancer. D-Limonene a dietary monoterpene and hispolon a bioactive polyphenol proven to be anticancer agents independently against several cancers. The current study is designed to examine complimentary anticancer effect of D-limonene-hispolonconcoction in COLO-205 and HCT-116 cell lines. Collectively, our cell viability, cell migration, clonogenic tests and CompuSyn analysis results exemplified that the combination of D-limonene and hispolonnatural products eminently effective against colon cancer cell lines.Gastric cancer patients are reported to develop severe side effects due to the currently available chemotherapy,our combinational anticancer therapy bydietary natural compounds would be highly beneficial to the patients.

Key words: Colorectal cancer, D-limonene, Hispolon.

Introduction

Misregulation of different biological pathways resulted from the genetic mutations, infections, environmental factors, etc., cause various diseases in the body. One of such dreadful disease is cancer, it is one of the major causes of mortality despite immense research in the cancer therapy and prevention worldwide [1]. Among all the cancers reported, colorectal cancer grabs at most attention as this is 2nd leading cancer in bothwomen and men[2]. Majority of colorectal cancers (CRCs) are sporadic, while 10% of them have genetic background. It is demonstrated that the aberrations in Ras and PI3K signalling pathway leads to development of CRC with enhanced risk of tumor[3].Hence, essentially these multi signalling pathways targeted with multidrug combinations would be highly beneficial. Natural compounds with anticancer activity and pleiotropic properties are involved in better chemo preventive and/or therapeutic alternatives [4].

A monoterpene natural compound D-limonene with a lemon-like odor available in several citrus oils like orange, lemon, lime, mandarin, and grapefruit. The food companies have been using D-limonene additives for flavor and fragrance. D-limonene is also used by clinicians for dissolving cholesterol containing gallstones [5], gastro esophageal reflux disorders,to relieve heartburns, and gastric acid neutralization in the stomach [6]. It is exemplified that D-limoneneis involved in regulating many cellular targets in cancer cells such as modulating chemical carcinogenesis, immune modulation, apoptosis, and antioxidant activity. D-limonene is an effective natural compound in preventing the growth of numerous cancer types including lymphomas [7], mammary [8], gastric [9], liver [10], lung [11] and prostate cancer [12] in preclinical cancer models.

Hispolon is a polyphenol isolated from various fungal species such as Phellinus igniarius, Phellinus linteus, and Inonotushispidus[13, 14,

Vol. 14 (3) 302-310, July 2020, ISSN 0973-8916 (Print), 2230-7303 (Online)
DOI: 10.5530/ctbp.2020.3.31

15]. It isidentifiedas an effective natural compound that show antiviral [16], hepatoprotective [17], immunomodulatory [18] and anti-proliferative activities [19, 20, 21] in different models. The role of hispolan is also demonstrated in induction of apoptosis, suppression of metastasis, and cell cycle[22, 23, 24, 25]. In 2008, Wei chen et al., demonstrated the ability of hispolon against gastric cancer and also demonstrated its reduced cytotoxic effect on the normal cells [26].

In the current study, we investigated the role of hispolon, D-limonene and the combination of hispolon and D-limonene against the colon cancer cell lines. Cell viability and cytotoxic assays results demonstrated that the synergistic effect of hispolon and D-limonene is shown significant effect against the COLO-205 and HCT-116.

Materials and Methods

The human colon cancer cell lines HCT 116 and COLO 205 was gifted from Dr. Royal Suresh (IIT, Chennai), RPMI 1640, McCoy's 5a, Fetal bovine serum (FBS) were purchased from GIBCO Ltd (Life Technologies TM., Grand Island, NY). MTT [3-(4, 5- dimethylthiazol-2-yl)-2, 5-diphenyl tetrazolium bromide], Hispolon, D-Limonene were purchased from Sigma (St. Louis, MO, USA). Stocks were prepared in dimethyl sulfoxide (DMSO) stored at -20ºC until use. All other chemicals of analytical grade were purchased from Sigma, USA.

Culturing and maintenance of COLO 205 and HCT 116 cells : COLO 205 and HCT 116 Cells were cultured respectively in RPMI 1640, McCoy's 5a medium with 10% heat-inactivated Fetal-Bovine Serum and 1% antibiotic solution (10,000 units of Penicillin, 10 mg Streptomycin and 25ìg amphotericin / ml). Cells were maintained at 37ºC in an incubator with 5% CO_2.

Determination of cell viability : MTT assay is used to determine the effect of hispolon and/or D-limonene on the cell viability of colon cancer cells. Concisely, cells were seeded at a density of 1 X 10^4 cells per well in 96-well plates and treated either with D-limonene or hispolon and also with their combinations, at specified concentrations for 24 and 48 hr. For combination effects the cells were treated with both the drugs concurrently as well as sequentially. In concurrent treatment, first the cells were treated with hispolon(10, 50, 100, 150, 200, 250, 300 µM) and D-limonene (100, 500, 1000, 1500, 2000, 2500, 3000 µM) separately and in case of combinations D-limonene and hispolon (1000+50, 1000+100, 1500+50, 1500+100) were taken for 24 and 48hr continuously. Whereas in sequential treatment, cells were pre-treated with either D-limonene or Hispolon for 12hr, followed by the exposure to the other agent for a total of 24 and 48hr. After that cells were incubated with the MTT reagent (5 mg/ml in DMEM) for 3hr at 37° C, followed by solubilization of the formazan crystals with DMSO for 10min on shaker. Absorbance was measured at 570 nm using a microplate analyzer (iMark Microplate Absorbance Reader, BioRad) [27]. The percent cell viability was calculated using the following

$$\% \text{ Cell viability} = \text{OD of sample} / \text{OD of control} \times 100$$

In vitro scratch assay : In vitro scratch assays are particularly appropriate for the cell migration analysis in the cell biology. Cells were seeded at a density of 5×10^4 in 6 well plates and the monolayer of 80% confluent cells were treated for 48hr with hispolon, D-limonene and with their combinations respectively. The concentration of serum in the complete media was decreased to diminish cell proliferation, but used sufficient enough to prevent cell detachment and/or apoptosis. After 48hr of treatment, themedium was removed and a scratch was created with a sterile p200 pipette tip and washed twice with 1X PBS to remove floating cells and plates were incubated after adding complete media with 5% FBS. Cell migration was monitored by capturing images at 0, 24 and 48hr using a bright field microscope (Olympus CX21FS1) [28]. Gap area was measured relative to the total cell-covered area with Wimasis image analysis software. The drug treatment effect was measured by a reduction in the % cell migration at each time interval compared

Vol. 14 (3) 302-310, July 2020, ISSN 0973-8916 (Print), 2230-7303 (Online)
DOI: 10.5530/ctbp.2020.3.31

to untreated control using the % Cell migration formula; % Cell migration = (Scratch area at 0hr-Scratch area at specific time point)/Scratch area at 0h x100.

Clonogenic assay : The clonogenic assay is used to determine the ability of a cell to proliferate indefinitely, thereby retaining its reproductive ability to form a large colony which is noticeable to the naked eye. Cells were seeded (5×10^4) in 6-well culture plates and treated with various doses of drugs either single or in combination, as indicated for 48hr. Then COLO 205 and HCT 116 cells were trypsinised and approximately 100 cells were seeded for each drug concentration into new and fresh 6-well culture plates and incubated for another 3 weeks with change of fresh media once in three days. The Colonies were exposedto glutaraldehyde (6% v/v) stained with crystal violet (0.5% w/v) for 30 minutes and counted under a microscope (Olympus CX21FS1) [29].

Analysis of combination effects : Further the anticancer effect of Hispolonand D-limonene combination in COLO-205 and HCT-116 cells were analyzed using CompuSyn software [30] for synergism, additive or antagonistic effects based on Combination Index (CI). If the Combination Index (CI) of more than 1 indicate antagonistic, CI is equal to 1 indicate additive and CI is less then to 1 indicate synergistic effect.

Statistical analysis : The obtained results are presented here as the mean ± standard deviation (SD) from three independent experiments. Differences were evaluated by the one-way analysis of variance (ANOVA) followed by Dunnett's multiple comparison test. The level of significance was set at *p* 0.05.

Results and Discussion

Natural products are proven as most reliable and effective sources for novel anticancer agents. Prognostic utility of natural compoundsin colorectal cancer are currently being investigated [31]. In the current study we demonstrated the synergistic effect of D-limonene and hispolon anticancer activity against COLO-205 and HCT-116 cancer cell lines.

The combinational effect of hispolon and D-limonene was initially screened by its cell viability using MTT assays. Cells were treated with increasing doses of D-limonene and Hispolon (10-300 ìM) for 24 & 48hr. Upon drug treatment, cells exhibited significant difference in cell viability compared to control ($P\leq0.05$). In dose and time dependent manner both the drugs tested individually and they inhibited the cell proliferation (Fig. 1). Under these experimental conditions, the calculated IC50 values in COLO-205 were at 1042 μM and 100 μM for D-limonene and hispolon respectively; whereas in HCT- 116 the IC 50 values for D-limonene and hispolon were at 1850 μM and 190 μM respectively. Both COLO 205 and HCT-116 were treated with different combinations of the drugs sequentially as well as simultaneously added and cell viability was identified as described before by MTT assay (27). The combination of varying doses of D-limonene and hispolon produced maximum antiproliferative activity at 48hr when compared with the treatment of either agents alone in both the cell lines. The combination of D-limonene and hispolon (LIM+HIS) at a concentration of 1500+100 produced highest antiproliferative activity in COLO-205; whereas in HCT-116 also the combination at a concentration of 1500+100 showed highest activity (Fig. 2.A.D). Antiproliferative effect was more when the cells were exposed to both drugs simultaneously than sequential treatment (84% vs. 70% or 65% for COLO-205: Fig. 2. A.B.C) and (86% vs. 68% or 62% for HCT-116: Fig. 2.D.E.F).

Effect of D-limonene and hispolon on cell migration : The cell migration experiments were conducted to study the synergistic effect of D-limonene and hispolon in COLO-205 & HCT-116 cell lines (Fig. 3.A.B). Lower doses of D-limonene (250, 500 μM) and hispolon (25, 50 μM) and their possible combinations were chosen for the study to minimize the cytotoxicity. In control group cell migration into the scratch was 100% in 48hr resulting complete closure of the gap, whereas

Vol. 14 (3) 302-310, July 2020, ISSN 0973-8916 (Print), 2230-7303 (Online)
DOI: 10.5530/ctbp.2020.3.31

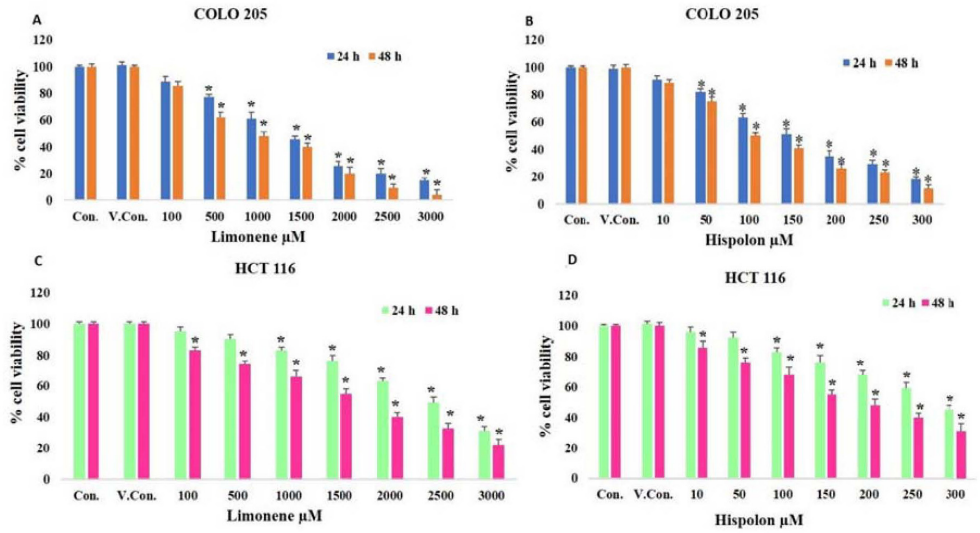

Fig. 1. Effect of D-limonene and hispolon on cell viability showing the effect of D-limonene and hispolon on cell viability in COLO-205 (A,B); HCT-116 (C,D) CRC cell lines. Cells were treated for 24 & 48 hr and viability was determined by MTT. Data were expressed as mean ± SD (n=3). *$p \leq 0.05$.

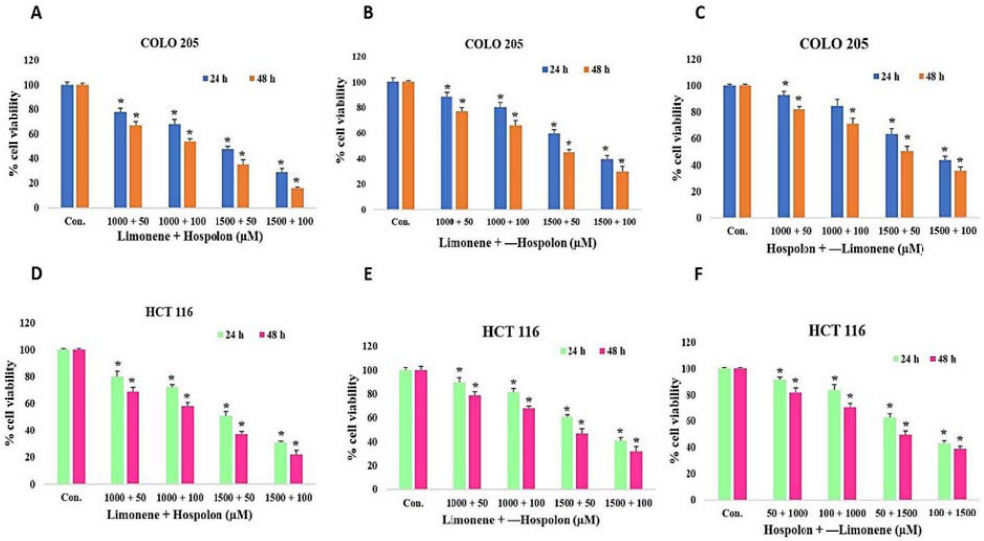

Fig. 2. Effect of D-limonene and hispolon combination on cell viability. Combination effect of D-limonene (LIM) and hispolon (HIS) on anti-proliferative activity in COLO-205 & HCT-116 cells. A.D: Cells were treated with D-limonene in combination with hispolon at the same time. B.E: Cells were pre-treated with D-limonene for 12hr followed by exposure to hispolon. C.F: Cells were pre-treated with hispolon for 12hr followed by exposure to D-limonene. Cells were treated for a total of 24 & 48hr and viability was determined by MTT. Data were expressed as mean ± SD (n=3). *$p \leq 0.05$.

Vol. 14 (3) 302-310, July 2020, ISSN 0973-8916 (Print), 2230-7303 (Online)
DOI: 10.5530/ctbp.2020.3.31

drug treatment alone or in combination caused a significant inhibition of cell migration in both the cell lines (P≤0.05). The maximum inhibition of % cell migration observed at 48hr was 63.65, 59.45 in COLO-205 and HCT-116 cells respectively at the highest concentration of LIM+HIS (500+50 µM).

Combination of D-limonene and hispolon

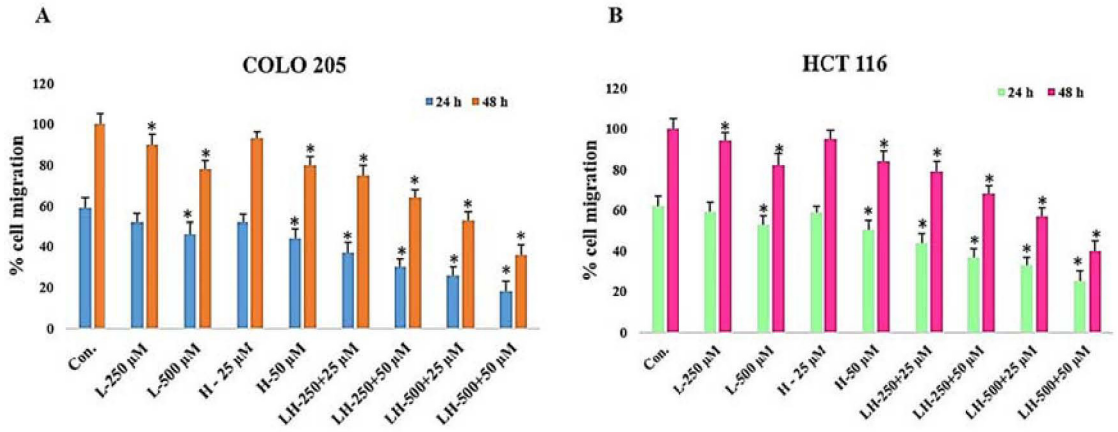

Fig. 3.D-limonene and hispolon inhibits cell migration. Effect of D-limonene and hispolon combinations on cell migration in COLO-205 (A); HCT-116 (B) cell lines. Cells were treated for 48hr and scratch images were captured at 0, 24 and 48hr and analyzed as described in materials and methods. The percent cell migration was expressed as mean ± SD (n=3). *p ≤ 0.05

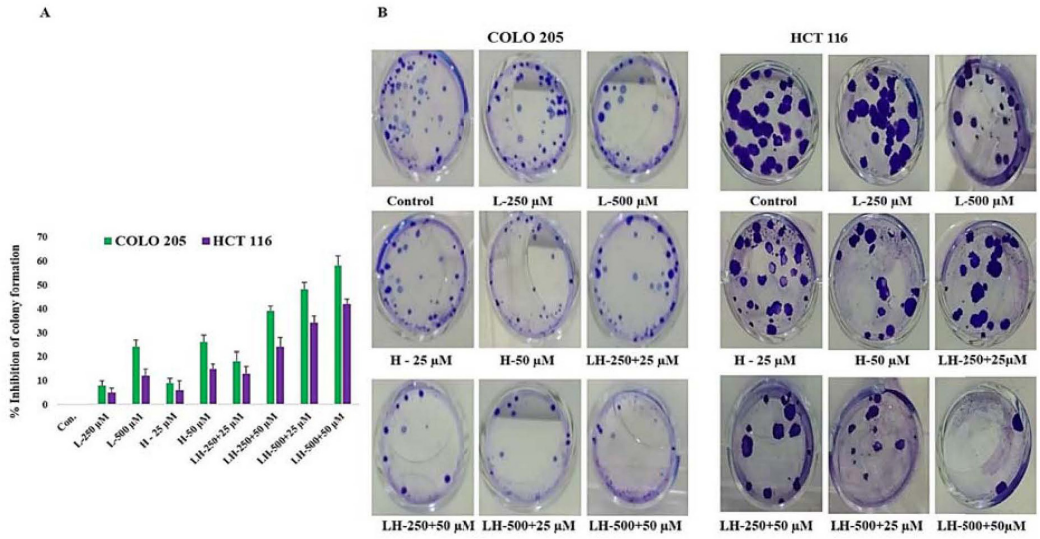

Fig. 4. D-limonene and hispolon inhibits colony formation. Effect of D-limonene and hispolon combinations on colony formation of COLO-205 and HCT-116 cell lines. A: The percent inhibition of colony formation at different drug combinations expressed relative to untreated cell control considering as zero; B: Images of colonies that were stained with 0.5% crystal violet reagent. The data were expressed as mean ± SD (n=3). *p ≤ 0.05.

inhibits colony formation : Clonogenic assay was performed to study the effects of D-limonene (250, 500 μM), hispolon (25, 50 μM) and their combinations (Fig. 4.A). Represent images of the assay were shown in (Fig. 4.B). Both the drugs at high concentrations resulted a significant inhibition of colony formation (%) compared to control (P≤0.05). Drug combinations were more effective than either of the drugs alone. LIM+HIS at high concentration (500+50) showed maximum inhibition of 53.66; 51.76 in COLO-205 & HCT-116 cells respectively.

Assessment of synergistic anticancer activity of D-limonene and hispolon : CompuSyn software (32) Drug combinations was analyzed by CompuSyn software and CI values were generated to determine synergy, additive or antagonistic effects. LIM+HIS on cell viability was strongly synergistic (CI≤1) at 1000+50; 1000+100 in COLO-205 when the drugs were exposed at the same time. In HCT-116 also at 1500+50; 1500+100 produced strong synergism in the same format. In case of pretreatment formats all the combinations were shown to be antagonistic (CI Ã1) in both the cell lines (Table 1.A). In COLO-205 the combination shows strong synergism on inhibition of cell migration at 250+50; 500+25 and 500+50; whereas it shows a weak synergistic interaction on colony formation at the dose of 500+25. However, in HCT-116 the combination at 500+25; 500+50 produced strong synergism on

Table 1. Combination Index (CI) values of D-limonene and hispolon combination effect on COLO-205 and HCT-116 cell lines A: Effect of combination treatment on anti-proliferative activity. Cells were treated with the drug combination simultaneously as well as sequentially as described in material & methods. B: Effect on cell migration and colony formation. Synergistic interaction is determined if CI<1, an additive interaction if CI=1 and antagonistic if CI >1.

A

	LIM + HIS (μM)	Cell viability		
		Both at once	Pre-treat with LIM	Pre-treat with HIS
COLO 205	500 + 50	1.9	2.1	2.1
	500 + 100	1.2	2.1	1.2
	1000 + 50	0.9	1.5	1.7
	1000 + 100	0.4	1.4	1.2
HCT 116	1000 + 50	2.3	3.5	1.4
	1000 + 100	1.5	2.7	1.3
	1500 + 50	0.8	1.4	1.3
	1500 + 100	0.5	1.3	1.2

B

LIM + HIS (μM)	COLO 205		HCT 116	
	Cell migration	Colony formation assay	Cell migration	Colony formation assay
250 + 25	2	1.2	2.2	1.4
250 + 50	0.7	1.2	1.8	1.2
500 + 25	0.4	0.8	0.9	0.8
500 + 50	0.5	1.1	0.5	0.9

Vol. 14 (3) 302-310, July 2020, ISSN 0973-8916 (Print), 2230-7303 (Online)
DOI: 10.5530/ctbp.2020.3.31

inhibition of cell migration and clonogenic ability (Table 1). Together our results demonstrated that the combination treatments of hispolon and D-limonene was more significant than the independent drug treatment. It is also evident from our results that exposure of both drugs at the same time was more effective than pre-treatment format. Results confirmed that COLO- 205 cells are more sensitive to anticancer activity of the hispolon and D-limonene.

Conclusion

In conclusion, overall our results revealed that the combination treatment of hispolon and D-limonene elicits synergistic anticancer effect in colon cancer cell lines (COLO-205 and HCT-116).These kind of combined natural compound treatmentsmay have further clinical utility for treating colon cancer, however the current findings requireadditional experimental evidence to identify anticancer effects of hispolon and D-limonene combinations in different cancer cell lines.Here we suggest that present study may be valuable to identify potential anticancer compounds and this kind of efficacious natural drugsas dietary products wouldhelp to combat against dreadful human diseaseswithout side effects.

Acknowledgements

The authors thank Sugen Life Sciences Pvt Ltd., Tirupati, India for their essential support.

Conflict of Interest

The authors declare no conflict of interest.

References

1. Baylin, S.B. and Ohm, J.E. (2006). Epigenetic gene silencing in cancer–a mechanism for early oncogenic pathway addiction Nature Reviews Cancer, 6:107-116.
2. American Cancer Society. (2015). Cancer Facts & Figures.
3. Baba, Y., Nosho, K., Shima, K., Hayashi, M. and Meyerhardt, J.A. (2011). Phosphorylated AKT expression is associated with PIK3CA mutation, low stage, and favorable outcome in 717 colorectal cancers. Cancer, 117: 1399-1408.
4. Brisdelli, F., D'Andrea, G. and Bozzi, A. (2009). Resveratrol: a natural polyphenol with multiple chemopreventive properties. Current drug metabolism, 10: 530-546.
5. Igimi, H., Hisatsugu, T. and Nishimura, M. (1976). The use of d-limonene preparation as a dissolving agent of gallstones. Am J Dig Dis, 21: 926-939.
6. Wilkins, J. (2002). Method for treating gastrointestinal disorder. U.S. Patent (642045).
7. Del Toro Arreola, S., Flores Torales, E., Torres Lozano, C., Del Toro Arreola, A., Tostado Pelayo, K., Guadalupe Ramirez Duenas, M. and Daneri Navarro, A. (2005). Effect of D-limonene on immune response in BALB/c mice with lymphoma. Int Immunopharmacol, 5: 829-838.
8. Maltzman, T.H., Hurt, L.M., Elson, C.E., Tanner, M.A. and Gould, M.N. (1989). The prevention of nitrosomethylurea-induced mammary tumors by D-limonene and orange oil. Carcinogenesis, 10: 781-783.
9. Lu, X.G., Zhan, L.B., Feng, B.A., Qu, M.Y., Yu, L.H. and Xie, J.H. (2004). Inhibition of growth and metastasis of human gastric cancer implanted in nude mice by D-limonene. World J Gastroenterol, 10: 2140-2144.
10. Kaji, I., Tatsuta, M., Iishi, H., Baba, M., Inoue, A. and Kasugai, H. (2001). Inhibition by D-limonene of experimental hepatocarcinogenesis in Sprague-Dawley rats does not involve p21 (ras) plasma membrane association. Int J Cancer, 93: 441-444.
11. Raphael, T.J. and Kuttan, G. (2003). Effect of naturally occurring monoterpenes carvone, limonene and perillic acid in the inhibition of experimental lung metastasis

Vol. 14 (3) 302-310, July 2020, ISSN 0973-8916 (Print), 2230-7303 (Online)
DOI: 10.5530/ctbp.2020.3.31

induced by B16F-10 melanoma cells. J Exp Clin Cancer Res, 22: 419-424.

12. Rabi, T. and Bishayee, A. (2009). D-Limonene sensitizes docetaxel induced cytotoxicity in human prostate cancer cells: generation of reactive oxygen species and induction of apoptosis. J Carcinog, 8: 1-19.

13. Ali, A.A., Janse, R., Pilgri, H., Liberra, K. and Lindequist, U. (1996). Hispolon, a yellow pigment from Inonotushispidus. Phytochemistry, 41: 927"929.

14. Mo, S., Wang, S., Zhou, G., Yang, Y., Li, Y., Chen, X. and Shi, J. (2004). Phelligridins C" F: Cytotoxic Pyrano [4, 3-c][2] benzopyran-1, 6-dione and Furo [3, 2-c] pyran-4-one Derivatives from the Fungus Phellinus igniarius. Journal of natural products, 67:823-828.

15. Wang, J., Hu, F., Luo, Y., Luo, H., Huang, N., Cheng, F., Deng, Z., Deng, W. and Zou, K. (2014). Estrogenic and anti-estrogenic activities of hispolon from Phellinus lonicerinus (Bond.) Bond. et sing. Fitoterapia, 95:93-101.

16. Ali, NA., Mothana, R.A.A., Lesnau, A., Pilgrim, H. and Lindequist, U. (2003). Antiviral activity of Inonotushispidus. Fitoterapia, 74: 483-485.

17. Huang, G.J., Deng, J.S., Chiu, C.S., Liao, J.C., Hsieh, W.T., Sheu, M.J. and Wu, C.H. (2012). Hispolon protects against acute liver damage inthe rat by inhibiting lipid peroxidation, proinflammatory cytokine, oxidative stress and down-regulating the expressions of iNOS, COX-2, and MMP-9. J. Evidence-Based Complementary Altern. Med, pp. 1-12.

18. Chang, H.Y., Sheu, M.J., Yang, C.H., Lu, T.C., Chang, Y.S., Peng, W.H., Huang, S.S. and Huang, G.J. (2011). Analgesic effects and the mechanisms of anti-inflammation of hispolon in mice. J. Evidence-Based Complementary Altern. Med, pp. 1-8.

19. Huang, G.J., Deng, J.S., Huang, S.S. and Hu, M.L. (2011). Hispoloninduces apoptosis and cell cycle arrest of human hepatocellular carcinoma Hep3B cells by modulating ERK phosphorylation. J. Agric.Food Chem, 59: 7104"7113.

20. Chen, Y.C., Chang, H.Y., Deng, J.S., Chen, J.J., Huang, S.S., Lin, I.H.,Kuo, W.L., Chao, W. and Huang, G.J. (2013). Hispolon from Phellinus linteus induces G0/G1 cell cycle arrest and apoptosis in NB4human leukaemia cells. Am. J. Chin. Med, 41: 1439"1457.

21. Wu, Q., Kang, Y., Zhang, H., Wang, H., Liu, Y. and Wang, J. (2014). The anticancer effects of hispolon on lung cancer cells. Biochem. Biophys. Res. Commun, 453: 385"391.

22. Chen, Y.C., Chang, H.Y., Deng, J.S., Chen, J.J., Huang, S.S., Lin, I.H., Kuo, W.L., Chao, W. and Huang, G.J. (2013). Hispolon from Phellinus linteus induces G0/G1 cell cycle arrest and apoptosis in NB4human leukaemia cells. Am. J. Chin. Med, 41: 1439"1457.

23. Chen, W., Zhao, Z., Li, L., Wu, B., Chen, S.F., Zhou, H., Wang, Y and Li, Y.Q. (2008). Hispolon induces apoptosis in human gastric cancer cells through a ROS- mediated mitochondrial pathway. Free Radical Biol.Med, 45: 60"72.

24. Huang, G.J., Yang, C.M., Chang, Y.S., Amagaya, S., Wang, H.C., Hou, W.C., Huang, S.S. and Hu, M.L. (2010). Hispolon suppresses SK-Hep1 human hepatoma cell metastasis by inhibiting matrix metal-loproteinase-2/9 and urokinase-plasminogen activator through thePI3K/Akt and ERK signaling pathways. J. Agric. Food Chem, 58: 9468"9475.

Vol. 14 (3) 302-310, July 2020, ISSN 0973-8916 (Print), 2230-7303 (Online)
DOI: 10.5530/ctbp.2020.3.31

25. Hsiao, P.C., Hsieh, Y.H., Chow, J.M., Yang, S.F., Hsiao, M., Hua, K.T., Lin, C.H., Chen, H.Y. and Chien, M.H. (2013). Hispolon induces apoptosis through JNK1/2-mediated activation of a Caspase-8, -9, and-3-dependent pathway in Acute Myeloid Leukemia (AML) cells and inhibits AML Xenograft tumor growth in vivo. J. Agric. Food Chem, 61: 10063"10073.

26. Ghosh, S. and Playford, R.J. (2003). Bioactive natural compounds for the treatment of gastrointestinal disorders. Clinical science, 104: 547-556.

27. Zheng, L., He, X., Ma, W., Dai, B., Zhan, Y., Zhang, Y. (2011) Ta1722, an antiangiogenesis inhibitor targeted on VEGFR-2 against human hepatoma. Biomed Pharmacother. 66(7):499-05.

28. Keane, M.M., Ettenberg, S.A., Nau, M.M., Russell, E.K. and Lipkowitz, S. (1999). Chemotherapy augments TRAIL-induced apoptosis in breast cell lines. Cancer Research, 59:734-741.

29. Shu, G., Mi, X., Cai. J., Zhang. X., Yin. W.,Yang, X., Li. Y., Chen, L., Deng. X. (2013). Brucine, an alkaloid from seeds of Strychnos nux-vomica Linn, represses hepato cellular carcinoma cell migration and metastasis: The role of hypoxia inducible factor 1 pathway. Toxicol Lett 222(2): 91-101.

30. Chou, T.C. (2006). Theoretical basis, experimental design, and computerized simulation of synergism and antagonism in drug combination studies. Pharmacological Reviews, 58: 621-681.

31. Karapetis, C.S., Khambata Ford, S., Jonker, D.J., O Callaghan, C.J., Tu, D., Tebbutt, N.C., Simes, R.J., Chalchal, H., Shapiro, J.D., Robitaille, S., Price, T.J., Shepherd, L., Au, H.J., Langer, C., Moore, M.J. and Zalcberg, J.R. (2008). K-ras mutations and benefit from cetuximab in advanced colorectal cancer. N Engl J Med, 359: 1757-1765.

Current Trends in Biotechnology and Pharmacy
Vol. 14 (3) 311-318, July 2020, ISSN 0973-8916 (Print), 2230-7303 (Online)
DOI: 10.5530/ctbp.2020.3.32

A simple and novel sample preparation approach for effective characterization of antibody low molecular weight impurities by CE-SDS method

Bala Reddy Bheemareddy[1], Pradeep Iyer[1], Kranthi Vemparala[1], Vijaya R. Dirisala*[2]
[1]R&D Division, Hetero Biopharma Limited, Jadcherla, Mahaboob Nagar, Telangana, India – 509301
[2]Department of Biotechnology, Vignan's University, Guntur, Andhra Pradesh, India-522213
*Corresponding author : drdirisala@gmail.com

Abstract

Product and process related impurities of biopharmaceuticals have serious implications on product safety and efficacy in clinical use. Low molecular weight (LMW) impurities are generated during process and stability studies are routinely analyzed using non-reducing capillary electrophoresis with SDS during different stages of product development and release. The current sample processing methodology with heat denaturation is known to induce fragmentation and interfere with the LMW impurity analysis. In this study, we compared different sample processing buffers with different compositions and pH and finally found a solution to the problem of sample artifacts generated during heat denaturation step of sample processing which interferes with the LMW impurity analysis by CE-SDS method. We compared three sample buffers (100 mM Tris-Cl, 25mM Citrate and 25mM citrate with Urea) in for their ability to maintain product integrity during sample processing at different pH and temperatures in the non-reducing CE-SDS analysis. This study suggests that, the sample processing with 25mM citrate with 8M Urea sample processing buffer does not require heat denaturation at higher temperatures and hence is the most appropriate buffer for sample processing in the LMW impurity analysis. The 25mM Citrate + 8M Urea buffer has shown better drug product stability and integrity compared to other buffers. Hence, we recommend the 25mM Citrate buffer with 8M Urea for sample processing in LMW impurity analysis by CE-SDS method.

Keywords: Sample buffer, capillary electrophoresis, anti-CD20 monoclonal antibody, pH, Low molecular weight impurities

Introduction

Therapeutic monoclonal antibodies (mAbs), which are produced with recombinant DNA technology constitute for majority of bio-pharmaceutical approvals in recent times (1). Therapeutic mAbs are commonly produced in the cells of murine/mammalian origin and their purification involves a variety of chromatography and filtration steps in the harsh conditions which may influence the structural and functional integrity of the antibodies and may generate process and product related impurities. Hence, the purity and quality of these antibodies is utmost critical for them to be used in the patients. To ascertain the purity of these antibodies, the process and product development as well as product release involves full structural and functional characterization using a battery of analytical methods. Analytical characterization of purity is crucial for the safety and efficacy of therapeutic monoclonal antibodies and for their commercial release (2). Testing the monoclonal antibody drug products for their stability is an important parameter for evaluating the product shelf life and is also a regulatory

Vol. 14 (3) 311-318, July 2020, ISSN 0973-8916 (Print), 2230-7303 (Online)
DOI: 10.5530/ctbp.2020.3.32

requirement. The product related impurities such as high and low molecular weight impurities and process related impurities must be well characterized and analyzed during in-process, stability and lot release stages of therapeutic mAb production. Most importantly stability studies at high temperature induce product degradation and these low molecular weight impurities such as degradation products of therapeutic mAbs must be thoroughly characterized.

High performance size exclusion chromatography (HP-SEC) is a commonly employed method for protein characterization based on its molecular weight (3). However, HP-SEC is low in sensitivity and resolving power for low molecular weight species. The other method, SDS-PAGE although has better sensitivity, it has some limitations such as manual operation, long run time, and inaccurate quantification (4). Non-reducing capillary electrophoresis- SDS (Non-reducing CE-SDS) is considered one of the best method to analyze low molecular weight impurities in therapeutic monoclonal antibody samples. Because of its automation, quantitative nature, capillary electrophoresis (CE) technology is the new bench mark for therapeutic antibody-purity analysis.

In the biopharmaceutical industry, currently CE-SDS is applied at all stages of the product development, which includes analysis of structural isoforms, analysis of size variants, carbohydrate occupancy, and in process development, and product release (5-8). For the product degradation or stability analysis, non-reducing CE-SDS is the most preferred method, which offer great aptitude of low molecular weight impurities detection. In the non-reduced CE-SDS analysis, the native protein is treated with SDS prior to CE separation to mask the protein native charges (9).

Sample processing and the choice of sample processing buffers are the most critical factors in the CE-SDS based impurity analysis as sample preparation itself known to induce antibody fragmentation and contribute to the increased LMW impurities in the samples (10,11). Some studies have also reported that the free sulfhydryl groups in the antibody itself induce disulfide bond catalysis, resulting in increased antibody degradation. To arrest the antibody degradation, some studies have suggested the addition of alkylating agents to the CE-SDS sample buffer to prevent artifacts generated due to harsh sample processing which involves heat denaturation and alkaline conditions of buffer (10-14). These alkylating agents have minimal impact on the sample artifacts generated due to heat denaturation as samples with constant concentration of Iodoacetamide (IAM) has shown lesser fragmentation at lower temperatures compared to the samples incubated at higher temperatures (15).Hence, heat induced antibody fragmentation and generation of low molecular weight (LMW) impurities during sample processing interferes with the CE-SDS based LMW impurity analysis and pose a greater challenge for non-reducing CE-SDS to be used in the analysis of low molecular weight impurities. Avoiding the sample artifacts during sample processing is highly recommended for accurate analysis of low molecular weight impurities. Unfortunately, with the existing sample processing buffers this cannot be achieved completely. Zhang *et al.* (16) used Citrate buffer in the pH range of 5.5 to 6.5 for sample processing to minimize sample artifacts. However, they are only marginally successful, because still heating at high temperature (65°C) is required and heating is known induce fragmentation. The only solution is to achieve effective sample processing at lower temperatures with pH maintained around neutral conditions. In this study we used Urea in combination with Citrate buffer with pH 6 to achieve good separation with lesser degradation products.

Materials and Methods

Preparation of reagents and buffers: The Tris-Cl sample buffer containing 100 mM Tris-Cl and 1%SDS with pH 9 was prepared by dissolving 605 mg of Tris base and 0.5 gm of SDS in 50 ml water for injection (WFI) and pH was adjusted

Vol. 14 (3) 311-318, July 2020, ISSN 0973-8916 (Print), 2230-7303 (Online)
DOI: 10.5530/ctbp.2020.3.32

using 1N HCl. The 25mM Citrate phosphate sample buffer pH was prepared as per previous literature (16). The 25mM citrate + 8M Urea buffer was prepared by dissolving 48 gm of Urea in 100ml 25mM citrate sample buffer with pH 6. The alkylating agent, 250 mM IAM was prepared by dissolving 23 mg of Iodoacetamide in 500 µl of filtered WFI. The other reagents like SDS-MW Gel buffer and 10kDa internal marker was prepared as per manufacturers recommendations.

Preparation of monoclonal antibody samples: Both the reference standard (Reference Medicinal Product from innovator) and the test samples were treated simultaneously. Test samples were processed in duplicates and injected individually while the standard was processed as singlet and injected in duplicates. The standards and test samples were diluted to 1 mg/ml with filtered WFI from the nominal concentration. To 45 µl aliquots of standard and test samples 50 µl of sample buffer, 2 µl of 10 kDa internal marker and 5 µl of 250 mM IAA solution were added and mixed thoroughly by vortexing in Eppendorf tubes followed by centrifugation at 300 g for 1 min at 25°C. The samples and standard were incubated at the respective temperatures (at 70°C and 90°C as per the experimental protocol) for 10 minutes followed by centrifugation at 300 g for 1 min at 25°C and taken 100 µl aliquots of samples and standard. The anti-CD20 mAb (Chimeric) sample and other anti-VEGF (Humanized) and anti-Her2 (humanized) mAbs samples (1 mg/ml) were incubated with 50 µl of Tris-Cl buffer pH 9, Citrate buffer pH 6 and Citrate buffer with 8M Urea pH 6 were processed as mentioned previously.

Non-reducing capillary electrophoresis – sodium dodecyl sulfate (NR CE-SDS): Capillary electrophoresis system (PA 800 plus) from Beckman coulter with bare fused silica capillary (Total length – 30.2 cm, Effective length – 20.2 cm, Inner diameter – 50 µm, Outer diameter – 375 µm) containing Photodiode array (PDA) detector was used for performing all the experiments. Reagents were aliquoted into the vials and were placed in the inlet and outlet trays. The Inlet and outlet and sample trays were placed on the arms of the instrument. Capillary cartridge was installed and method was created as per manufacturer's recommendation. System suitability was tested using reference standard and bracketing reference standard. Standard and samples (0.5mg/ml) were injected in duplicates with 7 kV voltage for 30 seconds. During separation, a voltage of 15kV with reverse polarity maximum current of 300µA was applied. The PDA detector was set with electropherogram channel 1 wavelength of 214nm and channel 2 wave length of 220nm and reference channel wavelength of 350nm containing band width of 10nm and the sampling rate of 2Hz for data collection. All experiments were carried with bare fuse silica capillaries and the capillary temperature was maintained at 25°C throughout the experiments. All the calculations were performed using corrected peak areas and migration times.

Capillary preconditioning: All the new capillaries were preconditioned through a rinse procedure starting with 0.1N NaOH for 10 min for cleaning the capillary surface, 0.1N HCl for 5min for neutralizing the capillary surface, water for 5min for removing the residual acid, using 20 psi pressure. A voltage of "15 kV was applied with reverse polarity to the capillary filled with running buffer for 5 min after the rinse.

Results and Discussion

Effect of heating, sample buffer composition and pH on the LMW profile of anti-CD20 monoclonal antibody: We found significant additional degradation induced by Heating in anti-CD20 mAb samples at 90°C compared to 70°C (Fig. 1 a & b). The sample preparation involving heat denaturation is contributing to the increased low molecular weight impurities, which are interfering the analysis. Interestingly, we found that the increased degradation at higher temperature (90°C) was primarily due to higher pH. The Tris-Cl buffer with pH 6 shown lesser degradation products and more intact mAb portion at both the temperatures (Fig.1 a & b). Zhang *et al*.[16] also observed the similar results with undisclosed

Vol. 14 (3) 311-318, July 2020, ISSN 0973-8916 (Print), 2230-7303 (Online)
DOI: 10.5530/ctbp.2020.3.32

antibody, and our results second their results. We have also evaluated the effect of Tris-Cl buffer pH (6 to 9) on LMWs% and intact mAb peak area (A %) at 70 °C for 10 mins incubation time. We found that the degradation pattern is linear in the range of pH 9 to 7 with intact mAb A% increased and LMW% decreased with decrease in pH proves that pH independently effect the product degradation during denaturation procedure (supplementary data set 1).

Although, Zhang *et al*. (16) reported the citrate buffer pH 6 shown better intact mAb peak area, they have not disclosed the antibody. Our results specifically suggested that, the temperature has a significant impact on fragmentation of anti-CD20 chimeric antibody, only at higher pH. Since, the Tris-Cl buffer with pH 6 is not stable for analysis, we tested the 25mM Citrate phosphate buffer with pH 6 for further experiments. We also compared the degradation profiles (LMWs) of both Chimeric and Humanized monoclonal antibodies in both 25 mM Citrate phosphate buffer and 100mM Tris-Cl buffer at 70°C and 90°C temperatures. To find whether the observed effect is mAb specific, we have also evaluated the effect of sample buffer and its pH on different therapeutic monoclonal antibodies with different engineering patterns such as chimeric and humanized antibodies at both the temperatures. Although both mAbs have exhibited more degradation in Tris-Cl buffer compared to citrate buffer, the extent of degradation was more in case of chimeric anti-CD20 monoclonal antibody suggesting antibody type may also influence the extent of degradation at both the temperatures (Fig. 2 a & b). The addition of alkylating agent IAM does not seem to have much effect on the heat induced degradation of anti-CD20 monoclonal antibody, as we observed similar LMW profile in with and without IAM (data not shown). Zhu *et al.* (15) also reported that the alkylating agents have minimal effect on fragmentation due to the variations in incubation times and concentration of IAM and due to variation in heating times of samples (15).

Table 1. Comparison of Degradation profile of three different antibodies in all three buffers

	Chimeric anti-CD20 mAb			**Humanized anti-VEGF mAb mAb**			**Humanized anti-HER2 mAb mAb**		
Buffer	Tris-Cl Buffe, pH9.0	Citrate Buffer, pH6.0	Citrate Buffer, pH 6.0 +8M Urea	Tris-Cl Buffe, pH9.0	Citrate Buffer, pH6.0	Citrate Buffer, pH 6.0 +8M Urea	Tris-Cl Buffer, pH6.0	Citrate Buffer, pH6.0	Citrate Buffer, pH 6.0 +8M Urea
Time	10 min.	10 min.	10 min.	10 min.	10 min.	10 min.	10 min.	10 min.	10 min.
Temp.	70 °C	70 °C	37 °C	70 °C	70 °C	37 °C	70 °C	70 °C	37 °C
LC	2.1	0.77	0.49	0.38	0.35	0.29	0.39	0.23	0.15
HC	0.14	0.14	0.11	0.16	0.15	0.13	0.04	0	0
1H1L	0.41	0.42	0.39	0.12	0.12	0.11	0.06	0.06	0.02
2HC	1.25	1.95	1.86	0.71	1.51	1.21	0.61	1.11	1.05
2H1L	5.59	1.95	1.55	0.94	0.73	0.62	0.71	0.23	0.17
Intact mAb	90.3	94.48	95.32	97.4	96.88	97.5	97.81	98.03	98.44

*LC – Light chain, HC – Heavy chain, 1H1L – 1 heavy and 1 Light chain, 2HC – 2 Heavy chains, 2H1L – 2 Heavy chains and 1 Light chains

Vol. 14 (3) 311-318, July 2020, ISSN 0973-8916 (Print), 2230-7303 (Online)
DOI: 10.5530/ctbp.2020.3.32

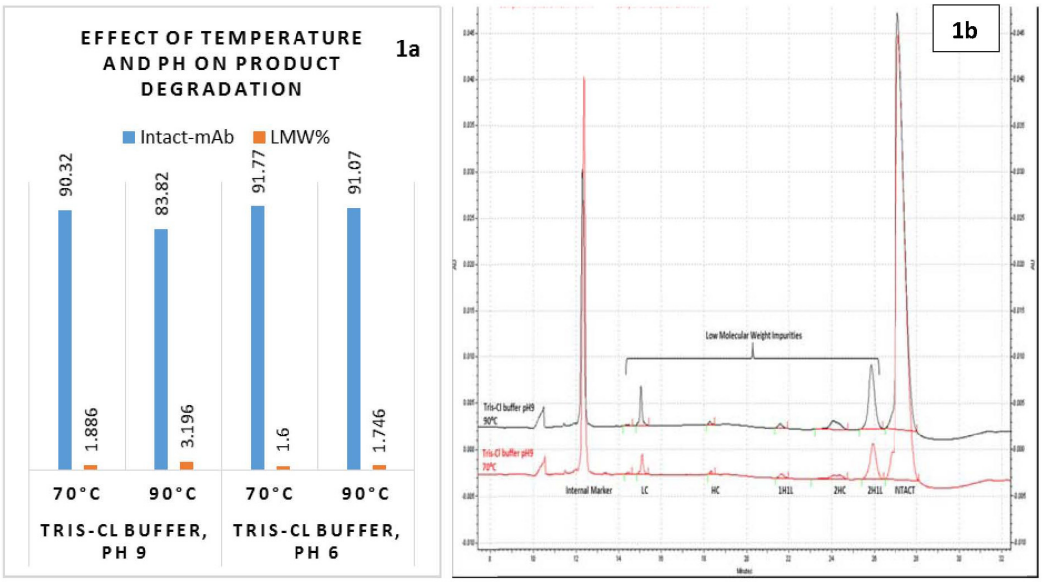

Fig. 1a & 1b. Effect of temperature and pH on product degradation profile in the Tris-Cl buffer

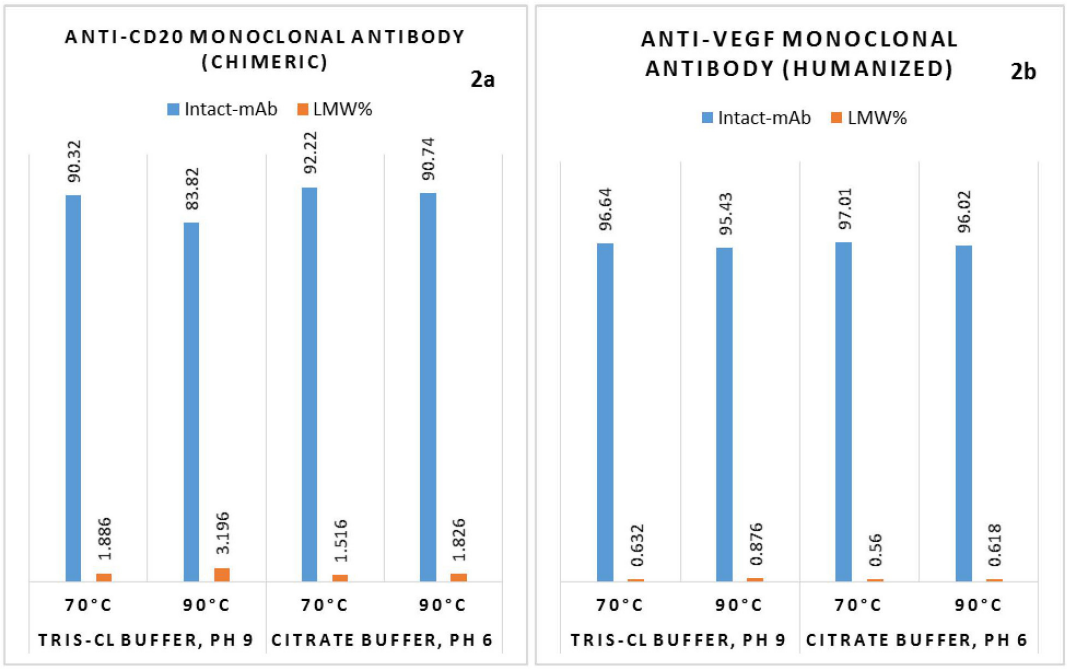

Fig. 2a & 2b. Effect of sample buffer on product degradation profile of two different therapeutic monoclonal antibodies

Effect of sample buffer composition and pH on LMW impurities analysis

Vol. 14 (3) 311-318, July 2020, ISSN 0973-8916 (Print), 2230-7303 (Online)
DOI: 10.5530/ctbp.2020.3.32

Urea as denaturing agent in sample preparation: Since, we observed heat denaturation increase the product degradation further and interferes with the analysis of inherent LMWs, we have evaluated the possibility of substituting heat denaturation with chemical denaturation using chaiotropic agents such as Urea. The samples were incubated with 25 mM Citrate phosphate Buffer containing 8M Urea (pH 6.0) at 37°C for 10 mins and compared with the samples subjected to routine heat denaturation at 70°C for 10 minutes in both Tris-Cl and Citrate buffers. We found the addition of urea to the citrate buffer marginally decreased the product degradation further at 37°C and improved the intact mAb peak area percentage at lower temperatures suggesting that Citrate buffer with Urea is better alternative to the Citrate buffer and Tris-Cl buffers which require heat denaturation during sample processing. However, Urea concentration (range 4 to 10M) does not seems to have any effect on degradation profile (See supplementary data set 2). This suggests the heat denaturation can be replaced by chemical denaturation with Urea for the analysis of LMW impurities by non-reducing CE-SDS. These results suggests that, the chemical denaturation by Urea has exhibited the similar resolving power and separation with better product integrity at 37°C compared to the 25mM Citrate buffer and Tris-Cl buffer run at 70°C.

Batch to batch variation of anti-CD20 chimeric mAb product degradation in all three buffers: We have compared this effect using the anti-CD20 monoclonal antibody product of innovator and in-house generated anti-CD20 antibody and found that the rate of degradation is more in the in-house generated antibody which may be attributed to quantity of other critical quality attributes of the antibody which may have an effect on the degradation profile (Fig. 3 a & b).

Variation in degradation profile of different antibodies with all three buffers: All three buffers including Citrate buffer containing urea are compared with three different classes of antibody such as chimeric, humanized and fully human

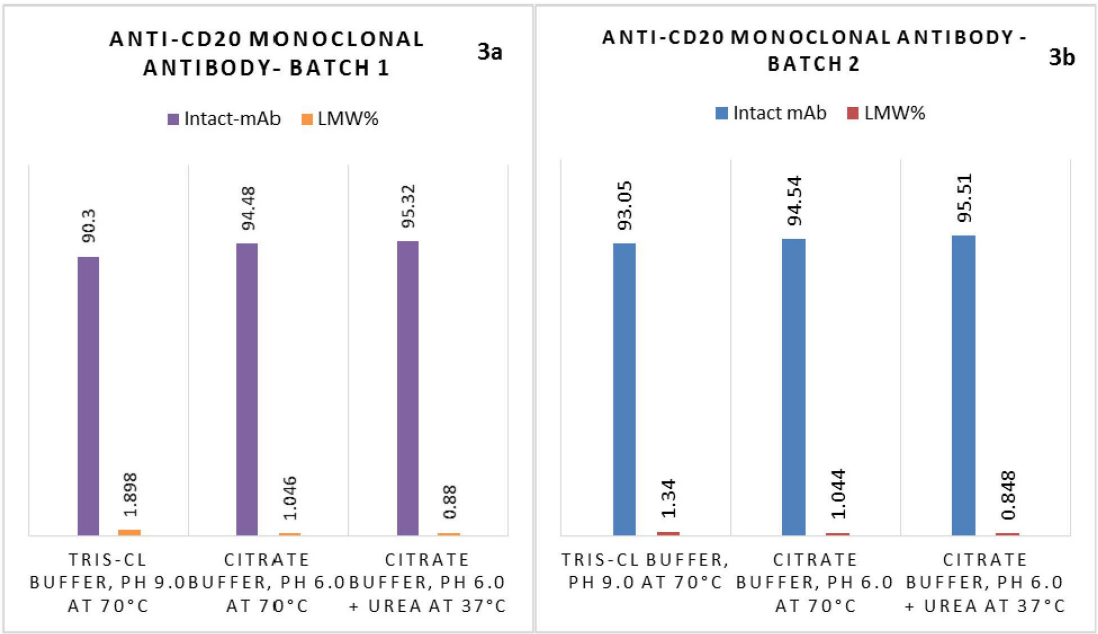

Fig. 3a & 3b. Batch to batch variation of product degradation in anti-CD20 mAb samples

Vol. 14 (3) 311-318, July 2020, ISSN 0973-8916 (Print), 2230-7303 (Online)
DOI: 10.5530/ctbp.2020.3.32

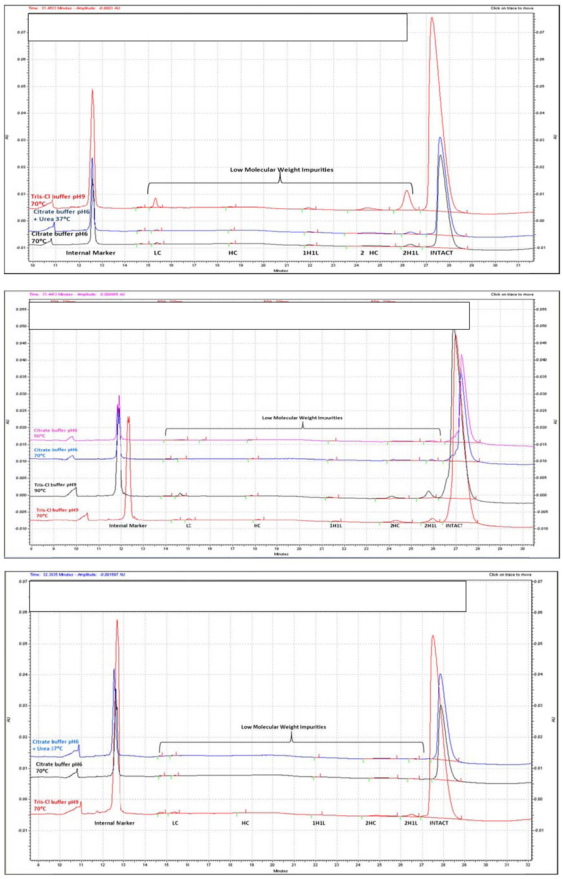

Fig. 4a, 4b & 4c. CE-SDS electrophoretograms of three different antibodies in all three butters

antibodies. All three antibodies shown better intact mAb A% in Citrate buffer with Urea and the extent of degradation was more in the case of chimeric anti-CD20 monoclonal antibody compared to the other two antibodies (Table 1) (Fig. 4 a, b & c). The peak heights in Citrate Buffer and Citrate Buffer with urea are nearly half when compared to Tris-Cl Buffer, which may be due to the conductivity variations in the buffers. The amount of protein entering the capillary is less due to conductivity and ionic strength of buffer. However, these variations does not show any effect on the results (data not shown). We found, the peaks irrespective of their molecular weight enter the capillary in a similar fashion both in both Tris-Cl buffer and Citrate Buffer.

Evaluation of urea sample preparation: We have also evaluated the role of Urea concentration (4, 6, 8 and 10 M) and incubation times (0, 5, 10, 15 min) at 37 °C and found that there is no significant impact of Urea concentration and incubation times in the specified ranges on the product degradation profile. However, we have observed base line drift and decreasing peak heights with increasing molarity of urea. IAM peak was not observed in samples treated with urea buffer.

Conclusion

Sample buffer composition, Temperature and pH affects the product degradation of therapeutic monoclonal antibodies. Antibodies with different engineering patterns such as chimeric and humanized show variations in the product degradation with chimeric having the highest degradation and humanized with low degradation profiles. The 25mM citrate sample buffer containing 8M urea is the most appropriate buffer for sample processing for LMW impurity analysis by CE-SDS method as heat denaturation step is not required for this buffer and hence the sample artifacts generated during heat denaturation which interferes with the LMW impurity analysis can be avoided with this buffer.

Acknowledgements

The authors would like to acknowledge the financial and Instrument support of Hetero Biopharma Limited and Vignan's University for this research.

Conflicts of interest : The authors declare there is no conflict of interest.

References

1. Ecker, D.M., Jones, S.D. and Levine H.L. (2015). The therapeutic monoclonal antibody market. MAbs. 7(1):9-14.

2. Berkowitz, S.A., Engen, J.R., Mazzeo, J.R. and Jones, G.B. (2012). Analytical tools for characterizing biopharmaceuticals and the implications for biosimilars. Nat Rev Drug Discov., 11(7):527-40.

Vol. 14 (3) 311-318, July 2020, ISSN 0973-8916 (Print), 2230-7303 (Online)
DOI: 10.5530/ctbp.2020.3.32

3. Kenney, A. and Fowell, S. (1992). Practical Protein Chromatography, Humana Press, Totowa, N.J, USA.

4. Zilberstein, G., Korol, L., Antonioli, P., Righetti, P.G. and Bukshpan, S. (2007). SDS-PAGE under Focusing Conditions: An Electrokinetic Transport Phenomenon Based on Charge Neutralization. Anal Chem., 79: 821–827.

5. Rustandi, R., Washabaugh, M., and Wang, Y. (2008). Applications of CE SDS gel in development of biopharmaceutical antibody-based products. Electrophoresis, 29: 3612–3620.

6. Guo, A., Han, M., Martinez, T., Ketchem, R.R., Novick, S., Jochheim, C. and Balland, A. (2008). Electrophoretic evidence for the presence of structural isoforms specific for the IgG2 isotype. Electrophoresis. 29: 2550–2556.

7. Salas-Solano, O., Tomlinson, B., Du, S., Parker, M. and Strahan, A. (2006). Optimization and validation of a quantitative capillary electrophoresis sodium dodecyl sulfate method for quality control and stability monitoring of monoclonal antibodies. Anal Chem., 78: 6583–6594.

8. Good, D.L., Cummins-Bitz, S., Fields, R.M. and Nunnally, B.K. (2004). Methods in Molecular Biology, vol. 276: Capillary Electrophoresis of Proteins and Peptides Editors: M. A. Strege and A. L. Lagu Humana Press Inc., Totowa, NJ, USA.

9. Chantal, F. and Oscar, S.S. (2018). Capillary Electrophoresis in Quality Control: PART II: CE-SDS: Method Development and Robustness. Cited, IB-16385A. Available from: https://sciex.com/Documents/Applications/AIB-16385.pdf.

10. Liu, H., Gaza-Bulseco, G., Chumsae, C. and Newby-Kew, A. (2007). Characterization of lower molecular weight artifact bands of recombinant monoclonal IgG1 antibodies on non-reducing SDS-PAGE. Biotechnol Lett., 29: 1611–1622.

11. Rustandi, R.R., Washabaugh, M.W. and Wang, Y. (2008). Applications of CE SDS gel in development of biopharmaceutical antibody-based products. Electrophoresis, 29: 3612–3620.

12. Lacher, N.A., Wang, Q., Roberts, R.K., Holovics, H.J, Aykent, S., Schlittler, M.R., Thompson M.R. and Demarest, C.W. (2010). Development of a capillary gel electrophoresis method for monitoring disulfide isomer heterogeneity in IgG2 antibodies. Electrophoresis. 31: 448–458.

13. Guo, A., Han, M., Martinez, T., Ketchem, R.R., Novick, S., Jochheim, C. and Balland, A. (2008). Electrophoretic evidence for the presence of structural isoforms specific for the IgG2 isotype. Electrophoresis. 29: 2550–2556.

14. Taylor, F.R., Prentice, H.L., Garber, E.A., Fajardo, H.A., Vasilyeva, E. and Blake Pepinsky, R. (2006). Suppression of sodium dodecyl sulfate-polyacrylamide gel electrophoresis sample preparation artifacts for analysis of IgG4 half-antibody. Anal Biochem., 353: 204–208.

15. Zhu, Z.C., Chen, Y., Ackerman, M.S., Wang, B., Wu, W., Li, B., Obenauer-Kutner, L., Zhao, R., Tao, L., Ihnat, P.M., Liu, J., Gandhi, R.B. and Qiu, B. (2013). Investigation of monoclonal antibody fragmentation artifacts in non-reducing SDS-PAGE., 83: 89-95.

16. Zhang, J., Burman, S., Gunturi, S. and Foley, J.P. (2010). Method development and validation of capillary sodium dodecyl sulfate gel electrophoresis for the characterization of a monoclonal antibody. J of Pharm and Biomed Anal., 53: 1236–1243.

Current Trends in Biotechnology and Pharmacy
Vol. 14 (3) 319-326, July 2020, ISSN 0973-8916 (Print), 2230-7303 (Online)
DOI: 10.5530/ctbp.2020.3.33

Production and characterization of a haloalkaline pectinase from *Halomonas pantellerinsis* strain SSL8 isolated from Sambhar lake, Rajasthan

Makarand N. Cherekar and Anupama P. Pathak*
School of Life Sciences, Swami Ramanand Teerth Marathwada University, Nanded-431606
*Corresponding author : anupama.micro@rediffmail.com

Abstract

Haloalkaliphilic bacterium producing a pectinase was isolated from the Sambhar soda lake, Rajasthan, India. Chemical composition of water sample was analyzed. Pectinase production was studied in submerged fermentation, an appropriate medium for the growth and production was orange peel powder. The bacterium was gram negative and identified as *Halomonas pantellerinsis* strain SSL8 using biochemical tests and 16S rRNA sequencing. It was able to grow and produced pectinase that was stable and active at high pH, temperature and high NaCl concentration. Maximum pectinase production from isolate was observed after 120hr of incubation (0.70U/mL). The maximum pectinase activity was found at 9 pH (0.79U/mL), 40°C Temperature (0.70U/mL) and 10% NaCl concentration (0.85U/mL). Partially purified pectinase enzyme was used for the fruit juice extraction and clarification.

Keywords: Haloalkaliphilic, *Halomonas pantellerinsis,* Sambhar lake, orange peel powder, Pectinase

Introduction

Pectinase constitute a unique group of enzymes which catalyze the degradation of pectic polymers present in the plant cell walls. Pectinases are commercially used in many processes and nearly 25% of the global enzymes sales are attributed to pectinases (1, 2).

In the industrial sector, acidic pectinases are used in the production and clarification of fruit juices, in maceration and solubilization of fruit pulps whereas alkaline pectinases are finding immense use in the degumming of ramie fibers retting of flax, textile processing, coffee and tea fermentations, paper and pulp industry, and in oil extraction (3). Pectinases are produced by many organisms such as bacteria, fungi, yeasts, insects, nematodes, protozoa and plants. A quarter of the global food enzymes sale is met with microbial pectinases. Although the major sources of acidic pectinases are fungi, alkaline pectinases are produced from alkaliphilic bacteria (4)

The present paper describes isolation and identification of a haloalkaliphilic *Halomonas pantellerinsis* strain SSL8 from the hypersaline Sambhar Lake and production of extracellular haloalkaliphilic pectinase from such fruits and vegetable waste to minimize the cost by the selected isolate.

Material and Methods

Site description and sample collection: The Sambhar Lake is the largest inland saline lake located in Thar Desert of Rajasthan, India (26° 52'- 27° 2' N, 74° 53'- 75° 13'E) (Fig. 1). It is an elliptical and shallow lake, with the maximum length of 22.5 km. The width of the lake ranges from 3.2 km to 11.2 km. The total catchments area of the lake is 7560 km^2, most of which lies to

Vol. 14 (3) 319-326, July 2020, ISSN 0973-8916 (Print), 2230-7303 (Online)
DOI: 10.5530/ctbp.2020.3.33

the north and northeast. The lake has occupied an area of about approximately 225 Sq. Km and average depth of water is about 1 m whereas the maximum depth is about 3m (5, 6, 7). The surface (SU) and Sediment (SD) water samples were collected from four sampling stations located in main lake and salt pans towards Sambhar Lake city. Samples were collected in presterilized bottles in post-monsoon, season. The samples collected from each station were average of ten samples spanning the whole sampling point.

Abiotic characterization of water: The parameters like Temperature, pH were measured at the time of sampling by using Digital Thermometer and Digital pen pH meter respectively. Samples were transported to laboratory in cold box. The samples were filtered and stored in refrigerator during investigation (8).

Various physicochemical parameters were determined for both the samples individually. TS, TDS, TSS were analyzed according to procedures described in APHA. The salinity was measured by using Refractometer (Erma, Tokyo). The dissolved oxygen content (DO) was determined by azide modification method, Biological oxygen demand (BOD) and chemical oxygen demand (COD) were determined by potassium dichromate oxidation method. Chloride was determined by argentometric and sulphate by gravimetric methods. Sodium and potassium were measured directly using the flame photometer (Model Elico CL 361). Carbonates and bicarbonates were measured titrimetrically. Calcium and magnesium were determined by EDTA titrimetric method. Metal ions like Fe, Mn, Zn, As, Cr, Pb, Cu, and Cd were directly analyzed by atomic absorption spectrophotometer. (Model S2 Thermo- USA) (9, 10).

Enrichment, Isolation and cultivations of haloalkaliphiles: The 5ml water and Brine sample was inoculated into nine different media such as Alkaliphilic media at pH- 10.0,[A], Marine agar pH- 10.5 [MA], Nutrient broth at pH- 10.5 [ANA] with 30 % sodium chloride, Halophilic medium [H], modified Horikoshi II medium [H II], Synthetic Sea water medium[S], Alkaline peptone water [AP], Alkaline Bacillus medium (AB) and Tindal's medium [T].. Inoculated media flasks were incubated in shaking incubator for 8 days at 30°C temperature and 150 rpm speed. Incubated samples were further inoculated on respective agar plates. Inoculated agar plates were incubated for 15-20 days at 30°C temperature (11-14).

Screening of isolates for efficient pectinase producer: Isolates were tested qualitatively by growing the culture on modified alkaliphilic pectin agar medium followed by observing zone of hydrolysis around colonies. After incubation the plates were flooded with Iodine-potassium iodide solution (0.3 % iodine, 0.6 % potassium iodide solution) to enhance the clarity of zone. The isolate showing largest zone was selected for further production (2, 15, 16)

Identification of selected strain of the bacterium: Selected isolate was subjected to morphological and Biochemical observation. Sugar utilization pattern of selected isolate was determined using glucose, galactose, mannose, arabinose, fructose, ribose and lactose. Enzyme utilization profile was determined using starch, casein, gelatin, pectin substrates (17).

DNA extraction, amplification and 16S rRNA sequencing: 16S rRNA analysis was performed by extracting DNA of isolates. For DNA extraction isolates were suspended in an extraction buffer (10 mM Tris HCL, pH 8.0; 1 mM EDTA, pH 8.0). Proteinase K solution was added to a final concentration of 100 ug/ml and incubated at 55°C for 2 h with continuous shaking. 0.5 M NaCl was added and incubated at 72°C for 30 min. DNA was extracted by phenol–chloroform extraction. DNA was washed with 70% ethanol and dissolved in Tris–EDTA buffer (pH 8.0). Extracted DNA was analyzed by electrophoresis on a 1% agarose gel and visualized by ethidium bromide staining (18)

The amplification of 16S rRNA fragments were performed by using (PCR) thermocycler, (Eppendorf) with 530F (52 GTGCCAGC

Vol. 14 (3) 319-326, July 2020, ISSN 0973-8916 (Print), 2230-7303 (Online)
DOI: 10.5530/ctbp.2020.3.33

AGCCGCGG 32) and 1392R (52 ACGGG CGGTG T GTAC 32) primer pair. The PCR reaction mixture contained 1.5 mM $MgCl_2$, 200 uM dNTP mixture and 0.3 μM of each primer and 1 U of Taq DNA polymerase with a reaction mixture supplied by the manufacturer in a total volume of 100 μl. Reaction mixture was first denatured at 94°C for 3 min, followed denaturation at 94°C for 30 s, annealing at 52°C for 30 s and extension at 72°C for 1 min. Amplification was completed by a final extension step at 72°C for 7 min reaction was carried out for 30 cycles. PCR products were run on a 1% agarose gel. PCR products were purified by the PEG/NaCl method (19) and directly sequenced using Applied Biosystem model 3730 DNA analyzer (Foster, California, USA). The 16S rRNA sequences were initially analyzed using BLAST program (www.ncbi.nlm.nih.gov/blast/blast.cgi). Multiple sequence alignments of approximately 800 base pair sequences were performed using CLUSTALW2 program version 2.1. Phylogenetic tree was constructed using the neighbor joining method (20). Tree files were generated by PHYLIP and viewed by TREE VIEW program. Bootstrap analysis was applied.

***Pectinase production using synthetic and crude media**:* Pectinase production was carried out submerged fermentation using synthetic and crude media. Presterilized medium containing yeast extract, 1; pectin, 5; KH_2PO_4, 4; NaCl, 200; $MgSO_4.7H_2O$, 1; $MnSO_4$, 0.05; $FeSO_4.7H_2O$, 0.05; $CaCl_2.2H_2O$, 2; NH_4Cl, 2 grams per liter was inoculated and incubated at 30°C temperature and 150 rpm speed at pH 9.

Presterilized crude medium contain 10g orange peel powder mixed with mineral salt solution contain 1% KH_2PO_4, 15% NaCl, 0.1% $MgSO_4.7H_2O$, 0.1% $CaCl_2$ was also inoculated and incubated at same conditions (21, 22).

Assay of pectinase activity: Polygalacturonase activity was determined by quantifying the amount of reducing groups expressed as galacturonic acid units, liberated during the incubation of 1 ml of 1% (w/v) citrus pectin, prepared in 0.2 M phosphate buffer (pH 8.2) with 500 ìl of the enzyme at 37°C for 30 min, by DNSA method. One unit of polygalacturonase activity was defined as the amount of enzyme required to release 1 ìmol of galacturonic acid per minute under standard assay conditions and expressed as units per litre (U/l). Specific activity was defined as the amount of enzyme required to release 1 μmol of galacturonic acid per minute per milligram of total enzyme protein and expressed as units per milligram (U/mg) (16, 21, 22).

Partial purification of pectinase: The crude pectinase enzyme supernatant was partially purified using chilled acetone and ammonium sulphate precipitation method. The precipitate was dissolved in 10 ml of 0.2 M phosphate buffer (pH 8.5) and desalting was carried out by dialysis (2).

Determination of protein content: The protein contents of the crude and purified pectinases were determined by the method specified by Lowry *et al.*, using bovine serum albumin as the standard (23).

Effect of pH, temperature, salt and reaction times on pectinase activity : The optimum pH and temperature of the pectinase activity was studied over pH range of 5 to 12 and temperature range from 20 to 50 °C respectively. The effect of various salt concentrations and reaction times on pectinase activity was measured over range of 5 to 30% and 10, 20, 30, 40, and 50 min respectively (2, 24, 25).

Application of pectinase in fruit juice extraction and fruit juice clarification: Fruits (apples) were obtained from a local market Nanded. For the extraction of juice from apple, the apples were chopped into small cubes (3-5mm in size). Ten grams of material were incubated with 1 ml of crude enzymatic extract for 1 h in a shaking water bath with a shaking rate of 100 rpm, at 40 °C. Later the samples were incubated in a boiling water bath for 5 min to inactivate the enzyme. After cooling to room temperature, the juice was filtered by vacuum through filter paper and the volume of juice obtained was measured

Vol. 14 (3) 319-326, July 2020, ISSN 0973-8916 (Print), 2230-7303 (Online)
DOI: 10.5530/ctbp.2020.3.33

by using 100 mL graduated cylinders. Inactivated enzyme was used as a control and for study the fruit juice clarification, 10 mL portion of juice was taken and centrifuged at 3000 rpm for 10 minutes. The clarity of fruit juice was determined by measuring at 450nm using UV-VIS spectrophotometer (9, 28).

Result and Discussion:

Abiotic characterization of water: Abiotic characterization of Sambhar lake water samples collected in post-monsoon season has yielded diverse results. The colour of post-monsoon water sample was pale green at the time of collection. The typical rotten egg like smell was experienced in the lake atmosphere. The average pH recorded was 10 for water sample.

The Total Solids (TS) and Total dissolved Solids (TDS) were recorded as 131050 mg/l and 88263 mg/l respectively. The Total Solids (TS) and Total dissolved Solids (TDS) recorded in present investigation were higher as compared to the very well studied African soda lake and Kenyan Soda Lake.[22]. Some anionic and cationic concentrations of water were recorded, among all dominating cations and anions were sodium (9930 mg/l) and chloride (7356 mg/l) and the divalent cations Ca^{2+} (1550 mg/l) and Mg^{2+}(1870 mg/l). Carbonates (396 mg/l) and sulphate (9152 mg/l)) anions also recorded in considerable amount.

Also in the water sample the metal concentrations were recorded. The Trace amount of chromium (0.01 mg/l) and arsenic (0.01mg/l) were recorded. Also lead (0.05mg/l), Zinc (0.36 mg/l) and cadmium (0.7mg/l) were present in considerable amount in water sample (27, 28).

Screening of bacterial isolates for Haloalkaliphilic pectinase production: Out of nine broth media used during enrichment the agar media have supported highest diversity and faster growths of haloalkaliphiles were used in further investigation. Out of total 10 isolates which have shown zone of clearance on pectin agar plates, and showing distinct colony characters were selected from alkaliphilc medium (A), synthetic Sea agar (SS), alkaline nutrient agar (ANA) and Marine agar (MA) plates. Small colonies were appeared after incubation of 10 days, further incubation of 10 days have yielded large colonies. Non pigmented and pigmented colonies were observed. Pigmented colonies showed cream, yellow, pink, and red colour pigment. Out of ten morphologically distinct isolates SSL8 rapidly growing extreme haloalkaliphilic strain was selected for further investigation which showing maximum zone of clearance on pectin agar plates. It is motile, cream pigmented, Gram negative, rod shaped bacterium growing at optimum 9 pH, 10% salt concentration and 40°C temperature. It is Catalase and oxidase positive, produces H_2S. The sugars Glucose, Fructose, Mannose, Ribose, Arabinose, Galactose and Lactose are not utilized It is negative for hydrolysis of starch, Casein and Gelatin (14, 28) (Table 1).

Based on morphological, physiological, biochemical characteristic and Phylogenetic analysis of its 16S rRNA gene sequence it was identified as *Halomonas pantellerinsis* strain SSL8 (Fig. 1). The 16S rRNA gene sequence was submitted to NCBI Genbank with accession number KC 434456

Alkaline pectinase production was recorded with two substrates orange peel powder and pectin. Maximum production was observed in growth medium containing orange peel as source of substrate (Fig. 2). Maximum pectinase production from *Halomonas pantellerinsis* strain SSL8 was observed after 120hr or 5 days of incubation (0.70U/mL). A gradual increase in the enzyme level was detected till the 120hr of the fermentation process, whereas, there was a steep decline in the pectinase activity after the 120hr of incubation, as shown in Fig 2. Beyond this period the enzyme production drastically reduced, probably due to the depletion of essential nutrients in the medium and/or accumulation of toxic secondary metabolites.

Effect of temperature: The effect temperature on the alkaline pectinase enzyme production was studied using alkaliphilic medium by conducting

Vol. 14 (3) 319-326, July 2020, ISSN 0973-8916 (Print), 2230-7303 (Online)
DOI: 10.5530/ctbp.2020.3.33

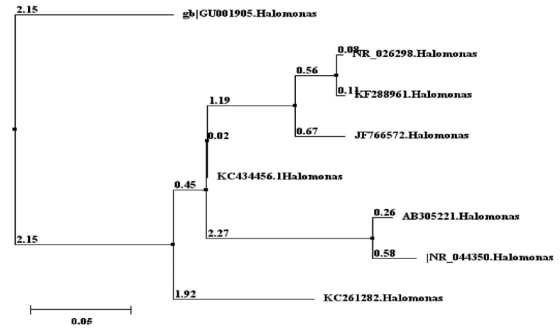

Fig. 1. Phylogenetic tree of isolate SSL8 to other Halomonas.Each number on a branch indicates the bootstrap values. The scale bar indicates 0.05 substitutions per nucleotide position

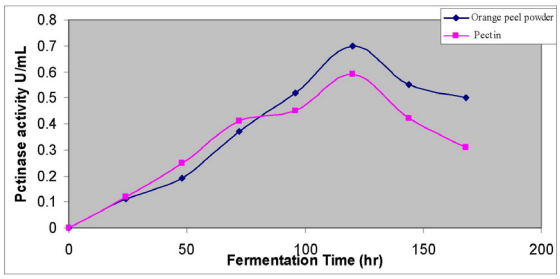

Fig. 2. Effect of fermentation time on pectinase production

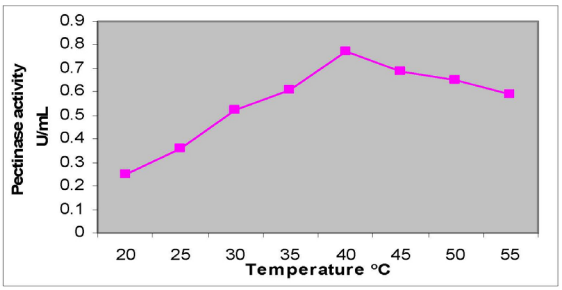

Fig. 3. Effect of Temperature on pectinase Activity

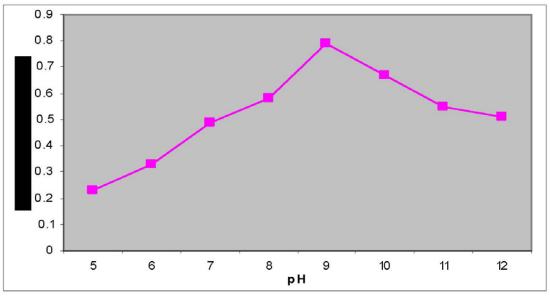

Fig. 4. Effect of pH on pectinase Activity

Table 1. Morphological and Biochemical characterization of Strain SSL8

Characters	SSL8
Morphology	Rod
Gram nature	-
Size (mm)	0.5-2
Colony pigmentation	Cream
Motility	Motile
Oxidase	+
Catalase	+
pH range	08-Nov
Optimum pH	9
Salt range	5-15%
Optimum Salt Concentration	10%
Temperature range (°C)	20-40
Urease	+
Nitrate reduction	+
H2S production	+
Hydrolysis of:	
Casein	-
Gelatin	-
Starch	-
Utilization of:	
Arabinose	-
Fructose	-
D-Glucose	-
D-Galactose	-
Mannose	-
Ribose	-
Lactose	-

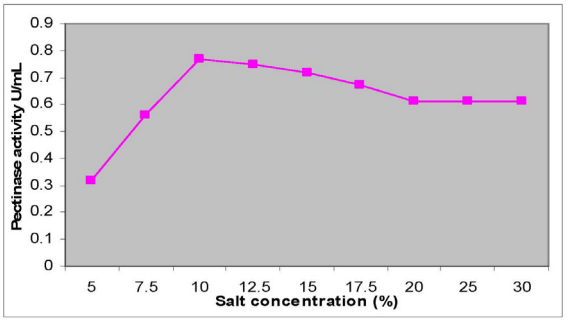

Fig. 5. Effect of Salt concentration on pectinase Activity

Vol. 14 (3) 319-326, July 2020, ISSN 0973-8916 (Print), 2230-7303 (Online)
DOI: 10.5530/ctbp.2020.3.33

experiments at different temperatures, keeping all other conditions constant for the fermentation. As a temperature increase the pectinase enzyme activity was found to increase and maximum pectinase activity of 0.77 U/ml was found at 40°C (Fig. 3). Further increase in temperature beyond 40°C decreased the pectinase activity till the end of fermentation. Hence optimum temperature was 40°C and was used for further studies. The decrease in enzyme activity at higher temperature may be due to enzyme denaturation.

Effect of pH: The effect of pH on the pectinase production was studied by conducting experiments at different pH (pH range 5, 6, 7, 8, 9, 10, 11, 12) and by keeping temperature at 40 °C. As initial pH was increased from pH 5 to pH 9, the pectinase activity was found to increase. Further increase in initial pH beyond pH 9, the pectinase activity was found to decrease. The decrease in enzyme activity at higher pH may be due to growth and metabolism of organism. A maximum pectinase activity of 0.79U/ml was observed at a fermentation period of 6 days at temperature 40°C and at pH value of 9. Hence optimum pH value was selected as pH 9 (Fig. 4).

***Effect of salt concentration*:** The effect Salt concentration on the alkaline pectinase enzyme production was studied using alkaliphilic medium by varying Salt concentrations (5, 10, 15, 20, 25 and 30% w/v) keeping all other conditions constant. The maximum pectinase activity of 0.85U/ml was found at 10% Salt concentration (Fig. 5).

Pectinase for fruit juice extraction and clarification : The fruit juice extraction by using the pectinase enzyme as well as mixture of other enzymes (cellulose) with pectinase was showed significant results of fruit juice extraction. 31 mL of fruit juice was extracted when apple without peel was treated with pure pectinase and 24 mL juice was extracted when treated with crud pectinase. 17 mL juice was extracted when crude pectinase treatment was given to apple with peel. Whenever the treatment of cellulase on the fruit without peel was given, 26 mL juice was extracted and 19 mL was extracted from apple with peel. (1) 26.5 mL juice was extracted when treatment of crude pectinase and crude cellulose given to the fruit without peel and 19.7 mL was extracted from the same treatment on the fruits with peel. And the apple juice which was extracted by the treatment of crude pectinase has the more clarity as compare to other enzymatic treatment

Conclusions

A haloalkaliphilic bacterial strain isolated from the Sambhar salt lake of India was identified as *Halomonas pantellerinsis* strain SSL8. It produced halo alkaline pectinase that was stable and active at high pH, temperature and high salt concentration. It is showing optimum activity at pH 9, temperature 40 °C and at 10 % salt concentration. The *Halomonas pantellerinsis* strain SSL8 pectinase gives maximum production in fruit juice extraction and also showed good result in fruit juice clarification. Similar study was carried out by Kashyap et al. in 2000 (1).

Considering the high activity and stability in high alkaline pH and temperature, the *Halomonas pantellerinsis* strain SSL8 pectinase may find potential application in the degumming of ramie fibers, retting of flax, textile processing, coffee and tea fermentations, paper and pulp industry, and in oil extraction (25).

Acknowledgments

Honorable Vice Chancellor of Swami Ramanand Teerth Marathwada, University is thanked for providing infrastructure facility.

Reference

1. Kashyap, D. R., Chandra, S., Kaul A. and Tewari, R. (2000). Production, purification and characterization of pectinase from a *Bacillus sp*. DT7., World Journal of Microbiology & Biotechnology 16: 277 -282.
2. Kashyap, D.R., Vohra, P. K., Chopra, S. and Tewari, R. (2001). Applications of pectinases in the commercial sector: a review, Bioresource Technol*.,* 77, 215-227.
3. Hoondal, G. S., Tiwari, R. P., Tiwari, R. Dahiya, N. and Beg, Q.K. (2000). Microbial

Vol. 14 (3) 319-326, July 2020, ISSN 0973-8916 (Print), 2230-7303 (Online)
DOI: 10.5530/ctbp.2020.3.33

alkaline pectinases and their applications: a review. Appl Microbiol Biotechnol, 59, 409–18.

4. Horikoshi, Koki (1972). Production of Alkaline Enzymes by Alkalophilic Microorganisms Part III. Alkaline Pectinase of Bacillus No. P-4-N Agr. Biol. Chem., Vol. 36, No. 2, p. 285-293.
5. Upasani, V. N. (2008). Microbiological studies on Sambhar lake (Salt of Earth). Rajasthan, India. *Proc of Taal* 2007: The 12th World Lake Conference, 448-50.
6. Yadav, D. N., Sarin, M. M. (2009). Ra-Po-Pb isotope systemics in waters of Sambhar Salt Lake, Rajasthan (India): geochemical characterization and particulate reactivity. J of Environmental Radioactivity, 100, 17-22.
7. Yadav, D. N., Sarin, M. M., krisnaswami, S. (2007). Hydrogeochemistry of Sambhar salt Lake, Rajasthan: Implication to recycling of salt and annual salt budget. J of the Geological society of India, 69, 139-152.
8. Bhadja, P. and Kundu, R. (2012). Status of the seawater quality at few industrially important coasts of Gujarat (India) off Arabian Sea. Indian J of Geo-Marine Sciences, 41, 954-61.
9. American Public Health Association (APHA) 1992. In: Greenberg A, Clesceri L, Eaton A (eds) Standard methods for the examination of water and wastewater, 18th edn. American Public Health Association.
10. Trivedi, R. K. and Goel, P. K. (1986). Chemical and Biological methods for water pollution studies (Environment pollution V. C. College of Sci. Karad.
11. Deshmukh, K. B., Pathak, A. P. and Karuppayil M. S. (2011). Bacterial Diversity of Lonar Soda Lake of India. Indian J Microbiol, 51(1), 107-111.
12. Sahay, H., Mahfooz, S., Singh, A. K., Singh, S., Kaushik, R., Saxena, A. K., and Arora, D. K. (2012). Exploration and characterization of agriculturally and industrially important haloalkaliphilic Exploration and characterization bacteria from environmental samples of hypersaline Sambhar lake, India World J Microbiol Biotechnol, (DOI 10.1007/s11274-012-1131-1), 28, 3207-3217.
13. Upasani, V. N. (1990). Sambhar Salt Lake: Chemical composition of the brines and studies on Haloalkaliphilic archaeobacteria, Archies of Microbiology 154: 589-593.
14. Cherekar, M. N. and Pathak, A. P. (2015). Studies on Haloalkaliphilic gammaproteobacteria from hypersaline Sambhar lake, Rajasthan, India, Indian Journal of Geo-Marine Sciences, vol 44(10), pp 1646-1653.
15. Banu, A. R., Devi, M. K., Gnanaprabha,l G. R., Pradeep, B. V. and Palaniswamy, M. (2010). Production and characterization of pectinase enzyme from *Penicillium chrysogenum,* Indian J Sci. Technol**.,** 3(4)**,** 377- 381.
16. Kuhad, R.C., Kapoor, M. and Rustagi, R. (2004). Enhanced Production of an alkaline pectinase by *Streptomyces* sp. RCK-SC by whole-cell immobilization and solid-state cultivation, World J Microbiol Biot*,* 20, 257-263.
17. Aneja, K. R. (2007). Experimnts in Microbiology, Plant pathology and biotechnology. 4th edition (New Internationsal publishers, New Delhi) 2007.
18. Ausubel, F. M., Brent, R., Kingston, R. E., Moore D. D., Seidman, J. G., Smith, J. A, Struhl, K. (2002). The polymerase chain reaction. In: Short protocols in molecular biology, 5th Edn. Vol II. Wiley, New York.
19. Yates, C, Gilling, M. R., Davison, A. D., Altavilla, N., Veal, D. A. (1997). PCR amplification of crude microbial DNA extracted from soil. Lett Appl Microbiol. 1997; 25:303–307.

Vol. 14 (3) 319-326, July 2020, ISSN 0973-8916 (Print), 2230-7303 (Online)
DOI: 10.5530/ctbp.2020.3.33

20. Saitou, N., Nei, M. (1987). The neighbour joining method a new method for reconstructing phylogenetic trees. Mol Biol Evol. 1987; 4:406–425.

21. Silva, D., Martins, E. S., Silva R. and Gomes, E. (2002). Pectinase production by *Penicillium viridicatum* RFC3 by solid state fermentation using agro-industrial by-products, Braz. J Microbiol., 33, 318-324.

22. Zu-ming, L., Bo, J., Hong-xun, Z., Zhi-hui, B., Wen-tong, X. and Hong-yu, L. (2008). Purification and characterization of three alkaline endopolygalacturonases from a newly isolated *Bacillus gibsonii,* China. J Process Eng., 8(4), 768- 773

23. Lowry O.H., Rosebrough N.J., Farr A.L. and Randall R.J. (1951) Protein measurement with folin phenol reagent, J Biol.Chem., 193, 265-275.

24. Deshmukh, K. B., Pathak, A. P., (2012). Alkaline protease production, Extraction and characterization from alkaliphilic *Bacillus licheniformis* KBDL 4: A Lonar Soda Lake isolate, Indian J of Experimental Biology, Vol. 50, pp 569-576

25. Kapoor, M., Beg, Q. K., Bhushan, B., Singh, K., Dadich, K. S. and Hoondal, G. S., (2001). Application of alkaline and thermostable polygalacturonase from Bacillus sp. MG-cp-2 in degumming of ramie (Boehmeria nivea) and sunn hemp (Crotolaria juncia) bast fibers. Process Biochem, 36, 803–807.

26. Soares, M., Da Silva, R., Carmona, E. C., Gomes E. (2001). Pectinolytic enzyme production by Bacillus species and their potential application on juice extraction, World Journal of Microbiology and Biotechnology 17: 79. https://doi.org/10.1023/A:1016667930174.

27. Pathak, A. P. and Cherekar, M. N. (2015). Hydrobiology of hypersaline Sambhar salt Lake a Ramsar site Rajasthan, India, Indian Journal of Geo-Marine Sciences, vol 44 (10), pp 1640-1645.

28. Cherekar, M. N. and Pathak, A. P. (2016). Chemical assessment of Sambhar Soda Lake, a Ramsar site in India, J. Water Chem. Technol. 38: 244. https://doi.org/10.3103/S1063455X1604010X.

Current Trends in Biotechnology and Pharmacy
Vol. 14 (3) 327-339, July 2020, ISSN 0973-8916 (Print), 2230-7303 (Online)
DOI: 10.5530/ctbp.2020.3.34

Chrysin pretreatment improves mitochondrial enzymes and angiotensin converting enzymes in L-NAME induced hypertensive rats

Veerappan Ramanathan[1], GV Swarnalatha[2], B. Manimegalai[1], A. Dominic amalraj[1], Senthilkumar Rajagopal[2*]

[1]Department of Biochemistry, Enathi Rajappa Arts and Science College, Pattukkottai, TN, India
[2]Department of Biochemistry, Rayalaseema University, Kurnool, AP, India
*Corresponding author : senthilanal@yahoo.com

Abstract

Hypertension is one among the important factors that causes cardiovascular disorders. Nω-nitro-L-arginine methyl ester (L-NAME) induces hypertension by blocking nitric oxide (NO) synthesis. Aim of present study was to investigate the effects of chrysin is one of major flavnoids, on L-NAME-induced hypertensive rats. Induces hypertension in adult male wistar rats weighing 180-220 g by oral treated of L-NAME (40 mg/kg/day) dissolved in drinking water daily for 8 weeks. Experimental rats were oral treated with chrysin (25 mg/kg b.w). Both the systolic and diastolic blood pressure of control and experimental rats were measured by tail cuff plethysmography system.

In our studies results showed an increase in the levels of systolic and diastolic blood pressure, heart, liver, kidney, body weight, plasma, and aortic Angiotension converting enzymes (ACE), Sodium (Na^+), Chloride (Cl^-) levels in L-NAME treated rats. At the same time in L-NAME treated rats, there was a decrease in the levels of potassium (K^+), Plasma and heart- aortic nitrite/nitrate level, mitochondrial enzymes in liver such as Isocitrate dehydrogenase (ICDH), á-ketoglutarate dehydrogenase (á-KGDH), Succinate dehydrogenase (SDH) and Malate dehydrogenase (MDH). Chrysin treatment prevented the increase in systolic and diastolic blood pressure in the L-NAME-treated rats. Blood pressure (BP) reduction was interrelated with a reduction in Na^+, Cl^-, ACE activity and increased K^+, plasma and heart, aortic nitrite/nitrate levels. In contrast, L-NAME had opposite effects on mitochondrial liver enzymes, electrolytes, ACE and NO by treatment of chrysin.

Hence, the present findings might suggest that chrysin improve the balance between circulating nitric oxide and rennin-angiotensin system and beneficial effects on cardiovascular tissue through its ACE inhibitor activity.

Key words: Angiotensin II, Chrysin, hydroxyproline, β - ketoglutarate dehydrogenase, nitric oxide, renin-angiotensin system.

Abbreviations: ACE - Angiotension converting enzymes; BP - Blood pressure; eNOS - endothelial nitricoxide synthase; ICDH - isocitrate dehydrogenase; L-NAME- Nω-nitro-l-arginine methyl; SDH - succinate dehydrogenase.

Introduction

Hypertension is acknowledged to be a 'silent killer, which causes no signs and symptoms for so many years, even decades, until it finally damages certain vital organs [1]. Both Dyslipidemia and hypertension are the major risk factors for cardiovascular disease [2]. Hypertension is one of the risk factor responsible for cardiovascular diseases to accounts for about 54% of deaths through stroke and 47% of deaths

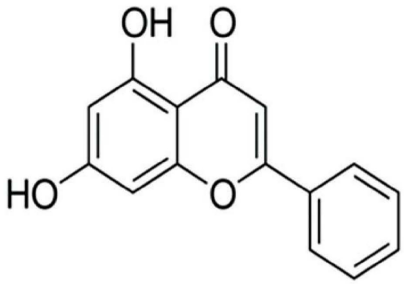

Fig. 1. Chemical structure of chrysin (5,7 dihydroxyflavone)

through coronary heart disease in adults worldwide [3]. Changes in lifestyle and dietary habits in modern worlds may affect blood pressure (BP) and increases cardiovascular risk factors. Studies have reported that nitric oxide (NO) and angiotensin II (Ang II) are the primary key factors that regulate BP and cardiovascular tissue structures [4]. NO has been proved to have important role in the maintenance of normal BP and body fluid homeostasis [5]. Is one of the biologically active molecules that are produced from L-arginine by nitric oxide synthase (NOS). There exist three isoforms of these enzymes: neuronal (nNOS), inducible (iNOS) and endothelial (eNOS) [6]. NO helps to maintain vascular tone and is a regulator of platelet activation inhibitor of endothelial cell stimulation [7]. The chronic administration of NOs inhibitors provides an experimental animal model for hypertension [8]. Bioavailability of NO can be enhanced by inhibition of oxidative stress, and therefore the agents with antioxidant properties inactivating free radicals, increase NO bioavailability [9]. Endothelial dysfunction exhibits a reduction in NO bioavailability that may also cause cardiovascular remodeling through the activation of the RAS to produce Ang II. Treatment of hypertension with ACE inhibitors may inhibit the formation of Ang II and thus, suppress vasoconstriction, oxidative stress and lower BP [10]. The RAS or the rennin angiotensin-aldosterone system (RAAS) is a major endocrine/paracrine system that plays a vital role in BP regulation, fluid and electrolyte homoeostasis. The RAAS regulates BP via angiotensin release and blood electrolyte content through release of aldosterone [11]. The ACE is a carboxypeptidase is involved in the conversion of angiotensin I (Ang I) into the biologically active Ang II [12]. ACE is important in the production of Ang II. Treatment with ACE inhibitors in rats with L-NAME induced hypertension was reported not only to reduce BP but also to prevent the progression of cardio renal remodeling [13].

Plant polyphenolic compounds the flavanoids consist of number of classes, as flavanols, flavones and flavans. A naturally occurring flavones, Chrysin (5, 7-dihydroxy flavones structure shown in Fig. 1) contained in flowers blue passion flower (*Passiflora caerulea*), Indian trumpet flower, as well as in edible of mushrooms [14], honey and propolis [15]. At the same time it possess antioxidant capacity, anti-inflammatory activity, anti-allergic, anti-cancer, antiestrogenic, anxiolytic [16], antihypertensive properties [17]. Chrysin has tyrosinase inhibitory activity, moderate aromatase inhibitory activity, and also inhibits estradiol-induced DNA synthesis. C-iso-prenylated hydrophobic derivatives of chrysin are potential P-glycoprotein modulators in tumour cells [18]. The earlier study showed that chrysin has antihypertensive effects, and reduces hepatic, renal damages and endothelial dysfunction in L-NAME induced hypertensive rats [19]. The present study aimed to evaluate the effect of chrysin on Electrolytes, mitochondrial liver enzymes, ACE, nitric oxide metabolites (nitrite and nitrate) in the L NAME induced hypertensive rats against the control and unsupplemented groups.

Materials and Methods

Chemicals : Chrysin and L-NAME was purchased from Sigma Chemical Co. (St. Louis, MO, USA). All other chemicals used in this study were of analytical grade and obtained from E-Merck or HIMEDIA, Mumbai, India.

Animals *:* All the animal handling and experimental procedures were approved by the Institutional Animal Ethics Committee of Bharathidasan University and animals were cared

for in accordance with the Indian National Law on Animal Care and Use. Male Wistar rats (180-220 g) were purchased from the Indian Institute of Science, Bangalore, India. Rats were housed in plastic cages with filter tops under controlled conditions of a 12 h light-dark cycle, 50% humidity and temperature of 28ºC. All rats received a standard pellet diet (Lipton Lever Mumbai, India) and water *ad libitum*.

Induction of L-NAME induced hypertension: L-NAME (40 mg/kg B.W) was dissolved in drinking water and given to rats at an interval of 24 h for 8 weeks. Mean arterial blood pressure (MAP) was measured using tail cuff method. MAP measurements were performed during the time of 1-8 weeks [16].

Blood pressure measurements: Systolic and diastolic blood pressures were determined by the tail-cuff method (IITC, model 31, Woodland Hills, CA, USA). The animals were placed in a heated chamber at an ambient temperature of 30-34°C for 15 minutes and from each animal one to nine blood pressure values were recorded. The lowest three readings were averaged to obtain a mean blood pressure. All recordings and data analyses were done using a computerized data acquisition system and software.

Study design: Animals were divided into four groups of six rats each and all were fed the standard pellet diet. The rats were grouped as given below.

Group I	:	Control.
Group II	:	Normal + Chrysin (25 mg/kg of B.W) after 4th week.
Group III	:	L-NAME induced hypertension (40 mg/kg of B.W).
Group IV	:	L-NAME induced hypertension (40 mg/kg of B.W) + Chrysin (25 mg/kg of B.W) after 4th week.

Chrysin (25 mg/kg of B.W) was administered orally once in a day in the morning for 4 weeks. Chrysin dose (25 mg/kg of B.W) based on our previous study. The compound was suspended in 2% dimethyl sulfoxide solution and fed by intubation. After 8 weeks, the animals were sacrificed by cervical dislocation. The blood was collected in clean dry test tubes and allowed to coagulate at ambient temperature for 30 minutes. Serum was separated by centrifugation at 2000 rpm for 10 minutes. The blood, collected in a heparinized centrifuge tube, was centrifuged at 2000 rpm for 10 minutes and the plasma separated was removed by aspiration and was used for estimations.

Biochemical estimation and Heart weight and collagen content : The Heart, aorta and kidney was dissected out and then weighed. Heart weight-to-body weight ratio was calculated. Hydroxyproline concentration was estimated in heart and aorta samples and the determined from standard curve and expressed as mg/g dry weight [20].

The electrolytes such as sodium (Na^+) and chloride (Cl^-) along with potassium (K^+) were analyzed by AVL 9180 Electrolyte analyzer (ROCHE-USSR). Methodology is based on the ion selective electrode measurement principle to precisely determine the measurement values Burtis and Ashwood [21].

The activities of isocitrate dehydrogenase (ICDH), succinate dehydrogenase (SDH), malate dehydrogenase (MDH), á- ketoglutarate dehydrogenase (á-KGDH) were assayed by the methods of silambarasan et al., [22] respectively.

Nitric oxide metabolites level : Nitrite/nitrate (stable NO metabolites) in the aorta and heart samples were measured based on the Griess reaction Green et al., [23] in which a chromophore with a strong absorbance at 550 nm is formed by reaction of nitrate with a mixture of naphthyl ethylene diamine and -sulfanilamide. The nitrate was reduced to nitrite by 30 minutes incubation with nitrate reductase in the presence of NADPH. The amount of nitrite/nitrate present in the aorta and heart sample was estimated from the standard curve obtained. Nitrite/nitrate levels were expressed as nmol/mg protein.

ACE assay : ACE (USCN Life, West Lake, and Wuhan, China) activity was analyzed in cardiac samples using commercially available kits following the manufacturer's instructions. The colored end product of this enzyme was measured by a microplate reader (Molecular Devices, Sunnyvale, CA, USA) at 450 nm [24].

Statistical analysis : Statistical analysis were analysed by one-way analysis of variance (ANOVA) followed by Duncan's multiple range test (DMRT) using a commercially available Software Package for the Social Science (SPSS) software package version 11.0. Results were expressed as mean ± S.D. for six rats in each group. For all the statistical tests, values of $P < 0.05$ were statistically significant.

Results

Table 1 shows the effect of chrysin on the weight of heart, aorta and kidney weights, and heart weight-to-body weight ratio in control and L-NAME induced hypertensive rats. L-NAME induced hypertensive rats had significantly increased heart, aorta and kidney weights, heart weight-to-body weight ratio and hydroxyproline weights. Treatment with chrysin (25 mg/kg) significantly ($P < 0.05$) reduced the heart, aorta and kidney weights and weight-to-body weight ratio.

Fig.2 shows effect of chrysin in cardiac and aortic hydroxyproline in experimental rats. In cardiac and aorta hydroxyproline concentration levels are increased in L-NAME induced hypertension as compared to control. Supplementation of chrysin significantly ($P < 0.05$) reduces in cardiac and aorta levels of hydroxyproline in group IV as compared to group I. There is no significant difference between group I and II.

Table 2 shows the effect of chrysin on the levels of plasma electrolytes such as Na^+, K^+ and Cl^- in control and L-NAME hypertensive rats. L-

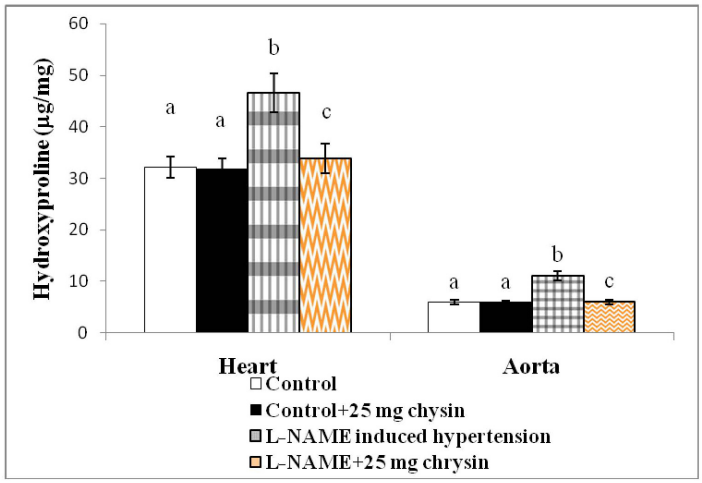

Columns are mean ± S.D. for six rats in each group.
Columns not sharing common superscript are significant with each other at P<0.05 (Duncan's multiple range test).

Fig. 2. Effect of chrysin in hydroxyproline levels in heart and aorta in various expermintal groups

NAME rats had significantly ($P < 0.05$) increased Na^+, Cl^- levels and decreased K^+ levels. Supplementation with chrysin significantly ($P < 0.05$) brought back these values towards near to normal levels. No significant differences between Group I and II.

Activities of ICDH, SDH, MDH, and á-KGDH were significantly ($P < 0.05$, Table 3) decreased in the liver mitochondria of L-NAME rats. Oral treatment with chrysin significantly ($P < 0.05$, Table 3) increased the activities of these enzymes when compared to untreated L-NAME rats. No significant difference between group I and II.

Plasma and heart, aortic nitrite/nitrate level was significantly ($P < 0.05$) reduced in L-NAME rats whereas chrysin treatment for 4 weeks significantly ($P < 0.05$) increased the above to normal (Fig. 3.A.B.). There is no significant change of group I and II.

L-NAME hypertension significantly ($P < 0.05$) enhanced the activity of ACE in heart and aorta compared with control and this increase was attenuated by chrysin treatment (Fig. 4.A.B.).

Discussion

In previous studies it was reported that in L-NAME treated rats there was a significant increase of heart, kidney, liver and aorta weights [25]. Our studies also supported that L-NAME induced hypertensive rats has significantly increased heart, aorta, and kidney weights. Supplementation of chrysin dose (25 mg/kg) significantly reduces the aortic, renal and cardiac hypertrophy that might be due to the BP lowering effect of chrysin. Because it has been also proved to reduce BP and antihypertensive effects on our previous study [18].

Cardiac and aorta tissues hydroxyproline concentration levels are increased in L-NAME

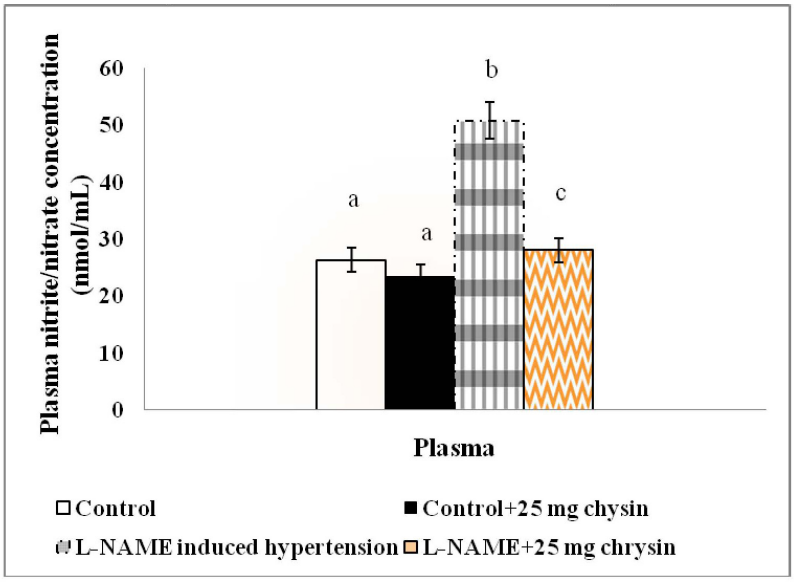

Columns are mean ± S.D. for six rats in each group.
Columns not sharing common superscript are significant with each other at $P<0.05$ (Duncan's multiple range test).

Fig.3. A. Effect of chrysin in Nitrite/nitrate concentrations in plasma in various experimental groups.

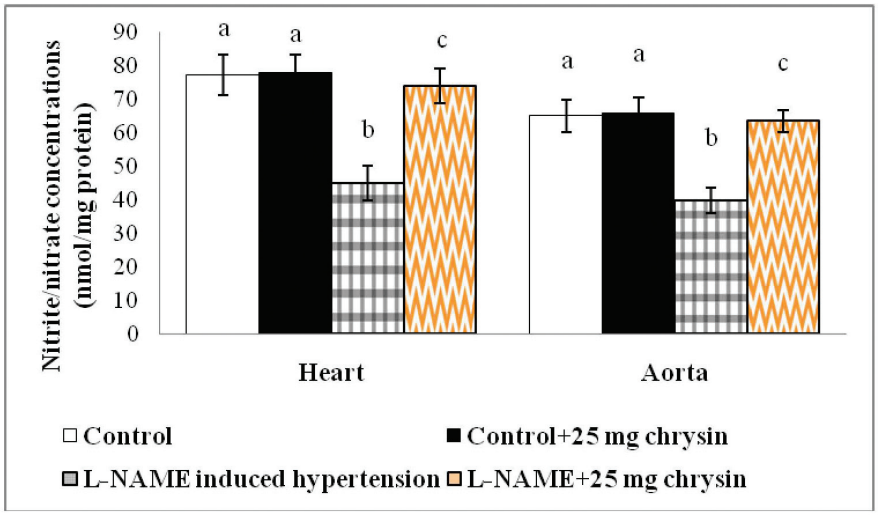

Columns are mean ± S.D. for six rats in each group.
Columns not sharing common superscript are significant with each other at P<0.05 (Duncan's multiple range test).

Fig.3. B. Effect of chrysin in Nitrite/nitrate concentrations in heart and aorta in various experimental groups.

induced hypertension as compared to control rats. Cardiac hypertrophy is propositional with increased BP, increased fibrosis, collagen deposition, and reduced cardiac function. Hydroxyproline is major component of collagen and its concentration is a quantitative index of fibrosis. During heart failure the collagen get deposited in heart causing stiffening of the heart walls, impaired relaxation, impaired filling, and reduced cardiac output [26]. In aortic wall components, it is shown that collagen with highest elastic modulus and, therefore, appears as major determinant of aortic stiffness. In our proposed study we have determined the level of hydroxyproline which is the collagen marker in aorta as wells as cardiac tissue. Chrysin has the capability of preventing the accumulation of collagen in aorta. At the same time the elevated cardiac weight in hypertension was evidently suppressed by supplementation of chrysin. The antihypertensive potential of chrysin is main reason for reducing pressure load with induced hypertrophy. Treatment of L-NAME significantly elevates BP and ACE levels which cause cardiovascular system and kidneys injuries that might be leads to aggravation of hypertension. Renal NO synthesis plays an important role in acute and chronic regulation of sodium balance. In experimental rats maintained on high salt diet, the expression of all three NOS is forms are increased in the inner medulla. An important characteristic of renal body fluid feedback control system is the pressure naturituresis or the ability of the kidneys to play central role in reducing BP by altering the renal excretion of salt and water such as sodium balance, extracellular fluid volume and BP homeostasis. In addition to playing a major role in long term BP adjustment, the sodium transporters along the nephron are very dynamic, even responding quickly to normal fluctuations of BP. Increased ANG II and pressure-induced oxidative stress alter mitochondria and electrolyte

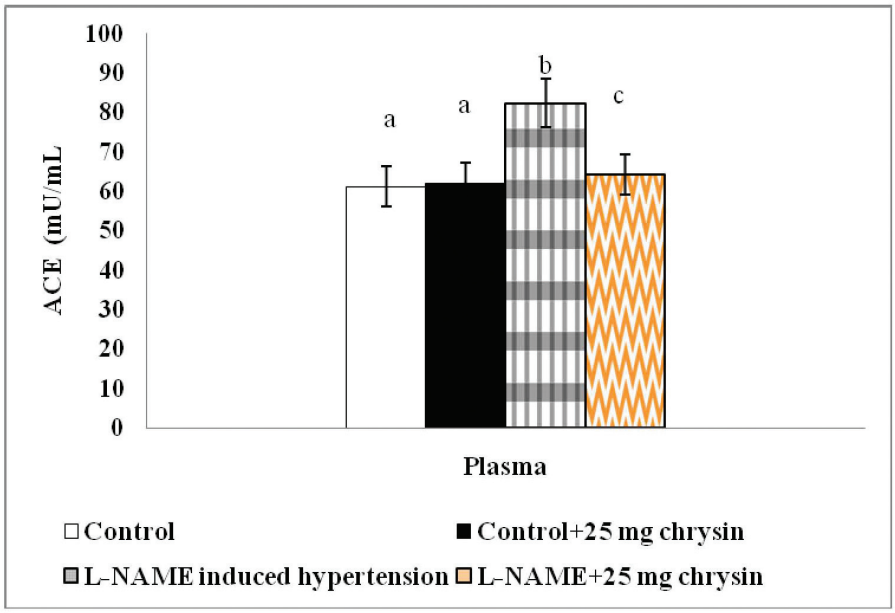

Columns are mean ± S.D. for six rats in each group.
Columns not sharing common superscript are significant with each other at P<0.05 (Duncan's multiple range test).
Fig.4. A. Effect of chrysin in ACE in plasma in various experimental groups

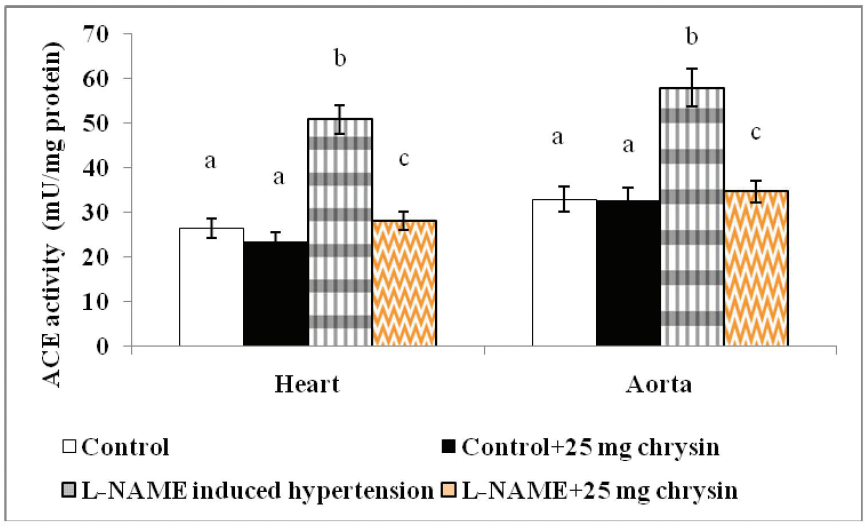

Columns are mean ± S.D. for six rats in each group.
Columns not sharing common superscript are significant with each other at P<0.05 (Duncan's multiple range test).
Fig.4. B. Effect of chrysin in ACE in Heart and aorta in various experimental groups.

transport efficiency, which together reduce kidney oxygen tension and can cause tissue hypoxia. In our studies plasma electrolytes such as Na^+, K^+ and Cl^- are kept in control and in L-NAME hypertensive rats. It is shown that L-NAME rats has significantly ($P < 0.05$) increased Na^+, Cl^- levels and decreased K^+ levels. The electrolytes Na^+, K^+ play critical role in the normal regulation of blood pressure. These electrolytes have has main impact in the control of arterial resistance [27]. Number of research suggests that intracellular sodium overload and potassium depletion are important for pathophysiology of hypertension [28]. As previously reported increased level of Na^+ and Cl^- along with a decreased level of potassium results with chronic inhibition of NOS by L-NAME [29] is observed in our studies. Administration of chrysin brought back these parameters to near normal values similar to control rats.

On the same time NO synthase substrate, it should be remembered that arginine participates in other metabolic functions, including a-ketoglutarate metabolism and polyamine synthesis. (Fumarase catalyzes the reversible conversion between fumarate and L-malate in the tricarboxylic acid cycle in mitochondria. L-malate can be converted to oxaloacetate, aspartate, argininosuccinate, and L-arginine, the substrate of nitric oxide (NO) synthase.). Our studies have shown that activities of ICDH, SDH, MDH, and á-KGDH, which were significantly ($P < 0.05$), decreased in the liver mitochondria of L-NAME rats. It was already explored that under oxidative stress conditions the functions of several key tricarboxylic acid cycle enzymes were perturbed [30]. Giribabu et al., [31] reported that *Vitis vinifera* seed extract has ability for preventing the decrease in ICDH, SDH and MDH in liver homogenates respective to decrease in liver oxidative stress in diabetes. In our study is also accepted the earlier report, chrysin, it is observed to increase the activities of liver mitochondrial enzymes and which might be the effect of oxidative stress.

Hypertension is one of the most important risk factors associated with the development of vascular diseases. The modulation of vascular tone results from NO synthesis and release by endothelial cells [32]. The use of NO is not limited but in other cellular events, such as vascular smooth muscle cell proliferation [33]. Chronic inhibition of NO synthase persuaded by administration of L-NAME resulting in induction of hypertension, hypertrophy, cardiac remodelling [34]. Treatment with L-NAME-induces hypertension and provides an experimental model to study hypertension. It has been shown that ventricular hypertrophyin L-NAME model of hypertension increase the chance of fibrosis and left ventricle hypertrophy [35].

In this study on treating with chronic inhibition of NOS by nitric oxide deficient hypertensive rats we observed the significant decrease of plasma, heart and aorta NOx levels. Moreover, our findings are in consistent with several other reports which showed the association between chronic NO deficiency and hypertension [36]. It shown that chrysin protects NO from free radicals, increasing the bioavailability of NO and also increase the activity of eNOS resulting in decreased BP. There are no significant changes between group I and II. With antioxidant property, chrysin is believed to reduce oxidative damage and lower cardiovascular diseases as shown in our studies.

RAAS is important physiological role in BP control and sodium volume homeostasis. In this study, it is observed that plasma, heart and aortic ACE activity are increased in L-NAME induced hypertensive rats. ACE converts Ang I to Ang II. In general the reduction of ACE activity leads to a reduction in blood pressure because of the reduction in Ang II synthesis. Ang II acts as a potent vasoconstrictor. Ang II exacerbates oxidative stress by increasing the production of superoxide [37]. Increased ACE activity and oxidative stress was observed in hypertensive animals. Increased plasma Ang II availability was reported in L-NAME-treated rats because of

Table 1. Estimation of heart, kidney, aorta weights and heart weight-to-body weight ratio levels in various experimental groups.

	Control	Control+25 mg chrysin	L-NAME induced hypertension	L-NAME+25 mg chrysin
Heart Weight (mg)	821.12± 31.28[a]	819.24 ± 32.12 [a]	1099.57 ± 42.68 [b]	861.57 ± 39.29 [c]
Kidney weight (mg)	872.39± 35.81[a]	869.41 ± 34.20 [a]	1486.92 ± 49.11[b]	901.14 ± 38.24 [c]
Aorta weight (mg)	98.59± 5.19[a]	97.41 ± 4.76 [a]	121.85 ± 9.59 [b]	103.23 ± 5.27 [c]
HW/BW (mg/g)	3.08 ± 0.19[a]	3.06 ± 0.18 [a]	5.24 ± 0.32 [b]	3.14 ± 0.17[c]
LVW/BW (mg/g)	1.21 ± 0.06 [a]	1.20 ± 0.06 [a]	1.58± 0.05[b]	1.25 ± 0.05 [c]
RVW/BW (mg/g)	0.43 ± 0.05 [a]	0.42 ± 0.06 [a]	0.31 ±0.04[b]	0.41 ± 0.05 [c]

Values are mean ± S.D. for six rats in each group.
Values not sharing common superscript are significant with each other at P < 0.05 (Duncan's multiple range test).

Table 2. Effect of chrysin on Electrolytes of control and L-NAME induced hypertensive rats

	Control	Control+25 mg chysin	L-NAME induced hypertension	L-NAME+25 mg chrysin
Plasma sodium (mmol/L)	146.23 ± 8.12a	145.12 ± 7.27a	169.55 ± 9.63b	150.67 ± 6.38c
Plasma potassium (mmol/L)	4.81 ± 0.39a	4.82 ± 0.40a	2.39 ± 0.19b	4.52 ± 0.40c
Plasma chloride (mmol/L)	99.53 ± 4.27a	98.11 ± 4.57a	127.27 ± 8.16b	104.17 ± 6.75c

Values are mean ± S.D. for six rats in each group.
Values not sharing common superscript are significant with each other at P < 0.05 (Duncan's multiple range test).

endothelial NO synthase (eNOS) inhibition [38]. The increase of BP and ACE levels further causes pathological injuries to the cardiovascular system and kidneys, which in turn leads to aggravation of hypertension [39]. In current study, chrysin have reduced plasma, cardiac and aortic ACE activity in L-NAME received rats. This result suggests that the antioxidant properties of chrysin proportional to the reduction of the enzyme activity. The effect of chrysin on ACE in this study in accordance with Kataoka et al., [40] has reported that anti-inflammatory and antioxidant effects of calcium channel blockers might be a result of the inhibition of the local RAS.

Table 3. Effect of chrysin on the activities of mitochondrial enzymes in liver in control and L-NAME induced hypertensive rats

	Control	Control+25 mg chysin	L-NAME induced hypertension	L-NAME+25 mg chrysin
ICDH	596.9 ± 35.1 a	598.4 ± 34.6 a	407.5 ± 28.1 b	588.3 ± 36.2 c
a-KGDH	57.4 ± 3.6 a	58.1 ± 3.3 a	30.6 ± 2.9 b	45.2 ± 2.4 c
SDH	226.3 ± 19.7a	229.4 ± 19.6 a	126.1 ± 9.4 b	219.5 ± 12.4 c
MDH	298.5 ± 15.7 a	299.7 ± 15.2 a	216.3 ± 12.4 b	295.3 ± 12.3 c

ICDH: Isocitrate dehydrogenase; a-KGDH: a-ketoglutarate dehydrogenase; SDH: Succinate dehydrogenase; MDH: Malate dehydrogenase; NADH: Nicotinamide adenine dinucleotide.
Activity is expressed as nM of NADH oxidized/h/mg protein for ICDH
nM of ferrocyanide formed/h/mg protein for a-KGDH
nM of succinate oxidized/min/mg protein for SDH
nM of NADH oxidized/min/mg protein for MDH.
Values are mean ± S.D. for six rats in each group.
Values not sharing common superscript are significant with each other at $P<0.05$ (Duncan's multiple range test).

Conclusion

The present study demonstrated that chrysin attenuates the hypertension and there by protects cardiovascular function against damages from endothelial dysfunction through its ACE inhibitor activity. Chrysin at a dose of 25 mg/kg regulates the L-NAME-induced BP and in chain shows a reduction in plasma electrolytes, cardiac and aortic hydroxyproline cardiac, aortic and plasma ACE activity. Chrysin also increases mitochondrial enzymes, plasma, heart, aortic nitrite/nitrate concentration. On the basis of these results, we suggest that chrysin may be a useful therapeutic drug treatment for cardiovascular disease and hypertension.

Acknowledgements

The support provided by UGC-BSR Fellowship to Dr. G. Archunan, Bharthidasan University, TN to complete this work in a successful manner is gratefully acknowledged.

Conflict of interest statement

None declared

References

1. Hyun-Sub Kim and Dae-Geun Kim, (2013). Effect of long-term resistance exercise on body composition, blood lipid factors, and vascular compliance in the hypertensive elderly men. J Exerc Rehabil, 9(2): 271–277.
2. Cohuet, G. and Struijker-Boudier, H. (2006). Mechanisms of target organ damage caused by hypertension: therapeutic potential. Pharmacol Ther, 111: 81–98.
3. Lawes. CM., Vander Hoorn. S. and Rodgers. A. (2008). Global burden of blood-pressure-related disease, 2001. Lancet, 371: 1513–1518.
4. Yanga. H.Y., Yangb. S.C., Chenb. S.T. and Chenb. J.R. (2008). Soy protein hydrolysate ameliorates cardiovascular remodeling in

rats with L-NAME-induced hypertension. J Nutr Biochem, 19: 833–839.

5. Saravanakumar, M. and Raja, B. (2011). Veratric acid, a phenolic acid attenuates blood pressure and oxidative stress in L-NAME induced hypertensive rats. Eur J Pharmacol, 671: 87–94.

6. Veerappan, RM. And Malarvili, T. (2018). Chrysin pretreatment improves angiotensin system, cGMP concentration in L-NAME induced hypertensive rats. Ind J Clin Biochem, 1–8.

7. Morrell, CN., Matsushita, K., Chiles, K., Scharpf, RB., Yamakuchi, M., Mason, RJ., Bergmeier, W., Mankowski, JL., Baldwin, WM 3rd., Faraday, N. and Lowenstein CJ. (2005). Regulation of platelet granule exocytosis by S-nitrosylation. Proc Natl Acad Sci, USA. 102: 3782–3787.

8. Silva-Herdade, A. and Saldanha, C. (2011). Hemorheological effects of valsartan in L-NAME induced hypertension in rats. Open Circul Vasc J, 4: 1–5.

9. Kumar, S., Saravanakumar, M. and Raja, B. (2010). Efficacy of piperine, an alkaloidal constituent of pepper on nitric oxide, antioxidants and lipid peroxidation markers in L-NAME induced hypertensive rats. Int J Res Pharm Sci, 1: 300–307

10. Ceconi, C., Fox, KM., Remme, WJ., Simoons, ML., Bertrand, M., Parrinello, G., Kluft, C., Blann, A., Cokkinos, D. and Ferrari, R. (2007). ACE inhibition with perindopril and endothelial function. Results of a sub study of the EUROPA study: PERTINENT. Cardiovasc Res, 73: 237–246.

11. Maddury Srinivasa Rao. (2010). Inhibition of the Renin Angiotensin Aldosterone System: Focus on Aliskiren. JAPI, 58: 102–108.

12. Giani, JF,, Janjulia, T,, Kamat, N. Seth, D.M., Blackwell, W.L.B., Kandarp H, Xiao, Z. S., Sebastien, F., Eric, D., Jorge, E.T., Kenneth, E.B., Alicia, A.M. and Romer A.G. (2014). Renal Angiotensin-converting enzyme is essential for the hypertension induced by nitric oxide synthesis inhibition. J Am Soc Nephrol, 25: 2752–2763.

13. Pereira, L.M., Bezerra, D.G., Machado, D.L. and Mandarim-de-Lacerda, C.A. (2004). Enalapril attenuates cardiorenal damage in nitric-oxide-deficient spontaneously hypertensive rats. Clin Sci (Lond), 106: 337–343.

14. Jayakumar, T., Thomas, PA. and Geraldine, P. (2009) In-vitro antioxidant activities of an ethanolic extract of the oyster mushroom, *Pleurotus ostreatus*. Innov Food Sci Emerg Technol, 10: 228–34.

15. Williams, CA., Harborne, JB., Newman, M. Greenham, J. and Eagles, J. (1997). Chrysin and other leaf exudate flavonoids in the genus *Pelargonium*. Phytochemistry, 46; 1349–1353.

16. Malarvili, T. and Veerappan, RM. (2014). Effects of chrysin on free radicals and enzymic antioxidants in Nù-nitro-l-arginine methyl ester: Induced hypertensive rats. Int J Nutr Pharmaco Neurol Dis, 4: 112–117.

17. Veerappan, RM. and Malarvili, T. (2014). Role of chrysin on hepatic and renal activities of $N^{ù}$-nitro-l-arginine-methylester induced hypertensive rats. Int J Nutr Pharmacol Neurol Dis, 4: 58–63.

18. Veerappan, RM. and Senthilkumar, R. (2015). Chrysin enhances antioxidants and oxidative stress in L-NAME-induced hypertensive rats. Int J Nutr Pharmacol Neurol Dis, 5: 20–27.

19. Veerappan, RM., Malarvili, T. and Aruchunan, G. (2014). Effects on chrysin on lipid and xenobiotic metabolizing enzymes in l-NAME induced hypertension. Int J Nutr Pharmacol Neurol Dis, 4: 17–22.

20. Silambarasan, T., Manivannan, J., Krishna Priya, M., Suganya, N., Chatterjee, S. and Raja, B. (2014). Sinapic acid prevents hypertension and cardiovascular remodeling in pharmacological model of nitric oxide inhibited rats. PLoS ONE, 9(12): e115682 1–20.

21. Burtis, C.A. and Ashwood, E.R. (1994). Tietz Text Book of Clinical Chemistry, 2nd ed. WB Saunders Company, Philadelphia, USA. pp. 1354–1370.

22. Silambarasan, T., Manivannan, J., Raja, B. and Chatterjee, S. (2016). Prevention of cardiac dysfunction, kidney fibrosis and lipid metabolic alterations in L-NAME hypertensive rats by sinapic acid-Role of HMG-CoA reductase. Euro J Pharmacol, 777: 113–123.

23. Green, L.C., Wagner, D.A., Glogowski, J., Skipper, P.L., Wishnok, J.S. and Tannenbaum S.R. (1982). Analysis of nitrate and [^{15}N] nitrite in biological fluids. Analyt Biochem, 126: 131–138.

24. Jaarin, K., Foong, WD., Yeoh, MH., Kamarul, ZY., Qodriyah HM, Azman A, Japar Sidik F.Z., Abdul Hamid, J. and Yusof Kamisah. (2015). Mechanisms of the antihypertensive effects of Nigella sativa oil in L-NAME-induced hypertensive rats. Clinics, 70(11): 751–757.

25. Kumar. S., Prahalathan, P. and Raja, B. (2014). Vanillic acid: a potential inhibitor of cardiac and aortic wall remodeling in L-NAME induced hypertension through upregulation of endothelial nitric oxide synthase. Environ Toxicol Pharmacol, 38(2): 643–652.

26. Seymour, EM., Singer, AM., Bennink, MR., Parikh, RV., Kirakosyan. A., Kaufman, PB. and Bolling, SF. (2008). Chronic intake of a phytochemical-enriched diet reduces cardiac fibrosis and diastolic dysfunction caused by prolonged salt sensitive hypertension. J Gerontol A Biol Sci Med Sci, 63: 1034–1042.

27. Karppanen, H. (1991). Minerals and blood pressure. Ann Med, 23: 299–305.

28. Leiba, A., Vald, A., Peleg, E. and Shamiss, A. and Grossman, E. (2005). Does dietary recall adequately asses sodium, potassium and calcium intake in hypertensive patients? Nutrition, 21: 462–466.

29. Kang, D.G., Sohn, E.J., Lee, Y.M., Lee, A.S., Han, J.H., Kim, T.Y. and Lee, HS. (2004). Effects of Bulbusfritillaria water extract on blood pressure and renal functions in the L-NAME-induced hypertensive rats. J Ethnopharmacol, 91: 51–56.

30. Mailloux. R.J., Bériault, R., Lemire, J., Singh, R., Chénier, D.R., Hamel, R.D. and Appanna VD. (2007). The tricarboxylic acid cycle, an ancient metabolic network with a novel twist. PLoS One, 2: e690.

31. Giribabu, N., Eswar Kumar, K., Rekha, S.S., Muniandy, S. and Salleh, N. (2014). *Vitis vinifera* (Muscat variety) seed ethanolic extract preserves activity levels of enzymes and histology of the liver in adult male rats with diabetes. Evidence-Based Complementary and Alternative Medicine, Article ID 542026.

32. Katsumi, H., Nishikawa, M. and Hashida, H. (2007). Development of nitric oxide donors for the treatment of cardiovascular diseases. Cardiovasc Hematol Agents Med Chem, 5: 204–208.

33. Kumar, S., Prahalathan, P. and Raja, B. (2011). Antihypertensive and antioxidant potential of vanillic acid, a phenolic compound in L-NAME-induced hypertensive rats: A dose-dependence study. Redox Report. 16: 208–215

34. Ulker, S., McKeown, PP. and Bayraktutan, U. (2003). Vitamins reverse endothelial

dysfunction through regulation of eNOS and NAD(P)H oxidase activities. Hypertension. 2003; 41: 534–539.

35. Michalska, A. and echter, A.N. (2011). Dietary nitrite and nitrate: a review of potential mechanisms of cardiovascular benefits. Eur J Nutr, 50: 293–303.

36. Tsukahara, H., Hiraoka, M., Kobata, R., Hata, I., Ohshima, Y., Jiang MZ, Noiri, E. and Mayumi M. (2000). Increased oxidative stress in rats with chronic nitric oxide depletion: measurement of urinary 8-hydroxy-2'-deoxyguanosine excretion. Redox Rep. 5: 23–28.

37. Hong, D., Bai, YP., Shi, RZ., Tan, GS., Hu. CP. and Zhang, GG. (2014). Inhibitory effect of reinioside C on vascular smooth muscle cells proliferation induced by angiotensin II via inhibiting NADPH oxidase-ROS-ENK1/2-NF-kappaBAP-1 pathway. Pharmazie, 69(9): 698–703.

38. Toba, H., Nakagawa, Y., Miki, H., Shimizu, T., Yoshimura, A., Inoue, R., Asayama, J., Kobara, M. and Nakata, T. (2005). Calcium channel blockage exhibits anti-inflammatory and anti-oxidative effects by augmentation of endothelial nitric oxide synthase and inhibition of angiotensin converting enzymes in the N-nitro-L arginine methyl ester induced hypertensive rat aorta: Vosoprotective effects beyond the blood pressure lowering effect of amlodipine and manidipine. Hypertens Res, 28(8): 689–700.

39. Yanga, H.Y., Yangb, S.C., Chenb, S.T. and Chenb, J.R. (2008). Soy protein hydrolysate ameliorates cardiovascular remodeling in rats with L-NAME-induced hypertension. J Nutr Biochem. 19: 833–839.

40. Katoaka, C., Egashira, K. and Ishibashi, M. (2004). Novel anti-inflammatory action of amlodipine in a rat model of atherosclerosis induced by long term inhibition of nitric oxide synthesis. Am J Physiol Heart Circ Physiol, 286(2): H768–774.

Current Trends in Biotechnology and Pharmacy
Vol. 14 (3) 340-346, July 2020, ISSN 0973-8916 (Print), 2230-7303 (Online)
DOI: 10.5530/ctbp.2020.3.35

Morphological and biochemical characterization of fluorescent *Pseudomonads* from groundnut rhizosphere

Padma Gurucharan Jogi[*],L.Nirmala jyothi,* K. Vijay Krishna Kumar[1], P. Osman Basha[*] and E.C. Surendranatha Reddy[*@]

*Department of Genetics and Genomics, Yogi Vemana University, YSR Kadapa, A.P., India
[1] Acharya N G Ranga Agricultural University, Regional Agricultural Research Station, Maruteru, Andhra Pradesh, India.
@Corresponding author : surendraeddula@gmail.com

Abstract

Groundnut is an important grain legume and oil seed crop grown all over the world. Fluorescent Pseudomonads are beneficial bacteria that inhabit the root zone of plants and increase the growth of plants by a wide variety of mechanisms. In our studies,, we have assessed the morphological and biochemical characteristics of 24 fluorescent pseudomonads isolated from groundnut rhizosphere collected from Rayalaseema region of Andhra Pradesh. All the *Pseudomonas fluorescens* (Pf) strains showed development of fluorescent pigments under UV light. Morphological studies indicated that they have displayed (i) rod-shaped, (ii) smooth shiny surface, (iii) gram-negative reaction (iv) motility and (v) growth even at 41^{0}C. None of the strains were positive for the indole, and voges-proskauer test. All strains were positive for oxidase, citrate, catalase, and gelatin liquefaction test; 58% were starch hydrolysis-positive, 29.16% were methyl red-positive and 62.5% were H_2S-positive. The present study proved that these Pf strains have potential plant growth-promoting activities. Our future studies are directed in establishing the plant growth-promoting effects of these Pf strains under Greenhouse and field conditions on groundnut.

Key Words: Groundnut, rhizosphere, Pseudomonas fluorescens, Plant Growth Promotion

Introduction

Groundnut (*Arachis hypogaea* L.) is an important grain legume and oilseed crop grown all over the world. At the global level, the groundnut area during 2018-'19 was 27.34 Mha, with a production of 46.17 MMT and a productivity of 1.69 Metric Tons per hectare . In Andhra Pradesh, during 2017-'18, the groundnut crop was cultivated in 735,000 hectares with a production of 10, 48,000.10 tons and a yield of 1426 kg ha^{-1} (Indiastat). Indiscriminate use of chemical pesticides and fungicides have harmful effects on human health and to the environment. Moreover, the problem of resistance gain by pathogens to chemical fungicides is not uncommon as in groundnut by Sclerotium rolfsii, the stem rot pathogen . The application of microbial bio-agents in agriculture to control pests and diseases is fast catching up and has been well established in several crops against various pests and diseases (Govindasamy *et al*., 2011). Plant Growth-Promoting Rhizobacteria (PGPR) are used world-wide for the control of plant diseases. The PGPR such as *Pseudomonas florescens*, *Pseudomonas putida* etc are widely used and their efficacy is well established in sustainable management. These PGPR are a group of bacteria that increase plant growth through the production of plant growth hormones, N fixation, P-solubilizing activity and biological activity

(Deshwal *et al*., 2003). These *P. fluorescens* and P. *putida* were identified as important organisms and are capable of promoting plant growth and effective plant diseases management (Belker and Gade, 2012).

Pseudomonas fluorescens is one of the PGPR species characterized by a gram negative, rod shaped bacterium with a proven Plant-Growth Promoting (PGP) and disease control capability in various crops. Earlier *P. fluorescens* were used either individually or in conjunction with other management options for managing stem rot and other diseases. The Pseudomonas Endo rhizospheric inhabiting bacteria strains were used to promote sunflower (*Helianthus annus*) plant growth (Pandey *et.al*. 2013). Keeping this in view, the present investigation is aimed to isolate the elite *P. fluoroscens* strains from groundnut rhizospheric soil, and these strains were characterized morphologically and biochemically.

Material and Methods:

Collection of groundnut rhizosphere soil samples : A random survey was undertaken in the major groundnut growing districts of Rayalaseema. Twenty four soil samples were collected from Rayalaseema region (Ananthapuram, Chittor, Kadapa, Kurnool districts) of Andhra Pradesh, India. The soil samples were collected up to the depth of 10-15cms from groundnut plants rhizosphere. In addition, the soil adhering to the roots were also collected.

***Isolation of Pseudomonas fluorescens strains*:** For the isolation of P. fluorescens strains, one gram of collected soil sample was taken in a 10 ml of sterile distilled water. The samples were mixed thoroughly by vortexing for 15 min. 1 ml of the suspension from the first dilution (10^{-1}) was aseptically transferred to another tube having 9 ml (10^{-2} dilution) of sterile distilled water and thus diluting the original suspension up to 10^{-5}dilutions. Then, 100 µl of 10^{-5} diluted soil samples were spread on sterilized petriplates containing King's B media and incubated at 28±2°C for 48 h. After incubation, colonies with yellowish green, bluish green and blue pigments were detected under UV light. The selected colonies were transferred to fresh King's B slants and pure cultures were maintained.

Cultural characterization of Pseudomonas fluorescens strains : Twenty four bacterial strains were studied for their colony morphology, cell morphology (Gram reaction), pigmentation and sporulation as per Bergey's Manual of Determinative Bacteriology (Holt *et al*., 1994).

Biochemical characterization of Pseudomonas fluorescens isolates : The different biochemical tests performed for the isolated Pf strains were as described below.

1. Catalase test*:* The test was conducted to study the presence of catalase enzyme activity in the isolated Pseudomonas strains. Overnight grown 24 pure isolates were taken on glass slides and few drops of 3% H_2O_2 was added and observed for the production of gas bubbles. Production of bubbles indicated the presence of catalase activity (Schaad, 1992).

2. Starch hydrolysis test : Freshly grown Pseudomonas strains were placed on sterile starch agar plates and the plates were incubated at 28±2° C for 48 hrs. After incubation, the plates were flooded with iodine solution and observed for the clear zone around the colony. The formation of a transparent zone around the colony was taken as positive reaction for the test (Eckford, 1927)

3. Methyl Red Test : To perform the Methyl red test, glucose- phosphate broth was prepared and sterilized. One ml of sterilised glucose phosphate broth was taken into an autoclaved test tube and single colony of Pseudomonas culture was inoculated, followed by incubation at 28±2 ^{0} C for 48h. After incubation, seven drops of methyl red indicator was added to each tube and gently shaken. Red colour production was taken as positive and yellow colour production was taken as negative for the test.

5. Voges prausker's Test : To the pre-sterilized glucose-phosphate broth slants, the overnight grown Pseudomonas cultures were inoculated and incubated at 28°C for 48h. After incubation,

ten drops of Baritt's reagent-A was added and vigorously shaken followed by the addition of 10 drops of Baritt's reagent-B. Appearance of pink colour in the broth was taken as positive result for the test.

5. Oxidase test : All bacteria that are oxidase positive are aerobic, and can use oxygen as a terminal electron acceptor in respiration. The 24 hrs old Pseudomonas bacterial cultures were spotted on sterile trypicase soy agar and incubated at 28±2°C for one day. Five drops of Wurster's reagent (N, N, N', N'- tetramethyl- p-phenylenediamine dihydrochloride) was added on the surface of grown culture placed on them. The cultures showing blue colouration were taken as positive result for aerobic bacteria.

6. Citrate utilization test : Citrate test was used to detect the ability of an organism which can utilize citrate as a sole source of carbon for their metabolism. The overnight grown fresh pseudomonas bacterial cultures were streaked on Simmon's citrate agar slants and incubated at 28±2 °C for 24h. Appearance of Prussian blue colour indicates positive reaction for citrate utilization (Simmons 1926).

7. Kovac's indole test : To identify the Indole production capacity of isolated Pseudomonas cultures, SIM agar media was prepared and poured into tubes followed by sterilization. After sterilization, the overnight grown bacterial culture was inoculated to SIM agar slants and incubated at 48 h at 28±2°C. After incubation, ten drops of Kovac's reagent was placed on *Pseudomonas* culture. Appearance of red colour was taken as positive result for Indole production

8. Hydrogen sulfide (H_2S) test : The overnight grown Pseudomonas cultures were inoculated along the walls of the tubes containing Sulfide Indole Motility Medium (SIM). These cultures were incubated at 28 ± 2°C for 48 h. Visualisation of black colour all along the line of inoculation indicated a positive result.

9. Gelatin liquefaction : Gelatin liquefaction method was used to detect whether the bacterial isolates has the capacity to produce proteolytic enzymes (Kohn, 1953). The overnight grown bacterial cultures were inoculated to sterilized nutrient gelatin deep tubes and incubated at 28±2°C for 48 hrs. After incubation the tubes were kept in a refrigerator at 4°C for 30 minutes. The isolates showing liquefied gelatin were taken as positive and those that solidified on refrigeration were taken as negative result (Blazevic and Ederer, 1975).

Results and Discussion:

Morphological characterization: Rhizosphere soil samples were collected from different regions of Rayalaseema, Andhra Pradesh and the colonies that exhibited fluorescence were isolated using King's B media by serial dilution method. The colonies which showed fluorescence under UV light were selected and pure cultures were obtained by spread plate method. Total twenty four pure strains were selected which showed fluorescence and used for further morphological and biochemical characterization. The selected pseudomonas isolates were named according to the strain and crop character i.e. "P" stands for *Pseudomonas florescence*, "G" stands for groundnut and "Y" stands for Yogi Vemana University (PGY) (Table 1). Morphological characterization results revealed that all the isolated 24 strains were showed rod shape, smooth shiny surface and motility without sporulation, when observed under microscope (Table1). The gram staining results classified all the isolated strains into gram negative group (Table 1). The isolates showed yellowish green, light green, bluish green or dull white pigmentation when the strains were grown in *Pseudomonas* agar F medium (Table 1). The florescence and pigmentation results confirmed all the isolated stains belong to pseudomonas group. Out of twenty four isolates, a total of 11 isolates (45.83%) showed yellowish green pigmentation, two isolates (8.33%) showed bluish green pigmentation, two isolates (8.33%) showed light green pigmentation and the remaining isolates showed dull white colonies under UV light (Table 1).

Table 1: Morphological characteristics of Pseudomonas fluorescens isolates

S. No	Isolates	Shape	Pigmentation	Surface	Gram reaction	Motility test	Sporulation	Growth at 41°C
1	PGY1	Rod	Yellowish green	Smooth shiny	Negative	Motile	Negative	+
2	PGY2	Rod	Yellowish green	Smooth shiny	Negative	Motile	Negative	+
3	PGY3	Rod	Yellowish green	Smooth shiny	Negative	Motile	Negative	+
4	PGY4	Rod	Yellowish green	Smooth shiny	Negative	Motile	Negative	+
5	PGY5	Rod	White	Smooth shiny	Negative	Motile	Negative	+
6	PGY6	Rod	White	Smooth shiny	Negative	Motile	Negative	+
7	PGY7	Rod	Yellowish green	Smooth shiny	Negative	Motile	Negative	+
8	PGY8	Rod	Bluish green	Smooth shiny	Negative	Motile	Negative	+
9	PGY9	Rod	Light green	Smooth shiny	Negative	Motile	Negative	+
10	PGY10	Rod	White	Smooth shiny	Negative	Motile	Negative	+
11	PGY11	Rod	Yellowish green	Smooth shiny	Negative	Motile	Negative	+
12	PGY12	Rod	Bluish green	Smooth shiny	Negative	Motile	Negative	+
13	PGY13	Rod	White	Smooth shiny	Negative	Motile	Negative	+
14	PGY14	Rod	Yellowish	Smooth shiny	Negative	Motile	Negative	+
15	PGY15	Rod	Light green	Smooth shiny	Negative	Motile	Negative	+
16	PGY16	Rod	White	Smooth shiny	Negative	Motile	Negative	+
17	PGY17	Rod	Yellowish green	Smooth shiny	Negative	Motile	Negative	+
18	PGY18	Rod	Dull white green	Smooth shiny	Negative	Motile	Negative	+
19	PGY19	Rod	Yellowish green	Smooth shiny	Negative	Motile	Negative	+
20	PGY20	Rod	Dull white	Smooth shiny	Negativ	Motile	Negative	+
21	PGY21	Rod	Dull white	Smooth shiny	Negative	Motile	Negative	+
22	PGY22	Rod	White	Smooth shiny	Negative	Motile	Negative	+
23	PGY23	Rod	Yellowish green	Smooth shiny	Negative	Motile	Negative	+
24	PGY24	Rod	Yellowish green	Smooth shiny	Negative	Motile	Negative	+

Biochemical characterization: After morphological characterization, emphasis was placed on the range of variation among the isolated *Pseudomonas fluorescens* strains at different biochemical test such as Starch hydrolysis test, Methyl red test, Voges praskaur's test, Oxidase test, Citrate test, Indole test, H_2S test, Catalase test and Gelatin liquefaction test. The results of the biochemical test are shown in Table 2 for all the Pf strains.

All 24 strains were catalase positive, since catalase is common enzyme in almost all living organism which exposed to oxygen. Catalase is the enzyme which breakdown the harmful substance H2O2 into water and oxygen (Chelikani *et al.,* 2004), thus helping to avoid oxidative damage to cells caused by H_2O_2. Twenty four isolates have the ability to produce gelatinase enzyme hence strains gives positive result of gelatin liquefication test. Gelatinase enzyme break down the gelatin protein into poly peptide, peptide and amino acids and these could be absorbed by isolates cell membrane. All strains showed positive result for oxidase test and the test confirm the presence of Oxidase enzyme. The oxidase enzyme transfers electrons from donor to O_2 and oxidase positive organisms are aerobes. All the Twenty four *Pseudomonas fluorescens* isolates showed positive results for Citrate test. The citrate test identifies the capability of an isolates to utilize citrate as only source of carbon and energy. Positive results were noted for catalase activity, oxidase test, gelatin liqufication test and citrate utilisation test for all the isolated strains. Similar results were reported by Suman *et al*., 2015.

None of the 24 isolates were positive for Voges praskaur's test and Indole test. The Voges praskaur's test performed to identify the ability of organism to catabolise the glucose through butanediol pathway. The indole test is the biochemical test used to perform the ability of bacteria to convert tryptophan into indole. It was noted that PGY2, PGY5, PGY8, PGY10, PGY15, PGY16 and PGY23 strains were positive for methyl red test (MR). The methyl red test (MR) performed to identify the capacity of strains capability of catabolising glucose in the formation of formic acid, acetic acid, lactic acid, ethanol etc. This mixed acid fermentation reduced the pH of the media which in turn give positive result for methyl red test.

Out of Twenty four isolates, PGY1, PGY3, PGY4, PGY6, PGY 8, PGY9, PGY10, PGY12, PGY14, PGY16, PGY17, PGY19, PGY22 and PGY23 isolates showed positive results for starch hydrolysis. Starch hydrolysis reaction tests the capacity of isolates to release exoenzymes which hydrolysed the starch molecules. Starch molecules are too large to transport in the bacteria, hence few strains has the capacity to secrete exoenzymes to degrade the starch molecules that can be transported in bacteria easily through bacterial membrane. Sixty two percent of the isolated strains were positive for hydrogen sulphide production activity. The PGY2, PGY4, PGY5, PGY6, PGY8, PGY10, PGY11, PGY13, PGY14, PGY16, PGY18, PGY19, PGY21, PGY22 and PGY24 strains H2S production was detected by its reaction with lead acetate strips placed above the surface of the medium.

Microbes of the rizhobacteria plays an important role in nutrient acquirement, enhanced soil texture, production of secondary metabolites and various compounds, all leading to enhancement of plant growth (Becker *et al* 2018). Extensive research demonstrated that plant growth-promoting rizho bacteria (PGPR) are very diverse as bio control agents and their action can showed via local antagonism to soil-borne pathogens (Beneduzi et al 2012). The present study was carried out by employing various morphological and biochemical methods for characterization and assessment of diversity among the twenty four *Pseudomonas florescence* isolates. Similarly, researchers have isolated fluorescent pseudomonads from suppressive soil of different ecosystems for the management of soil borne and foliar diseases (Prabhukarthikeyan et al 2015; Meera and Balabhaskar, 2012).

Table 2: Biochemical and physiological characterization of Pseudomonas fluorescens isolates isolated from groundnut rhizosphere

S. No	Isolates	Starch hydrolysis	M R test	VP test	Oxidase test	Citrate test	Indole test	H_2S test	Catalase e test	Gelatin liquefac-tion test
1	PGY1	+	"	"	+	+	"	"	+	+
2	PGY2	"	+	"	+	+	"	+	+	+
3	PGY3	+	"	"	+	+	"	"	+	+
4	PGY4	+	"	"	+	+	"	+	+	+
5	PGY5	"	+	"	+	+	"	+	+	+
6	PGY6	+	"	"	+	+	"	+	+	+
7	PGY7	"	"	"	+	+	"	"	+	+
8	PGY8	+	+	"	+	+	"	+	+	+
9	PGY9	+	"	"	+	+	"	"	+	+
10	PGY10	+	+	"	+	+	"	+	+	+
11	PGY11	"	"	"	+	+	"	+	+	+
12	PGY12	+	"	"	+	+	"	"	+	+
13	PGY13	"	"	"	+	+	"	+	+	+
14	PGY14	+	"	"	+	+	"	+	+	+
15	PGY15	"	+	"	+	+	"	"	+	+
16	PGY16	+	+	"	+	+	"	+	+	+
17	PGY17	+	"	"	+	+	"	"	+	+
18	PGY18	"	"	"	+	+	"	+	+	+
19	PGY19	+	"	"	+	+	"	+	+	+
20	PGY20	"	"	"	+	+	"	"	+	+
21	PGY21	"	"	"	+	+	"	+	+	+
22	PGY22	+	"	"	+	+	"	+	+	+
23	PGY23	+	+	"	+	+	"	"	+	+
24	PGY24	"	"	"	+	+	"	+	+	+

Conclusions:

Biochemical characteristization shows that isolates of *Pseudomonas fluorescence* have the ability to secrete extracellular amylse and gelatinase enzymes. *P. fluorescence* with plant growth-promoting rhizobacteria (PGPR) with pathogen resistance capacity was valuable resource in the formulation of new inoculants and is an effective replacement for pesticides and fertilizers and becomes environmentally friendly biological control of plant diseases. In the present study, *P. fluorescens* isolated strains may have a positive prospect and high capability to be bio-control agent of important plant pathogens and promote plant growth. Our future studies are aimed at identifying potential *P. fluorescens* isolates among the 24 isolates with 2; 4-DAPG production and siderophores producing capacity together with greenhouse and field assessment studies against stem rot pathogen diseases.

References

1. Backer et al., Plant Growth-Promoting Rhizobacteria: Context, Mechanisms of Action, and Roadmap to Commercialization of Biostimulants for Sustainable Agriculture. 2018; 9: 1473

2. Belkar, Y.K. and Gade, R.M. 2012. Biochemical characterization and growth promotion activities of Pseudomonas fluorescens. J.Pl.Dis.Sci. 7(2): 170 – 174.

3. Beneduzi et al., Plant growth-promoting rhizobacteria (PGPR): Their potential as antagonists and biocontrol agents. 2012 Dec; 35(4 Suppl): 1044–1051

4. Blazevic, D. J. and Ederer, G. M. (1975). Principles of Biochemical Tests in Diagnostic Microbiology, Wiley and Company, New York. pp.13 - 45

Deshwal VK, Pandey P, Kang SC, Maheshwari DK. Rhizobia as a biological control agent against soil borne plant pathogenic fungi. Indian Journal of Experimental Biology. 2003; 41:1160-1164

5. Eckford, m.d., 1927, Thermophilic bacteria in Milk. *American Journal of Hygiene,* 7: 201-202.

6. Govindasamy, V., Senthilkumar, M., Magheshwaran, V., Kumar, U., Bose, P., Sharma, V., Annapurna, K., 2011. Bacillus and Paenibacillus spp. Potential PGPR for sustainable agriculture. Plant Growth and Health Promoting Bacteria. Microbiology Monographs. 18: 333-364. 8.

7. Holt, J.G., Krieg, N.R., Sneath, P.H.A., Staley, J.T and Williams, S.T. 1994. Bergey's Manual of Determinative Bacteriology, 9th ed, Willams and Wilkins Co. Baltimore

8. Kohn, J. (1953). A preliminary report of a new gelatin liquefaction method. J. clin. Path. 6, 249.

9. P. Chelikani et al., 2004. Diversity of structures and properties among catalases. CMLS, Cell. Mol. Life Sci. 61 (2004) 192–208.

10. Pandey R, Chavan PN, Walokar NM, Sharma N, Tripathi V, Khetmalas MB. Pseudomonas stutzeri RP1: A versatile plant growth promoting endorhizospheric bacteria inhabiting sunflower (Helianthus annus). Res. J. Biotechnol. 2013; 8(7):48-55

11. S. R. Prabhukarthikeyan et al., 2015. Biochemical characterization of fluorescent pseudomonads from turmeric rhizosphere. Biochem. Cell. Arch. Vol. 15, No. 1, pp. 299-303, ISSN 0972-5075.

12. Schaad, N.W., 1992, *Laboratory Guide for Identification of Plant Pathogenic Bacteria,* 2nd Edn. International Book Distributing Co., Lucknow, pp.44-58.

13. Simmons, J.S., 1926. A culture medium for differentiating organisms of typhoid-colon aerogenes groups and for isolation of certain fungi. J. Infectious Diseases, 93: 209-241.Dennis and Webster, 1971.

14. T. Meera and P. Balabaskar. Isolation and characterization of pseudomonas fluorescens from rice fields 2012; 2277-209x

Current Trends in Biotechnology and Pharmacy
Vol. 14 (3) 347-358, July 2020, ISSN 0973-8916 (Print), 2230-7303 (Online)
DOI: 10.5530/ctbp.2020.3.36

Assessment of free radical scavenging activities and antioxidative potential of the tuber extracts of *Stemona tuberosa* Lour.

C. Lalmuansangi, Marina Lalremruati and Zothansiama*
Department of Zoology
Mizoram University, Aizawl-796 004, India
* Corresponding author : zothans@gmail.com

Abstract

This study evaluates the phytochemical constituents, free radical scavenging activities and antioxidative potential of the tuber extracts of *Stemona tuberosa* (ST). The preliminary phytochemical screening revealed the presence of alkaloids, cardiac glycosides, saponins, steroids, tannins and terpenoids from various solvent extracts of ST. The methanolic extract of ST showed the highest phenolic (715.20 ± 2.42 mg GAE/g dry extract) and flavonoid (3864.25 ± 7.54 mg quercetin/g dry extract) contents. *S. tuberosa* extracts were analyzed for their scavenging activities based on 1,1-diphenyl-2-picrylhydrazyl (DPPH), 2, 2'-azino-bis-(3-ethylbenzothiazoline-6-sulfonic acid (ABTS), and superoxide anions ($O_2^{\cdot-}$) in a cell free system. Different extracts of ST inhibited the generation of DPPH, ABTS and $O_2^{\cdot-}$ in a concentration dependent manner. Among the various extracts of ST, the methanolic extract showed the highest scavenging activities for ABTS and $O_2^{\cdot-}$ with IC_{50} of 36.20 ± 0.832 µg/ml and 98.93 ± 3.37 µg/ml respectively. The scavenging activity of methanolic extract for ABTS and $O_2^{\cdot-}$ was significantly higher than the standard ascorbic acid. However, chloroform extract was found to possess the highest scavenging activity for DPPH with IC_{50} of 7.36 ± 0.081 µg/ml. The total reducing power of ST extracts was also determined by measuring the transformation of Fe^{3+} into Fe^{2+} and the methanolic extract was found to exhibit the highest reducing power. The extracts were also analyzed for their anti-haemolytic activity and inhibitory effect on lipid peroxidation in an *ex vivo* condition using mice erythrocyte and liver, respectively. The anti-haemolytic activity of ST extracts also increased with the increase in concentration of the extract. Chloroform extract was found to possess the highest anti-haemolytic activity with 68.81 % inhibition followed by methanolic extract (38.57 %) and aqueous extract (20.81 %). Methanolic extract showed the highest inhibitory activity on lipid peroxidation (80.5 %) followed by chloroform extract (67.8 %) and then aqueous extract (62.63 %). Our study suggests that ST extracts have free radical scavenging and antioxidative potential, probably due to their high phenolic and flavonoid contents.

Keywords: *Stemona tuberosa,* Free radicals, Antioxidants, Lipid peroxidation.

Introduction

During normal cellular metabolism, molecular oxygen results in production of reactive oxygen species (ROS) such as superoxide ($O_2^{\cdot-}$), hydrogen peroxide (H_2O_2), hydroxyl radicals ($^{\cdot}OH$) and singlet oxygen ($^1O_2$). At low to moderate concentrations, ROS are fundamental in modulating various physiological functions of the body, representing an essential part of aerobic

life and metabolism (1 and 2). However, excessive generation of ROS hampers the antioxidant defense systems of the body leading to a condition called 'oxidative stress'ensuing tissue damage, and have been reported to be associated with diseases including coronary heart disease, neurodegenerative disorders, diabetes, arthritis, inflammation, lung damage and cancer (3 and 4). Certain plants have been reported to contain various phytochemicals that are generally non-toxic, act as natural antioxidants and useful for the treatment of different diseases (5). Since, antioxidants are capable of preventing oxidative damage, use of plants and plant-derived products as a source of natural antioxidants has been employed as a conventional method for maintaining oxidative balance in the body.

Stemona tuberosa is an elegant plant belonging to the family Stemonaceae. It is native to China, Southeast Asia, North-east India and New Guinea, and is one of the 50 fundamental herbs used in traditional Chinese medicine (6). Roots of *S. tuberosa* has been traditionally used for the treatment of cough and chest pains (7), infestations with lice and treatment of enterobiasis, and in revitalization of the body and provision of sexual stimulant (8). Among the genus *Stemona, S. collinsae* has been reported for its antifungal property, *S. japonica* for its antimicrobial activity (9). Other species such as *S. sessifolia* and *S. curtisii* have also been reported to contain certain alkaloids that may possess antifungal, anti-inflammatory and antitussive activities (10). Antioxidative potential is widely used as a parameter to assess medicinal property of natural products or the bioactive components of plants. *In vitro* screening methods have been commonly used for chemical elucidation and pharmacological investigations of medicinal plants (11). Therefore, the present study aimed to evaluate the free radical scavenging activity and antioxidant potential of the tuber extracts of *Stemona tuberosa.*

Materials and Methods

Chemicals used : Gallic acid, quercetin dihydrate, methanol, ferric chloride, sodium nitrite, nitrobluetetrazolium (NBT), nicotinamide adenine dinucleotide (NADH), phenazinemethosulfate (PMS), 2-deoxyribose, 2,2'-azino-bis-(3-ethylbenzothiazoline-6-sulfonic acid) (ABTS), di-sodium hydrogen phosphate, potassium persulfate and hydrogen peroxide (H_2O_2) were obtained from HiMedia Laboratories Pvt., Ltd.(Mumbai, India). 1,1-diphenyl-2-picrylhydrazyl radicals (DPPH) and thiobarbituric acid (TBA), were obtained from Sigma Aldrich Inc (Louis, Germany). Trichloroacetic acid (TCA), Folin-ciocalteu's reagent, sodium hydroxide, sodium carbonate, ascorbic acid and ferrous sulphate were obtained from SD fine–chem Ltd. (Mumbai, India). Alluminium chloride and sodium di-hydrogen phosphate were obtained from Merck Specialities Pvt., Ltd. (Mumbai, India). Ethylene diamine tetraacetic acid (EDTA) was obtained from Qualigens Fine Chemicals (Mumbai, India). Potassium ferricyanide was obtained from LobaChemie Pvt., Ltd. (Mumbai, India).

Preparation of extracts *:* The plant *Stemona tuberosa* (ST) was identified and collected from Phura, Siaha District, Mizoram. The roots were washed and chopped into smaller pieces and then shade dried at room temperature. The dried roots were grounded to powder using a mixer grinder and then sequentially extracted with petroleum ether, chloroform, methanol and distilled water based on their increasing polarity using Soxhlet apparatus at their respective boiling points for a minimum of 40 cycles each. The liquid extracts were filtered, allowed to evaporate and finally freeze dried so as to obtain a fine powder of the extract. Henceforth, the chloroform extract, methanolic extract and aqueous extract of ST will be called as STCE, STME and STAE respectively.

Phytochemical analysis : The following phytochemicals were screened for their presence in various extracts of *S. tuberosa* using standard protocols.

Alkaloids *:* The presence of alkaloids in ST extracts was confirmed by employing the Dragendorff's test. Briefly, 0.1 g of different extracts of ST was mixed with 0.5 ml of

Dragendorff's reagent. The development of reddish brown precipitate indicates the presence of alkaloids (12).

Cardiac glycosides : ST extract (0.1 g) was treated with 2 ml of glacial acetic acid containing one drop of ferric chloride solution with an under laying of 1 ml of concentrated H_2SO_4. The appearance of brown ring at the interface indicated the presence of deoxysugar, which is a characteristic of cardenolides (13).

Saponins : ST extracts (0.1 g) was mixed with 3 drops of olive oil and shaken vigorously for few min. The formation of a fairly stable emulsion indicated the presence of saponins (13).

Steroids : The presence of steroid in various extracts of ST was determined by Salkowski's test. Briefly 0.1 g of ST extract dissolved in their respective solvents was mixed with a few drops of concentrated H_2SO_4. The development of red colour at lower layer indicated the presence of steroids (12).

Tannins : Presence of tannin was determined by Ferric chloride test. Brieftly, 0.1 g of ST extract was dissolved in their respective solvents and a few drops of 0.1% ferric chloride were added. The formation of brownish green or a blue-black colour indicated the presence of tannins (13).

Terpenoids : The presence of terpenoids in various extracts of ST was detected using Salkowski's test. 5 ml of each extract (0.1 g/ml) was mixed with 2 ml of chloroform followed by careful addition of 3 ml concentrated H_2SO_4 so as to allow the formation of a layer. The formation of a reddish brown colour at the interface confirmed the presence of terpenoids (12).

Phlobatannins : Different extracts of ST (0.1 g) was boiled in 1% aqueous hydrochloric acid and deposition of a red precipitate indicated the presence of phlobatannins (13).

Quantitative estimation of phytochemicals

Determination of total phenolic content : The total phenolic content of various extracts of ST was determined using the method described earlier (14). Briefly, 5 ml of Folin-ciocalteau reagent (diluted ten-fold) was mixed with 1 ml of plant extracts (STCE, STME, STAE) dissolved in their respective solvent, at the concentration ranging from 0.25-8.0 mg/ml. Sodium carbonate (4 ml, 0.115 mg/ml) was added to the mixture after 5 min of incubation at room temperature. Then, the mixture was incubated for 2 hr in the dark at room temperature followed by measuring the absorbance at 765 nm using UV-Visible spectrophotometer (SW 3.5.1.0. Bio-spectrometer, Eppendorf, India Ltd., Chennai) Calibration curve was also prepared by mixing methanolic solution of gallic acid (1 ml, 0.25–4.0 mg/ml) with the reagents above and absorbance was measured at 765 nm. All determinations were carried out in triplicate. The total phenolic content in each extract was expressed as gallic acid equivalents (GAE) mg/g of the dry extract.

Determination of the total flavonoids : Total flavonoid content was determined using the method described earlier (15). Briefly, 0.25 ml of different fractions of the extract (0.25-4.0 mg/ml; dissolved in respective solvent) and quercetin standard solution was mixed with 1.25 ml of distilled water followed by the addition of 75 µl of 5% (w/v) sodium nitrite solution. After few min, 150 µl of 10% (w/v) aluminum chloride solution was added and allowed to stand for further 5 min before the addition of 0.5 ml of 1 M NaOH. The mixture was then made up to 2.5 ml with distilled water and mixed well. Absorbance was measured immediately at 510 nm. The result was expressed as quercetin equivalents (mg/g extract) All estimations were performed in triplicate.

***In vitro* antioxidant assays**

DPPH radical scavenging activity : DPPH radical scavenging activity was carried out according to the method described earlier (16) with slight modifications. To different concentrations of various extracts of ST (0.5 ml, 1-400 µg/ml), 1 ml of methanolic solution of 0.1 mM DPPH was added. The mixture was then allowed to stand in the dark for 30 min and absorbance was measured at 523 nm. Methanol

was utilized as the baseline correction. The results were compared with that of the control prepared as above without sample. The antioxidant activity of the extract was expressed as IC_{50}, the concentration (µg/ml) of extract that inhibited 50 % of DPPH radicals. Ascorbic acid was used as the positive control and each study was performed in triplicate. The scavenging activity was then estimated using the formula:

$$\% \text{ scavenging} = [(A_{blank} - A_{sample}) / A_{blank}] \times 100$$

Where, A_{blank} is the absorbance of the control reaction (containing all reagents except the test compound) and A_{sample} is the absorbance of the test compound.

Superoxide radical scavenging activity : Superoxide scavenging activity was determined by the nitrobluetetrazolium (NBT) reduction method (17) with minor modifications. To the reaction mixture containing 0.2 ml of NBT (1mg/ml in DMSO) and 0.6 ml of extract (1- 800 mg/ml), 2 ml of alkaline DMSO (1 ml DMSO in 5 mM NaOH) was added to give a final volume of 2.8 ml. The absorbance was recorded at 560 nm. The blank consisted of pure DMSO instead of alkaline DMSO. Ascorbic acid was used as the standard and the ability of ST extracts to scavenge the superoxide radical was calculated using the formula:

$$\% \text{ scavenging} = (A_e - A_o / A_e) \times 100$$

Where, A_o is absorbance without sample and A_e is absorbance with sample.

ABTS radical scavenging activity : The scavenging activity of ST extracts for ABTS radical was determined using the method of Re *et al*. (18). A stock solution was prepared by mixing equal volumes of 7 mM ABTS solution and 2.45 mM potassium persulfate solution. The solution was incubated at room temperature in the dark for 12 hr to yield a dark-coloured solution containing $ABTS^{\cdot+}$ radicals. A working solution was prepared freshly before each assay by diluting the stock solution with 50% methanol for an initial absorbance of about 0.700 (±0.02) at 745 nm. The scavenging activity was then assessed by mixing 150 µl of different fractions of various extracts (1-200 µg/ml, dissolved in their respective solvents) with 1.5 ml of ABTS working standard. The decrease in absorbance was measured immediately at 745 nm. Each experiment was done in triplicate. Ascorbic acid was used as positive control. The scavenging activity was then estimated based on the formula:

$$\% \text{ scavenging} = [(A_{blank} - A_{sample}) / A_{blank}] \ 100$$

Where, A_{blank} is the absorbance of the control reaction (containing all reagents except the test compound) and A_{sample} is the absorbance of the test compound.

Reducing power : The reducing power of ST extracts was determined using the method described earlier (19) with slight modifications. Different extracts of ST dissolved in their respective solvent (1-1000 mg/ml) was mixed with 2.5 ml of 0.2 M phosphate buffer (pH- 6.6) and 2.5 ml of 1% potassium ferricyanide solution. The mixture was incubated at 50°C for 20 min after which 2.5 ml of 10% TCA was added. The mixture was then centrifuged at 3000 rpm for 10 min and 2.5 ml of the supernatant was mixed with 2.5 ml of distilled water and 0.5 ml of 1% ferric chloride solution. Absorbance was measured at 700 nm. Increased absorbance of the reaction mixture indicated increase in reducing power of the extract.

Ex vivo antioxidant assay

Anti-hemolytic activity : The antioxidant activity of different extracts of ST was measured according to the inhibition of erythrocyte hemolysis (20). Blood was collected from mice of same age group (10-12 w) and body weights (25-27 g) by means of heart puncture in a heparinized tube. The mice erythrocyte hemolysis was performed with H_2O_2 as free radical initiator. To 0.5 ml of 5% (v/v) suspension of RBC in PBS, 0.4 ml (0.5 mg/ml) of different extracts and 100 µl of 1 mol/L H_2O_2 was added. The reaction mixture was shaken gently while being incubated at 37°C for 3 hr. After incubation the reaction mixture was again diluted with 4 ml of PBS and centrifuged at 2000

rpm for 10 min. The supernatant was collected and absorbance was measured at 540 nm. The rate of inhibition of erythrocyte hemolysis was calculated using the formula:

Inhibition rate % = [1 - (A1 – A2)/ A_0] × 100

Where, A_0 is the absorbance of control (without extract), A1 is the absorbance in the presence of the extract and A2 is the absorbance without sample (RBC).

Lipid peroxidation inhibition assay : Lipid peroxidation in mice liver was induced by $FeCl_2$-H_2O_2 (21). Briefly, liver was excised from mice and 1% liver homogenate was prepared. The liver homogenate was centrifuged at 3000 rpm at 4ºC for 10 min and the supernatant was used for the assay. The supernatant (0.5 ml) was mixed with 0.5 ml (0.5 mg/ml) of extracts and then incubated at 37ºC for 1 hr after mixing with 0.25 ml each of 0.5 mol/L $FeCl_2$ and H_2O_2. After incubation, the formation of malonaldehyde (MDA) was measured at 535 nm. The inhibitory effect was calculated as:

Inhibition rate % = [1 - (A1 – A2)/ A_0] × 100

Where, A_0 is the absorbance of control (without extract), A1 is the absorbance in the presence of the extract whereas A2 is the absorbance without liver homogenate.

Animal model : The inbred Swiss albino mice colony is being maintained under controlled conditions of temperature (22 ° C ± 5°C) and 12 h light-dark cycles (Frontier Euro Digital Timer, Taiwan) at the Animal Care Facility of the Department of Zoology, Mizoram University, Aizawl, India. The animals were fed with commercially available food pellets and water *ad libitum.* The animal care and handling was carried out according to the guidelines issued by World Health Organization, Geneva, Switzerland. The study was approved by the Institutional Animal Ethical Committee, Mizoram University, India vide approval No. MZU-IAEC/2018/09.

Statistical analysis : Data are expressed as mean ± standard error of mean. The IC_{50} values were calculated using Graph pad prism software ver. 6.0 by plotting the values against the log doses. One-way analysis of variance (ANOVA) was performed to test the significant variations on phytochemical contents and the antioxidant assays of various extracts followed by Tukey multiple comparision of means. SPSS ver.16.0 software (SPSS Inc, Chicago, Illinois, USA) and Graph pad prism software ver. 6.0 were used for the statistical and graphical evaluations. A p-value of less than 0.05 was considered statistically significant.

Results and Discussion

Phytochemical analysis : Qualitative screening revealed the presence of various active and naturally occurring phytochemicals such as alkaloids, cardiac glycosides, saponins, steroids, tannins and terpenoids in different extracts of *S. tuberosa* (Table 1). These phytochemicals belongs to polyphenolic compounds and have been reported to possesses numerous pharmacological values including anti-malarial (22), astringents (23), anti-inflammatory (24), anti-ulcer and antimicrobial activities (25).

Total phenolic and flavonoid contents: The total phenolic content of ST extracts increased in a concentration dependent manner (Fig. 1). At 8 mg/ml, STME has significantly higher ($p<0.001$) total phenolic content (715.20 ± 2.42 mg gallic acid equivalent/g of dry extract) than that of STCE (549.49 ± 16.67 mg gallic acid equivalent/g of dry extract) and STAE (367.92 ± 2.47 mg gallic equivalent/g of dry extract). The total flavonoid content of various extracts of ST also increased with the increase in concentration of the extracts (Fig. 2). At 8 mg/ml of extracts, STME has the highest ($p<0.001$) total flavonoid content (4890.13 ± 8.97 mg quercetin equivalent/g of dry extract) as compared to other fractions of the ST extracts (4556.94 ± 13.70 mg quercetin equivalent/g of dry extract for STAE; 2902.48 ± 6.26 mg quercetin equivalent/g of dry extract for STCE). The present study indicated the presence of significant amounts of flavonoid and phenolic compounds in ST extracts. Phenolic compounds have been reported to show antioxidant activity by scavenging or stabilizing free radicals due to their conjugated

Table 1: Phytochemical screening of various extracts of S. tuberosa. ('+' indicates presence of phytochemicals and '–' indicates absence of phytochemicals).

Phytochemicals	Reagent	Colour Indication	STCE	STME	STAE
Alkaloids	Dragendorff's Reagent	Reddish brown precipitate	+	+	+
Cardiac glycosides	Glacial Acetic Acid Ferric Chloride Sulphuric Acid	Brown ring	+	+	+
Saponins	Olive oil	Whitish Emulsion	+	+	+
Steroids	Sulphuric Acid	Red Colour	+	-	-
Tannins	Ferric Chloride	Brownish Green or blue-black	+	+	+
Terpenoids	Sulphuric acid	Reddish Brown	+	+	+
Phlobatannins	Hydrochloric acid	Red precipitate	-	-	-

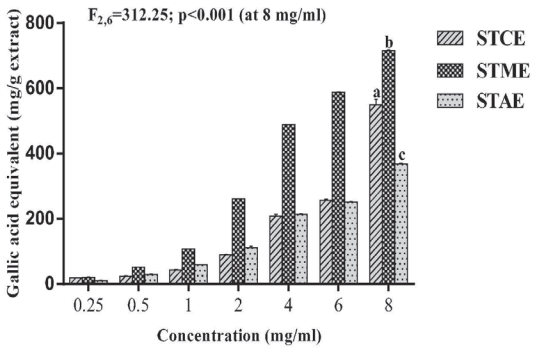

Fig. 1: Phenolic content of various extracts of *S. tuberosa* determined as gallic acid equivalent. Values are expressed as Mean ± SEM, n=3. Different letters indicate significant variation.

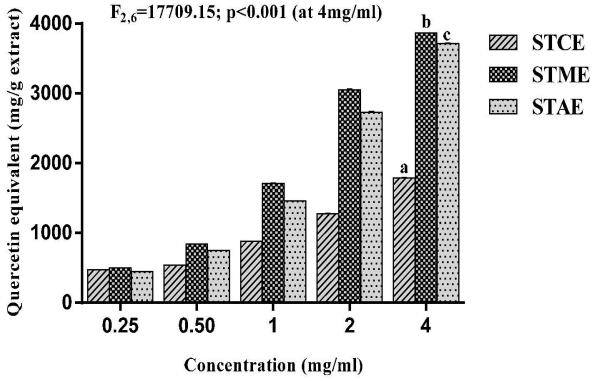

Fig. 2: Flavonoid content of various extracts of *S. tuberosa* determined as Quercetin equivalent. Values are expressed as Mean ± SEM, n=3. Different letters indicate significant variation.

ring structures and presence of hydroxyl groups (26 and 27). Phenolic compounds have also been reported to exhibited antiallergenic, antimicrobial, anti-artherogenic, antithrombotic, anti-inflammatory, vasodilatory and cardioprotective effects (28 and 29). Similarly, flavonoids are also reported to have antioxidative action through scavenging or chelating process (30).

In vitro antioxidant assay

DPPH radical scavenging activity : Various extracts of ST showed a concentration dependent increase in the scavenging of DPPH radicals as indicated by the discoloration of DPPH. Maximum scavenging was observed at a concentration of 200 µg/ml for all the extracts. Log-doses of various extracts of *S. tuberosa* and standard ascorbic acid (ASA) were plotted against DPPH inhibition (%) for the calculation of IC_{50} (Fig. 3). STCE showed the highest scavenging activity (lowest IC_{50}; 7.36 ± 0.08 µg/ml) followed by STME (IC_{50}; 13.46 ± 0.04 µg/ml) and STAE (IC_{50}; 18.41 ± 0.16 µg/ml). The IC_{50} of STCE does not significantly differ ($p > 0.05$) from that of the standard ASA (IC_{50};6.57 ±1.01 µg/ml) (Fig. 4). It has been reported that the reducing capability of the methanolic DPPH solution to a non-radical DPPH-H form by various compounds such as cystein, glutathione, ascorbic acid and tocopherol was due to their hydrogen donating ability (31 and 32). In the present study, various solvent extracts of ST effectively reduced the stable radical DPPH to the yellow-colored diphenyl-picrylhydrazine probably due to presence of certain active compounds that are capable of donating hydrogen to a free radical in order to remove odd electron.

Superoxide radical scavenging activity : Superoxide radical scavenging activity of various extracts of ST showed a concentration dependent inhibition of superoxide radical generation. Maximum $O_2^{\cdot-}$ scavenging activity was observed at a concentration of 800 µg/ml for STME and STAE. STME possessed the highest scavenging activity (IC_{50}; 98.93 ± 3.37 ìg/ml) followed by STAE (241.83 ± 3.15 µg/ml) while the IC_{50} of STCE was indeterminable within the given concentration (800 µg/ml). The IC_{50} of STME and STAE are significantly higher ($p < 0.01$) than that of the standard ascorbic acid (IC_{50}; 262.20 ± 4.25 ìg/ml) (Figure 6). Superoxide ($O_2^{\cdot-}$) radical serves as a precursor of most of the reactive oxygen species (33) and can be decomposed to form stronger oxidative species such as singlet oxygen and hydroxyl radicals, which are very harmful to the cellular components and can initiate lipid peroxidation (34). Thus, neutralization of superoxide radical will inhibit the chain of ROS generation and protect the cells from oxidative stress. It has also been reported that antioxidant properties of some flavonoids are effective mainly through scavenging of superoxide anion radical (35). Thus, the presence of significant amount of flavonoids in ST extracts might be responsible for

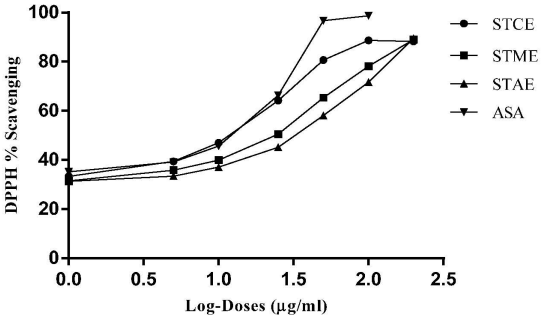

Fig. 3: Plots of log-doses of various extracts of *S. tuberosa* and standard ascorbic acid (ASA) against DPPH inhibition (%) for the calculation of IC_{50}.

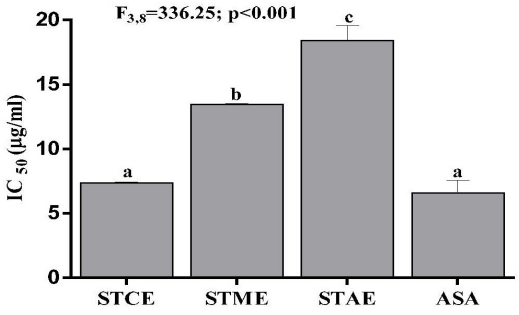

Fig. 4: IC_{50} (ìg/ml) for DPPH of various extracts of *S. tuberosa* and standard ascorbic acid. Values are expressed as Mean ± SEM, n=3. Different letters indicate significant variation.

their scavenging activity against superoxide radical. Interestingly, the scavenging potentials of STME and STAE were even better than the standard ascorbic acid.

ABTS radical scavenging activity : $ABTS^{\bullet+}$ radical scavenging activity of ST extracts increased in a concentration dependent manner as indicated by discoloration of the $ABTS^{\bullet+}$, which was measured spectrophotometrically at 745 nm. Maximum scavenging activity was observed at a concentration of 200 µg/ml for all the extracts. Log-doses of various extracts of *S. tuberosa* and the standard ascorbic acid (ASA) were plotted against $ABTS^{\bullet+}$ inhibition (%) for the calculation of IC_{50} (Fig. 7). Among the various extracts, STME possessed the highest $ABTS^{\bullet+}$ scavenging activity (IC_{50}; 36.20 ± 0.83 µg/ml) followed by STAE (IC_{50}; 45.12 ± 0.79 µg/ml) and STCE (IC_{50}; 66.8 ± 1.04 µg/ml) (Fig. 8). The effectiveness of any compound in stabilization of the preformed $ABTS^{\bullet+}$ to ABTS depends on the molecular weight of phenolic compounds, the number of aromatic rings and nature of hydroxyl group's substitution than the specific functional groups (36). Hence, the $ABTS^{\bullet+}$ scavenging activity of ST extracts might be due to the presence of high molecular weight phenolics such as catechin, and rutin derivatives.

Reducing power : The reducing power of various extracts of ST was determined by measuring the

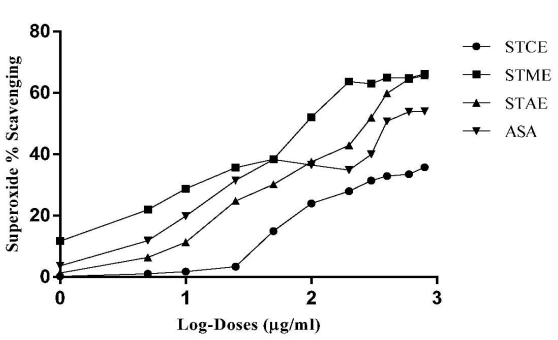

Fig. 5: Plots of log-doses of various extracts of *S. tuberosa* and standard ascorbic acid (ASA) against superoxide radical inhibition (%) for the calculation of IC_{50}.

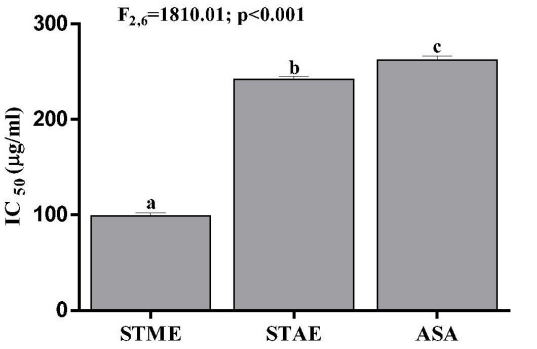

Fig. 6: IC_{50} (ig/ml) for superoxide radical inhibition of various extracts of *S. tuberosa* and standard ascorbic acid. Values are expressed as Mean ± SEM, n=3. Different letters indicate significant variation.

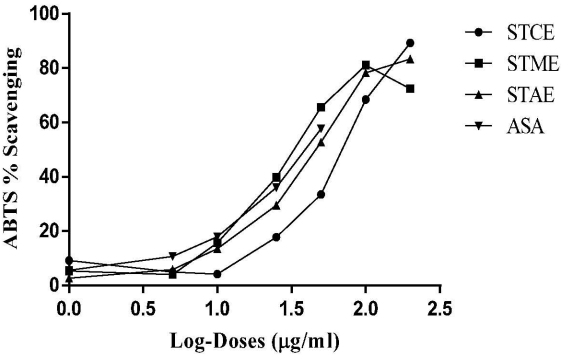

Fig. 7: Plots of log-doses of various extracts of *S. tuberosa* and standard ascorbic acid (ASA) against ABTS inhibition (%) for the calculation of IC_{50}.

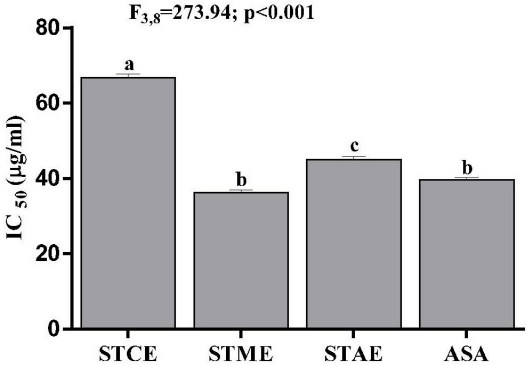

Fig. 8: IC_{50} (ig/ml) for ABTS of various extracts of *S. tuberosa* and standard ascorbic acid. Values are expressed as Mean ± SEM, n=3. Different letters indicate significant variation.

transformation of Fe^{3+} to Fe^{2+}. The reducing activity of ST extracts increased in a concentration dependent manner (Figure 9). At 1000 ìg/ml, the highest reducing activity was shown by STME (1.975 ± 0.002) followed by STCE (1.952 ± 0.005) and STAE (1.016 ± 0.007). The reducing power of a compound may serve as a significant indicator of its potential antioxidant activity. However, the activity of antioxidants has been assigned to various mechanisms such as prevention of chain initiation, binding of transition-metal ion catalysts, decomposition of peroxides and prevention of continued hydrogen abstraction, reductive capacity and radical scavenging (37). The dose dependent increase in the reducing power of the ST extracts also suggested their potent antioxidant activity.

Ex-vivo antioxidant assay

Anti-hemolytic activity : Erythrocytes were considered to be the major target of free radicals, leading to membrane damage and consequently to hemolysis (38 and 39). The anti-hemolytic activity of various extracts of ST increased in a concentration dependent manner (Fig. 10). At 1 mg/ml, STCE possessed the highest ($p < 0.001$) inhibitory activity against erythrocyte hemolysis with an inhibition rate of 68.82 % followed by STME and STAE with the inhibition rate of 38.58 % and 20.81 % respectively (Fig. 10). The protective effect of ST extracts on erythrocyte hemolysis could be due to the presence of significant amounts of phenolic and flavonoid compounds. Certain phenolic compounds have been reported to partition in the cell membrane, hindering diffusion of free radicals and consequently decreasing the kinetics of free radicals reactions (40). In addition, flavonoids upon binding to the erythrocytes membrane inhibit lipid peroxidation and improved their integrity against cell lyses (41).

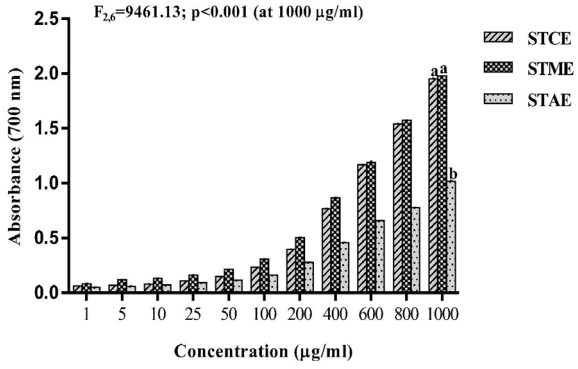

Fig. 9: Reducing power of various extracts of *S. tuberosa*. Values are expressed as Mean ± SEM, n=3.Values are expressed as Mean ± SEM, n=3. Different letters indicate significant variation.

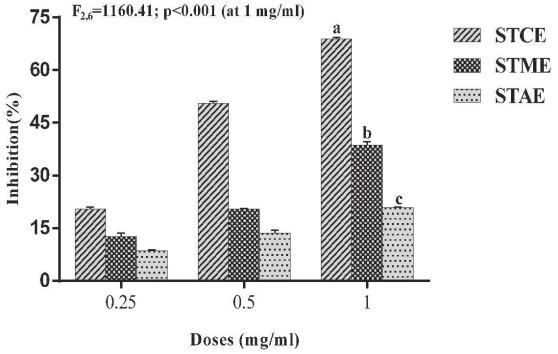

Fig. 10: Anti-hemolytic activity of various extracts of *S. tuberosa*. Values are expressed as Mean ± SEM, n=3. Different letters indicate significant variation.

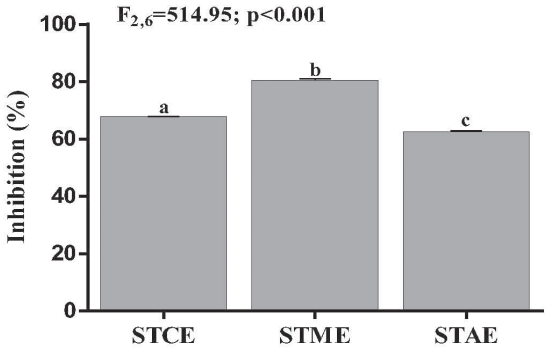

Fig. 11: Lipid peroxidation inhibition of various extracts of *S. tuberosa*at a concentration of 0.5 mg/ml. Values are expressed as Mean ± SEM, n=3. Different letters indicate significant variation.

The study indicated that the tuber extracts of ST contains molecules that might interacts with the membrane lipids of erythrocyte membrane and providing protective action against hemolysis.

Lipid peroxidation inhibition : In biological systems, lipid peroxidation generates certain degradation products such as MDA that are considered to be an important cause of cell membrane destruction and cell damage (21). *S. tuberosa* extracts exhibited moderate activity against lipid peroxidation inhibition in liver homogenate. At a concentration of 0.5 mg/ml, inhibition rates were significantly different among various extracts of ST ($F_{2,6}$=514.95) and STME possessed the highest ($p<0.001$) inhibitory activity against lipid peroxidation with an inhibition rate of 80.55 % followed by STCE and STAE with the inhibition rate of 67.81 % and 62.64 % respectively (Fig. 11).

Conclusions

The present study revealed the presence of significant amounts of phenolic and flavonoid compounds along with various active polyphenolic compounds such as alkaloid, cardiac glycosides, saponins, steroids, tannins and terpenoids. This study also demonstrates that various solvent extracts of *Stemona tuberosa* exhibit a concentration dependent inhibition of free radicals, ferric reducing power, anti-hemolytic and inhibitory action against lipid peroxidation. The radicals scavenging activity and the antioxidative property of ST might be due to presence of significant phytochemical contents. However, an effort to understand the mechanism(s) through which ST exerts antioxidant activities need to be investigated further.

References

1. Halliwell, B. and Gutteridge, J. M. (1998). Free Radicals in Biology and Medicine. Oxford University Press, Oxford, UK.
2. Tiwari, A. K. (2001). Imbalance in antioxidant defence and human diseases: multiple approach of natural antioxidants therapy. Current Science, 81 (9): 1179-1187.
3. Stadtman, E. R. (1992). Protein oxidation and aging. Science, 257 (5074): 1220-1224.
4. Maxwell, S. J. R. (1995). Prospects for the use of antioxidant therapies. Drugs, 49 (3): 345-361.
5. Cordel, G. A. (2011). Sustainable Medicines and Global Health Care. Planta Medica, 77: 1129-1138.
6. Loureiro, and Cochinch, F. L. (1790). *Stemona tuberosa*. Flora of China, 2: 404.
7. Nohayati, I., Zharil, I. and Muzlifah, A. M. (1999). Malaysian Medicinal Plant Index. Kuala Selangor: Victus Semulajadi, pp. 61.
8. Joseph, P. H. and Youyu, J. (2005). The healing power of Chinese herbs and medicinal recipes. Howard Press, New York, pp. 370-372.
9. Pacher, T., Seger, C., Engelmeier, D., Vajrodaya, S., Hofer, O. and Greger, H. (2002). Antifungal stilbenoids from *Stemona tuberosa*. Journal of Natural Products, 65(6): 820-827.
10. Guo, A., Jin, L., Deng, Z., Kai, S., Guo, S. and Lin, W. (2008). New *Stemona* Alkaloids from the Roots of *Stemona sessilifolia*. Chemistry & Biodiversity, 5: 598-605.
11. El-Zalabani, S. M., Mahmoud, I. I., Ahmed, F. I., and Shehab, N. G. (1999). Protein, carbohydrate, mineral and vitamin contents of *Sonchus oleraceus*. Journal of Pharmaceutical Sciences, 23: 46-54.
12. Harborne, J. B. (1998). Phytochemical methods: A guide to modern techniques of plant analysis (3rd edition).
13. Doughari, J. H. (2012). Phytochemicals: extraction methods, basic structures and mode of action as potential chemotherapeutic agents, phytochemicals – A global perspective of their role in nutrition and health. In: Venketeshwer Rao (edition). InTech, Rijeka, Croatia.

14. Singleton, V. L. and Rossi, J. A. (1996). Calorimetry of total phenolics with phosphomolybdicphosphotungstic acid reagents. American Journal of Enology and Viticulture, 16: 144-153.

15. Sakanaka, S., Tachibana, Y. and Okada, Y. (2005). Preparation and antioxidant properties of extracts of Japanese Persimmon leaf tea (*kakinoha-cha*). Food Chemistry, 89: 569-575.

16. Leong, L. P. and Shui, G. (2002). An investigation of antioxidant capacity of fruits in Singapore markets. Food Chemistry, 76: 69-75.

17. Hyland, K., Voisin, E., Banoun, H. and Auclair, C. (1983). Superoxide Dismutase Assay Using Alkaline Dimethylsulfoxide as Superoxide Anion-Generating System. Analytical Biochemistry, 135: 280-287.

18. Re, R., Pelligrini, N., Proteggente, A., Pannala, A., Yong, M. and Rice-Evas, C. (1999). Antioxidant activity applying an improved ABTS radical cation decoloursation assay. Free Radical Biology and Medicine, 26: 1231-1237.

19. Oyaizu, M. (1986). Studies on product of browning reaction prepared from glucose amine. Japanese Journal of Nutrition and Dietetics, 44: 307-315.

20. Li, N., Alam, J., Venkatesan, M. I., Eiguren-Fernandez, A., Schmitz, D., Stefano, E. D., Slaughter, N., Killeen, E., Wang, X., Huang, A., Wang, M., Miquel, A. H., Cho, A., Sioutas, C. and Nel, A. E. (2004). Nrf2 Is a Key Transcription Factor That Regulates Antioxidant Defense in Macrophages and Epithelial Cells: Protecting against the Pro-inflammatory and Oxidizing Effects of Diesel Exhaust Chemicals. Journal of Immunology, 173(5): 3467-3481.

21. Rajinder, K. A. K. and Thukral, S. A. (2010). Attenuation of free radicals by an aqueous extract of peels of Safedmusli tubers (*Chlorophytum borivilianum* Santet. Fernand). Journal of Chinese Clinical medicine, 5: 7-11.

22. Wink, M., Schmeller, T. and Latz-Bruning, B. (1998). Modes of action of allelochemical alkaloids: Interaction with neuroreceptors, DNA, and other molecular targets. Journal of Chemical Ecology, 44(11): 1881-1937.

23. Pieters, Rik, and Warlop, L. (1999). Visual attention during brand choice : The impact of time pressure and task motivation. International Journal of Research in Marketing, 16: 1-17.

24. Dolara, P., Luceri, C., Filippo, C. D., Femia, A. P., Giovannelli, L., Caderni, G., Cecchini, C., Silvi, S., Orpianesi, C. and Cresci, A. (2005). Red wine polyphenols influence carcinogenesis, intestinal microflora, oxidative damage and gene expression profiles of colonic mucosa in F344 rats. Mutation Research – Fundamental and Molecular Mechanisms of Mutagenesis, 591: 237-246.

25. Dudareva, N., Pichersky. andGershenzon, J. (2004). Biochemistry of Plant Volatiles. Plant Physiology, 135: 1893-1902.

26. Diplock, A. T. (1997). Will the good fairies please prove us that vitamin E lessens human degenerative disease. Free Radical Research, 27: 511-532.

27. Amic, D., Davidovic-Amic, D., Beslo, D. and Trinajstic, N. (2003). Structure-radical scavenging activity relationship of flavonoids. Croatica Chemica Acta, 76: 55-61.

28. Middleton, E., Kandaswami, C. and Theoharides, T. C. (2000). The effects of plant flavonoids on mammalian cells: Implications for inflammation, heart disease and cancer. Pharmacological Reviews, 52: 673-751.

29. Alpinar, K., Ozyurek, M., Kolak, U., Guclu, K., Aras, C., Altun, M., Celik, S. E., Berker, K. I., Bektasoglu, B. and Apak, R. (2009).

Antioxidant Capacities of Some Food Plants Wildly Grown in Ayvalik of Turkey. Food Science and Technology Research, 15: 59-64.

30. Cook, N. C. and Samman, S. (1996). Flavonoids-Chemistry, metabolism, cardioprotective effects and dietary sources. Journal of Nutritional Biochemistry, 7 (2): 66-76.

31. Blois, M. S. (1958). Antioxidant determinations by the use of a stable free radical. Nature, 181: 1199-1200.

32. Moon, K., Katolkar, P. and Khadabadi, S. S. (2010). In vitro antioxidant activity of methanolic extract of Erythriniaindica. Der Pharmacia Lettre, 2: 16-21.

33. Kirkinezosa, I. G. and Morae, C. T. (2001). Reactive oxygen species and mitochondrial diseases. Cell and Developmental Biology, 12: 449-457.

34. Yen, G. C. and Duth, P. D. (1994). Scavenging effect of methanolic extracts of peanut hulls on free radical and active-oxygen species. Journal of Agricultural Food and Chemistry, 42: 629-632.

35. Robak, J. and Gryglewski, R. J. (1988). Flavonoids are scavengers of superoxide anions. Biochemical Pharmacology, 37 (5): 837-841.

36. Hagerman, A. E., Reidl, K. M., Jones, G. A., Sovik, K. N., Ritchard, N. T. and Hartzfeld, P. W. (1998). High Molecular Weight Plant Polyphenolics (tannins) as biological antioxidants. Journal of Agricultural Food and Chemistry, 46: 1887-1892.

37. Fahn, S. and Cohen, G. (1992). The antioxidant stress hypothesis in Parkinson's disease: evidence supporting it. Annals of Neurology, 32: 804-812.

38. Wang, J. and Yao, H. (2005). Antioxidant activity of feruloylated oligosaccharides from wheat bran. Food Chemistry, 90 (4): 759-764.

39. Ebrahimzadeh, M. A., Ehsanifer, S. and Eslami, B. (2009). Sambu cusebulu selburensis fruits: a good source for antioxidants. Pharmacognosy Magazine, 4 (9): 213-218.

40. Singh, N. and Rajini, P. S. (2008). Antioxidant-mediated protective effects of potato peel extract in erythrocytes against oxidative damage. Chemico Biological Interactions, 173 (2): 97-104.

41. Chaudhuri, S., Banerjee, A., Basu, K., Sengupta, B. and Sengupta, P. K. (2007). Interaction of flavonoids with red blood cell membrane lipids and proteins: Antioxidant and antihemolytic effects. International Journal of Biological Macromolecules, 41 (1): 42-48.

Registered with Registrar of News Papers for India
Regn. No. APENG/2008/28877

Association of Biotechnology and Pharmacy

(Regn. No. 28OF 2007)

Executive Council

Hon. President
Prof. B. Suresh

Hon. Secretary
Prof. K. Chinnaswamy

President Elect
Prof. T. V. Narayana
Bangalore

General Secretary
Prof. K.R.S. Sambasiva Rao
Guntur

Vice-Presidents
Prof. M. Vijayalakshmi
Guntur
Prof. T. K. Ravi
Coimbatore

Treasurer
Prof. P. Sudhakar

Advisory Board

Prof. C. K. Kokate, Belgaum
Prof. B. K. Gupta, Kolkata
Prof. Y. Madhusudhana Rao, Warangal
Prof. M. D. Karwekar, Bangalore
Prof. K. P. R.Chowdary, Vizag
Dr. V. S.V. Rao Vadlamudi, Hyderabad

Executive Members

Prof. V. Ravichandran, Chennai
Prof. Gabhe, Mumbai
Prof. Unnikrishna Phanicker, Trivandrum
Prof. R. Nagaraju, Tirupathi
Prof. S. Jaipal Reddy, Hyderabad
Prof. C. S. V. Ramachandra Rao, Vijayawada
Dr. C. Gopala Krishna, Guntur
Dr. K. Ammani, Guntur
Dr. J. Ramesh Babu, Guntur
Prof. G. Vidyasagar, Kutch
Prof. T. Somasekhar, Bangalore
Prof. S. Vidyadhara,Guntur
Prof. K. S. R. G. Prasad,Tirupathi
Prof. G. Devala Rao, Vijayawada
Prof. B. Jayakar, Salem
Prof. S. C. Marihal, Goa
M. B. R. Prasad, Vijayawada
Dr. M. Subba Rao, Nuzividu
Prof. Y. Rajendra Prasad, Vizag
Prof. P. M.Gaikwad, Ahamednagar

Printed, Published and owned by Association of Bio-Technology and Pharmacy # 6-69-64 : 6/19, Brodipet, Guntur - 522 002, Andhra pradesh, India. **Printed at :** Don Bosco Tech. School Press, Ring Road, Guntur - 522 007. A.P., India **Published at :** Association of Bio-Technology and Pharmacy # 6-69-64 : 6/19, Brodipet, Guntur - 522 002, Andhra pradesh, India.
Editors : Prof. K.R.S. Sambasiva Rao, Prof. Karnam S. Murthy